



**CATALYTIC WET AIR OXIDATION OF PHENOL OVER ACTIVE CARBON IN  
FIXED BED REACTOR: STEADY STATE AND PERIODIC OPERATION**  
**Nigus Gabbiye Habtu**

ISBN:  
Dipòsit Legal: T.1262-2011

**ADVERTIMENT.** La consulta d'aquesta tesi queda condicionada a l'acceptació de les següents condicions d'ús: La difusió d'aquesta tesi per mitjà del servei TDX ([www.tesisenxarxa.net](http://www.tesisenxarxa.net)) ha estat autoritzada pels titulars dels drets de propietat intel·lectual únicament per a usos privats emmarcats en activitats d'investigació i docència. No s'autoritza la seva reproducció amb finalitats de lucre ni la seva difusió i posada a disposició des d'un lloc aliè al servei TDX. No s'autoritza la presentació del seu contingut en una finestra o marc aliè a TDX (framing). Aquesta reserva de drets afecta tant al resum de presentació de la tesi com als seus continguts. En la utilització o cita de parts de la tesi és obligat indicar el nom de la persona autora.

**ADVERTENCIA.** La consulta de esta tesis queda condicionada a la aceptación de las siguientes condiciones de uso: La difusión de esta tesis por medio del servicio TDR ([www.tesisenred.net](http://www.tesisenred.net)) ha sido autorizada por los titulares de los derechos de propiedad intelectual únicamente para usos privados enmarcados en actividades de investigación y docencia. No se autoriza su reproducción con finalidades de lucro ni su difusión y puesta a disposición desde un sitio ajeno al servicio TDR. No se autoriza la presentación de su contenido en una ventana o marco ajeno a TDR (framing). Esta reserva de derechos afecta tanto al resumen de presentación de la tesis como a sus contenidos. En la utilización o cita de partes de la tesis es obligado indicar el nombre de la persona autora.

**WARNING.** On having consulted this thesis you're accepting the following use conditions: Spreading this thesis by the TDX ([www.tesisenxarxa.net](http://www.tesisenxarxa.net)) service has been authorized by the titular of the intellectual property rights only for private uses placed in investigation and teaching activities. Reproduction with lucrative aims is not authorized neither its spreading and availability from a site foreign to the TDX service. Introducing its content in a window or frame foreign to the TDX service is not authorized (framing). This rights affect to the presentation summary of the thesis as well as to its contents. In the using or citation of parts of the thesis it's obliged to indicate the name of the author.

# DOCTORAL THESIS

Nigus Gabbiye Habtu

Catalytic Wet Air Oxidation of Phenol over Active Carbon in Fixed  
Bed Reactor: Steady State and Periodic Operation



UNIVERSITAT ROVIRA I VIRGILI







---

# Catalytic Wet Air Oxidation of Phenol over Active Carbon in Fixed Bed Reactor: Steady State and Periodic Operation

Memòria presentada per optar al títol de

**Doctor per la Universitat Rovira i Virgili**

**Nigus Gabbiye Habtu**

Departament d'Enginyeria Química  
Escola Tècnica Superior d'Enginyeria Química  
Universitat Rovira i Virgili  
Av. Països Catalans 26  
43007 Tarragona



UNIVERSITAT ROVIRA I VIRGILI

Tesi dirigida per el Dr. Frank Stüber





UNIVERSITAT  
ROVIRA I VIRGILI

Escola Tècnica Superior d'Enginyeria Química  
Departament d'Enginyeria Química

Avinguda dels Països Catalans, 26  
43007 Tarragona (Spain)  
Tel.: +34 977 559700  
Fax: +34 977 559699

I, Dr. Frank Stüber, professor of the Department of Chemical Engineering of the Rovira i Virgili University,

CERTIFY:

That the present study, entitled "Catalytic Wet Air Oxidation of Phenol over Active Carbon in Fixed Bed Reactor: Steady State and Periodic Operation", presented by Nigus Gabbiye Habtu for the award of the degree of Doctor, has been carried out under my supervision at the Department of Chemical Engineering of this university, and that it fulfils all the requirements to be eligible for the European Doctorate Award.

**Frank Stüber**  
Professor Titular  
Departament d'Enginyeria Química  
Universitat Rovira i Virgili

Tarragona, April 30, 2011



# Acknowledgements

Honestly speaking, PhD thesis is not only a personal effort rather a contribution of ideas, suggestion, help and encouragement of different people, to whom I would like to express my deepest gratitude.

First and foremost I would like to thank my supervisor Dr. F. Stüber for his patience, guidance and critical spirit through out my work. Apart from improving my skill on Catalytic Wet Air Oxidation process in three phase reactors, you taught me to not pay no attention for small things in a scientific world.

Within the Chemical Reaction Engineering and Process Intensification Group, to Dr. J. Font and Dr. A. Fortuny who, through numerous discussions, clarified many of my doubts. To Dr. C. Bengoa and Dr. A. Fabregat who have been attendant to provide the material support necessary for the realization of this work. I would like to thank you, Esther for your cooperation in providing materials for my work. Specially thanks for your patience in supplying regularly the high pressure gas system which I guess my trickle is a major consumer. Ana, Xavier, Rita and Gergo thank you for the unforgettable time we spent in the laboratory and discussion about our research topics. My office mates Ivone, Selamawit, Natalia, Magida and Sunil, thank you for the time we spent in a small office.

I would like to express my deepest gratitude for Prof. dr. ir. Jaap Schouten for allowing me to share the research experience of his group and Dr. ir. T.A. Nijhuis (Xander) for his hospitality and encouragement during my visit.

I am grateful to acknowledge Dr. Delmas (INP de Toulouse), Dr. Fabregat (Rovira i Virgili University), Dr. Contreras (Rovira i Virgili University), Dr. Julcour-Lebigue (INP de Toulouse) and Dr. Suárez-Ojeda (Universidad Autnoma de Barcelona) for accepting to participate in the examining committee of this PhD thesis, as well as Dr. Font (Rovira i Virgili University) and Dr. Fortuny (Universitat Politcnica de Catalunya ) who are the substitute members of the committee. Also I am thankful to Dr. Besson (Universit Claude Bernard Lyon 1) and Dr. Ayral (Orege society) for accepting to review the reports that enabled this work to be eligible for European PhD award, and for their comments regarding the manuscript.

I would like to acknowledge the University of Rovira i Virgili for providing me a four year scholarship to accomplish my PhD thesis and the Ministry of education of Spain for financial sup-

port of three month research stage at Technical University of Eindhoven.

Within the Chemical Engineering Department I am grateful to thank Ms. Nuria Juanpere and Merche Maurn for their administrative help from the beginning to the end of my study.

My deepest gratitude goes to my elder sister, Wudinesh Gabbiye, for her attention and encouragement throughout my study.

Last, but not least, my lovely wife Aberash and daughter Sara, life in Tarragona would not have been so pleasant without you.

---

## Resumen

Los recursos naturales disponibles de agua dulce están cada vez más expuestos a la contaminación sistemática debido al aumento de su extracción por diversas actividades humanas. De hecho, la rápida industrialización y urbanización mundial han creado un gran número de nuevos efluentes acuosos que contienen contaminantes tóxicos y peligrosos, siendo en su mayoría muy refractarios para ser modificados de forma natural. En particular, los compuestos orgánicos como los fenoles se encuentran entre las sustancias más tóxicas y no biodegradables que se encuentran con frecuencia en muchas aplicaciones industriales. Por lo tanto, el tratamiento y control para el re uso de aguas residuales provenientes de procesos industriales son una contribución obligatoria para el suministro sostenible de agua dulce para las futuras generaciones. Por otra parte, las legislaciones ambientales son cada vez más estrictas, lo cual promueve el desarrollo de investigaciones referentes al impulso de tecnologías más eficientes y de bajo costes; pues las soluciones existentes (incineración, tratamientos biológicos) ya no son viables. En la literatura existes referente a este tema se ha mostrado que CWAO sobre carbón activado llevada a cabo en un reactor de lecho fijo, puede ser una prometedora alternativa de bajo costo para la destrucción de determinados contaminantes fenólicos. Sin embargo, parece poco probable lograr satisfactoriamente la estabilidad del catalizador a largo plazo en los reactores de lecho fijo en estado estacionario; debido a la combustión lenta del carbón activado y a la adsorción irreversible de los productos de condensación en la superficie del carbón activado, a las típicas condiciones de CWAO.

Una evaluación conjunta entre los aspectos químicos y de ingeniería de procesos podrían permitir la mejora en el rendimiento CWAO para una aplicación exitosa a escala industrial. En esta tesis, el potencial del carbón activado para la CWAO de fenol fue estudiado en aplicaciones de reactores de lecho fijo. Tantos experimentos en estado estacionario como en estado transitorio fueron realizaron para flujos ascendentes y descendentes con una amplia gama de condiciones de operación. Para la operación en estado estacionario, el régimen cinético, la dinámica de flujo de los hidrdrinámico y la adecuada puesta en marcha del reactor fueron determinados previamente para llevar a cabo mediciones de cinética intrínseca de la oxidación de fenol sobre carbón activo. Los experimentos con operación periódico fueron realizados con la finalidad estudiar tanto la transferencia de calor en la columna de lecho fijo por goteo como la mejora de la estabilidad del carbón activado. Un modelo de pseudo homogéneo para la transferencia de calor desarrollado por los Profs. A. Ayude y P. Haure (INTEMA Universidad de Mar del Plata) fue utilizado para examinar los perfiles de temperatura axial obtenidos en la columna de lecho empacado bajo condiciones no reactivas.

Los resultados de la hidrodinámica del flujo y régimen cinético mostraron que la oxidación de fenol sobre carbón activo puede llevarse a cabo sin las limitaciones de transporte externo e interno en el reactor de lecho fijo por goteo utilizado. En el estado estacionario, la actividad y la estabilidad del carbón activado están fuertemente influenciadas por las condiciones de operación

( $T$ ,  $P_{O_2}$ ,  $C_{Ph}$ ) y por el procedimiento de arranque (saturación lecho de carbón activado). La alta actividad y estabilidad del catalizador fueron logradas cuando la formación, la adsorción y la destrucción de los productos de acoplamiento oxidativos estaban equilibradas en la superficie del carbón activado, donde se destaca la importancia de oxígeno disuelto en la fase líquida en el estado inicial de CWAO. Ha sido observado que las conversiones de fenol y TOC también se ven afectadas por la concentración de la alimentación de fenol, lo que sugiere que la oxidación de fenol sobre el carbón activado no puede seguir simple cinética de primer orden. En ese caso, la medición de la superficie heterogénea cinética para la disociación del oxígeno puede explicar mejor los resultados observados.

Altos grados de conversión de fenol ( $> 99\%$ ) y de mineralización (más del 85% de conversión TOC) pueden ser alcanzados en un TBR utilizando carbón activado como catalizador en condiciones típicas CWAO (160 °C, 2 bar de presión de oxígeno). Sin embargo, una pérdida de la actividad lenta y progresiva, debido principalmente a la quema del catalizador, fue apreciada a estas condiciones, previniendo a su aplicación exitosa a escala industrial. Para disminuir este inconveniente, la operación del reactor periódico (variación de la temperatura de la alimentación y flujo del líquido) ha sido probada como un concepto novedoso para la realización de CWAO de fenol sobre el carbón activado. En la primera parte, la transferencia de calor en el reactor de lecho fijo por goteo fue estudiada para definir el modelado final de la CWAO para la variación de la temperatura de alimentación. Los experimentos fueron llevados a cabo, sin reacción, en una columna de lecho fijo a diferentes condiciones de presión total y a diferentes tasas de flujo de líquido y gas ( $P_t$ ,  $F_L$  and  $F_G$ ) en el estado estacionario o con variación de la temperatura de alimentación. Los resultados de transferencia de calor en el estado de estacionario obtenidos revelaron que la presión de operación y el flujo de líquido tienen la mayor influencia tanto en el coeficiente global de transferencia de calor ( $U$ ) como en el coeficiente de transferencia desde el lecho hasta la pared ( $h_w$ ) del reactor. Por otra parte, el modelado de los perfiles de temperatura dinámicos se logró con el modelo de transferencia de calor pseudo homogéneo de un parámetro, usando los valores previamente establecidos del coeficiente de transferencia de calor global. El desempeño del modelo da confianza para su aplicación definitiva en el modelo de CWAO de fenol sobre carbón activado, llevado a cabo en un TBR con variación de la temperatura de alimentación. En la segunda parte, la temperatura de alimentación modular de la CWAO fue investigada en el TBR para diferentes cortes y combinaciones de ciclos periódicos, mientras que los experimentos de variación de flujo de líquido se realizaron en el modo de flujo ascendente. Al parecer la variación de la temperatura de alimentación es una estrategia operativa eficaz para retrasar la quema del carbón activado. La actividad del catalizador permaneció estable durante aproximadamente 150 h de variación de temperatura de la alimentación en la CWAO, este comportamiento se observó a  $p = 1$  h,  $s = 0.8$ , 163 °C y 2 bar de presión de oxígeno. En estas condiciones, la quema del carbón activado pudo ser evitada por completo dando conversiones de fenol aceptables, entre 60-65%. Además, la aplicación de la variación de flujo de líquido en la CWAO parece ser satisfactoria. La conversión de fenol mejoró

en un 65% para un período más corto y para un corte de 0,2 horas y 0,5, respectivamente. Sin embargo, la fuerte pérdida de capacidad de adsorción en el caso de la variación de la temperatura de alimentación y el considerable desgaste del catalizador con la posterior obstrucción del tubo por la variación de flujo de líquido fueron observados durante los experimentos. Estos fenómenos representan el estado real de la principal barrera para lograr una mayor conversión de fenol ( $X_{Ph} > 80\%$ ).

## Summary

The earth's available fresh water resources are more and more exposed to a systematic pollution due to an increasing water abstraction by diverse human activities. In fact, the fast world industrialization and urbanization have created a large number of new sources of aqueous effluents containing toxic and hazardous pollutants, which are in most cases too refractory to amend naturally. In particular, organic compounds such as phenols are amongst the most toxic and non-biodegradable substances frequently found in many industrial applications. Thus, wastewater treatment and controlled re-use of these treated industrial process water are one mandatory mayor contribution to the sustainable supply of fresh water for future generation. Moreover, the increasingly stringent environmental legislation has reinforced the research on more efficient low cost remediation technologies since the existing solutions (incineration, biological treatments) are not longer feasible. A review of the specific literature points out that CWAO over activated carbon (AC), conducted in a fixed bed reactor can be a promising low cost alternative for the destruction of certain phenolic pollutants. However, it seems unlikely to achieve satisfactory long term catalyst stability in fixed bed reactors under steady state operation, due to the slow combustion of AC and irreversible adsorption of condensation products on the AC surface at typical CWAO conditions.

A combined assessment of the process chemistry and engineering aspects may allow improving CWAO performance for a successful application at industrial scale. In this thesis, the potential of AC for the CWAO of phenol was thus explored focusing on the application of fixed bed reactors. Both steady state and unsteady state experiments were conducted in down and upflow mode for a broad range of operating conditions. For steady state operation, kinetic regime, flow hydrodynamics and adequate reactor startup were previously determined to conduct intrinsic kinetic measurements of phenol oxidation over active carbon. Periodic operation experiments were done to study both the heat transfer in a trickle bed column and the improvement of activated carbon stability. A pseudo homogeneous one parameter heat transfer model developed by Profs. A. Ayude and P. Haure (INTEMA University Mar del Plata) was used to examine the axial temperature profiles obtained in the packed bed column under nonreactive conditions.

The results on flow hydrodynamics and kinetic regime showed that phenol oxidation over active carbon can proceed without external and internal transport limitations in our trickle bed reactor. At steady state, the activity and stability of AC is strongly influenced by operating conditions ( $T$ ,  $P_{O_2}$ ,  $C_{Ph}$ ) and reactor startup procedure (AC bed saturation). High activity and stability were achieved if the formation, adsorption and destruction of oxidative coupling products are balanced on the AC surface underlying the importance of oxygen dissolved in the liquid phase at the initial state of CWAO. It has been observed that phenol and TOC conversions are also affected by phenol feed concentration suggesting that the oxidation of phenol over AC may not follow simple first order kinetics. In that case, heterogeneous surface kinetics accounting for oxygen dissociation may better explain the observed results.

High degrees of phenol conversion (>99%) and mineralization (over 85% TOC conversion) can be achieved in a TBR using AC as a catalyst and typical CWAO conditions (160°C, 2 bar oxygen pressure). However, a slow and progressive activity loss mainly due to carbon burn-off was found takes place at these conditions preventing thereby a successful application at industrial scale. To alleviate this drawback, periodic reactor operation (feed temperature and liquid flow modulation) has been tested as a novel concept for conducting CWAO of phenol over AC. In the first part, heat transfer in trickle bed was studied for the ultimate modelling of CWAO under feed temperature modulation. Experiments without reaction were conducted in an insulated trickle bed column at different conditions of  $P_T$ ,  $F_L$  and  $F_G$  in steady state or with feed temperature modulation. The steady state heat transfer results obtained revealed that operating pressure and liquid flow rates have the strongest influence on both the overall ( $U$ ) and bed to wall ( $h_w$ ) heat transfer coefficients. Moreover, accurate modelling of the dynamic temperature profiles was achieved with the dynamic pseudo homogenous one parameter heat transfer model using the previously fitted values of the overall heat transfer coefficient. The performance of the model give confidence for its ultimate application to model CWAO of phenol over AC conducted in a TBR under temperature feed modulation. In the second part, feed temperature modulated CWAO was investigated in TBR for different split and cycle period combinations, while on-off liquid flow modulation experiments were conducted in upflow mode. It appears that temperature feed modulation is an effective operating strategy to delay AC burn-off. Stable catalyst activity during 150 h of feed temperature modulated CWAO was observed for  $p = 1$  h,  $s = 0.8$ , 163 °C and 2 bar of oxygen pressure. At these conditions, AC burn-off was completely avoided leading to acceptable phenol conversion of 60-65%. Also, application of liquid flow modulation to CWAO appears promising. Phenol conversion being improved to 65% for a shorter period and split of 0.2 h and 0.5, respectively. Nevertheless, strong loss of adsorption capacity in case of feed temperature modulation and considerable catalyst attrition and subsequent tube clogging for liquid flow modulation were observed during the experiments. These phenomena represent at the actual state a main barrier for achieving higher phenol conversion ( $X_{Ph} > 80\%$ ).



April 30, 2011



# Contents

<b>I</b>	<b>Literature Review</b>	<b>1</b>
<b>1</b>	<b>Introduction</b>	<b>3</b>
1.1	Global water distribution and abstraction . . . . .	3
1.2	Water pollution . . . . .	4
1.3	Wastewater treatment . . . . .	6
<b>2</b>	<b>Catalytic Wet Air Oxidation</b>	<b>13</b>
2.1	CWAO Catalysts . . . . .	14
2.1.1	Noble metal and metal oxide supported catalysts . . . . .	14
2.1.2	Activated carbon catalyst . . . . .	16
2.1.2.1	Activity of AC . . . . .	18
2.1.2.2	Stability of AC . . . . .	29
2.1.2.3	Role of AC in CWAO of phenol . . . . .	35
2.2	Multi-phase Reactors for CWAO . . . . .	42
2.2.1	Reactor choice . . . . .	42
2.2.2	Periodic operation of fixed bed reactors . . . . .	46
2.3	Conclusion . . . . .	52
<b>3</b>	<b>Hypothesis and Objective</b>	<b>55</b>
3.1	Hypothesis . . . . .	55
3.2	Objective . . . . .	55
<b>II</b>	<b>Methodology</b>	<b>57</b>
<b>4</b>	<b>Experimental</b>	<b>59</b>
4.1	Materials used . . . . .	59
4.2	Trickle Bed Reactor experiments at steady state . . . . .	60
4.2.1	Experimental set-up . . . . .	60

---

4.2.2	Phenol adsorption experiments . . . . .	62
4.2.3	Reactor start-up experiments . . . . .	62
4.2.4	Kinetic experiments . . . . .	63
4.3	Fixed Bed Reactor Experiments with Periodic Operation . . . . .	66
4.3.1	Gas-liquid feed temperature modulated TBR . . . . .	66
4.3.1.1	Experimental set-up . . . . .	66
4.3.1.2	Heat transfer study . . . . .	67
4.3.1.3	Feed temperature modulation without reaction . . . . .	69
4.3.1.4	Feed temperature modulation with reaction . . . . .	70
4.3.2	On-off liquid flow modulated upflow FBR . . . . .	71
4.3.2.1	Experimental set-up . . . . .	71
4.3.2.2	On-off liquid flow modulation experiments . . . . .	72
4.4	Analytical Methods . . . . .	73
4.4.1	Liquid effluent analysis . . . . .	73
4.4.2	Catalyst characterization . . . . .	74
<b>5</b>	<b>Modelling of Heat Transfer in Trickle Bed without Reaction</b>	<b>77</b>
5.1	Model equations and numerical solutions . . . . .	77
5.2	Determination of overall (U) and wall to bed heat transfer coefficient ( $h_w$ ) . . . . .	79
<b>III</b>	<b>Results and Discussion</b>	<b>81</b>
<b>6</b>	<b>CWAO of Phenol over AC in Steady State Trickle Bed Reactor</b>	<b>83</b>
6.1	Reactor Start-up . . . . .	84
6.1.1	Adsorption of phenol over AC under anoxic condition . . . . .	84
6.1.2	Influence of initial AC saturation . . . . .	84
6.1.3	Influence of AC pre-wetting . . . . .	89
6.1.4	Conclusion . . . . .	90
6.2	Phenol oxidation over AC in TBR . . . . .	91
6.2.1	Determination of kinetic regime in TBR . . . . .	91
6.2.2	Influence of phenol feed concentration . . . . .	96
6.2.3	Influence of oxygen partial pressure . . . . .	98
6.2.4	Influence of temperature . . . . .	100
6.2.5	Influence of solution pH . . . . .	103
6.2.6	Influence of WAO and free radical scavengers . . . . .	104
6.2.7	Conclusion . . . . .	106

---

<b>7</b>	<b>CWAO of Phenol in Periodically operated Fixed Bed Reactor</b>	<b>109</b>
7.1	Heat Transfer in Trickle Bed . . . . .	110
7.1.1	Influence of insulation materials . . . . .	110
7.1.2	Axial temperature profiles . . . . .	111
7.1.3	Influence of operating conditions . . . . .	114
7.1.4	Determination of overall heat transfer coefficient (U) . . . . .	114
7.1.5	Determination of bed to wall heat transfer coefficient ( $h_w$ ) . . . . .	118
7.1.6	Conclusion . . . . .	120
7.2	Feed Temperature Modulated CWAO in Trickle Bed Reactor . . . . .	122
7.2.1	Temperature feed modulation without reaction . . . . .	122
7.2.2	Temperature feed modulation with reaction . . . . .	125
7.2.2.1	Adiabatic operation . . . . .	125
7.2.2.2	Influence of period and split on phenol conversion . . . . .	125
7.2.2.3	Influence of cycle parameters on catalyst stability . . . . .	129
7.2.3	Conclusion . . . . .	135
7.3	Liquid Flow Modulated CWAO in Fixed Bed Upflow Reactor . . . . .	136
7.3.1	Influence of period and split on phenol conversion . . . . .	136
7.3.2	Influence of cycle parameters on AC stability . . . . .	139
7.3.3	Conclusion . . . . .	141
<b>IV</b>	<b>Concluding Remarks</b>	<b>143</b>
<b>8</b>	<b>Conclusions and Outlook</b>	<b>145</b>
8.1	Conclusions . . . . .	145
8.2	Outlook . . . . .	147
	<b>Bibliography</b>	<b>149</b>
<b>A</b>	<b>Appendix</b>	<b>163</b>
<b>B</b>	<b>Appendix</b>	<b>167</b>
B.1	Experimental Profiles obtained in Adsorption and Kinetic Measurement	167
<b>C</b>	<b>Appendix</b>	<b>183</b>
C.1	Axial temperature profiles . . . . .	183
<b>D</b>	<b>Appendix</b>	<b>197</b>
D.1	Conversion and temperature profiles for feed temperature modulation	197
D.2	Conversion and temperature profiles for liquid flow modulation . . . . .	208



## List of Figures

1.1	Projection of the increasing worldwide demand for water . . . . .	4
1.2	CALIPHOX process for catalytic liquid-phase oxidation of organic pollutants with an adsorber unit for pre-concentration . . . . .	10
2.1	Performance of different activated carbons. . . . .	20
2.2	CWAO of different compounds over Merck AC . . . . .	21
2.3	Phenol conversion measured during CWAO over parent and modified Merck ACs . . . . .	22
2.4	Performance of different CWAO catalysts in batch oxidation of phenol solution. . . . .	23
2.5	AC weight evolution during CWAO for different oxygen pressures . .	30
2.6	AC weigh evolution during CWAO for different phenol inlet concentration . . . . .	31
2.7	Evolution of phenol conversion, carbon weight, textural properties and C/O ratio during CWAO . . . . .	34
2.8	Mechanism for $O_2 / O_3$ decomposition and $H_2O_2$ formation over activated carbon . . . . .	37
2.9	Reaction pathways proposed for CWAO of phenol over AC catalyst .	39
2.10	Reaction pathway proposed for CWAO of phenol over Fe/AC catalyst	41
2.11	Configuration of three phase catalytic reactors . . . . .	42
4.1	Trickle Bed Reactor for steady state experiments . . . . .	61
4.2	Trickle Bed Reactor for feed temperature modulation experiments . .	67
4.3	Fixed Bed Reactor for liquid flow modulation experiments . . . . .	72
6.1	Phenol adsorption/desorption measured in a trickle bed column at three temperatures . . . . .	85
6.2	Phenol conversion profile for different active carbon bed saturations .	87

6.3	Effect of inert AC bed saturation on the activity and stability of AC catalyst . . . . .	88
6.4	Phenol conversion as function of time on stream for different pre-wetting procedures . . . . .	90
6.5	Effect of particle size and gas flow rate on phenol conversion during CWAO over AC. . . . .	92
6.6	Phenol and TOC conversion as a function of liquid flow rate . . . . .	93
6.7	Phenol conversion as a function of liquid space time for different hydrodynamic configurations . . . . .	94
6.8	Phenol conversion obtained in upflow and downflow mode of operations versus space time . . . . .	95
6.9	Phenol conversion for sequentially dilution of phenol feed concentration . . . . .	97
6.10	Phenol and TOC conversion as a function of space time and different feed concentration. . . . .	99
6.11	Phenol and TOC conversion as function of oxygen partial pressure: . . . . .	100
6.12	Phenol and TOC conversion as a function of time on stream for sequential temperature variation . . . . .	101
6.13	Phenol and TOC conversion as function of space time for different temperatures . . . . .	102
6.14	Phenol conversion as function of pH during CWAO of phenol over AC . . . . .	103
6.15	Phenol conversion as function of space time during WAO/CWAO in TBR . . . . .	104
6.16	Phenol conversion as function of feed concentration of different free radical scavenger . . . . .	106
7.1	Influence of different insulating material on axial temperature profile in a trickle bed column . . . . .	110
7.2	Evolution of axial temperature during a standard heating experiment . . . . .	112
7.3	Axial temperature profiles for different liquid flow rates and pressures . . . . .	113
7.4	Axial temperature gradient as function of system pressure for different liquid and gas flow rates . . . . .	115
7.5	Overall heat transfer coefficient as a function of system pressure for different liquid at constant gas flow rates . . . . .	117
7.6	Overall heat transfer coefficient as a function of system pressure for different gas flow rates at constant liquid flow rate . . . . .	119
7.7	Parity plot for experimentally determined $h_w$ and values calculated from the correlation proposed . . . . .	120
7.8	Evolution of axial temperatures during operation with imposed feed temperature modulation . . . . .	123

7.9	Adsorption-desorption dynamics of phenol concentration under temperature feed modulation without reaction . . . . .	124
7.10	Phenol conversion and temperature profiles for adiabatic and isothermal steady state TBR operation . . . . .	126
7.11	Effect of period and split on phenol conversion and temperature observed during modulated CWAO of phenol over AC . . . . .	127
7.12	Mean cycle phenol conversion after 50 h of CWAO operation versus cycle period . . . . .	128
7.13	Unsteady state phenol conversion and temperature profile as function of time on stream for ca. 150 h . . . . .	130
7.14	Phenol adsorption isotherm of fresh and CWAO spent AC samples obtained at $22 \pm 1$ °C . . . . .	131
7.15	Mean cycle phenol and TOC conversion as function of time on steam for different period . . . . .	132
7.16	Mean cycle phenol and TOC conversion with time on steam for different temperature . . . . .	134
7.17	Effect of period and split on phenol conversion under liquid flow modulation . . . . .	137
7.18	Mean cycle phenol conversion as function of split for different periods during liquid flow modulated CWAO . . . . .	138
7.19	Mean cycle phenol conversion as function of time on steam for different periods . . . . .	140
B.1	Phenomena adsorption/desorption over AC for different temperatures under inert conditions . . . . .	168
B.2	TGA data of fresh and spent AC for different AC saturation procedures	169
B.3	Phenol conversion as function of time on stream for different AC particle size . . . . .	170
B.4	Phenol and TOC conversion as function of time on stream for different gas flow rate . . . . .	171
B.5	Time on stream phenol conversion profile for subsequent variation of liquid flow rate (Low to high) . . . . .	172
B.6	Time on stream phenol conversion profile for subsequent change of liquid flow rate (High to Low) . . . . .	173
B.7	Phenol conversion versus time on stream for different reactor bed length	174
B.8	Time on stream phenol conversion profile for subsequent dilution of feed phenol concentration ( $\tau = 0.18$ h) . . . . .	175
B.9	Time on stream phenol conversion profile for subsequent dilution of feed phenol concentration ( $\tau = 0.07$ h) . . . . .	176

B.10	Phenol conversion as function of time on stream for subsequent variation of oxygen partial pressure . . . . .	177
B.11	Phenol conversion as function of time on stream for subsequent variation of reactor inlet temperature ( $\tau = 0.12$ h) . . . . .	178
B.12	Phenol conversion as function of time on stream for subsequent variation of reactor inlet temperature ( $\tau = 0.18$ h) . . . . .	179
B.13	Phenol conversion versus time on stream for different for different concentration of radical scavengers . . . . .	180
B.14	Evolution of phenol conversion and effluent pH with time on stream during CWAO over AC . . . . .	181
C.1	Trickle column axial temperature profile for different liquid and gas flow rates: $P_T = 9$ bar, Glass bead packing . . . . .	184
C.2	Trickle column axial temperature profile for different liquid and gas flow rates: $P_T = 12$ bar, Glass bead packing . . . . .	185
C.3	Trickle column axial temperature profile for different liquid and gas flow rates: $P_T = 15$ bar, Glass bead packing . . . . .	186
C.4	Trickle column axial temperature profile for different liquid and gas flow rates: $P_T = 20$ bar, Glass bead packing . . . . .	187
C.5	Trickle column axial temperature profile for different liquid and gas flow rates: $P_T = 25$ bar, Glass bead packing . . . . .	188
C.6	Trickle column axial temperature profile for different liquid and gas flow rates: $P_T = 9$ bar, AC packing . . . . .	189
C.7	Trickle column axial temperature profile for different liquid and gas flow rates: $P_T = 12$ bar, AC packing . . . . .	190
C.8	Trickle column axial temperature profile for different liquid and gas flow rates: $P_T = 20$ bar, AC packing . . . . .	191
C.9	Trickle column axial temperature profile for different liquid and gas flow rates: $P_T = 25$ bar, AC packing . . . . .	192
C.10	Axial temperature gradient as function of liquid flow rate for different system pressure and gas flow rates . . . . .	193
C.11	Axial temperature gradient as function of gas flow rate for different system pressure and liquid flow rates . . . . .	194
C.12	Dynamic temperature profile in trickle column for different system pressure and gas flow rates . . . . .	195
C.13	Dynamic temperature profile in trickle column for different system pressure and liquid flow rates . . . . .	196

---

D.1	Dynamic phenol conversion and temperature profile as function of time for different split and cycle period of 1 h . . . . .	198
D.2	Dynamic phenol conversion and temperature profile as function of time for different split and cycle period of 1.8 h . . . . .	199
D.3	Dynamic phenol conversion and temperature profile as function of time for different split and cycle period of 4h . . . . .	200
D.4	Cycle phenol conversion and temperature profile as function of time for long run dynamic experiments at different time on stream and period 0.5 h . . . . .	201
D.5	Cycle phenol conversion and temperature profile as function of time for long run dynamic experiments at different time on stream and period 1 h . . . . .	202
D.6	Cycle phenol conversion and temperature profile as function of time for long run dynamic experiments at different time on stream and period 1.8 h . . . . .	203
D.7	Mean cycle phenol conversion and temperature profile as function of time on stream for long run dynamic experiments: $p = 0.5$ h, $s = 0.8$ ,	204
D.8	Mean phenol conversion and temperature profile time on stream for long run dynamic experiments: $p = 1.8$ h, $s = 0.8$ . . . . .	205
D.9	Cycle phenol conversion and temperature profile as function of time for long run dynamic experiments at different time on stream : $p = 1$ h, $s = 0.8$ . . . . .	206
D.10	Cycle phenol conversion and temperature profile as function of time for long run dynamic experiments at different time on stream : $p = 1$ h, $s = 0.9$ . . . . .	207
D.11	Cycle phenol conversion and temperature profile with time at different time on stream for long run dynamic experiments: $p = 0.2$ h, $s = 0.5$	209
D.12	Cycle phenol conversion and temperature profile with time at different time on stream for long run dynamic experiments: $p = 1$ h, $s = 0.8$ .	210



## List of Tables

1.1	Chemical and physical properties of phenol [1]. . . . .	5
1.2	Annual release in 2009 of phenol and substituted-phenol in the United States of America . . . . .	6
1.3	Process conditions and performance of phenolic wastewater remediation. . . . .	8
2.1	Industrial catalytic and noncatalytic wet air oxidation processes. . . .	14
2.2	CWAO operating conditions using copper and mixed oxide catalysts. . . .	15
2.3	CWAO operating conditions using precious metal catalysts. . . . .	17
2.4	Reactions catalyzed by carbon and the type of surface chemistry or the nature of active site required . . . . .	18
2.5	CWAO studies of phenol and phenolic compounds over AC catalyst . . . .	25
2.6	Stability of AC in CWAO. . . . .	29
2.7	Review of studies dealing with periodically operated TBRs. . . . .	49
4.1	Physical properties of AC as provided by Merk. . . . .	60
4.2	Experimental conditions used and fixed bed reactor dimensions. . . .	62
4.3	Buffers used for pH variation in CWAO. . . . .	65
4.4	Operating conditions used for heat transfer and temperature feed modulation. . . . .	68
4.5	Characteristics of insulating systems used for heat transfer study. . .	68
4.6	Operating conditions used for liquid flow modulation. . . . .	71
6.1	Characteristics of fresh and ACs spent in CWAO . . . . .	89
6.2	Phenol conversion obtained after 20 h and 80 h of operation . . . . .	96
7.1	Phenol conversion and AC weight difference measured after ca.150 h TOS under feed temperature modulation . . . . .	135
7.2	Phenol conversion, AC weight and $S_{BET}$ measured after ca. 150 h of liquid flow modulation . . . . .	140

A.1	Thermo-physical properties of aqueous phenol solution . . . . .	163
A.2	Mineral content of fresh and CWAO spent AC . . . . .	163
A.3	List of operating conditions and main results for steady state CWAO of phenol over AC in TBR . . . . .	164

# Nomenclature

## Symbols and Abbreviations

$a_i$	interfacial area ( $\text{m}^3/\text{m}^2$ )
$c_p$	specific heat ( $\text{kJ}/\text{mol K}$ )
$D^{\text{eff}}$	effective diffusibility ( $\text{m}^2/\text{s}$ )
DI	internal diameter of reactor (m)
$d_p$	particle diameter (m)
F	flow rate ( $\text{m}^3/\text{s}$ )
Gr	Grashof number
$H_R$	height of reactor (m)
h	heat transfer coefficient ( $\text{W}/\text{m}^2\text{K}$ )
H	Henry constant ( $\text{Nm}/\text{kmol}$ )
k	thermal conductivity ( $\text{W}/\text{m K}$ )
L	length (m)
m	mass flow rate ( $\text{kg}/\text{s}$ )
Nu	Nusselt number
p	period (h)
P	pressure (MPa or bar)
Pe	Peclet number
Pr	Prandtl number
R	column radius (m)
$r_j$	species reaction rate ( $\text{mol}/\text{kg s}$ )
Ra	Rayleigh number
Re	Reynolds number ( $\frac{\rho u d_p}{\mu}$ )
Re'	Reynolds number ( $\frac{\rho u d_p}{\mu \epsilon}$ )
s	split
$S_{\text{BET}}$	BET surface area ( $\text{m}^2/\text{g}$ )
t	time (h)

T	temperature (°C)
u	superficial velocity (m/s)
U	overall heat transfer coefficient (W/m <sup>2</sup> K)
X	conversion
z	axial bed position (m)

### Greek Letters

$\Delta H^V$	evaporation enthalpy (kJ/mol)
$\alpha$	molar flow rate (mol/h)
$\beta$	Coefficient of thermal expansion
$\epsilon$	phase hold-up
$\epsilon_p$	particle voidage
$\epsilon_B$	bed voidage
$\gamma$	thermal conductivity of bed (W/m K)
$\eta$	wetting efficiency
$\rho$	density (g/m)
$\mu$	dynamic viscosity (g/m <sup>3</sup> s)
$\tau$	space time (h)

### Superscripts and Subscripts

0	inlet or initial
1	inner column radius
2	outer column radius
br	breakthrough
B	bed
ext	external
G	gas
IN	insulation
in	inlet
L	liquid
NAT	natural convection
N <sub>2</sub>	nitrogen
O <sub>2</sub>	oxygen
obs	observed reaction rate
out	outlet
Ph	phenol

sat	saturation
s	solid
T	total
v	vapor
w	water
W	wall

### Abbreviations

AC	Activated Carbon
AOP	Advanced Oxidation Process
CSTR	Continuous Stirred Tank Reactor
CWAO	Catalytic Wet Air Oxidation
HPLC	High Pressure Liquid Chromotography
diff	difference
GB	Glass bead
LFM	Liquid Flow Modulation
SWAO	Supercritical wet air oxidation
TBR	Trickle Bed Reactor
TFM	Temperature Feed Modulation
TGA	ThermoGravimetric Analysis
TOC	Total Organic Carbon
TOS	Time on Stream
TPD	Temperature programmed desorption
UFBR	Upflow Fixed Bed Reactor
WAO	Wet Air Oxidation
WWTPs	Wastewater treatment plants

# Part I

## Literature Review

UNIVERSITAT ROVIRA I VIRGLI

CATALYTIC WET AIR OXIDATION OF PHENOL OVER ACTIVE CARBON IN FIXED BED REACTOR: STEADY STATE  
AND PERIODIC OPERATION

Nigus Gabbiye Habtu

ISBN:/DL:T.1262-2011

# Chapter 1

## Introduction

### 1.1 Global water distribution and abstraction

Water is the most abundant substance that exists on our planet covering ca. 70 % of its total surface. Of the total amount of the earth's water, 97% is contained in the ocean as salt water and only the remaining 3% is fresh water. Moreover, only 0.3% of the latter is easy available as surface water in lakes (87%), rivers and soil (13%), the remaining 99.7% belongs to the glaciers, icecap and groundwater, respectively. This data is quite demonstrative of that the amount of fresh water accessible for human activity is very scarce.

The distribution and abstraction of the available surface water for human activities is strongly dependent on geographical location, hence varies from region to region. According to the United Nation World Water Development (UNWWD) 2009 report [3], arid and semi-arid regions abstract high amounts of water for irrigation purpose. In contrast, industries are the major water users in Europe and North America. Figure 1.1 displays the trend of water demand predicted for each human activity. Thus, the total water demand increases rapidly for the coming 60 years being the higher abstraction due to agricultural activities (70%). The increase is due to the fact that the world population is increasing at an alarming rate of 80 million people per year requiring about 64 billion cubic meters of extra fresh water (UNWWD 2009 report) [3]. This data clearly underlines that the available fresh water resources need protection against contamination to guaranty sustainable supply of fresh water for the future generations.

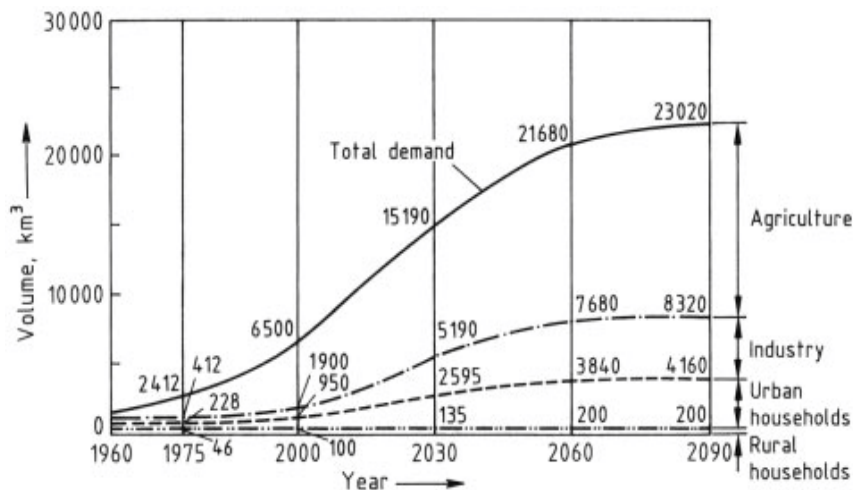


Figure 1.1: Projection of the increasing worldwide demand for water [2]

## 1.2 Water pollution

During the extensive exploitation of the available fresh water resources by human activities, water pollution arises from so-called point or non-point sources. Point sources of water pollution occur when hazardous or toxic substances are discharged directly into the water body at a single point of discharge. Most industrial effluents are considered as a point source of water pollution. A non-point source on the other hand, arises from a wide range of unspecified area, which causes water pollution difficult to control. For example, fertilizes and pesticides washed out from agricultural fields by rain fall are considered as a non-point sources of water pollution.

Wastewater coming from a point source can be classified into four broad categories, according to its origin: domestic, industrial, public and service system loss [4]. Of the total volume discharged, industrial wastewater and domestic wastewater take the highest fraction, accounting for 42.4 and 36.4% respectively. All this polluted water, irrespective of its source has a heterogeneous compositions, which however can be characterized by the following main groups:

- Suspended solids,
- Dissolved inorganic compounds and heavy metals,
- Biodegradable organics and nutrients,

- Non-biodegradable organics and pathogens.

In particular, wastewater with high organic loads (degradable and non-degradable bio-toxic organics) and/or inorganic hazardous compounds resulting from numerous industrial activities has become a worldwide concern for conventional wastewater treatment facilities. Within this context, the importance of refractory and bio-toxic aromatics compounds such as phenol and substituted phenols has to be highlighted. This pollutant family will therefore be discussed more in detail in the following paragraph.

Phenol was discovered in 1834 by the German chemist Runge, who isolated it from coal tar for the first time. It is an aromatic hydroscopic white crystalline compound at ambient conditions. Phenol is soluble in ethyl alcohol, in ether and in several polar solvents, as well as in hydrocarbons such as benzene. It weakly solubise in water and behaves as a week acid in aqueous solution. Some of its chemical and physical properties are listed in Table 1.1.

Today, phenol is produced at a rate of about 6 million T/y worldwide, with a significant increasing trend in the near future [5]. It is a common raw material for the production of a wide variety of organic compounds for instance, dies, pharmaceuticals, antioxidants, resins etc. Since phenols are mainly of coal tar origin, they

Table 1.1: Chemical and physical properties of phenol [1].

Formula	$C_6H_5OH$
$M_W$ (g/mol)	94.11
$T_m$ (°C)	40.9
$T_b$ (°C)	181.75
water solubility	9.3 g <sub>Phenol</sub> /100 ml <sub>H2O</sub>
pKa	9.89
Flammability limits	1.7 (lower)
in air (vol%)	8.6 (higher)
Flash point (°C)	79 (closed cup)
Autoignition (°C)	715

are also present in the effluent of refinery (6-500 mg/L), coking operations (28-3900 mg/L), coal processing (9-6800 mg/L), and manufacture of petrochemicals (2.8-1220 mg/L) [1]. Accordingly, high volumes of wastewater containing these compounds are discharged to the environment each year (see Table 1.2).

The problem of phenols and substituted phenols for water pollution abatement

Table 1.2: Annual release in 2009 of phenol and substituted-phenol in the United States of America [6].

Compound	Emission (T/y)
Phenol	2870
Aniline	490
Hydroquinone	212.7
Pentachlorophenol	66.5
Chlorophenol	31
2,4-Dinitrophenol	28.3
O-cresol	16.4
Catechol	8.3
2-Nitrophenol	6.6
4-Nitrophenol	0.07
Quinone	0.07

stems from the extreme toxicity even at trace level to the aquatic life and their resulting resistance to biodegradation [7]. Phenol is thus considered as a priority substance (EC 1179/94, OJ L131, 26.5.94, p.3.) under regulation 793/93 according to the European environmental agency (EEA)[8]. Despite the legislation restrictions (Threshold limit, 0.02 T/y), high amount of phenolic compounds are still discharged into the environment. For example, ca. 900 T of phenol are directly and/or indirectly discharge per year to the water body in Europe (PRTR 2008 report [8]). Similarly, as shown in Table 1.2, ca. 4000 T of phenol and substituted phenols are directly discharged to the environment in United States [6].

### 1.3 Wastewater treatment

Adequate in-situ management and/or treatment and reuse of (all types of) treated wastewater could be a mayor contribution for reducing the increasing stress on the available fresh water resources. Accordingly, wastewater containing organic compounds such as phenol and its derivatives should be prevented preferentially at the origin from being discharged to the environment. Also, as most of the pollutants emission, do not respect national boundaries, a global effort to monitor their transportation is necessary.

A review of the available treatments of phenolic pollutants contained in wastewater are summarized in Table 1.3. Up to date, the most common abatement technology for organic pollutant is the conventional biological treatment. Nevertheless,

it is an extremely slow process and produces large volumes of sewage sludge that have to be disposed off by land fill or incineration, the latter being a costly process [9, 10]. Moreover, it may be unsuitable for wastewater that is too concentrated, toxic or refractory to microbial actions. In general, organic wastes like phenol and its derivatives with concentrations exceeding 0.5 g/L should not be treated in a biological wastewater treatment plant, even though acclimatised cultivates in laboratory tests have performed depollution of up to 2 g/L of phenol solutions [11]. Another well-known non-reactive wastewater treatment is active carbon adsorption [1]. Active carbon can effectively remove a wide range of organic pollutants from wastewater streams by physical adsorption. However, it only concentrates the waste requiring a posterior treatment of the carbon in order to regenerate it and/or safely dispose off it. Therefore, industrial wastewater containing bio-toxic organic compounds must be pre-treated by oxidative destruction techniques with acceptable energy requirements.

Several oxidative techniques such as incineration, catalytic and non-catalytic wet air oxidation (WAO), supercritical wet air oxidation (SWAO) and more recently advanced oxidation (AOP) have been considered as efficient treatment techniques for refractory industrial wastewater. Among them, the incineration of toxic organic wastes is well established. It can destroy the pollutant completely though at high-energy demand [9, 12] due to application of excessive temperatures (1000 to 1700 °C). In addition, in case of chlorinated compounds, even more toxic chemicals than the parent pollutant, such as dioxins and furans can be formed in the cooling section after the combustion.

Advanced oxidation processes (AOP), which use strong oxidants,  $O_3$  or  $H_2O_2$ , in combination with UV is an emerging oxidative treatment at ambient conditions [13, 14]. This process is mainly based on the presence of highly reactive radicals species such as OH radical, which can oxidize a wide range of organic pollutants due to its high oxidation potential, 2.8 V compared to  $O_3$  (2.07 V),  $H_2O_2$  (1.77 V) and  $Cl_2$  (1.36 V). Fenton's reaction is amongst a simplest AOP process, which has been used easily and effectively in wastewater treatment facilities. Nevertheless, the efficiency of AOP is restricted by several disadvantages: only treatment of low pollutant concentration, use of expensive oxidants and energy source for UV assisted AOP and need separation of iron after the reaction for Fenton's process.

Wet Air Oxidation (WAO) is today the most utilized oxidative technique to treat sewage sludge and a variety of medium to high concentrated industrial effluents [9, 15]. WAO oxidizes aqueous organic pollutants in the presence of a gaseous source of oxidants usually air at high temperature (125-320°C) and high pressure up to 200 bar to keep the reaction medium in the liquid phase with high reaction rates.

Table 1.3: Process conditions and performance of phenolic wastewater remediation.

Process	Conditions	Efficiency	Reactor	Process limitation
Distillation	95-180 °C 1 bar	100 %	Distillation column	<ul style="list-style-type: none"> <li>• Costly to recover phenol by distillation</li> </ul>
Extraction	120-150 °C 60-180 1 bar		Washing-Distillation	<ul style="list-style-type: none"> <li>• Commercial recovery of phenol is costly (equilibrium limitation)</li> <li>• High energy demanding</li> </ul>
Adsorption	20-50 °C 1 bar	100%	Fixed bed	<ul style="list-style-type: none"> <li>• Needs AC regeneration</li> <li>• Posterior treatment cost</li> </ul>
Biological treatment	20-50 °C 1 bar	100%	Bio reactor	<ul style="list-style-type: none"> <li>• Limited to very low pollutant concentration</li> <li>• Slow process, produce large volume of sewage sludge</li> <li>• Unsuitable for toxic and concentrated organic wastes.</li> </ul>
Incineration	1000-1700 °C 1 bar	>99%	Incinerator	<ul style="list-style-type: none"> <li>• Practically feasible if COD &gt; 300g/L)</li> <li>• Needs external fuel source for dilute wastes</li> <li>• Generate more toxic chemicals</li> </ul>
SWAO	> 400 °C >250 bar	>99.99%	Tubular	<ul style="list-style-type: none"> <li>• Corrosion problem due to salt precipitation.</li> <li>• High energy demand</li> </ul>
WAO	130 - 427 °C 200 bar	80 - 99%	Bubble column	<ul style="list-style-type: none"> <li>• Effective for COD range 20-200ppm</li> <li>• High energy demand</li> <li>• Inefficient for lower acids</li> </ul>
CWAO	120-250 °C 5-50 bar	75-99 %	Fixed bed	<ul style="list-style-type: none"> <li>• COD&gt;10 ppm</li> <li>• Need expensive catalyst</li> <li>• Catalyst stability problem</li> </ul>
AOP (O <sub>3</sub> , H <sub>2</sub> O <sub>2</sub> )	Ambient conditions	up to 100%		<ul style="list-style-type: none"> <li>• Use expensive chemicals such as H<sub>2</sub>O<sub>2</sub>, O<sub>3</sub></li> <li>• Needs posterior Separation of Fe from the effluent.</li> <li>• Low degree of mineralization.</li> </ul>

Since it does not use any chemical agent except for air, the process is extremely clean. As shown in Table 1.3, conversion of pollutant attains 80 to 99 % and COD reduction between 75 to 90%. Nevertheless, it may be prohibitively expensive when used to completely mineralized the parent organics [16] demanding special alloys that can resist corrosion at this severe conditions. For example, removal of acetic acid by WAO is negligible at temperatures less than 300 °C [9, 17]. Accordingly, WAO is mostly used as a pretreatment step for organic wastes, which then requires a posterior treatment process, e. g. biological treatment for final clean-up. Supercritical wet air oxidation (SWAO) exhibits a complete removal of organics from wastewater, typically up to 99.99% conversion of pollutants [18]. Similarly, this process demands a high-energy input due to the involvement of temperatures and pressures even higher than WAO, above the critical point of water (374.2 °C and 22.1 MPa). Its operating costs are 2-4 times higher than for the conventional WAO process [12, 19].

In 1992, Levec et al [20] demonstrated that the severity and efficiency of WAO can be significantly improved by the use of a catalyst. Since then, several homogeneous catalysts such as copper and iron salts and mixed oxides like Co/ Bi in solution were tested in oxidizing several organic compounds in the presence of air as oxidant [21, 22]. However, the inherent problem associated with the recovery of homogeneous catalysts from the effluent prevented a broad use at industrial scale. Moreover, their presence in the effluent in the range of concentration used is prohibited by environmental regulations. To overcome the problems associated with homogeneous catalysts, the application of heterogeneous catalysts has become attractive in the field of CWAO. Heterogeneous supported catalysts, mostly noble metals (Pt, Pd, Ru) and metals oxides have been tested in combination with all types of oxidants in removing organic wastes [21, 23–28]. Metal oxides show good activity but have series problem of leaching at typical conditions of CWAO resulting in a too short life-time for practical applications. On the other hand, noble metals exhibit excellent activity and are less susceptible for leaching, but their high costs limit their applicability at industrial scale for non-profit technologies such as wastewater treatment. Only, more recently, the potential of active carbon as a direct heterogeneous catalyst has become a focus of investigation. The most remarkable characteristics of ACs are their high surface area, the presence of oxygen surface groups and therefore a high metal dispersion capability [29, 30]. These studies have shown that a performance comparable to that of metal based catalysts can be achieved with AC catalysts [31, 32].

Concluding, the incorporation of heterogeneous catalysts allows softening the operating conditions of CWAO to < 3 MPa and < 200 °C. Under these conditions,



Based on these literature results, the use of activated carbon in CWAO or combined processes for organic wastewater treatment appears to be of interest. The following chapter 2 is therefore dedicated to review the state of art of CWAO of organic pollutants over heterogeneous catalysts, in particular over active carbon catalysts.



## Chapter 2

# Catalytic Wet Air Oxidation

The development of commercialized Catalytic Wet Air Oxidation (CWAO) started as early as the mid-fifties in the United States of America [40]. Since then, several industrial CWAO processes were developed based on both heterogeneous and homogeneous catalysts. Their respective operating conditions are summarized in Table 2.1. It is seen that several Japanese companies applied heterogeneous CWAO catalysts using precious metals deposited on titania or titania-zirconia oxides. In Europe, several CWAO processes relying on homogeneous catalysts (Ciba-Geigy, LOPROX, WPO, ORCAN and ATHOS) have been developed since 1990 [17].

In CWAO, the dissolved organic matter is also oxidized in the liquid phase in the presence of a gaseous source of oxygen or air but with an active catalyst at lower pressure and temperature compared to WAO. The operating pressure, however, has to be maintained well above the saturation pressure of water at the reaction temperatures (usually between 15-60 bar) so that the reaction takes place in the liquid phase. CWAO is more efficient than conventional WAO due to the reduced energy demand and faster oxidation rates achieved by the catalyst. Nevertheless, the reaction conditions of industrial CWAO processes as shown in Table 2.1 are still severe. Levec and Pintar et al [17] concluded that less expensive and more active materials are needed to make CWAO more competitive for industrial applications.

Table 2.1: Industrial catalytic and noncatalytic wet air oxidation processes.

Process	Waste type	Plants	Reactor type	T(°C)	P(MPa)	Catalyst
Zimpro	Sewage sludge	200	Bubble column	280-325	20	None
	Spent AC	20				
	Industrial	50				
Vertech	Sewage sludge	1	Deep shaft	< 280	<11	None
Wetox	-	-	Stirred tank	200-250	4	None
Kenox	-	-	Recirculation	<240	4.5	none
Oxyget	-	-	tubular jet	< 300	-	none
Ciba-Geigy	Industrial	3	-	300	-	Cu <sup>2+</sup>
LOPROX1	Industrial	>1	Bubble column	<200	5-20	Fe <sup>2+</sup>
NS-LC	-	-	Monolith	220	4	Pt-pd/ TiO <sub>2</sub> -ZrO <sub>2</sub>
Osaka	Coal gasifier	-	Slurry bubble	250	7	TiO <sub>2</sub> orZrO <sub>2</sub>
Gas	Coke oven		Column			with noble base metals
	Cyanide					
Kurita	Sewage sludge					supported Pt
	Ammonia	-	-	>100	-	

## 2.1 CWAO Catalysts

Among homogeneous and heterogeneous CWAO catalysts, the latter catalysts proved to be more promising because they do not need a posterior separation step. The catalytic activity of noble metals, metal oxides and their combination has thus been studied extensively using mostly phenol as model compound [12]. Contrary, the catalytic activity of active carbon (AC) or Fe/AC has become a focus of research only in the last decade [32].

### 2.1.1 Noble metal and metal oxide supported catalysts

**Metal oxides:** Unsupported and supported heterogeneous copper catalysts in the form of CuO and copper salts, or in combination with oxides of Co, Mo, Mn, Ni, Fe, Cr, Zn have been tested for CWAO of phenol [12, 23, 24, 41–47]. Some metal oxide catalyst employed in CWAO with their operating condition are summarizes in Table 2.2. It was found that Cu based catalysts were amongst the most active heterogeneous catalysts [12]. In general, the catalytic activity of metal oxides in phenol degradation was reported [12] in the following order :  $a_{CuO} > a_{CoO} > a_{Cr_2O}$

$a_{NiO} > a_{MnO_2} > a_{Fe_2O_3} > a_{YO_2} > a_{Cd_2O_3} > a_{ZnO} > a_{TiO_2} > a_{Bi_2O_2}$ . Up to 100% of phenol conversion and 75-90% mineralization to  $CO_2$  and  $H_2O$  was achieved using those catalysts.

Metal based oxides (Cu/Mn, Cu/Co, Cu/Co/Bi, and Cu/Bi/  $\gamma$ - $Al_2O_3$ ) in combination with CuO exhibited also relatively high activity towards phenol oxidation [21, 44]. It was found that CuO-MnO was the most active species from all combinations of CuO with oxides of Co, Mn, Fe or Zn [31]. Manganese oxide, ceria-oxides and promoted ceria catalyst developed for oxidation of ammonia-containing solutions have also proven very high activity for oxidation of various organic pollutants [21]. In general, those oxides containing metals with basic active site such as Bi, Co, Mn in combination with CuO show higher activities for destruction of phenolic wastes.

Nevertheless, base metal and transition metal catalysts are prone to deactivation due to leaching of the active phase [31, 55] and deposition of carbonaceous products [56] at typical conditions of CWAO. For example, Pintar and Levec et al [57] preformed CWAO of nitrophenol and chlorophenol over a catalyst containing CuO, ZnO and CoO in a liquid filled fixed bed reactor and detected corresponding

Table 2.2: CWAO operating conditions using copper and mixed oxide catalysts.

Catalyst	Support	T (°C)	$P_{O_2}$ (MPa)	$X_{Ph, max}$ (%)	Ref.
CeO <sub>2</sub> -TiO <sub>2</sub>	-	140	0.6	77 *	[23]
Fe	AC	100-130	0.8	70	[42]
CoO, Fe <sub>2</sub> O <sub>3</sub> , MnO or ZnO (10% CuO)	$\gamma$ - $Al_2O_3$	140	0.9	80-99	[48]
Mn, Fe, Co- CeO <sub>2</sub>	Ce <sub>0.65</sub> - $\gamma$ - $Al_2O_3$	150	0.424	>80	[44]
	SiO <sub>2</sub> TiO <sub>2</sub>	180	1.5	100	[26]
CuO	$\gamma$ - $Al_2O_3$	140	0.9	78	[31]
Ni and Cu	Zr <sub>0.35</sub> O <sub>2</sub>	110	0.5	94 *	[45]
Mn-Ce-O composites					
CuO, CuO-ZnO	$\gamma$ - $Al_2O_3$	110 - 145	0.1 -0.65	100	[49]
Cu-Chromate					
CuO	$\gamma$ - $Al_2O_3$	140	0.9	80	[50]
Cu	AC	140-160	0.46-1.6	80	[51]
CuO-ZnO	$\gamma$ - $Al_2O_3$	100-130	0.46-1.3	50	[52]
CuCe <sub>x</sub>	-	150	0.7	>95	[53]
Cu(II)	Chitosan	30 °C	0.21	60	[54]

\* TOC conversion.

metals ions in the final effluent. Fenoglio et al [58] and Massa et al [59], have observed leaching of copper ions during oxidation of phenol in trickle bed reactor over  $\text{CuO}/\gamma\text{-Al}_2\text{O}_3$  catalyst. Kim and Ihm [56] found carbonaceous deposits on the used transition metal catalyst during CWAO of phenol.

**Noble metal:** Some noble metal based catalyst employed in CWAO with their operating conditions are summarized in Table 2.3. Noble metal catalysts usually exhibited higher activities than copper or other base metal catalysts for the oxidation of organic pollutants such as phenols [30, 60–63], lower molecular weight carboxylic acids, including refractory acetic acid [62, 64], ammonia [30] and Kraft effluents [65]. They are mostly deposited in small quantities ranging from 0.1-5% on  $\gamma\text{-Al}_2\text{O}_3$ ,  $\text{SiO}_2$ ,  $\text{CeO}_2$ ,  $\text{TiO}_2$ ,  $\text{ZrO}_2$ , cement and active carbon supports. Their activity was tested using air as oxidant in the temperature range of 80-200 °C and oxygen partial pressures of 0.1-2 MPa. Under these conditions, up to 100% phenol conversion and 85-98% TOC and COD reduction was achieved. Mineralization of phenol to  $\text{CO}_2$  and  $\text{H}_2\text{O}$  was usually higher than that of metal oxide catalysts. This is due to their high reactivity for lower molecular refractory acids than metal oxide catalysts.

The activity of noble metal catalysts are also highly influenced by the nature and type of the supports used. Cao et al [30] studied the effect of three supporting materials on the performance of Pt catalyst for the oxidation of ammonia and phenol. The authors demonstrate that AC supported Pt catalysts outperform  $\text{TiO}_2$  and  $\gamma\text{-Al}_2\text{O}_3$  supported Pt catalysts. This was mainly attributed to the good metal dispersion and particle distribution capability of AC. Similarly, Castillejos-Lopez et al [73] studied the effect of three supporting materials on the performance of Ru catalysts for the oxidation of aniline and phenol. The authors demonstrated that AC supported Ru catalysts outperform  $\text{ZrO}_2$  and graphite supported Ru catalysts. Overall, considerable improvement has been achieved in the last decades in synthesizing a stable support and thus highly active noble metal catalyst for CWAO of phenol. Nevertheless, these catalysts are: 1) relatively expensive for non-profitable industrial applications as it is CWAO process, and 2) prone to deactivation due to fouling of carbonaceous deposits [66, 70, 75] coming from undesired polymerized side reactions and over oxidation of the support [74].

### 2.1.2 Activated carbon catalyst

Activated Carbon (AC) is a cheap material that can be derived from any renewable carbonaceous sources by high temperature pyrolysis and posterior physical or chemical activation. Depending on the preparation and activation conditions em-

Table 2.3: CWAO operating conditions using precious metal catalysts.

Catalyst	Support	T (°C)	P <sub>O<sub>2</sub></sub> (MPa)	X <sub>Ph, max</sub> (%)	Ref.
Pt, Ru	AC, $\gamma - Al_2O_3$	200	0.42	≈100	[30]
Pt	Graphite	120-180	0.01-08	>99	[60, 61]
RuO <sub>2</sub> -CeO <sub>2</sub>	$\gamma - Al_2O_3$	150	3	98	[63]
Pt, Pd, Ru	CeO <sub>2</sub>	170	2	≈100 *	[64]
Pt	CeO <sub>2</sub> , CexZr <sub>1-x</sub> O <sub>2</sub>	160	2	≈100	[66]
Pt	$\gamma - Al_2O_3$	175	0.5 -1.5	>99	[67]
Pt	4 · 5 % Ti <sub>2</sub> O <sub>3</sub>	150-200	3.4-8.2	≈100	[68]
Ru	AC	160	2	>99	[69]
Ru-CeO <sub>2</sub>					
Pt, Pd, Ru	CBS	120-160	0.96-1.5	>99	[27]
Pt, Ru	CeO <sub>2</sub> /Zr <sub>0.1</sub>				
	Ce <sub>0.75</sub> Pr <sub>0.250</sub> · 9 O <sub>2</sub>	160	02	>99	[70]
Ru	CeO <sub>2</sub> Al <sub>2</sub> O <sub>3</sub>	140	0.7	30	[71]
Ru	TiO <sub>2</sub>	250	0-10	≈100	[72]
Ru	ZrO <sub>2</sub> , AC	350	0.2	≈100	[73]
Ru	TiO <sub>2</sub> or ZrO <sub>2</sub>	140	6.5	93	[74]

\* COD conversion.

ployed, it can have a specific surface area ranging from 100 to 2500 m<sup>2</sup>/g and a pore size distribution including micro (<2 nm), meso (>2-50 nm) and macro (> 50 nm) pores. These textural properties together with its surface groups (surface chemistry) allow tailoring AC for specific applications as adsorbent, catalyst support or direct catalyst.

The most frequent utilization of AC is certainly as adsorbant in numerous physical separation processes including drinking water purification and wastewater treatment. As a catalyst, AC is used in the industrial production of phosgene and for the oxidation of harmful gases such as SO<sub>2</sub>, NO and H<sub>2</sub>S in air pollution control [32]. Given its excellent metal dispersion capability and chemical stability in both acidic and basic reaction media, it has been widely used as support material for noble metal catalysts in the oxidation of phenol and substituted phenols [30, 42, 51, 69, 76–80], carboxylic acids [64, 65] and ammonia [62].

It is already known since the seventies that carbon on itself has a high catalytic potential for different reactions such as oxidation, dehydrogenation, chlorination and dechlorination [81–83]. Table 2.4 provides a list of reactions that can be catalyzed

Table 2.4: Reactions that can be catalyzed by carbon and the type of surface chemistry or the nature of active site required [81].

Reactions	Surface chemistry/active sites
Gas phase	
Dehydration of alcohols	Carboxylic acids
Dehydrogenation of alcohols	Lewis acids and basic sites
NO <sub>x</sub> reduction (SCR with NH <sub>3</sub> )	Acidic surface oxides (carboxylic and lactone) basic sites (carbonyls )
Dehydrohalogenation	Pyridinic nitrogen sites
NO oxidation	Basic sites
SO <sub>2</sub> oxidation	Basic sites (pyridinic)
H <sub>2</sub> S oxidation	Basic sites
Oxidative dehydrogenation	Quinones
Liquid phase	
Hydrogen peroxide reactions	Basic sites
Catalytic ozonation	Basic sites
Catalytic wet air oxidation	Basic sites

by carbon catalysts, indicating that for all gas and liquid phase catalytic oxidation reactions, basic surface groups are proposed to be the active sites.

In particular, the ability of active carbon to oxidize diverse organic compounds was reported in the late seventies in studies related to the regeneration of spent activated carbon via WAO [84]. However, only 30 years later, the use of carbon as catalyst for CWAO has been highlighted in the pioneer works of Tukac et al [85, 86] and our research group in Tarragona [31]. Since then, AC has been tested as a direct catalyst for CWAO of organic pollutants (mostly phenols and substituted phenols) [31, 34, 42, 43, 85–102]. Occasionally, complex industrial effluents containing organic wastes were tested using a combination of low temperature, peroxide oxidants (H<sub>2</sub>O<sub>2</sub>) and granular active carbon [92, 103–105]. Excluding the patents and scientific literatures on AC regeneration via WAO, over 50 papers were published during the last 15 years on CWAO using carbon as a direct catalyst and the most important works are summarized in Table 2.5.

### 2.1.2.1 Activity of AC

From Table 2.5 it can be deduced that the activity of AC in CWAO relays on several factors among them the properties of AC (origin, textural properties, surface

chemistry, ash content), the nature of compounds oxidized and the operating conditions employed. Mainly aromatic pollutants including phenols and substituted phenols (m-xylene, o-cresol, 2-chlorophenol, 4-nitrophenol, 4-hydroxybenzoic acid, aniline, salicylic acid and 5-sulfo salicylic acid) [85, 91–93] and textile dyes (orange G, methylene blue and brilliant) [101] were studied as target compounds in CWAO over wood or coal based active carbon catalysts in batch or continuous reactors. The diverse batch and continuous AC catalyzed oxidations yielded almost complete compound conversion and up to 85-90% TOC or COD conversion for most of the compounds but not for all for temperatures ranging from 120 to 200°C, oxygen partial pressures from 0.1 to 1.6 and liquid space time or reaction time of 0.3 or from 3 to 6 h. These studies showed that temperature has a stronger influence on pollutant destruction due to an exponential increase in reaction rate constant ( $k$ ) with temperature, while the effect of oxygen pressure is less pronounced since the order of reaction with respect to oxygen concentration is between 0.5 to 1. Another particularity of AC catalyzed WAO is to provide refractory short chain carboxylic acids (mainly acetic acid), which account for the remaining TOC or COD measured in the liquid exited effluent.

**Origin of carbon:** One important factor determining the activity of carbon catalysts is the origin of the source material, i.e. from what precursor the AC is derived. Fortuny et al. [43] reported a 40, 15 and 8% phenol conversion in a TBR at 140°C and 0.9 MPa of oxygen pressure for wood, mineral and coconut based ACs, respectively. According to the authors, neither the surface area nor the mineral matter of the three carbons can explain the observed results. In that sense, the surface chemistry could play a key role for AC activity. Phenol conversion profiles obtained with ACs from different sources are illustrated in Figure 2.1 [90, 92–95, 106]. As mentioned before, active carbons derived from coal and wood seem to display a higher activity (almost 100% of phenol conversion). Quintanilla et al. [42] incorporated small amounts (2.5 w%) of Fe on AC for the CWAO of phenol at conditions of 127°C and 0.8 MPa of oxygen pressure. The conversion profile assessed for the Fe/AC catalyst is also illustrated in Figure 2.1. Similarly, complete conversions were achieved, however at milder temperature of 127°C. The same authors revealed that Fe/AC improves not only phenol conversion but also the degree of mineralization. Maretva et al [107] also studied CWAO of phenol over AC catalyst by eliminating effects of the textural AC structure and with Fe coating. The authors achieved a remarkable activity improvement (over 70%) at relatively mild operating conditions of 140°C and 2 bar using the Fe/AC catalyst.

Recently, an activity comparable with that of a commercial Chemvviron carbon

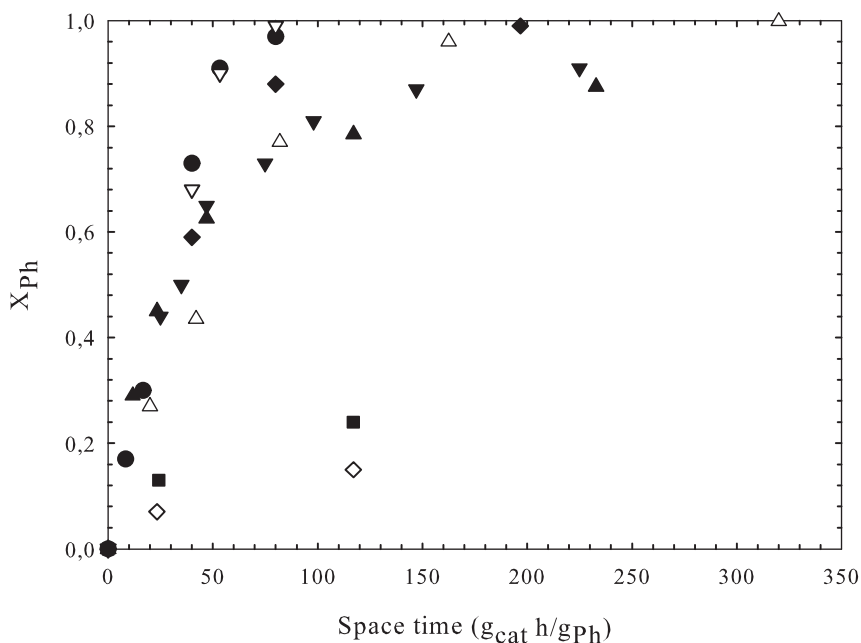


Figure 2.1: Performance of different active carbons: ( $\nabla$ ) Centaur, ( $\bullet$ ) Sonfocarb, ( $\blacklozenge$ ) Industrial React: 160°C, 1.6 MPa [106]; ( $\blacktriangle$ ) Merck (wood): 140°C, 0.2 MPa [92]; ( $\triangle$ ) Fe/AC(wood): 127°C, 0,8 MPa [90]; ( $\blacktriangledown$ ) Chemviron: 165°C, 0.9 MPa [94]; ( $\blacksquare$ ) Mineral, ( $\diamond$ ) Coconut: 0.2 MPa, 140°C [43]).

(AP4-X) has been displayed by diverse sewage sludge based activated carbon catalysts in the CWAO of phenol at 160°C and 4 bar of oxygen pressure (see Table 2.5) [96]. The activity of these sludge based carbons characterized by a high ash content was seen strongly influenced by the origin of the sludge and activation methods employed. Almost complete phenol conversion and high degree of pollutant mineralization ( $X_{\text{TOC}} > 76\%$ ) has been also achieved using multi-wall carbon nanotube with out deposition of any active phase during CWAO [108].

**Nature of compounds:** The activity of AC also depends on the nature of compounds to be oxidized. It is clear that there will exist substituted groups that activate or deactivate the phenol molecule. Suarez-Ojeda et al. [91] and Stüber et al. [92] studied the CWAO of different aromatic compounds over a commercial Merck carbon catalyst for oxygen pressures of 0.2 to 0.9 MPa, 140°C and liquid space time of 0.12 h. The conversion profiles measured for several compounds are

illustrated in Figure 2.2. As expected, the employed AC displays two conversion

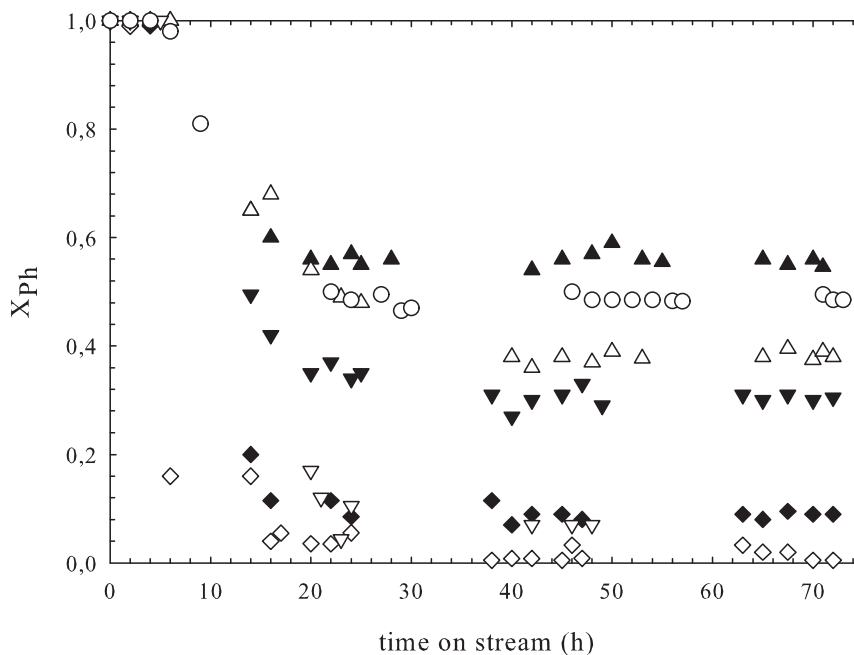


Figure 2.2: CWAO of different compounds over Merck AC in TBR: ( $\blacktriangle$ ) o-chlorophenol, ( $\circ$ ) Phenol, ( $\triangle$ ) o-cresol, ( $\blacktriangledown$ ) DBS, ( $\blacklozenge$ ) Aniline, ( $\diamond$ ) Sulfolane, ( $\nabla$ ) p-nitrophenol (0.9 MPa);  $P_{O_2} = 0.2$  MPa,  $T = 140^\circ\text{C}$ ,  $\tau = 0.12$  h,  $W_{\text{cat}} = 7$  g [91, 92].

zones: acceptable conversion for o-chlorophenol, phenol, o-cresol and DBS and very small conversion for aniline, p-nitrophenol and sulfolane. In general, the authors established the following reactivity order: m-xylene > o-cresol > o-chlorophenol > phenol > aniline  $\approx$  p-nitrophenol > sulfolane  $\approx$  nitrobenzene. A similar reactivity trend has been recently reported by Ayril et al [93] for CWAO of substituted phenols (4-chlorophenol > 4-hydroxybenzoic acid > 4-nitrophenol) in a batch slurry reactor at  $150^\circ\text{C}$  and 0.35 MPa of oxygen pressure for three different active carbons. According to the authors, the carbon with high amounts of basic surface groups displayed the highest activity towards mineralization, but also the strongest deactivation.

**Surface treatment of AC:** Liquid and gas phase treatments of active carbon can also lead to an important change of the carbon activity during CWAO [90, 95]. For

example, Santiago et al [95] tested the TBR activity of the Merck AC modified in the liquid phase with  $\text{HNO}_3$ ,  $(\text{NH}_4)_2\text{S}_2\text{O}_8$  or  $\text{H}_2\text{O}_2$ . Figure 2.3 presents the con-

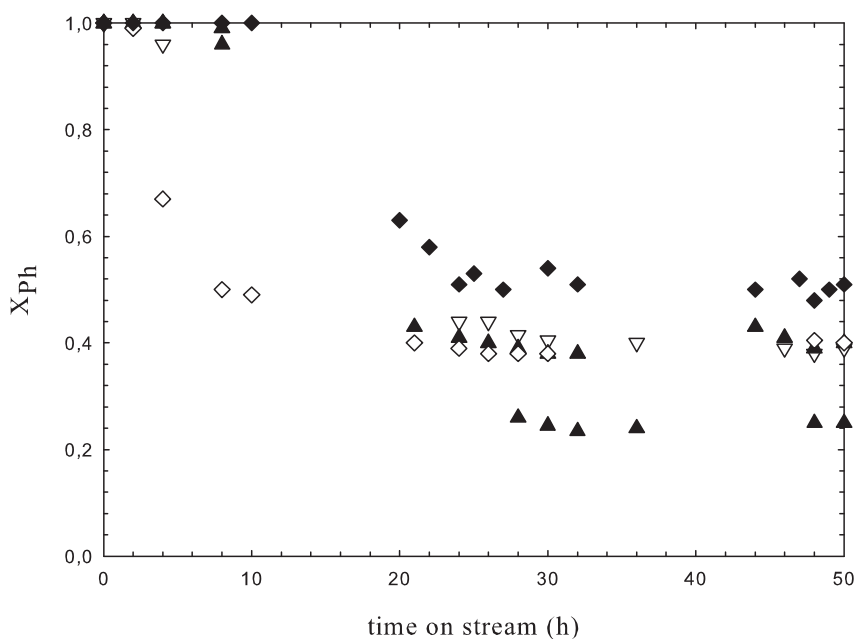


Figure 2.3: Phenol conversion measured during CWAO over parent and modified Merck ACs: (◆) AC, (▲) AC-P, (▽) AC-S, (◇) AC-N, (▼) AC-H;  $P_{\text{O}_2} = 0.2 \text{ MPa}$ ,  $T = 140^\circ\text{C}$ ,  $\tau = 0.12 \text{ h}$ ,  $W_{\text{cat}} = 7 \text{ g}$  [95].

version time profiles obtained in 50 h experiments. It appears from the figure that all liquid phase surface treatments induced a visible decrease of AC activity of 30 to 100% depending on the oxidant used. Boehm titration and ultimate analysis of the parent and modified ACs revealed a substantial reduction of basic oxygenated surface groups and a two fold increase in acidic surface groups being the maximum for  $\text{HNO}_3$  treated AC. These findings suggest that basic surface chemistry of AC can play an important role for the oxidation of phenol. The same authors claimed also that demineralization of AC by  $\text{HCl}$  reduces phenol conversion by a factor of two (see Figure 2.3).  $\text{HCl}$  washing dissolves metals from the ash fraction indicating that the high amount of Fe (0.4-0.6%) contained in the parent Merck AC may contribute significantly to the oxidation of phenol.

On the other hand, Quintanilla et al [90] studied CWAO of phenol in TBR using modified ACs via gas phase ( $\text{O}_2$ ) and liquid phase oxidation treatments ( $\text{HNO}_3$ ).

The authors found the following activity sequence:  $AC(HNO_3) \gg AC(O_2) > AC$  during CWAO of phenol in contrast to what has been observed by Santiago et al [95]. According to the authors, the activity of the catalyst for the oxidation of phenol is enhanced with increasing the initial amount of oxygen surface groups, i.e initial acidity of the carbon. These contradictory results show that the role of surface groups in CWAO is yet not fully understood.

**Comparison of AC with other CWAO catalysts:** Several investigators have demonstrated that AC without incorporation of any active phase can yield a comparable activity with transition metal catalysts such as copper catalyst [32, 43, 67, 106] and noble metal supported catalysts [27, 62, 70] for CWAO of phenol and substituted phenols. Figure 2.4 shows the phenol removal efficiency of some selected supported

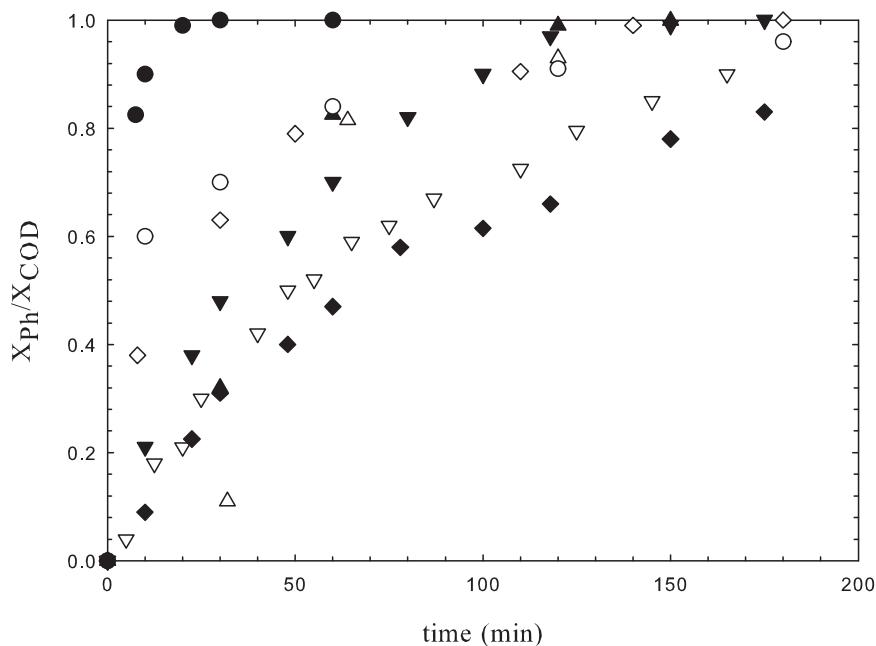


Figure 2.4: Performance of different CWAO catalysts in batch oxidation of 2 to 5 g/L phenol solution: (●) Mn/Ce: 130°C, 0.5 MPa [67]; (○) AC (Merck): 140°C, 0.71 MPa [109]; (▲) CeO<sub>2</sub>-TiO<sub>2</sub>: 150°C, 0.3 MPa, [23]; (△) AC (Chemviron): 160°C, 0.4 MPa [96]; (▼) Ru-Ce/AC, (▽) Ru/CeO<sub>2</sub>, (◆) Ru/AC: 150°C, 0.3 MPa [62]; (◇) Pt/Ce: 160°C, 2 MPa [70].

transition and nobel metal catalysts and ACs during CWAO of phenol in a batch slurry reactor. Mn/Ce (7:3) catalyst displays the highest performance followed by CeO<sub>2</sub>-TiO<sub>2</sub> (1:1). Complete phenol conversion and over 98% COD removal was achieved in 2 h with these catalysts. It appears also from figure 2.4 that the activity of AC falls in the intermediate region showing a comparable performance with nobel metal (Pt, Ru) supported catalyst for the destruction of phenol. Moreover, Santos et al [106] studied CWAO of phenol over three different ACs and found a better degree of mineralization than copper oxide based catalysts [110].

Summarizing, the diverse batch and continuous CWAO studies using virgin and surface modified carbons demonstrated that AC can be an alternative low cost bifunctional catalyst in the field of CWAO. However, up to date no clear correlation of texture, surface chemistry and mineral content of AC with its activity could have been established.

Table 2.5: CWAO studies of phenol and phenolic compounds over AC catalyst

Conditions	Substrate	Carbon	BET (m <sup>2</sup> /g)	Ash (%)	X <sub>Ph</sub> (%)	Comments	Ref.
TBR 140 °C 0.2 - 0.9 MPa $\tau = 0.12$ h 7 g of AC	phenol (5 g/L)	Wood Mineral Coconut	990 960 810	4 15 3	>40 15 8	Stable over 10 days, 140°C and 0.2 MPa, display better catalytic activity than copper based catalysts Activity can be related with Surface groups and surface area	[31] [43]
TBR 127 °C, 0.8 MPa $\tau = 320 \text{ g}_{\text{cat}} \text{ h g}_{\text{Ph}}^{-1}$	phenol (1 g/L)	Fe/AC (Wood)	890	-	> 99.9	Heterogeneous surface mechanism was proposed Insignificant metal leaching High degree of mineralization in the presence of iron	[42]
TBR 120 - 160 °C 0.1 - 0.2 MPa $\tau = 0.125$ h 7 g of AC	m-xylene (0.2 g/L) o.cresol (5 g/L) o-chloro phenol (5 g/L) phenol (5 g/L) aniline (5 g/L) p-nitro- phenol (5 g/L) sulfolane (5 g/L) nitro- benzene (2 g/L)	Wood 1480	990-	3.75	99.8 76 74 71 15 9 5 < 1	Conversions are for 140°C and 0.9 MPa PO <sub>2</sub> , complete conversion at 160°C, mineralization of the pollutant depends on the ring substituted group Nitrogen and sulfurs substituted phenols are very refractor	[92]
TBR 140 °C, 0.2 MPa $\tau = 0.12$ h 7.5 g of AC	phenol (5 g/L) o-cresol (5 g/L) 2-chloro- phenol (5 g/L) aniline (5 g/L) sulfolane (5 g/L) p-nitro- phenol (5 g/L)	Wood	1481	4.5	45 33 55 55 6	Catalyst activity depends on the substitute groups AC appears inefficient, for aniline, sulfolane and p-nitrophenol	[91]
TBR 140-160 °C Continued on Next Page...	phenol (5 g/L)	Wood	990	3.75	45-78	Mineralization depends on ring substitution group	[111]

Table 2.5 – Continued

Conditions	Substrate	Carbon	BET (m <sup>2</sup> /g)	Ash (%)	X <sub>Ph</sub> (%)	Comments	Ref.
0.2 - 0.9 MPa τ = 0.12 h 7 g of AC	o-cresol 5 (g/L) 2-chloro- phenol (5g/L)				58-62 33-83 97-90 55-75 60-80	Strong influence of temperature on activity, while pressure has a mild influence	
TBR 127 °C, 0.8 MPa τ = 320 g <sub>cat</sub> ·hg <sup>-1</sup> ·Ph	phenol (0.4-1 g/L)	AC (Wood) AC-T (>>) AC-N (>>) Fe/AC (>>)	974 990 881 890	4 4 4 4	60 78 95 >99	Total mineralization increases with initial acidity of AC Fe promotes the formation of additional surface oxygenated groups Activity towards carboxylic acids increase in the presence of Fe	[90]
TBR 140 °C 0.2 MPa τ = 0.12 h 7.5 g of AC	phenol (5 g/L)	CI (Wood) CI-N (>>) CI-S (>>) CI-P (>>) CI-H CII (Coconut)	1142 1160 806 1110 1089 602	4.5 1 1.1 1 1 1	50 35 37 37 25 8	Activity depends on mineral content Acid treatment of ACs introduce oxygenated surface groups Significant reduction basic surface groups	[95]
TBR 125-170°C 1-7 MPa (+H <sub>2</sub> O) tau = 0.05-1 h	phenol (all 5 g/L) 2-amino phenol salicylic acid 5-sulfo salicylic acid	Charcoal	1300	-	> 99 > 99 40 40	Activity depend on substituted group Partial wetting improve conversion Periodic operation improve overall performance of the catalyst	[94, 102]
TBR 127 °C, 0.17 MPa τ = 80 g <sub>cat</sub> ·hg <sub>Ph</sub> <sup>-1</sup>	phenol (1 g/L)	Coal	890	-	> 60	High mineralization with Fe/AC catalyst under oxic start up	[97]
UFBR 160 °C, 1.6 MPa Continued on Next Page...	phenol (0.4-1 g/L)	RTA-180 Centaur	1333 913	- -	60 70	Comparable activity with copper and copper oxide base catalysts	[106]

Table 2.5 – Continued

Conditions	Substrate	Carbon	BET (m <sup>2</sup> /g)	Ash (%)	X <sub>Ph</sub> (%)	Comments	Ref.
$\tau = 0.2 - 10.5$ g <sub>cat</sub> ·min·mL <sup>-1</sup>		IndReact	745	-	75	Leaching of active phase is avoided Higher mineralization can be achieved with AC catalyst	
UFBR 160 °C, 1.6 MPa $\tau = 2-3$ g <sub>cat</sub> ·min/mL 3.5 g of AC	phenol (1 g/L)	Coal	745	-	> 71	Stable activity over 200 h operating time Oxygen surface groups increase with course of CWAO reaction	[112]
UFBR 150 - 180 °C 0.718 MPa t <sub>R</sub> = 3.5 - 6.5 h 0.178 g NP/g AC	phenol p-nitro- phenol	Wood	450	-	>90	20-30% loss of initial surface, 80% can be recovered after regeneration (170 °C)	[99]
UFBR 160°C, 0.2 MPa $\tau=1-18$ g. min/mL 3.5 g of AC	orange G methylene blue (1 g/L) Brilliant green (1 g/L)	Coal	745	-	80 100 100	100% mineralization is difficult to achieve Detoxification depend on dyes	[101]
Batch reactor 100 - 160 °C 0.35 - 0.95 MPa t <sub>R</sub> = 0.03-0.3 h 4 g of AC	phenol (0.2 - 7 g/L)	Wood	1000	4	50-90	Deactivation due to totally blockage of the active active site of AC with oxidative coupling products	[109]
Batch Reactor 160 °C, 4.2 MPa 2 g of AC	phenol (5 g/L)	Sewage sludge based  Chemviron (AP4-X )	8.1  1013	26-83  11	28-93  97	Activity correlated with both mineral and surface textural properties, activity improved with chemical activation, high activity with basic carbons	[96]
Batch reactor 150°C, 0.35 MPa t <sub>R</sub> = 6 h 2 g of AC	phenol (1 g/L)	Coconut Wood Coal	1230 1860 985	3 8.3 12 12	100 95 >99	Activity relates to the acid-basic characteristics of the divers carbons, basic carbon shows higher activity	[93]

Continued on Next Page...

Table 2.5 – Continued

Conditions	Substrate	Carbon	BET (m <sup>2</sup> /g)	Ash (%)	X <sub>Ph</sub> (%)	Comments	Ref.
Batch Reactor 150 °C, 3.2 MPa 2 g of AC	phenol (5 g/L)	Sewage sludge PICA-F22 (coal)	90-265 985	60-80 12	15-60 70	Activity related mainly with ash content (Fe) Need improving mechanical strength	[98]
Batch reactor 160 °C, 2 MPa t = 120 min 0.8 g of MWCNT	phenol (1 g/L)	MWCNTs	194	-	100	Higher activity than CeO <sub>2</sub> and CeO <sub>2</sub> -TiO <sub>2</sub> catalyst Activity relates with surface groups	[108]
Batch Reactor 200 °C, 6.9 MPa 0.8 g of xerogel	aniline (2 g/L)	AC (ROX) xerogel	900 630	- -	97 99	Activity related to textural properties and surface groups	[100]
Batch reactor 200 °C, 0.7 MPa 2.7 g of AC	2,4-6 tri- nitrophenol (0.125 g/L)	Olive stone	121 1530	2.5	100	Heterogeneous mechanism on different range of micro-macro porosity	[113]
Batch reactor 110-160°C 3-5 MPa t <sub>R</sub> = 3 h 0.1-1 g of AC	phenol (5 g/L)	Chezacarb Charcoal	950 1049	Ni (0.25) Fe(0.016)	> 99 > 99	Strong effect of temperature catalyst activity Presence of trace amount of metal improves the degree of mineralization	[86, 102]

but deactivated very rapidly

### 2.1.2.2 Stability of AC

It has been shown that several ACs exhibited high catalytic activity in the oxidation of phenolic pollutants. However, one key issue for their successful application at industrial scale is an acceptable long term stability. In general, CWAO operating conditions are too mild to provoke sintering or solid-state transformation processes. Moreover, AC has proven to physically resist in both acidic and basic reaction environment [34, 106]. Stability of AC in CWAO can be thus related to variation in phenol or TOC conversion, weight, total surface area and surface group distribution of AC in the course of reaction. Table 2.6 summarizes the important results of some studies on AC stability during CWAO.

**Effect of operating conditions on carbon weight:** It appears from Table 2.6 that AC weight change is strongly linked with operating conditions ( $T$ ,  $P_{O_2}$ ,  $C_{Ph}$ , flow direction). Roughly, increasing the temperature and oxygen partial pressure leads to a substantial weight loss, while increasing the phenol inlet concentration has an opposite effect. Apparently constant weight has been also observed in upflow mode in contrast to downflow, which seems to favor carbon burn-off due to partial wetting of the carbon particles. Moreover, a substantial loss of AC has been also reported in SWAO of phenolic pollutants [116, 117] and oxidative dehydrogenation of ethylbenzene [118]. In particular, Fortuny et al [31, 43] studied the influence of oxygen pressure (0.1-0.9 MPa) on AC stability at 140°C and 0.12 h of liquid space time in TBR experiments over 10 days. The stability of the catalyst was monitored by measuring AC weight and phenol conversion after different TOS. Figure 2.5 il-

Table 2.6: Stability of AC in CWAO.

Reactor	Con. (g/L)	T (°C)	$P_{O_2}$ (MPa)	TOS (h)	$X_{Ph}$ (%)	$\Delta W_{AC}$ (g)	$\Delta S_{BET}$ (m <sup>2</sup> /g)	Ref.
TBR	5	140	0.9	240	48	-2.3	-627	[31, 43]
	5	140	0.4	240	42	-1.2	n.m	
	5	140	0.2	240	38	0.2	n.m	
	5	140	0.1	240	24	1.3	n.m	
TBR	1	160	0.2	100	51	-6	n.m	[32]
	2.5	160	0.2	100	53	-5	n.m	
	5	160	0.2	100	55	-1.8	n.m	
	7.5	160	0.2	100	35	-0.4	n.m	
10	160	0.2	100	38	2.4	n.m		
TBR	5	160	0.2	144	35	-5.7	n.m	[114]
TBR	5	160	0.2	144	60	-1.8*	n.m	[114, 115]
TBR	1	127	0.8	216	75	Stable**	-342	[97]
TBR	5	140	0.2	72	48	0.27	-1359	[91]
UFBR	5	160	0.2	140	18	0.1	n.m	[115]
UFBR	1	160	1.6	280	70	0.1	-529	[112]

\* Data from periodic operation; \*\* Fe/AC catalyst; n.m. not measured

illustrates the AC weight evolution for different oxygen pressures. During the first 20

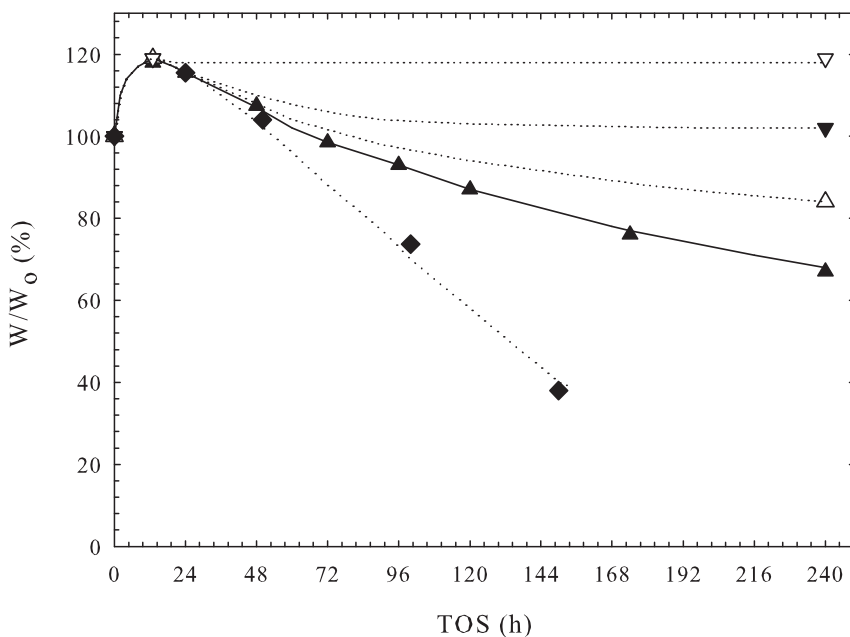


Figure 2.5: AC weight evolution during CWAO for different oxygen pressures: (∇) 0.1 MPa, (▼) 0.2 MPa, (△) 0.4 MPa, (▲) 0.9 MPa, (◆) 0.2 MPa,  $T = 160\text{ }^\circ\text{C}$ , lines show trends; Standard conditions:  $T = 140\text{ }^\circ\text{C}$ ,  $F_L = 58\text{ mL/h}$ ,  $F_g = 9\text{ NL/h}$ ,  $C_{ph} = 5\text{ g/L}$ ,  $W_{cat} = 7\text{ g}$  [31, 43].

h, the carbon weight is seen to increase and to reach a maximum, then remaining on a plateau or decreasing depending on the oxygen pressure and temperature employed. For example, at 0.9 and 0.4 MPa of oxygen pressure the AC weight decreases progressively to reach 66% and 84% of the initial weight, respectively. In contrast, a plateau was observed at lower pressures, which ultimately provide a final weight increment of 3 and 18% for 0.2 MPa and 0.1 MPa partial pressure of oxygen, respectively. A similarly trend, but with a fast carbon weight loss was observed when the temperature was increased to 160°C even for mild oxygen pressure of 0.2 MPa (see Figure 2.5). According to the authors the percentage weight increment observed in the initial period must be attributed to the fast formation and strong adsorption of oxidative coupling products. Once the formation, adsorption and destruction of these products reaches steady state however, combustion of AC may prevail at higher oxygen pressure, ultimately leading to a progressive loss of AC weight and a

similar conversion decline.

Stüber et al. [32] and Ayude et al. [114] reported on the effect of inlet phenol

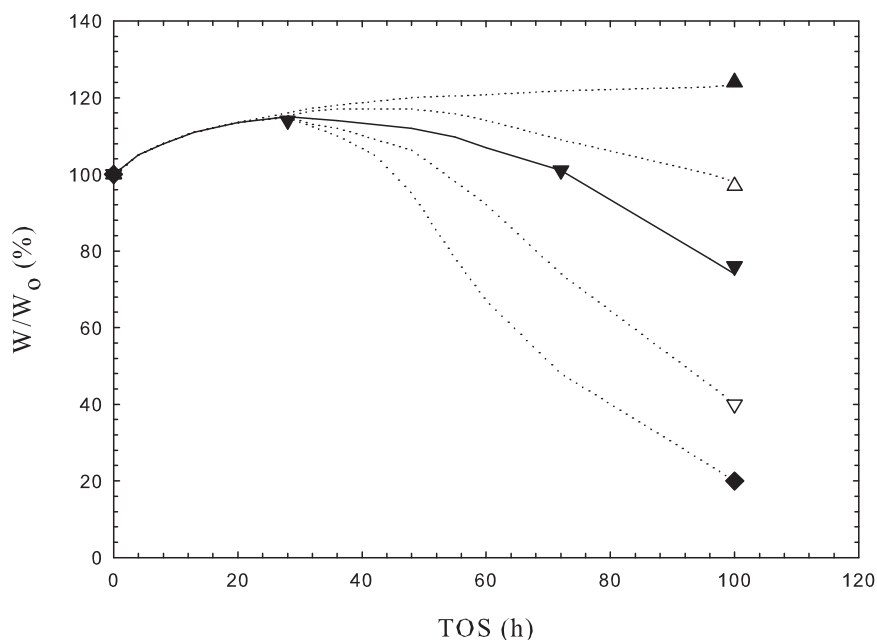


Figure 2.6: AC weight evolution during CWAO for different phenol inlet concentration: (▲) 10 g/L, (△) 7.5 g/L, (▼) 5 g/L, (▽) 2.5 g/L, (◆) 1 g/L, discontinuous lines show trends; Standard conditions:  $P_{O_2} = 2$  bar,  $T = 160$  °C,  $F_L = 58$  mL/h,  $F_g = 9$  NL/h,  $C_{ph} = 5$  g/L,  $W_{cat} = 7.5$  g [32].

concentration (from 1 to 10 g/L) on AC stability in a TBR at 160 °C, 2 bar of oxygen partial pressure and an initial AC load of 7.5 g. The resulting profiles of carbon weight are illustrated in Figure 2.6 for all phenol concentrations tested. Similarly, the initial carbon weight is increased in the first 20-40 h of operation and then decreases depending on the inlet phenol concentration tested with the exception of 10 g/L. An inspection of Figure 2.6 underlines that inlet phenol concentration has a strong influence on the degree of carbon consumption during CWAO. For example, only 1.5 g of the initial AC was recovered after 100 h of time on stream at 1 g/L feed phenol concentration, in contrast to 9.9 g (a 33% weight increment) for 10 g/L inlet phenol concentration. In general, a decrease/loss in carbon weight goes in hand with a similar decline with phenol conversion. According to the authors, the higher AC weight loss observed at lower inlet phenol concentration is attributed to the

lower phenol coverage on the AC surface, thereby directly exposing the AC surface to molecular oxygen and surface oxidation for prolonged period. This finding is in agreement with the work of Fortuny et al [31], who demonstrated that carbon consumption in a TBR was rapid in the absence of phenol at otherwise same conditions. At sever conditions, carbon combustion rates as high as 15-60 mg/min were even detected when the AC was subjected to supercritical water conditions of 400°C and 25 MPa [116, 117]. Accordingly, higher phenol concentration leads to higher surface coverage protecting the AC surface from being directly attacked by dissolved oxygen.

**Evolution of textural properties and surface groups during CWAO:** Several CWAO studies employing AC as catalyst reveal a significant modification of both texture ( $S_{\text{BET}}$ ,  $A_t$ ,  $V_{\text{micro}}$ ,  $V_{\text{meso}}$ ) and surface group distribution of the original AC in the course of the experiment [31, 34, 43, 90, 91, 97, 112]. In order to obtain a clearer picture, the results obtained from Quintanilla et al [97], Cordero et al [112] and Fortuny et al [31, 43] are illustrated in Figure 2.7. Fortuny et al [31, 43] studied the CWAO of phenol (5 g/L) over commercial active carbon (Merck) at 140°C, 0.9 MPa of oxygen pressure and 0.12 h of liquid space time in a TBR. The phenol conversion,  $S_{\text{BET}}$  and AC weight evolution are give in Figure 2.7 a. As it can be seen,  $S_{\text{BET}}$  and weight of AC decreased with run time to yield ca. 65% BET area and 33% AC weight reduction after 240 h, respectively. The decrease in AC weight and  $S_{\text{BET}}$  goes along with a decrease in phenol conversion. Quintanilla et al [97] also studied the CWAO of phenol (1 g/L) using commercial active carbon (Merck) coated with 2.5% of Fe at 127°C, 0.8 MPa of oxygen pressure and 0.083 h of liquid space time in a TBR. The evolution of textural properties and phenol conversion are depicted in Figure 2.7 b. BET area and micropore volume decrease rapidly in the first 40 h due to adsorbed oxidative coupling products, then stabilize in the further course of reaction, while external area and mesopore volume increases after ca. 100 h of TOS. Elemental analysis of the spent Fe/AC revealed a strong initial reduction of C/O ratio with time, which further proves the presence of surface oxidation of AC. Moreover, TPD analysis of the CWAO spent Fe/AC shows a double increase in the amount of CO and CO<sub>2</sub> evolved compared to the fresh one indicating that higher amounts of acidic surface groups (carboxylic acid, lactone and carboxylic anhydride) were formed during CWAO. With respect to conversion, fairly stable conversion was achieved for the range of conditions studied suggesting that the increased external and mesoporosity may compensate a possible activity loss due to the reduction of microporosity during the adsorption period. Cordero et al [112] studied the CWAO of phenol (1 g/L) over commercial active carbon (Chemviron) at 160°C, 1.6 MPa of oxygen pressure and 0.04 h of liquid space time in UFBR to highlight the modifi-

cation of AC via CWAO. The resulting conversion, textural properties and carbon to oxygen ratio profiles are also depicted in Figure 2.7 c. In their case, BET area, micropore volume and C/O ratio also rapidly decreased at the initial stage, whereas external area, mesopore volume accordingly increased with operating time reaching steady state values after ca.75 h. Similarly, stable conversion with a negligible AC weight loss (<3%) was achieved in agreement with the work of Quintanilla [97]. Not surprisingly, the authors found also a substantial reduction of carbon to C/O with operating time.

The important conclusion of this section is that AC does not only catalyze the oxidation of pollutants during CWAO, but also facilitates side reactions such as oxidative coupling, surface oxidation and ultimately self combustion of AC that all may induce modifications of textural properties and oxygen surface groups. Accordingly, the activity and stability of AC may change in the course of reaction. Besides the origin of the AC, the adsorption, formation and destruction of phenolic products together with the surface oxidation of AC occurring in the course of CWAO seems thus another important factor for the ultimate activity and stability of ACs in CWAO.

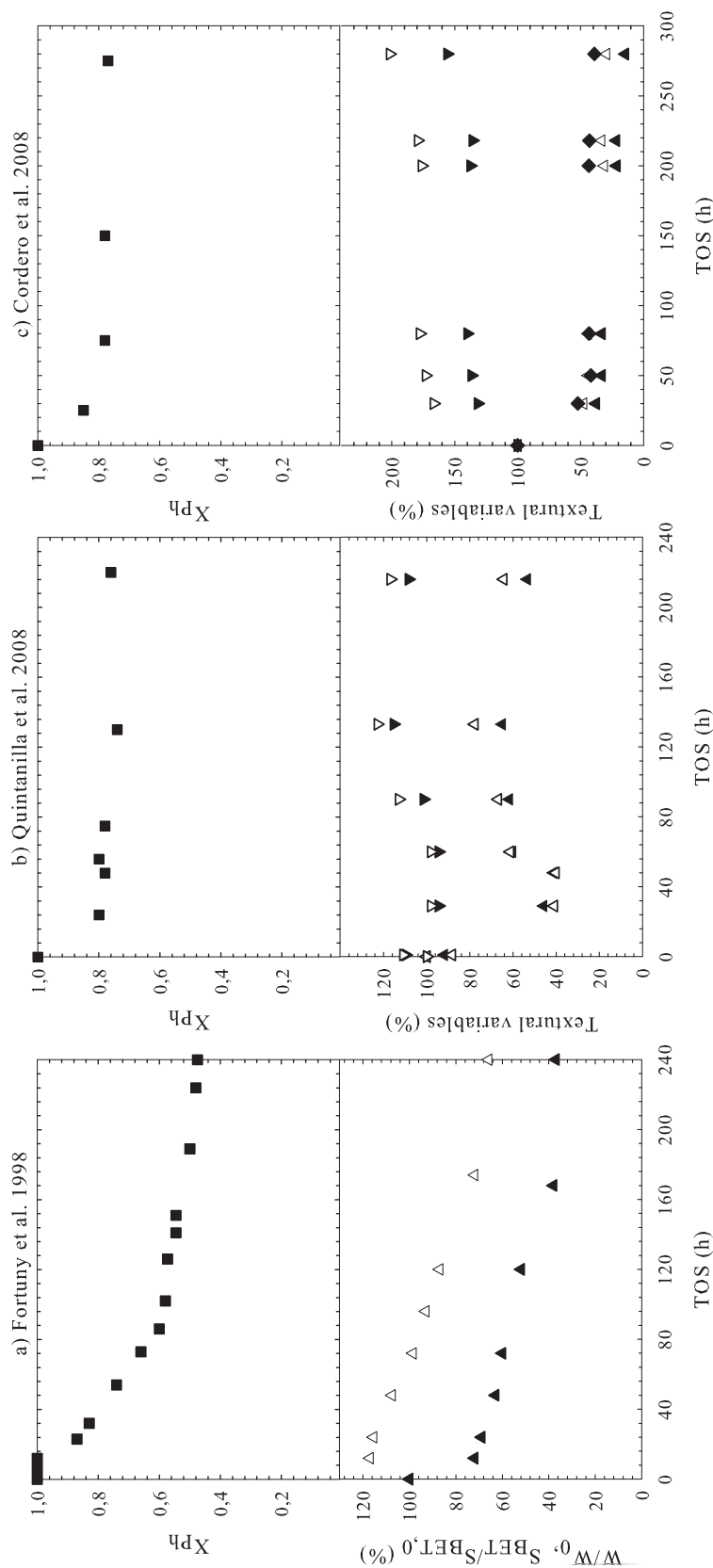


Figure 2.7: Evolution of phenol conversion, carbon weight, textural properties and C/O ratio during CWAO;  
 a) ( $\Delta$ ) AC weight, ( $\blacktriangle$ )  $S_{BET}$ :  $P_{O_2} = 2$  bar,  $T = 140^\circ C$ ,  $\tau = 0.12$  h,  $F_g = 9$  NL/h,  $C_{Ph} = 5$  g/L,  $W_{cat} = 7.5$  g [31];  
 b) ( $\Delta$ )  $V_{micro}$ , ( $\blacktriangle$ )  $S_{BET}$ , ( $\nabla$ )  $V_{meso}$ , ( $\blacktriangledown$ )  $A_t$ ;  $P_{O_2} = 0.8$  MPa,  $T = 127^\circ C$ ,  $F_L = 30$  mL/h,  $F_g = 92$  mL/min,  $C_{Ph} = 1$  g/L,  $W_{cat} = 2.5$  g [97];  
 c) ( $\Delta$ )  $V_{micro}$ , ( $\blacktriangle$ )  $S_{BET}$ , ( $\nabla$ )  $V_{meso}$ , ( $\blacktriangledown$ )  $A_t$ , ( $\blacklozenge$ ) C/O<sub>2</sub> ratio:  $P_{O_2} = 1.6$  MPa,  $T = 160^\circ C$ ,  $F_L = 90$  mL/h,  $F_g = 90$  mL/min,  $C_{Ph} = 1$  g/L,  $W_{cat} = 3.5$  g [112].

### 2.1.2.3 Role of AC in CWAO of phenol

Liquid phase catalytic wet air oxidation of phenolic compounds over AC is a complex process and the role of AC in CWAO is far from being well understood. This is certainly because AC does catalyze several reactions simultaneously during CWAO:

1. Oxidation of organics to intermediates and mineralization to  $\text{CO}_2$  and  $\text{H}_2\text{O}$  (desired reaction),
2. Oxidative coupling of aromatic compounds that strongly adsorb on AC surface (may block active sites),
3. Surface oxidation (may modify number of active site) and combustion of AC

Reactions 2 and 3 can alter the initial behavior of AC catalysts (textural and surface chemistry modification) during CWAO (see Figure 2.7). The question that arises is what is the role of AC during CWAO. A common point of all these reactions can be that they are initiated by free radical attack either in the liquid phase or on the carbon surface. Thus, the key for understanding AC catalyzed CWAO may be to elucidate how are the free radicals formed on the AC surface and the role that have surface chemistry and textural properties for the generation of oxygenated free radicals.

Significant effort has been made to relate the catalytic role of AC catalysts with surface chemistry; textural properties and mineral content though conclusive results have not been achieved [81, 112]. A fundamental study on the catalytic role of AC was published by Rivera-Ultrill and Sanchez [103] on the ozonation of 1,3,6-naphthalenetrisulphonic (NTS) acid using different activated carbons. According to these authors, high rates of pollutant degradation were achieved with carbons that have high concentration of oxygenated basic surface groups and mineral matter implying that carbon basicity (presence of pyrones or chromenes) is responsible for its catalytic activity. Eliminating the direct relationship with the physical properties of AC, Santiago et al [95] and Pereira et al [119] suggested that the surface chemistry of AC can play an important role for the catalytic activity of AC.

Several studies relate the role of AC to its ability to dissociate molecular oxygen, eventually through the formation of  $\text{H}_2\text{O}_2$ , yielding oxygenated free radicals responsible for attacking the organic pollutants [32, 79, 91, 95, 120–122]. Matsis [120] studied the interaction of dissolved oxygen with a coconut shell-derived active carbon. The authors found that the basic surface groups of AC decreased with sorption of oxygen. According to the author this is attributed to the deprotonation of the basic sites by the adsorbed oxygen molecule. To account for deprotonation process, Matsis et al [120] propose a chromene type mechanism (benzopyran-type structure) as it can be shown in Figure 2.8 a. In agreement with the proposed model, the

author detected small amount of  $H_2O_2$  during his sorption experiment.

Similarly, Rivera-Ultrill and Sanchez et al [103] (ozonization of NTS) state that the role of AC is to reduce (decompose) ozone to highly reactive radical such as  $OH^\bullet$ . According to the authors, the oxygenated basic surface groups (chromene and Pyrone) or the localized  $\pi$  electron system within the basal planes of carbon are responsible for the initiation of ozone or oxygen decomposition following reaction 1 and 2 in Figure 2.8 b. These decomposition reactions may ultimately yield  $H_2O_2$  through eventual formation of  $OH^\bullet$ .

Moreover, Ahumada et al [121] reported that the catalytic behavior of AC is related to the formation of  $H_2O_2$  in the presence of molecular oxygen in aqueous solution. The authors claim that oxygen surface groups alone do not have any catalytic activities rather they act as a reducing agent for molecular oxygen to form  $H_2O_2$  in aqueous solution. The authors verified their assumption through the oxidation of  $Fe^{2+}$  to  $Fe^{3+}$  using different oxidative treated AC. The authors found that AC with high concentration of oxygenated surface groups has a high activity towards  $Fe^{2+}$  oxidation. Based on their experimental observation, Ahumada et al [121] proposed the reaction mechanism illustrated in Figure 2.8 c for parent as well as oxidative treated ACs. As it can be seen in Figure 2.8 c, oxygen oxidation is initiated by  $C_{Red}^*$  sites in case of the parent AC, which can be a quinone type surface group to generate  $H_2O_2$ . On the other hand,  $Fe^{2+}$  can be oxidized in two parallel route with oxidative treated ACs. In this case,  $Fe^{2+}$  can be directly oxidized by oxygenated surface groups ( $C'_{Ox}$ ) with higher oxidation potential than the  $Fe^{3+}/Fe^{2+}$  (0.771 V) pair or through the mechanism stated in the parent AC to ultimately yield  $H_2O_2$ . In this context, Xie et al. [122] also reported the capability of AC to generate  $OH^\bullet$  radical using microwave irradiation in the presence of oxygen in aqueous solution.

The application of Multi-Wall Carbon Nanotube (MWCNTs) for CWAO of phenol has been also highlighted recently [108]. Yang et al. [108] realized that surface functionalities plays an important role for catalytic activity of MWCNTs through eventual formation of hydroperoxyl radical ( $HO_2^\bullet$ ) in the presence of oxygen. Accordingly, the authors proposed the mechanism illustrated in Figure 2.8 d for the production of hydroperoxyl radical ( $HO_2^\bullet$ ). Unlike the other mechanism, the adsorbed oxygen is reacted with the carboxylic group (COOH) to generate the active species (see Figure 2.8).

Nevertheless, doubts on the overall mechanism of CWAO over AC still remain. Georgi and Kopinke et al [123] studied the role of sorption for AC/ $H_2O_2$  catalyzed WAO of organic contaminants. Their findings clearly underline that the sorped fraction of the organics does not participate in the reaction indicating that the reaction should be between the dissolved organics entrapped in the pore and  $OH^\bullet$  radical

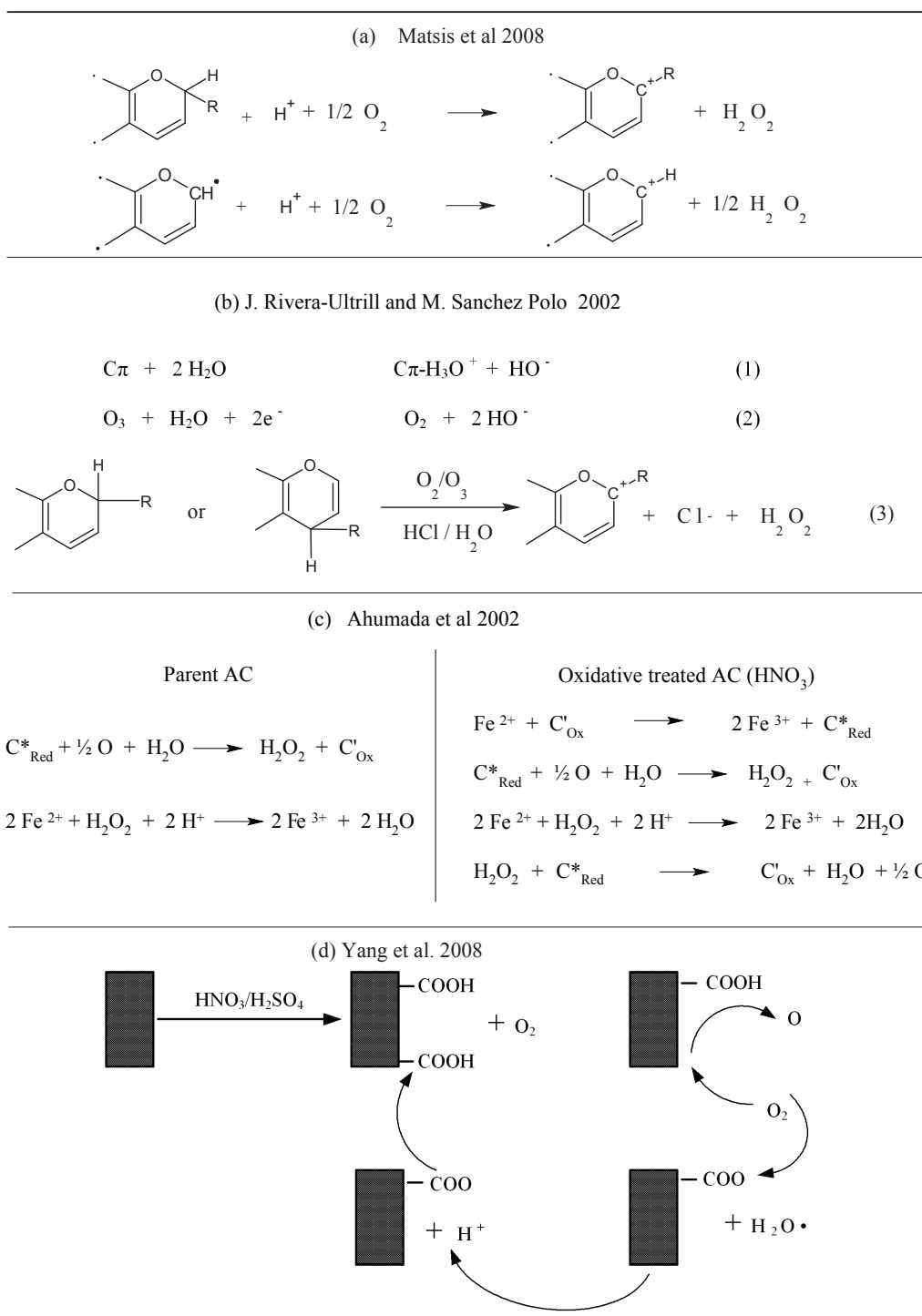


Figure 2.8: Mechanism for O<sub>2</sub> / O<sub>3</sub> decomposition and H<sub>2</sub>O<sub>2</sub> formation over activated carbon [103, 108, 120, 121].

generated by AC in the presence of  $H_2O_2$ . The authors proved this assumption by conducting oxidation reaction in the presence of, a well known free radical scavengers (methanol). According to their findings, the presence of methanol in the liquid phase strongly inhibit the degradation rate predominantly by scavenging the  $OH^\bullet$  radical. On other hand, the study of Farial et al [36] on the oxidation of oxamic and oxalic acid over AC using ozone as oxidant in the presence of tert-butanol as free radical scavenger underline the role of surface reaction. According to the authors, the presence of tert-butanol (which is known to not significantly adsorbed on the AC surface) does not affect the degradation of the compounds indicating that the reaction is mainly conducted on the AC surface.

Summarizing, the role of AC during CWAO could be the generation of oxygenated free radicals for the subsequent initiation of the aforementioned three reactions. However, the complete mechanism of AC catalyzed phenol oxidation based on free radicals is not established yet. Thus, future research work should be driven to explain in detail the mechanism of AC catalyzed CWAO process at molecular level.

In addition to the elementary reaction mechanism of AC for the generation of oxygenated radicals, which may initiate the oxidation reactions in CWAO processes, it is important to know the reaction pathway (route) that leads to complete mineralization towards  $CO_2$  and  $H_2O$ . Several reaction pathways have been proposed for oxidation of phenol over homogeneous or heterogeneous copper catalysts [125] and heterogeneous AC supported Ru, Pt, Pd and Fe [42, 60, 64] catalysts in the last decades all based on the work of Devlin and Harris [126]. On the other hand, studies related to reaction pathway of phenol oxidation over AC are scarce. The recent studies are the works of Quintinilla et al [42] over Fe/AC, Eftaxias et al. [127] and Santos et al [106].

Santos et al [106] extensively studied the wet oxidation of phenol and its cyclic intermediates over AC catalyst. The authors proposed the reaction scheme illustrated in Figure 2.9 b. As can be seen, phenol oxidation over AC follows three parallel routes to provides cyclic intermediate such as hydroquinone, p-benzoquinone, p-hydroxybenzoic acid and traces of catechol and short chain acids such as maleic, acetic and formic acid. In the first route, phenol is oxidized to hydroquinone, which further react to p-benzoquinone to provide short chain acids (formic or acetic acid) and  $CO_2$ . In the second route, phenol is oxidized to catechol leading to the formation of oxalic acid and  $CO_2$ . Lastly, phenol oxidizes to p-hydroxybenzoic acid to provide maleic acid and  $CO_2$ . According to the authors, the oxidation of the cyclic intermediates shows faster oxidation rate compared to phenol itself.

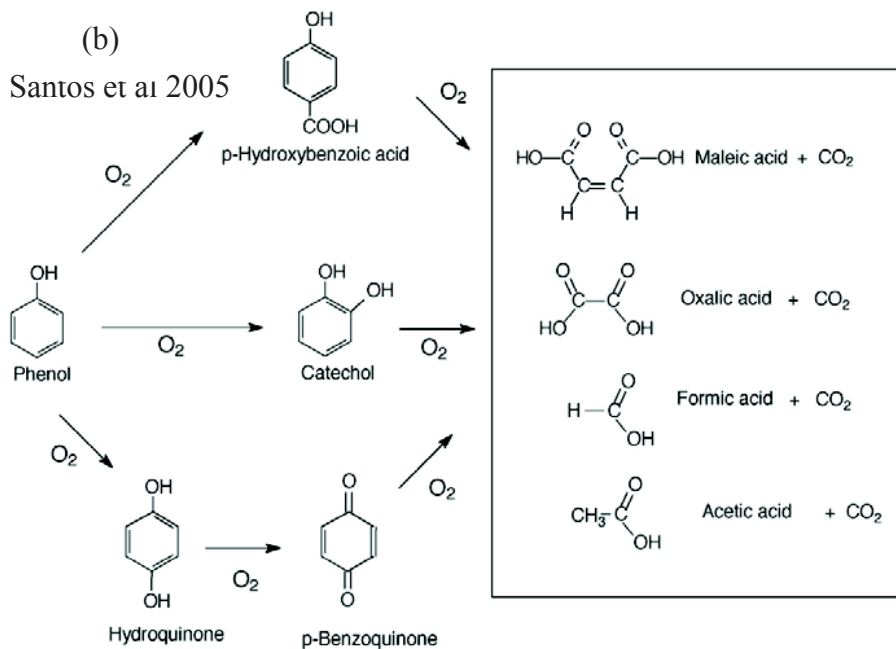
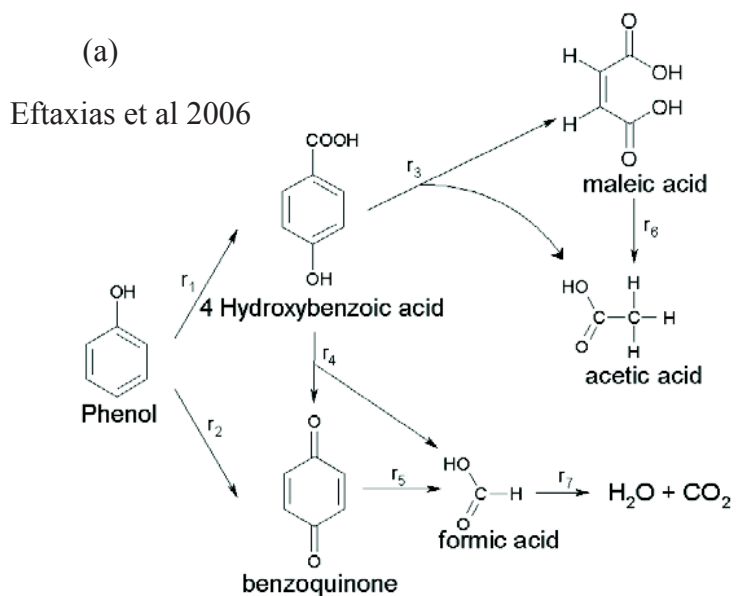


Figure 2.9: Reaction pathways proposed for CWAO of phenol over AC catalyst[106, 124].

Eftaxias et al [127] studied the oxidation of phenol over AC in a TBR. According to the authors, phenol oxidation yield cyclic intermediates such as 4-hydroxybenzoic acid (4-HBA), p-benzoquinone, trace catechol and hydroquinone, and short chain acids such as maleic, fumaric, acetic and formic acids in agreement with the work of Santos [106] using the same AC. Based on their experimental results and model predications, the authors proposed the reaction scheme illustrated in Figure 2.9 a. According to the authors, degradation of phenol follows two parallel routes: 1) oxidation to benzoquinone, which further oxidizes to maleic acid through acetic acid or 2) formation of 4-hydroxybenzoic acid. The latter leads to direct mineralization towards  $\text{CO}_2$  and  $\text{H}_2\text{O}$  through the formation of formic acid or is converted to refractory acetic acid.

Quintinilla et al. [42] also studied in detail the oxidation of phenol and intermediate compounds identified during CWAQ of phenol over Fe/AC catalyst. The authors proposed the reaction pathway illustrated in figure 2.10. As it can be seen, phenol oxidizes through two parallel routes: either oxidation to p-hydroxylated hydroquinone, which further oxidized to p-benzoquinone or through para-carboxylated hydroxybenzoic acid. The former leads to mineralization towards  $\text{CO}_2$  and  $\text{H}_2\text{O}$  through oxalic acid formation, whereas the latter gives raise to short chain acids such as refractory acetic acid. Oxidation results of individual compounds reveals that complete mineralization was achieved for formic acid in contrast to acetic acid where no conversion was observed at the tested conditions. Oxidation of oxalic, malonic and maleic on the other hand shows the formation of intermediates as confirmed by compound and TOC conversions. For example, acetic acid was detected as the main intermediate followed by formic acid during oxidation of malonic acid over Fe/AC catalyst. During the oxidation of maleic acid, fumaric, acetic and formic acids were detected as intermediate products. With respect to ring compounds, complete conversion has been achieved for p-benzoquinone with maleic, malonic, acetic and formic acids detected as intermediate products. The authors revealed that p-benzoquinone is mainly mineralized to  $\text{CO}_2$  and  $\text{H}_2\text{O}$  through the formation of oxalic acid. Hydroquinone was also oxidized rapidly when Fe/AC is used as a catalyst. p-benzoquinone was detected as intermediate product at lower space-times but as the liquid space-time is increased, its concentration decreased due to the rapid oxidation to lower molecular acids (maleic, acetic and formic acids). p-hydroxybenzoic acid on the other hand, oxidizes directly to short chain acids (maleic, acetic and formic acids). Its oxidation rate is slow compared to p-benzoquinone and hydroquinone.

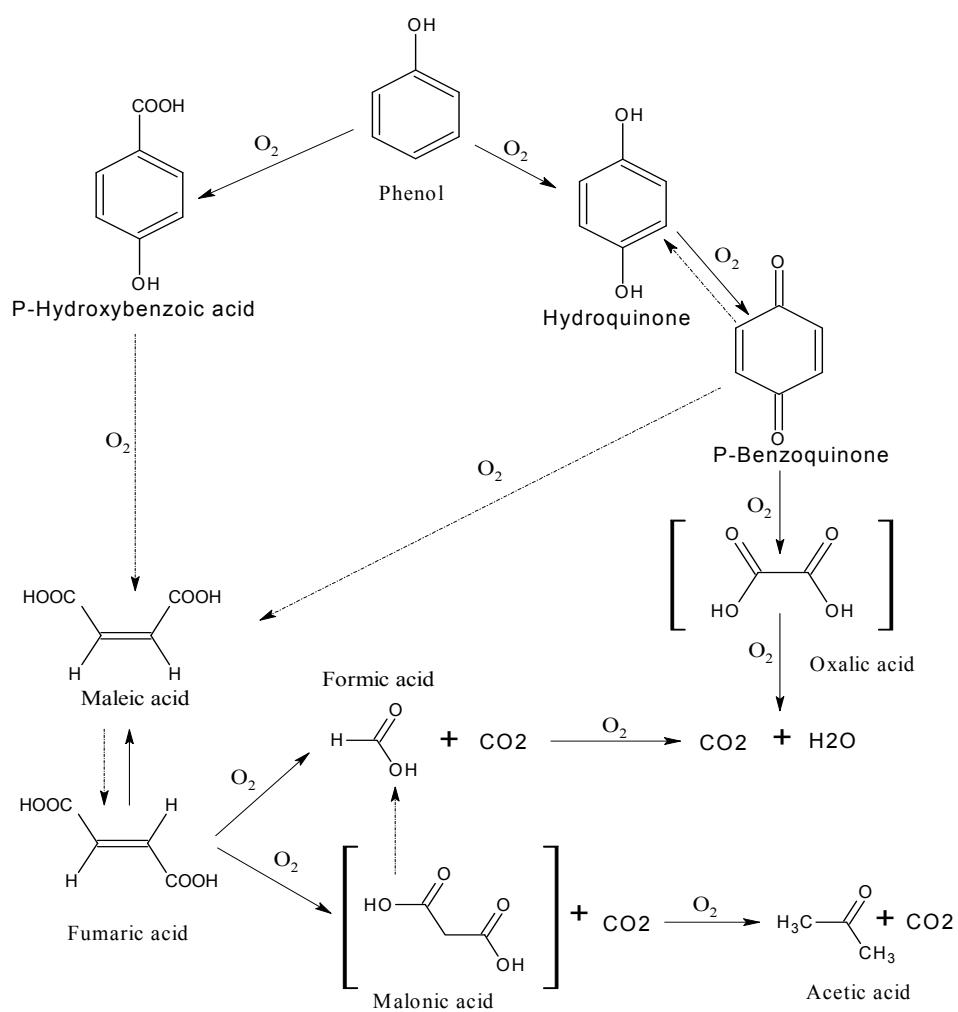


Figure 2.10: Reaction pathway proposed for CWAO of phenol over Fe/AC catalyst[42].

## 2.2 Multi-phase Reactors for CWAO

### 2.2.1 Reactor choice

Chemical reactions requiring the presence of three phases are frequently encountered in industrial liquid phase catalytic hydrogenations or oxidation reactions. The limiting steps in such types of reactors are normally internal and external mass transfer and heat transfer. Therefore, an important aspect of these reactors is the contacting between the phases. Two main reactor configurations are available: suspended or fluidized bed and fixed bed with cocurrent down or upflow as shown in Figure 2.11. The selection of adequate reactor type for a given application is not a straight forward task. The following factors including catalyst nature, activity and stability and reaction type and product distribution of multi-phase reaction systems should be considered. A short description of the reactors employed for CWAO will be given in the following section.

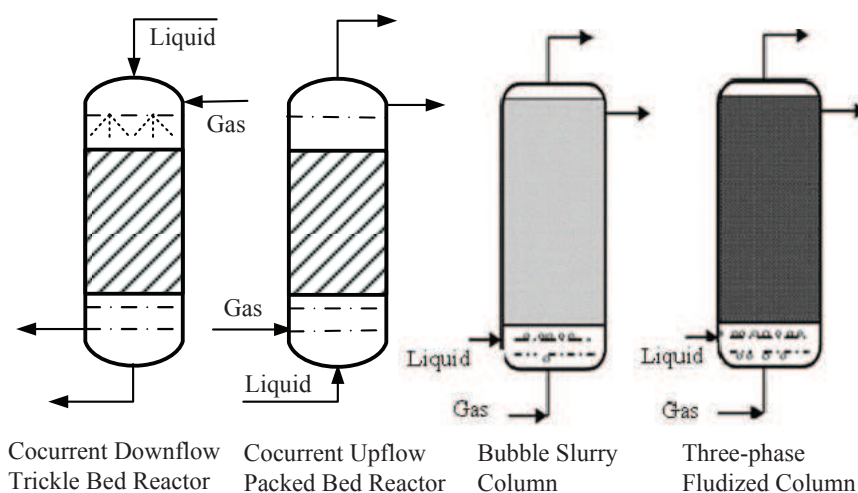


Figure 2.11: Configuration of three phase catalytic reactors [128]

#### 1) Slurry reactors

In a slurry reactor, fine catalyst particles are suspended in a liquid by mechanically agitation or a gas flow induced agitations in a batch and/or continuous mode of operations. The catalyst is suspended in a high liquid volume and therefore the catalyst effectiveness factor tends to unity. Temperature control is also relatively

simple due to large amount of liquid present in the reaction media. Batch mode is thus preferred for catalyst screening and kinetic measurements. For continuous slurry reactors, catalyst separation is a more difficult and costly task compared to fixed bed reactors. Since the residence time distribution of the reactant is close to that of an ideal continuous stirred tank reactor (CSTR), higher conversions are also difficult to achieve. Moreover, since organic pollutants, such as phenols have the tendency to undergo liquid phase polymerization reactions [55, 109], slurry reactors should not be a primary choice for CWAO studies.

## 2) Monolith reactors

Monolith reactors are constructed from a bundle of parallel tubular channels with specified dimension. The tubes are laminated with a thin layer of porous material containing the active component of the catalyst. Because of the short diffusion distance inside the thin layer of the structured catalysts, catalyst utilization factor tends to unity. Moreover, due to the presence of open channels, pressure drop in monolith reactor is very low compared to randomly packed bed reactors. Considering these advantages, Cybulski et al.[12] suggests monolith reactors as a potential candidate for CWAO of organic pollutants. Nevertheless, catalyst regeneration is an extremely difficult task in monolith reactors and must be done in-situ as the catalyst is coated on the channels and can not be removed.

## 3) Fixed bed reactors

Fixed bed reactors consist of a cylindrical tube in which the catalyst particles are randomly or structurally packed. In general, they are characterized by a high ratio of solid to liquid and catalyst utilization may be poor due to external and internal reactant transport limitations or liquid channeling. Temperature control can be also a difficult task in fixed bed reactors. Strong exothermic reaction can lead to a temperature rise inside the bed that may be prohibitive for several reasons: unfavorable equilibrium conversion, selectivity, catalyst stability and hot spot formation. However, despite their poor internal and external mass transport properties, fixed bed reactors are the most widely used reactors in industrial practice for their high production throughput and simple posterior catalyst recovery.

Within the fixed bed reactor configuration, two flow directions of gas phase and liquid phase are of industrial interest: co-current downflow (Trickle Bed Reactor) and co-current upflow (Packed Bed Reactor). Comparison of the two operation mode shows that upflow fixed bed reactor (UFBR) gives higher mixing (both radial and axial), higher gas-liquid mass-transfer coefficients, higher liquid holdup, better liquid distribution, better heat transfer between liquid and solid and to reactor wall

and less solid plugging than downflow fixed bed reactor (TBR). But, upflow reactor is also leads to higher pressure drop, poorer conversion, undesired liquid phase homogeneous reactions, larger catalyst attrition, and strong intraparticle diffusion effects than downflow operation. Partial external wetting occur in downflow mode, especially at low liquid flow rate which may have a positive effect for gas limiting reactions due to fast direct gas-solid mass transfer. On the contrary, when the main mass transfer limitation concern is for liquid reactant, partial wetting will have negative effects due to less solid liquid interfacial area.

The application of fixed bed reactors in CWAO of organic pollutants has been studied by several investigators in the last decades [43, 85, 110, 124, 129–132]. Eftaxias et al [124] studied the performance of down and upflow fixed bed reactors for the oxidation phenol over AC at 120-160°C and 0.1 to 0.2 MPa oxygen partial pressures. Higher phenol disappearance rates were achieved in downflow mode (TBR) for all temperature tested compared to upflow mode (UFBR) suggesting that mass transfer limitations exist in the fully wetted reactor (upflow reactor) at the given operating conditions. Nevertheless, care should be taken for the extent of catalyst wetting in TBR. For example, Tukac et al [85, 131] observed decreasing phenol conversion at higher liquid space times (small liquid flow rates). The authors attributed this result to the insufficient catalyst wetting at lower liquid flow rate (liquid reactant starvation on the catalyst surface) suggesting that the reaction is shifting to liquid limited reactions at a very small liquid flow rates.

In this context, Khadilkar et al [133] proposed the following unified criterion to identify the limiting reactant that helps in selecting the adequate direction of the gas-liquid flow.

$$\gamma = \frac{D_L^{eff} C_L}{\nu D_L^{eff} C_G} \quad (2.1)$$

where  $D^{eff}$  is the effective gas or liquid diffusion coefficient in the catalyst pore,  $C$  is the respective gas or liquid reactant concentration and  $\nu$  the stoichiometric coefficient of the gaseous reactant.

According to the above criterion, when  $\gamma \gg 1$ , the reaction is gas-reactant limited and downflow mode is preferred to obtain higher conversion. On the other hand, if  $\gamma \ll 1$  the reaction is liquid-reactant limited and upflow mode is recommended to have higher conversion.

It appears from the above discussion that CWAO of bio-toxic organic pollutants such as phenol using air as oxidant is a gaseous reactant limited process at a typical CWAO operating conditions. Moreover, these compounds have the tendency to undergo undesired liquid phase polymerization reaction at typical CWAO conditions in

high liquid to solid ratio reactors such as agitated slurry reactors or bubble column reactors [55, 109]. These facts suggest that fixed bed reactor operating in downflow mode (TBR) is a priority choice for CWAO phenol.

Despite a significant progress made on TBRs for the application of CWAO processes, aspects such as reactor startup and dynamic operation are scarcely treated in the open literature. For example, the pre-wetting procedure can influence the ultimate reactor performance due to different hydrodynamic parameters (pressure drop, catalyst wetting and liquid holdup) of the bed [134, 135] from the initial state. Baussaron et al. [136] reported that start-up with a prewetted bed can improve the wetting efficiency by more than 10% depending on liquid flow rate used. On the other hand, for CWAO using activated carbon as catalyst, the way in which the three phases are contacted is another important aspect that may affect overall reactor performance [61, 97], especially with respect to catalyst activity. Quintilla et al [97] studied CWAO of phenol over AC in TBR under startup with air or nitrogen flow. The authors found that startup of the reactor with air flow resulted in a better reactor overall performance. Similarly, Masende et al [61] studied the startup of continuous slurry stirred tank reactor (CSTR) for CWAO of organic pollutants using three different startup procedures (startup with  $N_2$ , startup with  $O_2$  and startup with three phases at once). The authors demonstrated that simultaneous contacting of the three phase results in a better reactor performance.

A further key point that needs to be investigated is the assessment of kinetic data for CWAO of phenol over AC catalyst in three phase reactors. Kinetic measurements for heterogeneous reactions are usually conducted in a batch slurry reactor to eliminate external and internal mass transfer limitations [20, 55, 109, 137–139]. In these reactors, however, due to their high liquid to solid ratio, homogeneous liquid phase polymerization reactions are enhanced and may leading to fast catalyst deactivation, most likely due to irreversible adsorption of the condensation products during CWAO of phenolic compounds [109]. Moreover, the intrinsic reaction rate could be over estimated due to the contribution of liquid phase homogeneous reactions. For example, Stüber et al [109] found a higher initial reaction rate constant in a batch slurry reactors compared a trickle bed reactor. According to the authors, this can be explained by enhanced fast polymerization reaction occurring in the slurry reactor. Also, Pinter and levec [55] formulated a kinetic expression that includes homogeneous and heterogeneous contribution to simulate the phenol degradation profile in a TBR. However, the kinetic expression could not match the performance of a TBR where the extent of the homogeneous side reaction is strongly reduced [55, 140].

The conclusion is that for the CWAO of phenol, it is not recommended to use

kinetic data obtained in batch slurry reactors for modelling, design and scale-up of heterogeneous catalytic reactors. Alternatively, Levec et al [140] studied CWAO of phenol in a liquid full fixed-bed reactor with oxygen pre-saturated liquid feed at conversions level smaller than 10% to avoid oxygen depletion in the reactor bed. The authors confirmed that differential, liquid full operated fixed-bed reactor can be effectively employed to provide the intrinsic kinetic data. Nevertheless, for phenol conversions of this magnitude, the progress of intermediate oxidation products cannot be satisfactorily monitored. In such cases, the use of trickle bed reactors appears to be more appropriate for heterogeneous kinetic study of compounds that tends to polymerized in a liquid filled reactor.

However, for intrinsic kinetic measurements in a TBR, one must take care that the reactor performance is exclusively determined by the true kinetic rate. This means to select operating conditions that ensure absence of internal and external mass and transfer limitations and the hydrodynamic interference. This is normally possible only for low rates of reaction, which is the case of CWAO, as the pollutant concentrations are low because they are diluted by water.

### 2.2.2 Periodic operation of fixed bed reactors

Industrial fixed bed reactors are usually operated under steady state conditions. However, recent studies have demonstrated that the reactor performance is significantly improved under forced periodic operation conditions both at laboratory and pilot plant scale [141]. The term 'periodic operation' refers to an operation, in which one or more operating parameters liquid flow rate, feed composition or temperatures are periodically varied in time [142? ]. Some studies on unsteady state TBR operation including CWAO of phenol are reviewed in Table 2.7.

In the last 15 years, most of these studies were dealing with liquid flow [94, 143–151], gas flow and composition [114, 115, 152] and reactant feed composition modulation [150, 153]. The enhancement observed in an unsteady state fixed bed reactor operation arises from the alteration of the gas and liquid phases for supplying reactant to the catalyst surface by periodically modifying the conditions of the gas-liquid hydrodynamics (pressure drop, liquid and gas holdup, partial wetting) and mass and heat transfer in the reactor. For example, the hydrogenation of  $\alpha$ -methyl styrene conducted in a periodically operated reactor (liquid flow modulation) performed an over 400% reaction rate enhancement compared to steady state operation [149, 152, 154]. According to the authors, the enhancement is mainly due to the improvement of the contacting between the two phase by reducing the gaseous reactant transport resistance, i.e better mass transfer due to the liquid pulse that

caused the removal of stagnant liquid pockets (film). Tukac et al [141] studied the hydrogenation of styrene and dicyclopentadiene in a pilot scale TBR under both steady state and periodic liquid flow modulation conditions. The authors found that a 30% higher reactor productivity compared to the corresponding state state operation. Again the authors stated that the improvement of wetting efficiency and heat transfer due to periodic variation of liquid flow was responsible for the higher productivity. Also, a 50% reaction rate enhancement over steady state was attained in removing  $\text{SO}_2$  in a periodically operated TBR packed using activated carbon as catalyst [147, 148]. According to the authors, the water flow during the on cycle continuously restores the catalyst activity by converting the strongly adsorbed  $\text{SO}_3$  into  $\text{H}_2\text{SO}_4$ . Due to such a strong improvement on reactor performance, it has been suggested that unsteady state reactor operation could be a promising tool for process intensification of three phase catalytic reactors [155].

Only a few works has been dedicated to periodic operation of liquid flow [94, 145] and gas flow and composition [114, 115] applied to the CWAO of phenol in fixed bed reactors in the last few years. As a matter of fact, Fixed Bed Reactors can be operated in many ways under periodic conditions, e.g. forced liquid and gas flow rate, reactant feed composition, pressure and temperature modulations [147]. It has been demonstrated that a 10% better reactor performance (conversion enhancement) can be achieved by applying liquid flow modulation to the CWAO of phenol over AC in a TBR [94]. According to the authors, this is mainly due to the modification of partial wetting of the catalyst bed that allows a direct transfer of gaseous reactant to the active site to initiate the oxidation reaction. Larruy et al. [115] and Ayude et al. [114] studied the effect of gas feed composition and gas feed flow modulation on CWAO of phenol over AC in TBR. The authors found a better long term AC performance with reasonable pollutant destruction at a typical CWAO conditions ( $160^\circ\text{C}$ , 2 bar of  $\text{O}_2$  pressure). At these conditions, AC burn-off could be reduced by about 60% for a cycle period of 1 to 2 h and 144 h time on stream maintaining an acceptable phenol conversion ( $>60\%$ ). The improvement is due to the adsorption-desorption dynamics that establish on the AC surface. During the nitrogen or air off period of the cycle, the reaction tends to halt due to the depletion of dissolved oxygen, thereby favouring phenol re-adsorption on the catalyst surface. On the other hand, when the air flow is switched on, the reaction will proceed with the incoming oxygen and the adsorbed phenol, without adversely affecting the carbon surface as long as a sufficient phenol surface coverage is maintained. In other words, periodically refreshing of the AC surface with phenol will help the carbon from being directly attacked by oxygenated radicals formed during CWAO. Nevertheless, during gas flow and composition modulations the temperature front inside the bed can

not fall below the oven temperature to induce more marked adsorption-desorption dynamics. Consequently, it is unlikely to avoid complete carbon burn-off using this strategy at the operating conditions tested. In this sense feed temperature modulation of TBR could be a more promising strategy to achieve the aforementioned goal.

So far, only indirect temperature modulation on TBR has been reported in the open literature [147, 149, 156] although its promising advantage on periodic operation of catalytic reactors has been already pointed out by Silveston [144]. Direct feed temperature modulation strategy has the advantage to exclude the interference of improvement obtained by hydrodynamic and mass transfer enhancement during stop flow in liquid flow modulation. Also, temperature feed modulation is expected to induce temperature driven adsorption-desorption cycle on the AC surface, thereby probably avoided the AC burn-off during CWAO. Summarizing, the ability of periodic operation of TBRs, in particular the application of direct temperature feed modulation for catalyst stability improvement should be investigated more in detail. Strong interest lies also in the modeling of periodic operation of TBR applied to CWAO over AC catalyst. For the particular case of feed temperature modulation, an important aspect is heat transfer in TBRs and therefore a short review on this topic will be included in what follows.

Table 2.7: Review of studies dealing with periodically operated TBRs.

Modulation	System studied	Conditions	Parameters	Catalyst	Ref.
Gas flow (on-off) (composition)	Phenol oxidation	$F_L = 60 \text{ mLh}^{-1}$ $F_G = 2.4 \text{ NLh}^{-1}$	$p = 1 - 4 \text{ h}$ $s = 0.33 - 0.8$	AC	[114]
Gas flow (on-off) (composition)	Phenol oxidation	$F_L = 60 \text{ mLh}^{-1}$ $F_G = 2.4 \text{ NLh}^{-1}$	$p = 0.3 - 4 \text{ h}$ $s = 0.3 - 0.8$	AC	[115]
Liquid flow (on-off)	Phenol oxidation	$F_L = 250 - 500 \text{ gh}^{-1}$ $Q_G = 23 \text{ NLh}^{-1}$	$p = 50 - 300 \text{ s}$ $s = 0.3 - 0.8$	AC	[94]
Liquid flow (on-off)	Phenol oxidation	$F_L = 0.06 - 12 \text{ mLh}^{-1}$ $F_G = 2.4 \text{ NLh}^{-1}$	$p = 3 - 10 \text{ min}$ $s = 0.2 - 0.5$	CuO/Al <sub>2</sub> O <sub>3</sub>	[145]
Liquid flow (on-off)	SO <sub>2</sub> oxidation	$u_L = 0.03 - 1.75 \text{ mms}^{-1}$ $u_G = 12 \text{ cms}^{-1}$	$p = 10-80 \text{ min}$ $s = 0.1-0.05$	AC	[147]
Liquid flow (on-off) Concentration	Dicyclopentadien Hydrogenation	$F_L = 15 \text{ mLmin}^{-1}$ $F_G = 500 \text{ mLmin}^{-1}$ $C = 0.78 \text{ molL}^{-1}$	$p = 60 - 480 \text{ s}$ -	Pd/Al <sub>2</sub> O <sub>3</sub>	[150]
Liquid flow (on-off)	Ethanol oxidation	$Q_{\text{Liss}} = 70 - 170 \text{ cm}^3 \text{min}^{-1}$ $Q_{\text{G}} = 200 \text{ cm}^3 \text{min}^{-1}$	$p = 3 - 9 \text{ min}$ $s = 0.3 - 0.7$	0.5% Pd/Al <sub>2</sub> O <sub>3</sub>	[151]
Liquid flow (on-off)	$\alpha - \text{AMS}$ hydrogenation	$Q_L = 127 \text{ mLh}^{-1}$ $Q_G = 900 \text{ Ls}^{-1}$	$p = 5 - 45 \text{ min}$ $s = 0.3 - 0.5$		[154]
Liquid flow (on-off)	Hydrogenation of olefins	$u_L = 0.8 - 5.3 \text{ mm/s}$ $u_G = 0.18 \text{ Nm/s}$	$p = 40 - 60 \text{ min}$ $s = 0.15 - 0.4$	Pd/Al <sub>2</sub> O <sub>3</sub>	[141]
Liquid flow (on-off)	Ethanol oxidation	$F_L = 0.54 - 0.72 \text{ kgm}^{-2} \text{s}^{-1}$ $F_G = 0.04 \text{ kgm}^{-2} \text{s}^{-1}$	$p = 10 - 900 \text{ s}$ $s = 0.33 - 0.67$	Pt/Al <sub>2</sub> O <sub>3</sub>	[157]
Liquid flow (on-off)	Ethanol, Benzyl alcohol oxidation	$F_L = 0.36 - 0.76 \text{ kgm}^{-2} \text{s}^{-1}$ $F_G = 0.04 \text{ kgm}^{-2} \text{s}^{-1}$	$p = 10 - 1800 \text{ s}$ $s = 0.5-0.67$	Pt/Al <sub>2</sub> O <sub>3</sub>	[158]
Liquid flow (on-off)	Hydrogenation of 2-thylanthraquinones	$u_L = 0.2 - 1.5 \text{ mms}^{-1}$ $u_G = 2.32 \text{ mms}^{-1}$	$p = 20 - 480 \text{ s}$ $s = 0.2 - 0.6$	Pt/Al <sub>2</sub> O <sub>3</sub>	[159]
Liquid flow (Base-peak) Continued on Next Page...	Oxidative coupling of propylene	$F_L = 50 - 150 \text{ mlmin}^{-1}$	$p = 80 \text{ s}$	Bi <sub>2</sub> O <sub>3</sub> -P <sub>2</sub> O <sub>5</sub>	[160]

Table 2.7 – Continued

Modulation	System studied	Conditions	Parameters	Catalyst	Ref.
Liquid flow (on-off) Concentration(on-off)	$\alpha$ -methyl styrene hydrogenation $\alpha$ - <i>AMS</i> hydrogenation	$F_L = 1 - 16 \text{ mms}^{-1}$ $F_G = 90 \text{ mms}^{-1}$ $F_L = 0.083 \text{ mLs}^{-1}$ $F_G = 20 \text{ NLh}^{-1}$ $C_o = 1 - 3.5 \text{ molL}^{-1}$	$p = 10 \text{ min}$ $s = 0.2 - 0.3$ $p = 0.576 - 1.914 \text{ s}$ $s = 0.2 - 0.5$	$\text{Pd/Al}_2\text{O}_3$ $\text{Pd/Al}_2\text{O}_3$	[161] [162]
Concentration (Composition)	NO reduction NO-CO reaction	$F_G = 50 \text{ cm}^3 \text{ min}^{-1}$ $C_{\text{NO}} = 500 - 2000 \text{ ppm}$ $C_{\text{CO}} = 1000 - 6000 \text{ ppm}$	$p = 30 - 180 \text{ s}$ $s = 0.5$	$\text{Rh/Al}_2\text{O}_3$	[163]
Composition	Cyclohexane hydrogenation	$Q_L = 80 - 250 \text{ mLmin}^{-1}$ Composition = 5 - 100 %	$p = 30 \text{ min}$ $s = 0.25 - 0.5$	$\text{Pd/Charcoa}$ $1\% \text{Pd/Al}_2\text{O}_3$	[152]

**Heat transfer in trickle bed reactor:** Over the last 40 years, numerous works on TBR appeared in the literature [164], providing useful information on flow regimes, hydrodynamics and mass transfer. In contrast, only a limited number of studies is available on heat transfer of fixed bed reactors and among them, few deal with heat transfer at low liquid and gas Reynolds number, typically encountered in laboratory TBR studies with reaction. Besides, most of the studies on TBR heat transfer have been carried out at near to ambient conditions with nonreactive system [165, 166] though TBR operation is usually carried out at elevated temperature and pressure [167].

Heat transfer in packed bed reactors has been usually investigated using 2-dimensional pseudo-homogeneous models considering that the phases (gas, liquid, solid) have the same temperature at any location in the reactor [166]. In that case the heterogeneity of the packed bed is usually described by the effective radial heat transfer  $\lambda_r$  in the bed and  $h_w$ , the latter taking into account a resistance to heat transfer close to the wall. accordingly, effective bed thermal conductivity ( $\lambda_r$ ) and effective bed to wall heat transfer coefficient ( $h_w$ ) have been a subject of several investigations [166, 168–173]. Lamine et al [166] presented a detailed study on heat transfer in packed bed reactors considering the hydrodynamics effects, bed and fluid properties. The authors showed that the bed thermal conductivity increases always with the liquid flow rate and particle diameter (1 to 6 mm). On the other hand, the effect of gas flow rate depends on the flow regime. The bed conductivity ( $\lambda_r$ ) is less sensitive (slightly influenced) to the gas flow rate in the low interaction regime (trickle flow), increases with gas flow rate in the bubble flow regime and decreases with gas flow rate in the high interaction regime (pulse flow). The same authors reveal also that liquid properties such as viscosity have a significant effect on bed conductivity. For example, a 20 to 50% higher thermal conductivity in the high interaction regime was observed for water compared to other viscous solutions while a negligible effect was observed in the low interaction regime. Mariani et al [171] studied heat transfer in a packed bed column with different aspect ratio (tube to particle diameter ratio) for a wide range of liquid and gas flow rates. The authors reported that  $\lambda_r$  is strongly influenced by the liquid flow rate while the gas flow rate has a marginal effect. Specchia and Baldi [169] also studied the effect of gas and liquid flow rates on the bed conductivity ( $\lambda_r$ ) in a TBR. The authors demonstrated that  $\lambda_r$  increased slightly with gas flow rate up to a certain range of liquid mass flow rate for both low and high interactive regime.

With respect to the bed to wall heat transfer ( $h_w$ ), Lamine et al [166] revealed that the bed to wall heat transfer coefficient increases monotonically with liquid flow rate in the low interaction regime (trickle flow) and decreases in the pulse flow

regime (high interaction regime), while gas flow rate has only a marginal effect on  $h_w$ . Mariani et al [171], Muroyama et al [170], Specchia and Baldi [169] also studied the effect of gas and liquid flow rate on the bed to wall heat transfer coefficient. Both authors found that  $h_w$  increases with gas and liquid flow rates.

## 2.3 Conclusion

The adequate management of the limited fresh water resources is a mandatory task to ensure a sustainable water supply for the growing world population. In this context, the in-situ pretreatment of all industrial effluents that are refractory or biotoxic and their subsequent reuse is one contribution that can help to achieve this goal. Among the available treatments, CWAO can be pointed out as an effective technique for the abatement of organic pollutants at medium to high concentrations, which are too resistant to the conventional biological wastepaper treatment.

Significant progress has been achieved in the field of CWAO with respect to the development of active noble metal or metal oxide based catalysts. However, the implementation of CWAO at industrial scale requires the availability of stable and less expensive catalysts. Certain activated carbons have demonstrated to be a cheap bi-functional material (adsorbent and catalyst) for effectively removing a variety of non-biodegradable phenolic compounds from wastewater at convenient temperatures and pressures. The CWAO of organic pollutants over AC catalyst follows a complex parallel-series reaction route towards the final products. The main oxidation routes are accompanied by other reactions such as AC combustion and oxidative coupling of phenol. For such complex reaction systems, detailed knowledge of the process chemistry is demanded and research studies should attempt to better elucidate the role that plays AC in the mechanism of CWAO. Moreover, the slow loss of AC due to burn-off at typical CWAO conditions seems unavoidable with the conventional steady state trickle bed reactor operation, preventing thereby its industrial application at a broader level.

It appears also from the literature review that less attention has been given to the optimization, design and scale-up of three phase catalytic reactors applied to CWAO over AC. TBRs that provide a low liquid to catalyst ratio compared to slurry type reactors are a good candidate for CWAO of phenol over AC, because this helps to reduce the extent of liquid phase homogeneous polymerization reactions. Moreover, due to the presence of partial wetting in TBR, gas-liquid mass transfer resistance may not a limiting step. Of course, evaluation of the overall process performance of continuous TBR is not a trivial task, especially with AC being prone to self-combustion under partial wetting conditions. With respect to the aforementioned

---

aspect, controlling the reactant concentration (phenol and oxygen concentration) on the AC surface is thus an import criterion to achieve to long-term catalyst stability during CWAO. In this context, the better performance of periodic operation, i.e. gas feed flow and composition modulation has been already highlighted for phenol CWAO over AC catalyst. Therefore, the present important work addresses in depth the concept of dynamic reactor operation with respect to long term catalyst stability. Feed temperature modulation seems an alternative of periodic operation to enlarge the catalyst life time and will be studied in the present PhD work



## Chapter 3

# Hypothesis and Objective

### 3.1 Hypothesis

Industrial effluents containing bio-toxic compounds are usually discharged to conventional wastewater treatment facilities such as biological wastewater treatment plants (WWTPs). However, these compounds have a negative effect on the microorganisms and therefore require a pre-treatment to reduce their bio-toxicity level. A review of the specific literature points out that catalytic wet air oxidation using active carbon (AC) as a catalyst in a trickle bed reactor can be one promising solution for the destruction of phenolic pollutants at medium to high concentrations. The drawback of using AC is the difficulty to achieve a satisfactory long term stability in TBRs under steady state operation, due to a slow AC combustion during the CWAO. ***The main hypothesis of this research work was therefore there exist an appropriate operating mode and conditions, for which a better catalyst stability and reactor performance will be achieved .***

### 3.2 Objective

Many CWAO studies have been dedicated to the search of active catalysts (mostly noble metal and metal oxide based catalysts) and the establishing of kinetic paths of organic pollutants, in particular of phenol. Alternative catalysts without any active metal phase based on carbon materials are emerging, but their potential is yet not fully established. Moreover, a combined assessment of the process chemistry and engineering aspects is necessary for the proper design and operation of CWAO processes at industrial scale. ***The main objective of this work*** was thus to

develop an appropriate reactor operation strategy for the CWAO of phenol using AC as catalyst. We focus on three aspects to extend the current state of art of CWAO over AC and three phase reactors: reactor start-up , kinetic measurements in TBR and periodic operation of fixed bed reactors. In particular, we formulate the following tasks for each item:

1. Reactor start up to:

- Investigate the effect of different saturation and prewetting procedures of AC on its activity and stability.

2. Kinetic measurement in TBR to:

- Provide conditions for kinetic regime.
  - absence of internal and external mass transfer limitations.
  - no effects of liquid mal distribution and catalyst wetting.
- Study phenol oxidation over AC in a broader range of operating conditions ( $P_{O_2}$ ,  $T$ ,  $F_L$ ,  $C_{Ph,O}$ ). Further attention was paid to the contribution of non-catalytic homogeneous oxidation and the effects of pH and free radical scavengers on phenol oxidation.

3. Periodic operation of Fixed Bed Reactors to:

- Investigate the steady state and dynamic heat transfer in a laboratory scale TBR for a given range of operating conditions ( $P_t$ ,  $F_L$ , and  $F_G$ ) without reaction.
- Use a dynamic pseudo homogeneous one parameter heat transfer model to fit the axial temperature profiles assessed in a packed bed column under nonreactive conditions.
- Investigate the effect of periodic temperature feed and liquid flow modulations on phenol conversion.
- Explore the potential of periodic operation for the long term performance of AC in CWAO.

# Part II

## Methodology

UNIVERSITAT ROVIRA I VIRGLI

CATALYTIC WET AIR OXIDATION OF PHENOL OVER ACTIVE CARBON IN FIXED BED REACTOR: STEADY STATE  
AND PERIODIC OPERATION

Nigus Gabbiye Habtu

ISBN:/DL:T.1262-2011

# Chapter 4

## Experimental

This chapter describes in detail the experimental methods used to study the CWAO of phenol over activated carbon catalyst in a laboratory fixed bed reactor operated in cocurrent gas-liquid down flow or upflow mode. The experimental data has been collected both at steady state and periodic operation conditions.

### 4.1 Materials used

Analytical-grade (>99.9%) phenol was purchased from Merck to prepare aqueous phenol solution using deionized water. Analytical grade tert-butanol, sodium bicarbonate and HPLC grade methanol also obtained from Merck were tested as free radical scavengers. High purity synthetic air was used as oxidant for all oxidation experiments. Pure nitrogen was used to pressurize the reactor prior to each experiment and to study the heat transfer characteristics of TBR under non-reactive conditions. The wood based activated carbon was purchased from Merck (Ref. 2518); its specific characteristics are given in Table 4.1.

Phenol adsorption tests under oxic atmosphere have shown a maximum capacity of  $370 \text{ mg}_{\text{ph}}/\text{g}_{\text{AC}}$  at  $20 \text{ }^\circ\text{C}$  for the active carbon employed. Prior to the CWAO experiments, the 2.5 mm carbon particles were crushed and sieved to obtain size fractions in the range of 0.3-2.5 mm. After crushing, each sample was washed with deionized water several times to remove fines, dried at  $105 \text{ }^\circ\text{C}$  overnight, and stored under inert atmosphere at room temperature. To study the non-catalytic homogeneous contribution to phenol oxidation, alumina particles of 0.5 mm were purchased from Sigma Aldrich.

Table 4.1: Physical properties of AC as provided by Merk.

Property	Value
Pellet size (mm)	2.5
Ash content	3.75%
Fe content	0.4-0.6%
Carbon density (g/L)	2000
Apparent density (g/L)	950
BET specific surface area (m <sup>2</sup> /g)	1156
Pore volume (m <sup>3</sup> /g)	0.55
Average pore diameter (nm)	1.4

## 4.2 Trickle Bed Reactor experiments at steady state

### 4.2.1 Experimental set-up

The original experimental set up used to study the oxidation of phenol in TBR was designed and constructed by Fortuny et al [174]. Figure 4.1 shows that it consists of the following three main sections:

1. Inlet zone including liquid feed and gas feed reservoirs with respective supply lines.
2. Reaction zone including mixing and pre-heating section and a fixed bed tubular reactor ( $L = 20$  cm, I.D = 1.1 cm.)
3. Post separation zone, including a sequence of sampling device, gas-liquid separator, needle valve and gas flow meter, all located at the reactor outlet.

Aqueous phenol solution prepared with deionized water was transported from the 5 L feed tank to the reactor by a high-pressure liquid pump (Eldex AA-100-S2, Napa, CA, USA) that can dispense flow rates between 0.01 and 0.15 L/h. Liquid flow rates were measured with a water calibrated mass flow meter installed in the exit line of the pump. Air and nitrogen were supplied from high-pressure gas cylinders at the required operating pressure adjusted with the help of a pressure-reducing valve. The reactor was carefully filled portion-by-portion with particles (2.5 to 7.5 g of AC with or without inert dilution) so as to ensure repeatable and uniform packing of particles [175]. The reactor tube was further equipped with a thermocouple axially introduced

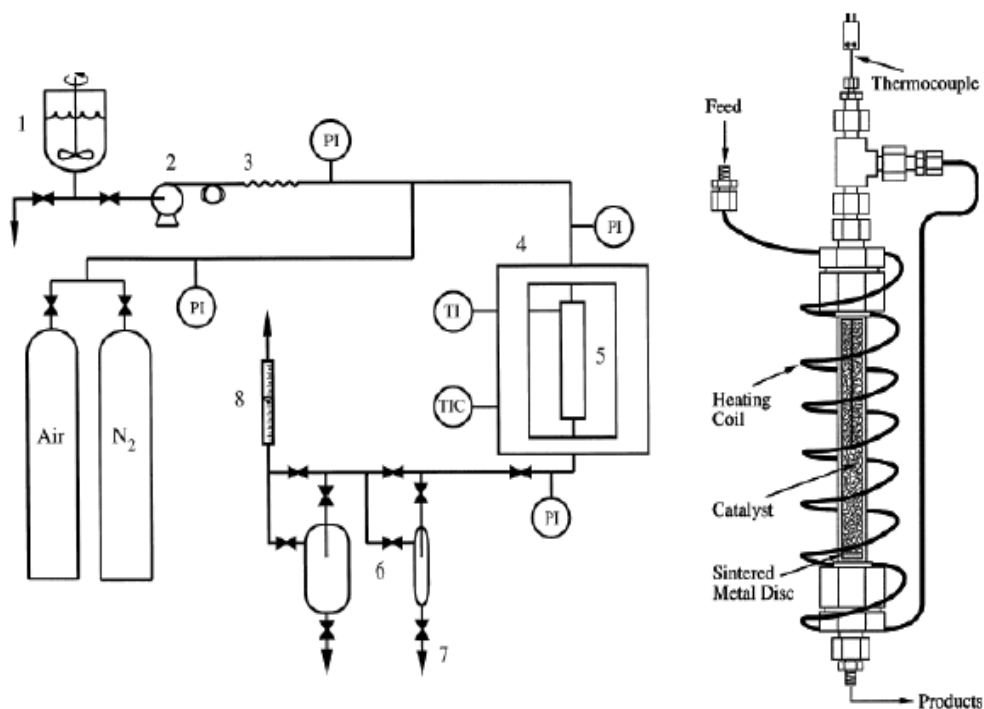


Figure 4.1: Trickle Bed Reactor for steady state experiments. (1) liquid feed tank, (2) pump, (3) flow regulator, (4) oven, (5) trickle bed reactor, (6) gas-liquid separator, (7) sampling valve, (8) gas flow meter.

from the top ( $z = 10$  cm) to monitor the temperature during the reaction and a 1 m long preheating coil. The reactor tube packed with activated carbon and/or inert materials and the coil were placed in an oven with temperature control ( $\pm 1^\circ\text{C}$ ) to attain the required reaction temperature. After tightening all the connections, the reactor was pressurized (25 bar) to check for leaks in the system. After trickling through the catalyst bed retained by two stainless steel metal grids, the exited gas-liquid flow was directed to the gas-liquid separator and the sampling device and finally stored in the gas-liquid separator (5 L). The gas flowing out of the separator was depressurized by means of a needle valve and vented through an air calibrated gas flow meter to measure its volumetric flow rate at ambient conditions of pressure and temperature. The experimental operating conditions and reactor dimensions are listed in Table 4.2.

Table 4.2: Experimental conditions used and fixed bed reactor dimensions.

Variable	Values
Reactor inner diameter, $d_R$ [cm]	1.1
Reactor Height, $H$ (cm)	20 - 25
Particle diameter, $d_p$ (mm)	0.3-2.5
Bed porosity, $\epsilon_B$	0.5
Bed density, $\rho_B$ (kg /m <sup>3</sup> )	0.4
Catalyst weight, $W_{cat}$ (g)	2.5 - 7.5
Inlet phenol concentration, $C_{Ph,o}$ (g/L)	0.5 -10
Temperature, $T$ (°C)	120 - 160
Oxygen partial pressure, $P$ (bar)	0.5 - 3.6
Liquid flow rate, $F_L$ (L/h)	0.03 - 0.11
Superficial liquid velocity, $u_L$ (mm /s)	0.044-0.3
Gas Flow rate, $F_G$ (NL/h)	1.5 - 24
Superficial gas velocity, $u_g$ (mm/s)	4 - 70
Space-time, $\tau$ (h)	0.04 - 0.24

### 4.2.2 Phenol adsorption experiments

Three continuous phenol adsorption-desorption experiments were conducted in the isothermally operated TBR at temperatures of 80, 120 and 160 °C, a total pressure of 15 bar, a liquid flow rate of 58 mL/h and a nitrogen flow rate of 9 NL/h. The reactor was loaded with 7 g of fresh AC and then contacted with phenol solution of 5 g/L and nitrogen flow at a rate of 9 NL/h. During the experiment, the phenol outlet concentration was assessed by taking liquid samples in regular time intervals to establish the breakthrough curve of phenol. On reaching saturation of the AC bed, the feed phenol solution was replaced by ultra-pure water in each experiment to perform phenol desorption under the same operating conditions.

### 4.2.3 Reactor start-up experiments

Four different procedures of reactor start-up (AC bed saturation) were tested with the original laboratory TBR. In the **standard saturation procedure** at 140°C, 2 bar of oxygen partial pressure,  $\tau = 0.12$  h,  $C_{Ph,o} = 5$  g/L and 7.5 g of AC, air and aqueous phenol solution were fed simultaneously into the reactor during 50 h to establish steady state of adsorption and reaction under so called "oxic" conditions.

In the **external AC saturation** procedure, the AC was first saturated in batch mode under vigorous stirring with an 8 g/L of phenol solution at room temperature and oxic conditions (1 bar of air). After saturation, the catalyst was filtered and dried at 105 °C over night and loaded into the TBR. Then, the oxidation experiment was performed with the pre-saturated AC at the operating conditions of the standard start-up procedure.

Likewise, 7.5 g of AC was saturated in-situ (**In-situ AC saturation**) employing a high phenol concentration (10 g/L) and a high liquid flow rate (100 mL/h) at 140 °C and 2 bar of oxygen partial pressure. After the induced fast AC saturation on detecting phenol breakthrough, inlet phenol concentration and liquid flow rate were set back to the standard values (5 g/L, 60 mL/h) to continue the oxidation reaction.

Finally, the presence of an inert atmosphere during reactor start up ("**anoxic**" **saturation**) was studied replacing by the air by nitrogen (flow of 9 NL/h) in the standard saturation procedure. On completing saturation of the catalyst bed, the nitrogen flow was changed to air flow to initiate phenol oxidation. In all cases, the evolution of activity and stability of the catalyst was monitored in terms of phenol and TOC conversion. Moreover, at the end of each experiment, the oven temperature was set to 105 °C to dry the catalyst overnight under nitrogen flow. Then, the catalyst was carefully recovered, weighed and stored under inert atmosphere for further characterization of the catalyst.

#### 4.2.4 Kinetic experiments

**Kinetic regime and flow hydrodynamics:** In order to establish operating conditions in the TBR that ensure kinetic control during phenol oxidation over AC, several oxidation experiments were conducted in the laboratory TBR under different conditions. In the first series, the extent of external mass transfer elimination was determined by varying the gas flow rate from 1.5 to 24 NL/h at 140 °C, 2 bar of oxygen partial pressure, a liquid space time of 0.12 h and a 5 g/L phenol solution. Likewise, catalyst particle sizes in the range of 0.3 - 2.5 mm were examined to determine the influence of intraparticle mass transfer on phenol oxidation at the aforementioned standard operating conditions.

The effect of flow irregularities (liquid mal distribution) on the reactor performance (phenol conversion) was checked by varying the liquid flow rate from 60 to 100 mL/h (constant bed height, at constant catalyst load of 7.5 g) to obtain liquid space time of 0.07 to 0.12 h or, changing the catalyst bed height corresponding to catalyst loads from 2.5 to 7.5 g at constant liquid flow rate of 60 mL/h. In all case

the liquid space time was calculated as follows:

$$\tau = \frac{m_{\text{cat}}}{m_L} \quad (4.1)$$

where  $m_{\text{cat}}$  is the mass of catalyst loaded in the reactor and  $m_L$  the liquid mass flow rate of the feed solution.

In additional experiments, the catalyst bed was diluted with inert  $\text{Al}_2\text{O}_3$  and/or glass bead particles of the same size maintaining the same bed length that corresponds to 7.5 g, and the liquid flow rate ranging from 60 to 100 mL/h.

Finally, the effect of initial catalyst wetting on reactor performance was investigated by conducting oxidation experiments in a pre-wetted TBR and flooded upflow fixed bed reactor. For the former experiment, the catalyst bed was pre-wetted under inert atmosphere at room temperature according to the method of Levec for Trickle Bed operation [134, 135, 176, 177]. Then, the oven temperature, reactor pressure and liquid flow rate were adjusted to start the oxidation reaction at 140 °C, 2 bar of oxygen partial pressure and 0.12 h of liquid space time. Additional oxidation experiments were conducted in an gas-liquid upflow fixed bed reactor for the same range of liquid space time (0.04 - 0.24 h) at 160 °C, 2 bar of oxygen partial pressure to obtain reactor data corresponding to completely wetted catalyst particles.

**Effect of main operating condition ( $C_{\text{Ph}}$ ,  $T$ ,  $P_{\text{O}_2}$ ,  $\text{pH}$ ):** Catalytic wet air oxidation experiments were conducted in a TBR in a wide range of operating conditions employing the standard reactor start-up procedure. Gas flow rate and particle diameter of 9 NL/h and 0.5 mm, respectively were used to avoid both external and internal mass transfer resistances in the experiments. Taking into account the experimental phenol conversions and the liquid flow rates employed, the total oxygen consumption during the runs was below 10% of the oxygen fed in the gas phase, except for the experiment at 160°C, 0.2 MPa and higher liquid flow rate of 100 mL/h, for which a gas phase oxygen consumption of up to 25% occurred [124]. Temperature, oxygen partial pressure, liquid flow rate and phenol inlet concentration were varied between 120 - 160°C, 0.5 - 3.6 bar, 30 - 100 mL/h and 0.5 - 10 g/L, respectively.

In order to minimize the total run time of each experiment series, on reaching first steady state of adsorption and reaction at 140°C and 2 bar of oxygen pressure, one sequential variation of phenol inlet concentration (from 5 to 2.5 to 1 to 0.5 back to 5 g and then to 10 g/L) was performed with fresh AC bed at a fixed space time. For each new phenol inlet concentration, the reaction was allowed to reach steady state of adsorption-reaction, monitored by immediately analyzing the liquid effluent via HPLC. In total, the experiment series lasted thus about 80 h. This procedure

Table 4.3: Buffers used for pH variation in CWAO.

Buffer used	Proportion	pH
$C_6H_8O_7$	19.2 g	3.0
$C_6H_5K_3O_7$	23 g	
$C_2H_4O_2$	5.7 mL	4.5
$C_2H_3NaO_2$	8.2 g	
$KH_2PO_4$	12.8 g	6.8
$K_2HPO_4$	15.8 g	
$H_3BO_3$	31.4 g	9.2
NaOH	4 g	

was repeated for different liquid space times to obtain phenol concentration profile for different phenol inlet concentration. At the end of each experimental series, a control check of the initial activity of the catalyst was done with 5 g/L of phenol solution.

A similar (sequential) strategy was adopted in all experiments conducted at different reactor inlet temperatures and oxygen partial pressures. The variation of reactor temperature and pressure were readily achieved by adjusting the oven temperature and the pressure reducer placed in the gas line before the mixed intersection of gas-liquid line. As for the phenol outlet concentration sequence, a fresh catalyst load was used in each experimental series to minimize catalyst deactivation.

With respect to the influence of pH on CWAO of phenol over AC, four experiments were carried out at standard conditions by adjusting the pH (3, 4.5, 6.8, 9.2) of feed solution with different buffer solutions. Table 4.3 lists the chemicals used for the preparation of each buffers solution. The specified proportion of each acid-salt couple gives concentrations of 0.1 M, when diluted to a one liter solution. The variation of pH of the buffer during preparation was adjusted with a drop wise addition of either 6 M HCl or 6 M NaOH.

**Wet air oxidation and free radical scavengers:** Experiments have been done to highlight both the contribution of non-catalytic wet oxidation and the influence of free radicals scavengers during CWAO of phenol over AC. For Wet Air Oxidation (WAO) experiments, the reactor was filled with inert glass beads and/ alumina of 0.5 mm to maintain the same flow hydrodynamics as for CWAO over AC. The homogeneous oxidation was carried out at 120-160 °C, 2 bar of oxygen partial pressure

and different liquid space times of 0.12-0.5 h. In addition, the contribution of small amount of homogeneous iron catalyst to the liquid phase oxidation of phenol was investigated by adding 25 ppm of  $\text{FeSO}_4$  to the phenol feed solution during WAO. The selected iron concentration ( $\text{Fe}^{2+} = 25$  ppm) corresponds to the maximum leached iron content detected in the CWAO effluent of phenol oxidation over AC in TBR at 160 °C. For the effect of radical scavenger experiments, the oxidation runs have been conducted with three different free radical scavengers (methanol, t-butanol and sodium bicarbonate) at variable feed concentration (1 - 10 g/L ) and at the standard operating conditions (140 °C, 2 bar of oxygen partial pressure and liquid space times of 0.12 h).

## 4.3 Fixed Bed Reactor Experiments with Periodic Operation

### 4.3.1 Gas-liquid feed temperature modulated TBR

#### 4.3.1.1 Experimental set-up

All experiments under reacting and non-reacting conditions were conducted in the modified TBR set-up shown in Figure 4.2.

The liquid and gas supply facilities were as described in section 4.2. After the mixing intersection of gas and liquid lines, a timer controlled three-way valve (5) was placed to enable continuous feeding of hot gas-liquid flow (pre-heated in a 1 m long coil) to the reactor or alternating cold with hot gas-liquid flow during column operation under feed temperature modulation.

Moreover, the old reactor tube was taken out of the oven and replaced by a new 25 cm long tube, thermally insulated and equipped with three thermocouples at axial distances from inlet of respectively 1.5, 10 and 20.5 cm to assess axial reactor temperature profiles. Tubing from the pre-heater outlet to the column inlet and from the column outlet to the gas-liquid separator was also insulated, in particular to reduce heat loss in the inlet section of the column. Moreover, for minimization of axial heat conduction through the tube walls and fitting connections, a system of two flanges thermally insulated has been mounted at the column outlet. After trickling through the packed bed retained by two metal grids, the exited gas-liquid was directed to the sampling device and finally stored in the 5 L gas-liquid separator. Table 4.4 summarizes the operating conditions employed in the experiments on heat transfer and feed temperature modulation.

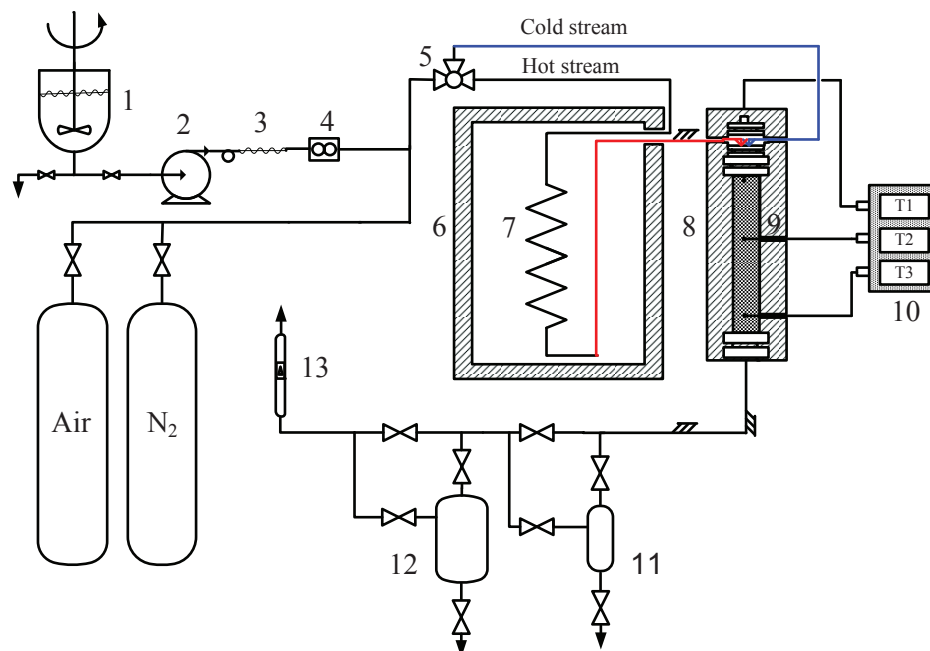


Figure 4.2: Trickle Bed Reactor for feed temperature modulation experiments;(1) liquid feed tank, (2) feed sampling valve,(3) high pressure liquid pump, (4) pulse dampener, (5) three-way valve, (6) heating coil (7) heat exchanger, (8) insulation foam, (9) trickle-bed reactor, (10) temperature display panel, (11) gas-liquid separator, (12) gas flow meter.

#### 4.3.1.2 Heat transfer study

The heat transfer study was performed operating the adapted trickle bed column (see Fig 4.2) at very low liquid (0.15 - 1) and gas (0.35 - 4.5) Reynolds numbers, however typically encountered in TBR studies at laboratory-scale. The ultimate aim of these experiments was to provide data on heat transfer required for the modelling of phenol CWAO over AC in TBR operated under feed temperature modulation.

Firstly, several insulating materials and geometries were tested to establish steady state axial temperature profiles in the trickle bed column suitable for the determination of heat transfer parameters. The following configurations were available: I) no insulation; II) two joint rectangular boards of dense ceramic fiber; III) a flexible cylindrical glass fiber wool mantle covered with aluminum foil; two joint half cylinders IV) of rock wool foam supported with PVC or V) of polyurethane supported with PVC. Characteristic data of the systems used is listed in Table 4.5. The tests

Table 4.4: Operating conditions used for heat transfer and temperature feed modulation.

Variable	Value
Reactor inner diameter, $d_R$ (cm)	0.93
Reactor height, $H$ (cm)	25
Bed weight, $W_{cat/inert}$ (g)	7.5 or 30
Particle, diameter, $d_p$ (mm)	0.5 or 2
Total pressure, $P_T$ (bar)	9 - 25
Reactor temperature, $T_{Inlet}$ ( $^{\circ}C$ )	120 - 180
Liquid flow rate, $F_L$ (L/h)	0.03 - 0.1
Superficial liquid velocity, $u_L$ (mm/s)	0.09 - 0.3
Liquid Reynold's number, $Re_L$	0.15 - 1
Gas flow rate, $F_G$ (NL/h)	3 - 18
Superficial gas velocity, $u_G$ (mm/s)	0.08 - 6.6
Gas Reynold's number, $Re_G$	0.35 - 4.5
Period (h)	0.5 - 4
Split	0.5 - 0.94

were conducted at the following conditions: oven temperature of  $170^{\circ}C$ , 16 bar of total pressure, water and nitrogen flow rates of respectively 100 mL/h and 18 NL/h using active carbon as packing material of the column.

A few experiments were undertaken with configuration II) and providing the

Table 4.5: Characteristics of insulating systems used for heat transfer study.

Material	Geometry	I.D. (cm)	O.D. (cm)	$\lambda_{heat}$
Polyurethane	cylindrical	1.1	15	0.016-0.020
Rock wool	cylindrical	1.1	10	0.045
Glass fiber	cylindrical	1.1	5	0.05
Ceramic fiber	rectangular	10 x 2.5 x 40	-	0.09

column outlet with a system of two assembled flanges to disrupt the axial heat flow through the outlet fittings of the column. To this end, all possible contact points between the two flanges (screws, nuts and flanges itself) were thermally insulated using seals with a low thermal heat conductivity. Experiments conducted with and without flanges at otherwise same operating conditions revealed no differences in

axial profiles indicating that the heat transfer due to axial wall conduction should not be relevant in our system.

With configuration IV and AC packing, the effect of operating variables ( $P_T$ ,  $F_L$  and  $F_G$ ) on the heat transfer was investigated at steady state conditions. In a standard experiment, a liquid flow rate of 100 mL/h was fixed for a given total pressure and gas flow rate to warm up the reactor until reaching stable temperatures. Subsequently, the liquid flow rate was decreased to 60 mL/h to establish a new steady state and finally to 30 mL/h. This standard procedure was repeated for different pressures (9-25 bar) and gas flow rates (3-18 NL/h). For each condition selected, an axial temperature profile was assessed at steady state for posterior determination of the overall and wall to bed heat transfer coefficient by fitting the experimental data to predictions of a one parameter heat transfer model as described in Chapter 5. Reproducibility of experiments has been confirmed by several repetition of the standard experiment resulting in same axial temperature profiles. Deviations were only observed after dismantling the insulating material of the column. In this case, the insulating material was dismantled and properly fixed again as to obtain reproducibility in the temperature profiles. To further avoid this problem, a maximum of experiments were done without dismantling the column.

#### 4.3.1.3 Feed temperature modulation without reaction

A first set of periodic operation experiments were performed in the absence of chemical reaction ( $N_2$  - Water - AC) to study the dynamics of trickle bed column. The standard procedure for column heating was as for continuous operation. Temperature cycling was initiated via the timer controlled three-way solenoid valve on reaching stable axial temperatures. Dynamic profiles were then assessed at least for two consecutive cycles by recording in regular time intervals of 3 to 6 min the temperature displayed by each of the three thermocouples mounted along the column. The range of operating parameters studied was limited to conditions that are of particular interest for periodically operated CWAO of phenol: cycle periods of ca. 1 - 2 h and splits between 0.8 - 0.9 h, water and nitrogen flow rates and total system pressure of 30 to 100 mL/h, 9 NL/h and 10 bar or 16 bar, respectively.

A second experiment was done to study the dynamics of adsorption/desorption phenol over AC without reaction ( $N_2$  - Phenol Solution - AC) but under feed temperature modulation. The trickle bed column, insulated with polyurethane foam (configuration V), was brought to steady temperature by continuously feeding the pre-heated nitrogen and aqueous phenol mixture to the reactor tube packed with AC. On reaching stable temperature, feed temperature cycling was started via the timer controlled three-way solenoid valve. Liquid phenol concentrations as well as

axial temperature profiles were subsequently measured at 2, 7, 10 and 25 h time on stream for the selected cycle period and split of 1.8 h and 0.83 respectively. The temperature displayed by each of the three thermocouples was registered in regular time intervals of 3 to 6 min. Accordingly, the phenol concentration profiles were obtained by taking liquid samples at the reactor outlet every 6 minutes and analyzing them immediately by HPLC. The other conditions of the experiments were:  $P_T = 16$  bar,  $T_{oven} = 168^\circ\text{C}$ ,  $F_L = 60$  mL/h and  $C_{Ph,o} = 5$  g/L.

#### 4.3.1.4 Feed temperature modulation with reaction

To compare isothermal and adiabatic reactor performance at steady state, an adiabatic oxidation experiment was conducted with the adopted TBR set up for 30 h operating time in the same conditions of  $163^\circ\text{C}$ , 2 bar of oxygen partial pressure and 0.12 h of liquid space time. During the experiment, liquid samples were withdrawn every 2 h and analyzed immediately with the help of HPLC. Also, axial temperature readings of the reactor were taken at steady state operation with the respective thermocouples.

For the CWAO experiments with feed temperature modulation (done with insulating configuration V), the oxygen partial pressure and, volumetric liquid and gas flow rates were kept constant at 2 bar and, 63 mL/h and 9 NL/h, respectively. The reactor inlet temperature used was 153 or  $163^\circ\text{C}$ .

Experiments were conducted over 50 h with different combinations of cycle period and split. In all cycling experiments, feed temperature modulation was only started on reaching steady state of adsorption and reaction (after ca. 25 h). The experiments were performed in slow mode with cycle period of 0.5, 1, 1.8 and 4 h and splits of 0.5, 0.6, 0.8 and 0.9. The split ( $s$ ) in feed temperature modulation is defined as the fraction of total cycle time ( $t_T$ ), during which the hot gas-liquid feed mixture flushes the catalyst bed ( $t_H$ ):  $s = t_H/t_T$ .

Similarly, liquid sample and temperature reading were taken every 6 minutes for one or two consecutive cycles depending on the period-split combination. A reference steady state catalytic wet air oxidation experiment was also conducted over ca. 50 h at the same conditions.

In the last series, catalytic wet air oxidation experiments were performed over ca. 150 h for two different reactor inlet temperatures of 163 and  $152^\circ\text{C}$  to assess the stability of AC. The modulation experiments were conducted with a split of 0.8 and different periods of 0.5 h, 1 h and 1.8 h. Corresponding continuous catalytic wet air oxidation experiments at steady state were also performed for ca. 150 h times on stream at  $163^\circ\text{C}$  and otherwise same operating conditions. Temperature evolution was monitored at the three axial positions and liquid samples were taken

every 6 min. After each CWAO experiment, the spent catalyst (AC) was dried overnight inside the reactor under nitrogen flow and then carefully recovered for weight measurement and BET surface area determination.

### 4.3.2 On-off liquid flow modulated upflow FBR

#### 4.3.2.1 Experimental set-up

The experimental set-up and conditions used in these experiments are shown in Figure 4.3 and Table 4.6, respectively. For modulation of the liquid flow rate, the gas feed line was equipped (upstream of the mixing intersection of gas and the liquid) with a by-pass (7) directly connected to the reactor inlet. The liquid line was also provided with a by-pass (tubing 8) to the gas-liquid separator. In this way, the timer controlled three-way valve (5) enables the liquid and gas to pass (tubing 7) through the reactor during the liquid on cycle interval or by-pass the liquid flow (tubing 8) to the gas-liquid separator during the liquid off cycle interval. In addition, the direction of the gas-liquid flow was inverted to operate the reactor under cocurrent gas-liquid upflow mode. The liquid and gas supply lines and post separation facilities are as described in section 4.2. The exited gas-liquid mixture flows to the sampling device and the gas-liquid separator, where the liquid fraction was finally stored.

Table 4.6: Operating conditions used for liquid flow modulation.

Variable	Value
Reactor inner diameter, $d_R$ (cm)	1.1
Reactor height, $H$ (cm)	20
Catalyst weight, $W_{cat}$ (g)	7
Particle diameter, $d_p$ (mm)	0.5
Oxygen partial pressure, $P_{O_2}$ (bar)	2
Reactor temperature, $T_R$ ( $^{\circ}C$ )	160
Liquid flow rate, $F_L$ (mL/h)	58
Gas flow rate, $F_G$ (NL/h)	9
Period (h)	0.5 - 4
Split	0.5 - 0.94

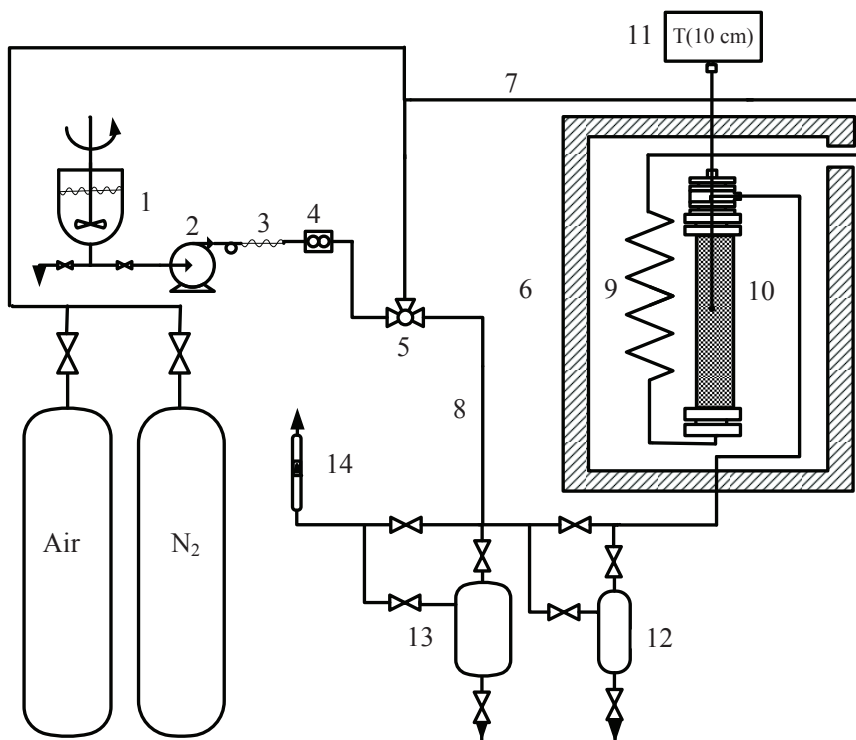


Figure 4.3: Fixed Bed Reactor for liquid flow modulation experiments: (1) feed, (2) HPL pump, (3) pulse dampener, (4) flow meter, (5) three way valve, (6) oven, (7) liquid-gas line, (8) liquid by-pass line, (9) heating coil, (10) fixed bed reactor, (11) temperature display panel, (12) sampling tube, (13) G-L separator, (14) gas flow meter.

#### 4.3.2.2 On-off liquid flow modulation experiments

Periodic CWAO experiments were conducted at a fixed oxygen partial pressure, gas flow rate and oven temperature of 2 bar, 9 NL/h and 158°C, respectively. For comparison, continuous experiments at steady state were also conducted at the corresponding mean volumetric liquid flow rates. Change of initial catalyst activity was also checked at the end of each experiment.

Different combinations of cycle period and split were tested in short term experiments (50 h time on stream) to highlight their effect on mean cycle conversion of phenol. For each cycling experiment, liquid flow modulation was initiated after ca. 25 h of standard reactor start up. In order to operate at the same liquid flow rate as in the steady state operation ( $Q_{ss}$ ), the cycle liquid flow rate ( $Q_{cyc}$ ) had to be

adjusted depending on the split used:  $Q_{cyc} = Q_{ss}/s$ . For liquid flow modulation, the split is defined as the ratio of the total time fraction during which the gas-liquid mixture flushes the catalyst bed over the total period length and was calculated as follows:  $s = t_{Li}/t_T$ . The experiments were performed in slow mode with periods of 0.2 h, 0.5 h, 1 h and 1.8 h and different splits of 0.5, 0.6, 0.8 and 0.9.

Accordingly, long-term experiments were conducted over ca. 150 h under liquid flow modulation using two periods of 0.2 or 0.5 h and splits of 0.5 and 0.8, respectively. To compare the periodic results, a steady state oxidation experiment was performed for ca. 150 h at otherwise same operating conditions. In all cases, reaction temperature was monitored with a thermocouple mounted at the center of the reactor ( $z = 10$  cm) and liquid samples were taken every 6 min at the reactor outlet for more than 10 consecutive cycles depending on the period-split combinations. The spent AC was dried over night under nitrogen flow and then carefully recovered for weight measurement.

## 4.4 Analytical Methods

### 4.4.1 Liquid effluent analysis

Liquid samples withdrawn during CWAO or adsorption experiments were analyzed with a high performance liquid chromatography (HPLC) equipped with an isocratic pump, an autosampler, a ProntoSIL C18 reverse phase column (250mm 4mm 5m) and a UV detector operated at 254 nm. The separation was achieved with a mobile phase mixture of ultra-pure water (acidified to pH =1.41 with  $H_2SO_4$ ) and HPLC grade methanol (35:65 by volume) programmed at 1 mL/h flow rate. The column was operated at a constant temperature of 30°C. Prior to injection into the analytical HPLC column, the samples were filtered in order to remove fines. The established phenol calibration curve was regularly checked with standard phenol solutions to correct deviations in column performance. Phenol conversion  $X_{Ph}$  was calculated by the following expression:

$$X_{Ph} = \frac{C_{Ph,in} - C_{Ph,out}}{C_{Ph,in}} \quad (4.2)$$

where  $C_{Ph,in}$  is the inlet phenol concentration and  $C_{Ph,out}$  the outlet phenol concentration measured during CWAO or adsorption experiments.

The total organic carbon content (TOC) of the liquid sample was measured using a TOC analyzer equipped with a reactor and non-dispersive infrared detector (NDIR). TOC was determined as the difference between total carbon (TC) and total

inorganic carbon (TIC) measured. The sample was acidified with 2 N HCl (pH =2) outside the analyzer to completely convert the inorganic carbon into dissolved CO<sub>2</sub>. The inorganic carbon free sample was drawn from the sparger and charged into the reactor. As phenol, TOC conversion was calculated as:

$$X_{\text{TOC}} = \frac{C_{\text{TOC},in} - C_{\text{TOC},out}}{C_{\text{TOC},in}} \quad (4.3)$$

where  $C_{\text{TOC},in}$  is the inlet total organic content and  $C_{\text{TOC},out}$  outlet total organic content.

The progress of the reaction was further followed by measuring effluent pH directly from the liquid samples using a pH meter (Model CRISON GL21) equipped with a K/KCl electrode.

#### 4.4.2 Catalyst characterization

The textural properties of AC were determined by N<sub>2</sub> adsorption isotherm at 77 K in a micromeritics instrument model ASAP 2000 surface area analyzer. Prior to analyzing, about 500 mg of AC was outgased under vacuum for 8 h at 120 °C. The surface area and micropore volume were calculated from BET surface area using the micromeritic software.

Thermogravimetric analysis (TGA) was carried out on a Perkin-Elmer TGA 7 microbalance (accuracy of 1 mg), which was equipped with an automatically programmed temperature controller. A sample of 20 mg was heated from 100 to 400 °C at a heating rate of 10 °C/min and hold at 400 °C for 1 h to remove any weakly physisorbed compounds. Then, the heating was continued to 900°C at the same heating rate.

Moreover, digestion and atomic absorption analysis was performed for some AC samples to determine their content of metals (Fe). A sample of 100 mg of AC was digested in 2 mL of concentrated nitric acid in a microwave digestion equipment (PAAR, model M627) for 30 min at 180 °C. The resulting colorless liquid was diluted with deionized water by a ratio of 2:50 and analyzed with atomic adsorption spectrophotometer. In addition, iron eventually leached from AC into effluent during CWAO was determined with atomic absorption analysis.

Adsorption isotherms were also determined for both AC samples spent at different CWAO operating conditions and fresh AC. These experiments were conducted in batch mode at room temperature and atmospheric pressure. The isotherms were assessed by introducing 0.25 g of AC in each of the flasks (100 mL) used, each flask containing 50 mL of aqueous phenol solution with a different initial concentration

(ranging from 0.5 to 10 g/L). The AC and phenol solution were equilibrated during 3 h under continuous stirring (500 rpm) and allowed to settle for 1 h. Finally, an aliquot of 1 mL was carefully taken from each flask with a micro-syringe and filtered using microfilter (0.45  $\mu$ m) to determine the equilibrium concentration of phenol in the liquid sample via HPLC.



## Chapter 5

# Modelling of Heat Transfer in Trickle Bed without Reaction

This chapter presents the model equations used to describe the heat transfer in a trickle bed column (non reaction) at steady and non-steady state conditions. The equations and their numerical solutions were developed by Profs. A. Ayude and P. Haure from INTEMA University Mar del Plata in the framework of a collaboration between our research groups.

### 5.1 Model equations and numerical solutions

In the absence of any chemical reaction, no significant interfacial temperature gradients will develop in the trickle-bed and the use of a pseudo-homogeneous one parameter plug flow model for heat transfer description is reasonable. Moreover, only flat temperature gradients should establish in radial direction given the particular geometry of our laboratory trickle-bed set-up: insulated narrow tube (0.93 cm in diameter) containing prewetted small carbon particles (0.5 mm) acting as an acceptable heat conductor. Thus, the model contemplates only one resistance to heat transfer inside the tube, i.e. from the trickle-bed to the inner tube wall at the vicinity of tube wall.

On the other hand, for small tube diameters, wall (flow) effects may become too influent and invalidate the plug flow assumption. However, the validity of plug flow appears to depend on the aspect ratio  $d_R/d_p$  rather than on  $d_R$  alone. Mariani et al. [171] concluded in their work that wall effects can be neglected as long as the aspect ratio is  $> 17$ . The aspect ratio of our trickle-bed takes thus an adequate value of 19 due to the reduced size of the carbon particles. As to axial dispersion of

heat, Mears et al. (1971) as cited in a review on criteria to ensure ideal behaviors in trickle-bed reactors (Mederos et al. [178]) established that axial dispersion of heat can be neglected for tube length to particle diameter ratio  $> 30$ , being as high as 500 in our case.

A last concern is related to the occurrence of liquid maldistribution at small liquid flow rates. To reduce undesired liquid maldistribution, both a narrow tube and small particles are required (the bed itself will then act as a gasliquid distributor). The importance of particle and tube diameter for flow homogeneity is also reflected in the criteria available in the review of Mederos et al.[178] for the estimation of liquid maldistribution ( $L_R > 0.25 d_R^2 / d_p^{0.5}$ ) and adequate wetting or even irrigation ( $W = \mu_L u_L / (\rho_L d^2 g) > 4 \times 10^6$ ). Accordingly, the verification of these criteria at the conditions of our study shows that both are fully met by at least one order of magnitude.

Summarizing, the heat transfer in the laboratory trickle bed column in the absence of phenol oxidation was modeled based on the following assumptions:

- Spherical and isothermal pellets,
- Complete internal wetted particle,
- Homogenous packed bed (constant bed porosity),
- Negligible pressure drop and radial gradients,
- No isothermal gradients between gas, liquid and solid phase,
- Heat transfer between packed bed and reactor wall,
- Instantaneous saturation of gas phase and with water vapour.

Taking into account these assumptions, the non steady state pseudo homogeneous energy balance over the bulk fluid phase at reactor length scale gives:

$$\frac{\partial T}{\partial t} = \frac{- (u_L c_p \rho_L + u_G c_p \rho_G) \frac{\partial T}{\partial z} - \frac{\partial \alpha_w}{\partial z} - \frac{\Delta H^v}{\pi \left(\frac{DI}{2}\right)^2} - U \frac{4}{DI} (T - T_w)}{\epsilon_L c_p \rho_L + \epsilon_G c_p \rho_G + (1 - \epsilon_L - \epsilon_G) \epsilon_L c_p \rho_L + (1 - \epsilon_L - \epsilon_G) (1 - \epsilon_p) c_p \rho_s} \quad (5.1)$$

where:

$$\frac{\partial \alpha_w^G}{\partial z} = \frac{(\alpha_T^G) \frac{\partial P_w^v}{\partial T} \frac{\partial T}{\partial z}}{P_T - P_w^v} = \left( \alpha_{Air}^G + \frac{\alpha_{Air}^G P_w^G}{P_t - P_w^v} \right) \frac{\partial P_w^v}{\partial T} \frac{\partial T}{\partial z} \quad (5.2)$$

The axial variation of the gas and liquid superficial velocity was calculated as follows:

$$\frac{\partial u_L}{\partial z} = \frac{M_w}{\rho_L \pi \left(\frac{DI}{2}\right)^2} \frac{\partial \alpha_w^L}{\partial z} + \frac{\partial \alpha_w^L}{\pi \left(\frac{DI}{2}\right)^2} \frac{\partial (1/\rho_L)}{\partial z} \quad (5.3)$$

$$\frac{\partial u_G}{\partial z} = \frac{R_w}{P_T \pi \left(\frac{DI}{2}\right)^2} \left[ \frac{T \partial \alpha_w^L}{\partial z} + \left( \alpha_w^G + \alpha_w^G \frac{P_w^v}{P_T - P_w^v} \right) \right] \frac{\partial T}{\partial z} \quad (5.4)$$

The inlet boundary conditions at reactor scale are as follows:

$$Z = 0; \quad T = T_0; \quad u_L = u_{L,o}; \quad u_G = u_{G,o}$$

For numerical solution, the resulting continuous differential equations were all replaced by their finite difference approximations. Solution to the heat balance in the bulk liquid was obtained with the help of explicit finite differences. A FORTRAN code was developed for the unsteady state model and various discretization strategies were tested to verify model convergence. The dynamic model was solved considering the operating conditions listed in Table 4.4 and the variation of physical properties of gas, liquid and solid phases with temperature. Static and dynamic liquid holdups were evaluated using the correlation proposed by Lange et al. [179] for low liquid and gas Reynolds numbers.

## 5.2 Determination of overall (U) and wall to bed heat transfer coefficient ( $h_w$ )

For an insulated cylindrical packed bed column with co-current gas-liquid flow, the overall heat transfer coefficient U, accounting for several radial resistance in series that can be expressed as follows (U is based on the column inside area,  $R_1$ ):

$$U = \frac{1}{1/h_w + \frac{\ln(R_{IN}/R_i)R_i}{k_{IN}} + \frac{R_i/R_{IN}}{h_{NAT}}} \quad (5.5)$$

where  $h_w$  represents the bed to reactor wall heat transfer,  $k_{IN}$  the thermal conductivity of the insulating material and  $h_{nat}$  the coefficient of heat transfer due to natural convection between the insulating wall and the surrounding air. Values of  $h_{nat}$  were calculated using the correlation proposed by Churchill and Chu et al [180] for laminar flow:

$$Nu_{NAT} = \frac{h_{NAT} d_p}{k_L} = 0.36 + \frac{0.518 Ra_D^{1/4}}{\left[1 + (0.559/Pr)^{9/16}\right]^{8/27}} \quad (5.6)$$

where the Rayleigh number is give by:  $Ra_D = Gr_D \cdot Pr = \frac{\beta \Delta T g D^3}{Pr \nu^2}$ .

In the first step, the overall heat transfer coefficient  $U$  was obtained for each experiment by searching the value of  $U$  that best fits the predicted to the experimental axial temperature profile at steady state. Moreover, it was possible to deduce the thermal conductivity of the insulating materials tested and experiments done with and without heat insulation at otherwise same operating conditions from equation 5.7.

$$k_{IN} = \frac{\ln(R_{IN}/R_1)R_1}{\left( \frac{1}{U_{IN}} - \frac{1}{U_{No,IN}} - \frac{R_1/R_{IN}}{h_{NAT,IN}} + \frac{R_1/R_2}{h_{NAT,NoIN}} \right)} \quad (5.7)$$

where  $U_{insu}$  and  $U_{Noinsu}$  are overall coefficients determined from fitted values of equation 5.1 with and without insulation, respectively. Similarly,  $h_{NAT,insu}$  and  $h_{NAT,Noinsu}$  are natural convection heat transfer coefficients obtained with and without insulating the reactor tube.  $R_1$  and  $R_2$  are inside and outside radius of the reactor tube, respectively.

The corresponding wall to bed heat transfer coefficients ( $h_w$ ) were subsequently evaluated from equation 5.8 using a know value of  $U$ ,  $k_{IN}$  and  $h_{NAT}$ .

$$\frac{1}{h_w} = \frac{1}{U} - \frac{\ln(R_{IN}/R_i)R_i}{k_{IN}} - \frac{R_i/R_{IN}}{h_{NAT}} \quad (5.8)$$

# Part III

## Results and Discussion

UNIVERSITAT ROVIRA I VIRGLI

CATALYTIC WET AIR OXIDATION OF PHENOL OVER ACTIVE CARBON IN FIXED BED REACTOR: STEADY STATE  
AND PERIODIC OPERATION

Nigus Gabbiye Habtu

ISBN:/DL:T.1262-2011

## Chapter 6

# CWAO of Phenol over AC in Steady State Trickle Bed Reactor

In general intrinsic reaction kinetics has to be studied in a reactor that ensures the absence of any flow hydrodynamic and mass and heat transfer effects. This can be readily achieved in a batch reactor by vigorous stirring and proper selection of catalyst particle size that sufficiently minimize external and internal transport limitations. Nevertheless, the high liquid to solid ratio could influence the intrinsic heterogeneous kinetics through enhanced contribution of liquid phase homogeneous reaction. Phenol is known to form condensation products in the liquid phase during CWAO [55], hence it may be impossible to conduct a sole heterogeneous kinetic study in a batch slurry reactor. Moreover, when the activity of catalyst gradually changes with course of reaction, as it is the case for AC catalysts, kinetic and catalyst deactivation cannot be easily decoupled in batch experiments. In such cases, TBRs appear to be a better candidate to study kinetics of CWAO [109, 140]. However, prior to do kinetic experiments it has to be ensured that the activity of AC is not limited by flow hydrodynamics of TBR and/or mass and heat transfer effects. Moreover, it is of interest to study the effect of reactor start up on the ultimate performance of AC catalysts during CWAO processes. Thus, the TBR kinetic measurements of phenol oxidation over AC were only performed after analyzing in detail the results obtained in the study of the hydrodynamics of the gas-liquid flow and reactor start up.

## 6.1 Reactor Start-up

### 6.1.1 Adsorption of phenol over AC under anoxic condition

Continuous phenol adsorption/desorption experiments were carried out in a trickle bed column packed with AC for three different temperatures (80, 120, 160°C). The determination of the breakthrough curves of phenol was done under "anoxic" conditions at standard operating conditions ( $C_{Ph} = 5$  g/L,  $F_L = 60$  mL/h,  $F_{N_2} = 9$  NL/h,  $P_T = 15$  bar), and results obtained are illustrated in Figure 6.1. Integration of the area between the phenol outlet concentration-time curve and the 5 g/L feed line multiplied by the corresponding liquid mass flow rate (see equation 6.1) provided the following equilibrium adsorption capacity ( $q_{eq}$ ) of 265, 233 and 181 mg Ph/g AC at 80, 120 and 160 °C, respectively:-

$$q_{eq} = \frac{F_L(\Delta t C_{Ph,0} - \int_0^{t_{br}} C_{Ph} dt)}{m_{AC}} \quad (6.1)$$

As expected, the adsorption capacity of AC decreased with increasing temperature in agreement with its exothermic nature [39]. Consequently, the AC bed saturation time was shortened towards higher temperatures nearly by a factor of two as shown in Figure 6.1.

Subsequently to saturation of the AC bed, the feed phenol solution was replaced in each experiment by ultrafilter pure water to desorb phenol from the carbon surface. As it is seen in the same figure, faster phenol desorption has been observed at high temperature, nevertheless, complete recovery of the adsorbed phenol seems difficult to achieve even after 15 h of flushing the bed with hot water. The outlet concentrations never reach zero even for desorption time two times longer than for adsorption. Interesting to note is that the total phenol uptake in the adsorption step could not be recovered during hot water stream flushing. Probably oxygenated surface groups are responsible for oxidative coupling reactions leading to formation of heavy molecules of phenolic dimers and trimmers that can be entrapped inside the pore thereby apparently lowering the total fraction of phenol recovered.

### 6.1.2 Influence of initial AC saturation

Four TBR bed saturation procedures have been investigated with respect to the ultimate performance of AC during CWAO of phenol. The evolution of phenol and TOC conversion and effluent pH are illustrated in Figure 6.2 for start up procedures at "oxic" conditions. A particularity of CWAO of phenol over AC is the start up,

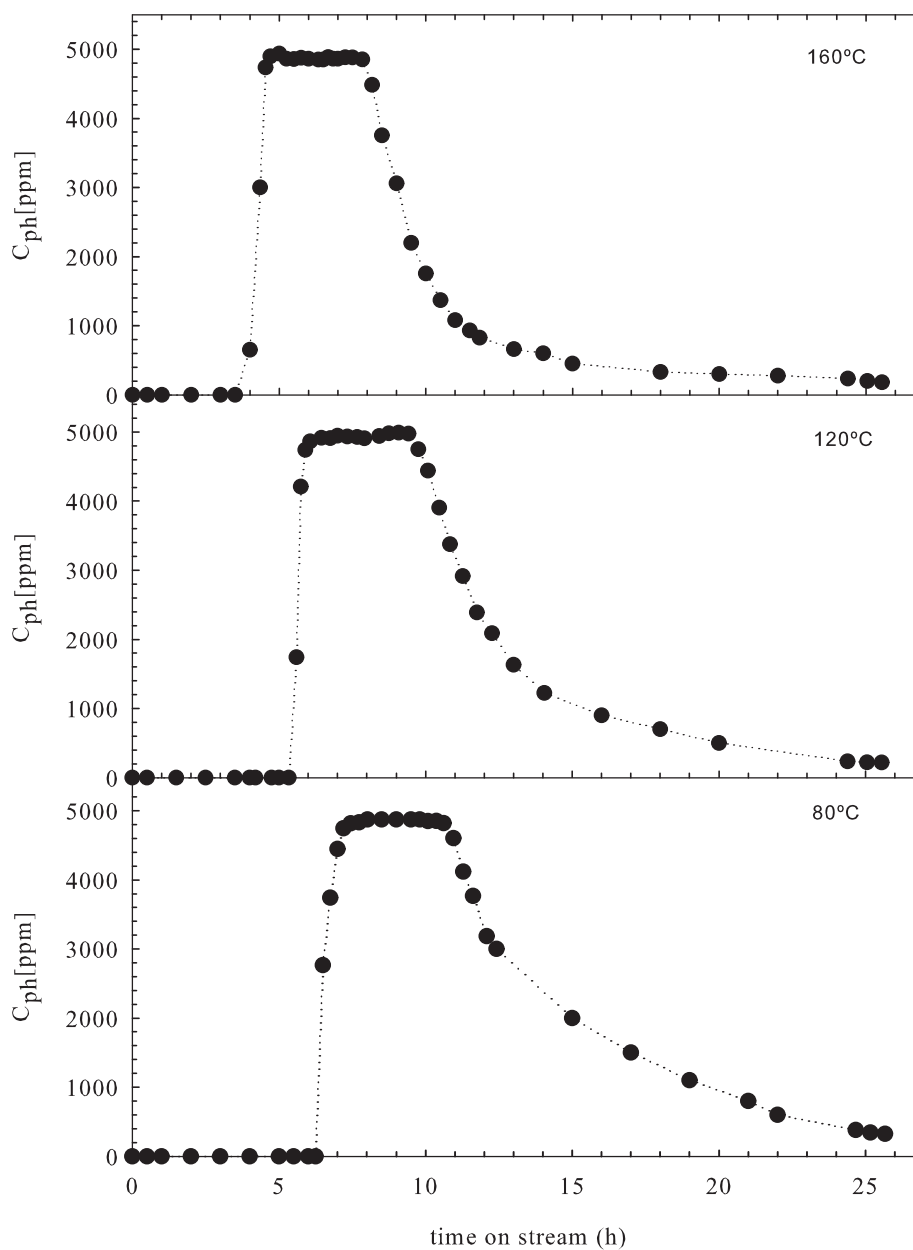


Figure 6.1: Phenol adsorption/desorption measured in a trickle bed column at three temperatures:  $P_T = 15$  bar,  $F_L = 58$  mL/h,  $F_G = 9$  NL/h,  $W_{cat} = 7$  g,  $C_{Ph} = 5$  g/L.

during which both adsorption and reaction have to reach steady state. Figure 6.2 reveals that complete bed saturation with phenol (apparent 100% conversion) takes about 10 h at standard conditions, while steady state of adsorption and reaction is only established after 20 h with a phenol conversion of 46% and TOC conversion of 30%. It appears also from Figure 6.2 that conducting experiments with external or fast in-situ bed saturation does not have the effect of reaching faster steady state. Moreover, a permanent decrease of phenol conversion to about 25-28% and TOC conversion to 17% is observed for both saturation modes. Similar trends are reflected in Figure 6.3, which compares the evolution of phenol and TOC conversion observed with standard and anoxic (nitrogen flow) bed saturation. Besides the noticeable initial deviation in the profiles, phenol and TOC conversion also need ca.10 h more to attain steady state of adsorption and reaction in the case of inert saturation. Although, conversion undergoes then a slight decline, values are always 15% higher for oxic bed saturation. Same findings were reported using a Fe/AC catalyst for the CWAO of phenol in a TBR [97].

It can be said in that the way how the carbon is contacted with phenol seems to modify significantly the initial activity of the active carbon, which evolves to a stable but different steady state conversion. The best long-term performance has been achieved for progressive (unforced) bed saturation in the presence of dissolved oxygen at the initial state of adsorption/reaction reflecting the importance of formation, adsorption and destruction of so called phenolic condensation products in the initial course of reaction. It is well known that AC enhances the formation of oxidative coupling in the liquid phase [181, 182], which can irreversibly adsorbed on its surface, thereby blocking the active sites in meso pores and mainly the access to active sites located in micro pores. The amount of adsorbed condensation products formed will be high (and so the initial decrease of activity) at conditions of high concentration of phenol in the liquid phase (external and fast saturation) and absence of dissolved oxygen. On the other hand, if enough dissolved oxygen is available from the beginning of the oxidation reactions, their formation and subsequent oxidation can be balanced in the course of reaction recovering partly the textural structure of the carbon surface, leading to a high activity.

With respect to the pH evolution of CWAO effluent (see Figure 6.2), it can be said that it decreases to ca. 2.5 once steady state adsorption-reaction regime has been reached. This is clearly caused by the formation of lower molecular weight carboxylic acids (acetic, formic acids) during CWAO of phenol over AC. In particular, AC seems to favor the accumulation of an easily biodegradable acetic acid, in CWAO of phenol [109]. The interesting point with respect to pH evolution for external saturation of AC is that the pH starts from 3.8, although conversion seen to

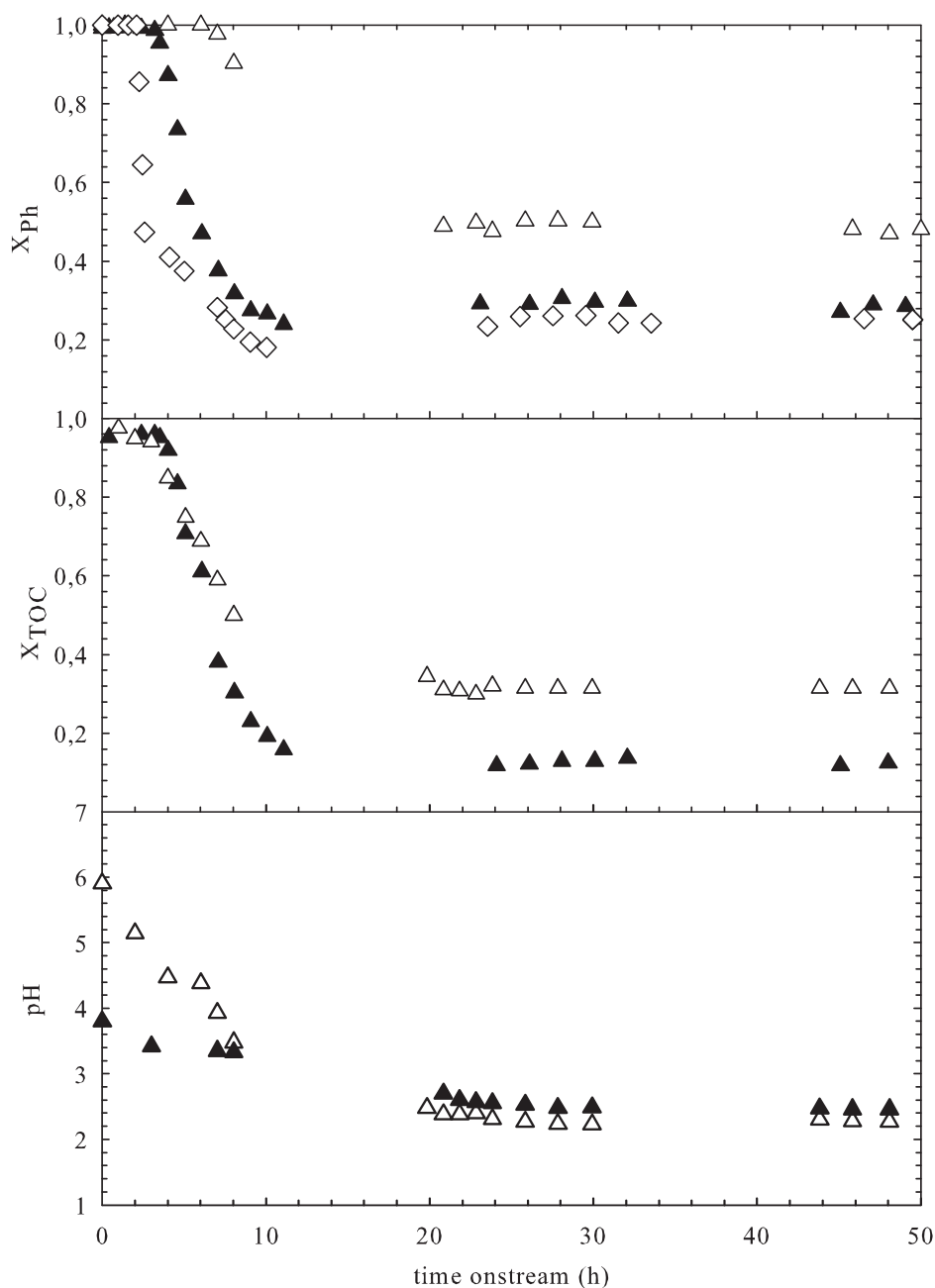


Figure 6.2: Phenol conversion profile for different active carbon bed saturations: ( $\Delta$ ) Standard procedure; ( $\blacktriangle$ ) Externally saturated AC; ( $\diamond$ ) Fast in-situ saturated AC:  $P_{O_2} = 2$  bar,  $T = 140^\circ\text{C}$ ,  $\tau = 0.12$  h,  $F_G = 9$  NL/h,  $W_{cat} = 7$  g,  $C_{Ph} = 5$  g/L.

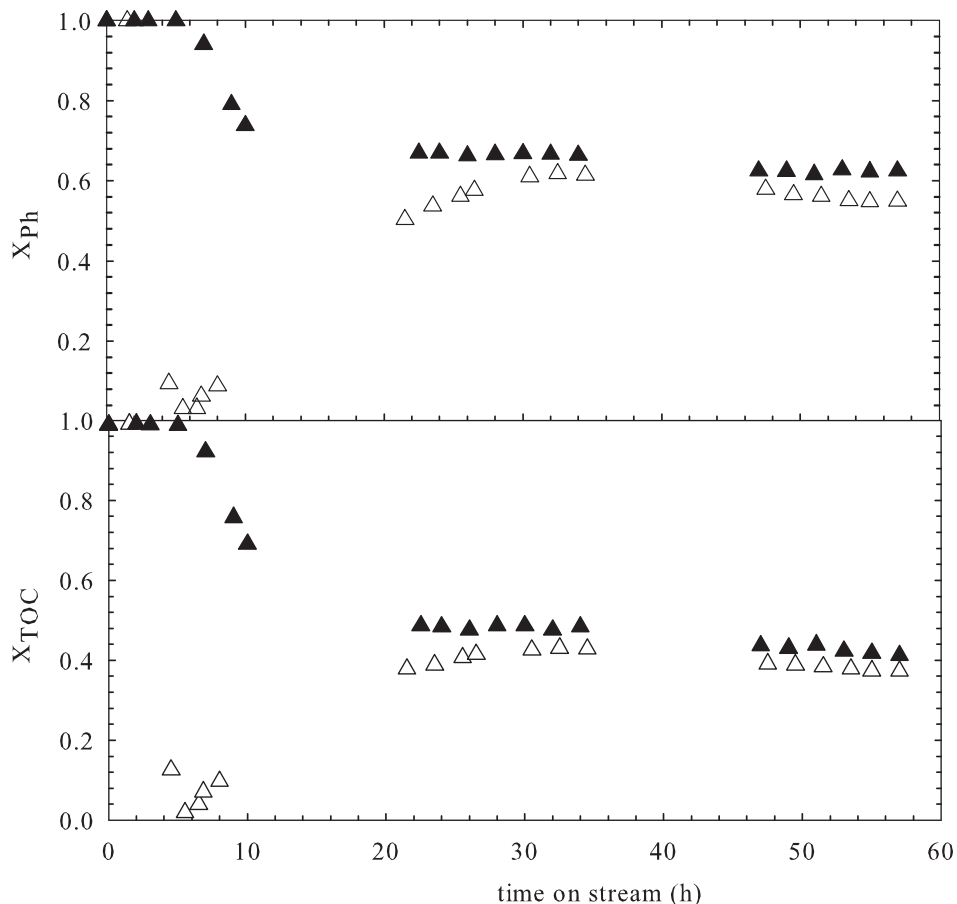


Figure 6.3: Effect of inert AC bed saturation on the activity and stability of AC catalyst: (▲) oxic saturation; (△) anoxic saturation:  $P_{O_2} = 2$  bar,  $T = 140^\circ\text{C}$ ,  $\tau = 0.12$  h,  $F_G = 9$  NL/h,  $W_{cat} = 7$  g,  $C_{Ph} = 5$  g/L.

be 100%. This indicates that the formation and release of acid products is enhanced for external saturation compared to standard saturation.

Analysis of the spent ACs (TGA, BET and weight measurements) was done in order to explain the aforementioned trends observed in the start up experiments and the results obtained are given in Table 6.1. From Table 6.1 it can be concluded that the carbons (external and fast in-situ saturation) that suffered the strongest decrease of conversion showed a particularly high reduction of surface area from ca.  $1200\text{ m}^2/\text{g}$  to  $70\text{-}80\text{ m}^2/\text{g}$  and at the same time a high weight gain during CWAO and a high weight loss in TGA. This loss in surface area must be mainly

Table 6.1: Characteristics of fresh and ACs spent in CWAO:  $P_{O_2} = 2$  bar,  $T = 140^\circ\text{C}$ ,  $\tau = 0.12$  h;  $F_G = 9$  NL/h,  $C_{Ph} = 5$  g/L,  $W_{AC} = 7$  g.

AC saturation	$S_{BET}$ ( $\text{m}^2/\text{g}$ )	$\Delta W_{TGA}$ (%)	$\Delta W_{CWAO}$ (%)	$X_{Ph}^*$	$X_{TOC}^*$
Fresh AC	1156	6	-	-	-
AC Standard saturation	306	14	10	1	1
AC Inert saturation	196	23	22	0.87	0.88
AC External saturation	80	23	22	0.61	0.60
AC In-situ saturation	70	25	28	0.56	0.57

\* based on the  $X_{Ph}$  or  $X_{TOC}$  measured at standard saturation.

attributed to initial though irreversible blockage of micro pores (by condensation products), which therefore can no longer participate in the oxidation of phenol after bed saturation.

### 6.1.3 Influence of AC pre-wetting

Gas-liquid flow irregularities and catalyst partial wetting can strongly impact on trickle bed reactor performance. At very low liquid flow rates, preferential flow may occur in a TBR leaving some catalyst particles completely dry throughout the reaction. This situation leads to incomplete utilization of the catalyst bed thereby reducing the overall performance of the reactor. Catalyst prewetting procedure could aid to establish a better gas-liquid flow distribution in TBR from the initial state and thereby a better catalyst utilization during CWAO over AC catalyst. The possible influence of initial bed wetting on reactor performance was investigated at  $140^\circ\text{C}$  and 2 bar of oxygen pressure for standard liquid flow rate of 60 mL/h following the method of Levec. The resulting time-phenol conversion profiles are illustrated in Figure 6.4. It is seen that prewetted and nonprewetted bed resulted in a very similar phenol conversion suggesting the establishment of adequate trickle flow regime in our laboratory scale TBR. Certainly, the pre-wetted catalyst bed evolved to its natural wetting conditions and consequently phenol conversion remained unaffected by pre-wetting procedures at the tested conditions.

Also, the effect of bed dilution with inert fines was investigated on the performance of TBR during CWAO of phenol over AC at  $140^\circ\text{C}$ , 2 bar of oxygen pressure and liquid flow rate of 60 mL/h. The results (not shown here) revealed that bed dilution with inert fine also did not cause any appreciable differences in phenol

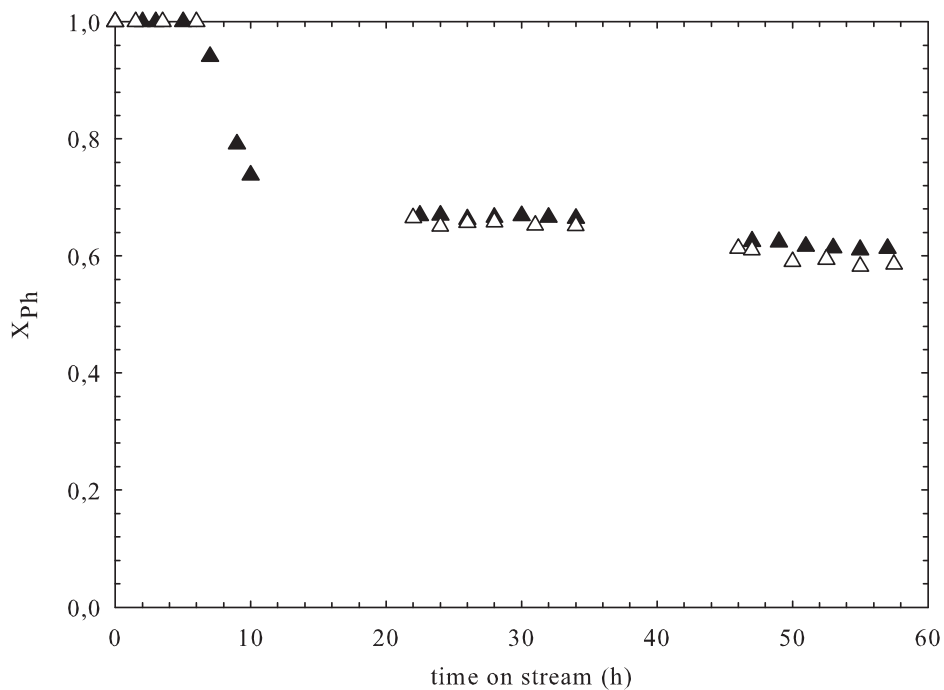


Figure 6.4: Phenol conversion as function of time on stream for different pre-wetting procedures of AC bed: ( $\blacktriangle$ ) Standard procedures ( $\triangle$ ) Levec mode :  $P_{O_2} = 2$  bar,  $T = 140^\circ\text{C}$ ,  $\tau = 0.12$  h,  $F_G = 9$  NL/h,  $W_{cat} = 7$  g,  $C_{Ph} = 5$  g/L

conversions in agreement with the result obtained for prewetting procedures.

#### 6.1.4 Conclusion

The ultimate activity of activated carbon for the CWAO of phenol conducted in our laboratory reactor scale was found largely affected by the way how the carbon is initially saturated with phenol (start-up procedures). The key for obtaining higher and stable activity is to balance the formation, irreversible adsorption and destruction of condensation products through the selection of adequate operating conditions (temperature and oxygen pressure) and start-up procedures. In particular, the presence of dissolved oxygen during the initial state appears very crucial for achieving a better long term activity. The laboratory reactor and the very small particle size being used in our experiments, the effect of initial catalyst wetting appears to be insignificant as nearly similar conversions were obtained for different bed

pre-wetting procedures and bed dilution with inert fines.

## 6.2 Phenol oxidation over AC in TBR

Eftaxias et al. [127] previously studied the effect of temperature and oxygen partial pressure on phenol and TOC removal over the same AC catalyst in order to obtain oxidation kinetics for the steady state modeling of CWAO process. However, the catalyst used in their study showed a significantly lower activity (by 40%) compared to the standard one. Also, the effect of phenol feed concentration on phenol oxidation was only scarcely studied [79, 109, 183]. It was therefore necessary to obtain data for updating the kinetic parameters of the previously developed kinetic expressions. The new kinetics will serve for the modeling of CWAO under gas flow and feed temperature modulation, which is currently in progress in our research group in collaboration with Prof. P. Haure and Prof. A. Ayude from INTEMA of University of Mar de Plata (Argentina).

### 6.2.1 Determination of kinetic regime in TBR

**Effect of particle size and gas flow rate:** In heterogeneous reaction systems, internal and external mass transfer resistances can be the limiting steps for the reaction rate. The intrinsic kinetics can thus be evaluated in a laboratory scale TBR, only if these resistances are sufficiently minimized at the conditions selected for the kinetic study. A series of experiments were thus carried out in TBR to assess the extent of internal and external mass transfer in phenol oxidation over activated carbon at 140 °C, 2 bar of oxygen partial pressure and 0.12 h of liquid space time. Figure 6.5 plots the measured steady state phenol conversion profile against particle diameter and gas flow rate. As it can be seen in, phenol conversion was strongly influenced by catalyst particle size (see Figure 6.5a)). It appears that for  $d_p > 0.5$  mm pore diffusion becomes a limiting step as reported for the CWAO of phenol over AC in a slurry batch reactor [109]. A related study [124] also showed that pressure drop for a particle diameter of 0.5 mm is not significant in our small TBR.

Similarly, external mass transfer limitation was evaluated by varying the gas flow rate at otherwise same operating condition. As it can be seen, two zones can be distinguished in the conversion-gas flow rate profile (see Figure 6.5b)). At the beginning, phenol conversion increased linearly for gas flow rates up to 3 NLh<sup>-1</sup> but then reaches a plateau of 45% at 12 NLh<sup>-1</sup>. Finally, the conversion diminishes marginally for a gas flow rate of 24 NLh<sup>-1</sup>. The almost linear dependency of conversion on gas flow rate at lower values is certainly due to a linear increase in

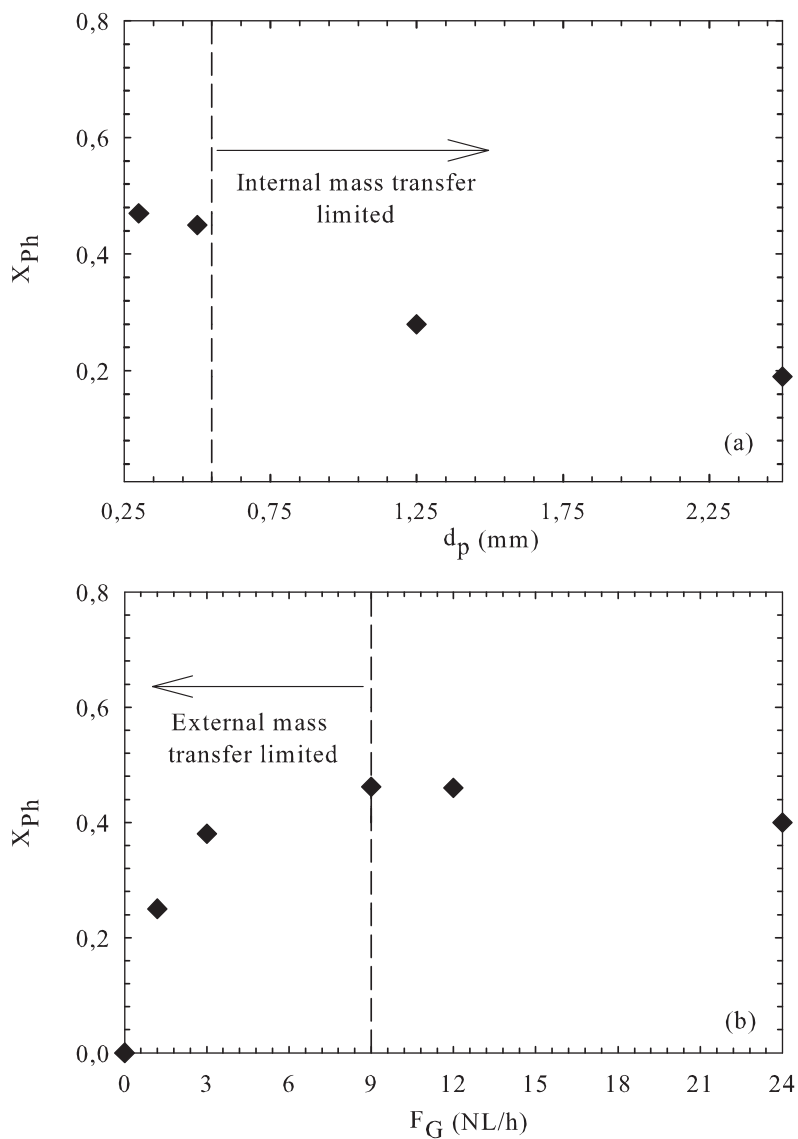


Figure 6.5: Effect of particle size (a) and gas flow rate (b) on phenol conversion during CWAO over AC: Standard conditions:  $P_{O_2} = 2$  bar,  $T = 140^\circ\text{C}$ ,  $\tau = 0.12$  h,  $F_G = 9$  NL/h,  $W_{cat} = 7$  g,  $C_{Ph} = 5$  g/L.

gas-liquid and liquid-solid mass transfer coefficients with gas velocity [184]. Hence, for all other kinetic experiments the gas flow rate and catalyst particle diameter of  $9 \text{ NLh}^{-1}$  and  $0.5 \text{ mm}$ , respectively, were used to avoid external and internal transport limitations.

**Flow hydrodynamics:** The influence of gas-liquid flow hydrodynamics on the ultimate trickle bed reactor performance was examined as described in Section 4.2.4. First of all, the effect of liquid flow rate on the steady state phenol and TOC conversion were examined at  $140^\circ\text{C}$  and  $2 \text{ bar}$  of oxygen pressure. The results obtained are illustrated in Figure 6.6. As it can be seen there, phenol and TOC conversion

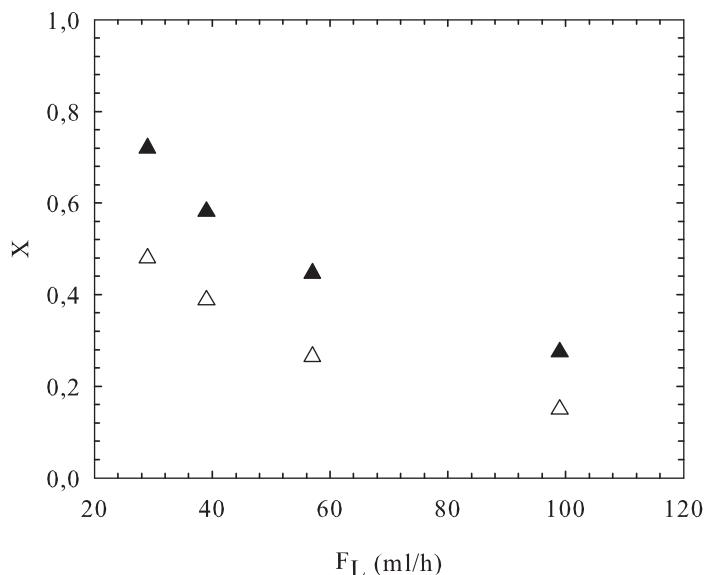


Figure 6.6: Phenol and TOC conversion as a function of liquid flow rate: (▲) phenol conversion, (△) TOC conversion:  $P_{\text{O}_2} = 2 \text{ bar}$ ,  $T = 140^\circ\text{C}$ ,  $\tau = 0.12 \text{ h}$ ,  $F_G = 9 \text{ NL/h}$ ,  $W_{\text{cat}} = 7 \text{ g}$ ,  $C_{\text{Ph}} = 5 \text{ g/L}$

increase steadily with decreasing volumetric liquid flow rate. At lower liquid flow rate (larger space time), the reactants have larger contact times that provide higher conversion of phenol and TOC. Moreover, as the liquid flow rate decreases, partial wetting of the catalyst bed is reduced, hence the extent of direct transfer of the gaseous reactant to the solid catalyst is increased thereby providing high conversion of phenol and TOC. Nevertheless, care should be taken for extremely low liquid flow rates where liquid reactant starvation (shifting the reaction from gas to liquid

limited) and liquid mal distribution could occur and limit the overall reaction rate [85, 131]. These phenomena, however were not observed in our experiment (see Figure 6.6). It seems that the  $D_R/d_p$  ratio of 22 selected for our laboratory reactor is adequate to prevent liquid flow mal distribution.

Moreover, axial dispersion should not be too influent the criteria of Mears being fulfilled even for the lowest liquid flow rates (lowest Bodenstein numbers) and highest phenol conversion (over 90%). However, initially non uniform bed irrigation could takes place in our TBR since no special gas-liquid distributor (only the grid that retains the catalyst particles) was placed at the entrance of the reactor. To check this, an experimental series was conducted with different bed length and liquid flow rate as explained in section 4.2.4 and standard operating conditions of 140°C and 2 bar of oxygen pressure. The steady state conversion-space time pro-

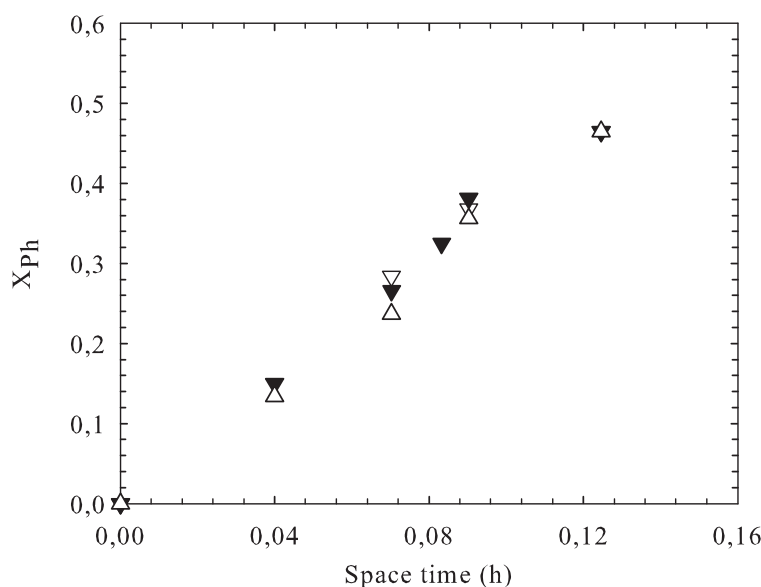


Figure 6.7: Phenol conversion as a function of liquid space time for different hydrodynamic configurations: ( $\nabla$ ) variable liquid flow rate, ( $\blacktriangledown$ ) variable catalyst load, ( $\triangle$ ) variable catalyst load with dilution:  $P_{O_2} = 2$  bar,  $T = 140^\circ\text{C}$ ,  $\tau = 0.12$  h,  $F_G = 9$  NL/h,  $W_{cat} = 7$  g,  $C_{Ph} = 5$  g/L.

files obtained are illustrated in Figure 6.7. As it can be concluded from Figure 6.7, all hydrodynamic conditions tested (variable bed length with or without catalyst dilution at fixed flow rate and variable liquid flow rate at fixed bed height) gave

very similar phenol conversion confirming again the small impact that may have hydrodynamics on the performance of our laboratory TBR operation in the range of liquid space time studied ( $\tau = 0.04 - 0.12$  h). Even for the shortest reactor bed length of 2.5 cm, effects of channeling and liquid back mixing which can reduce the overall reactor performance, were not observed.

On the other hand, due to the small and variable liquid flow rates employed

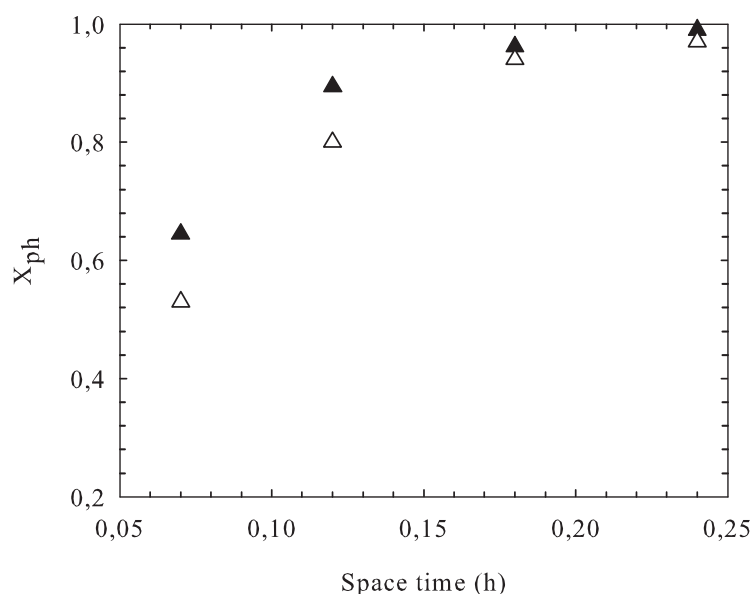


Figure 6.8: Phenol conversion obtained in upflow ( $\Delta$ ) and downflow ( $\blacktriangle$ ) mode versus space time:  $P_{O_2} = 2$  bar,  $T = 160^\circ C$ ,  $\tau = 0.12$  h,  $F_G = 9$  NL/h,  $W_{cat} = 7$  g,  $C_{Ph} = 5$  g/L

in our experiments (15 - 100 mL/h), catalyst wetting, however, is certainly not constant and the estimation of wetting efficiency from literature correlation gives quite small values ( $f_w = 0.2 - 0.5$ ). Upflow operation provides completely wetted catalyst particles and the knowledge of species availability at reaction sites is then useful to predict whether downflow or upflow mode would perform better. To this end, the criterion proposed by Kakildar et al. [133] was calculated at  $160^\circ C$  and 2 bar of oxygen partial pressure. The high value ( $\gamma = 17$ ) diagnoses that the limiting reactant is oxygen in the gas phase and thus trickle bed flow would be preferred over upflow mode. This was verified through CWAO experiments conducted in upflow and downflow operation at otherwise same conditions. Figure 6.8 illustrates the

respective phenol conversions versus liquid space time obtained at 160°C and 2 bar of oxygen partial pressure. It becomes evident from this figure that for the range of liquid flow rate studied downflow mode outperforms upflow mode the latter being limited by gas-liquid mass transfer of oxygen. However, the differences leveled off with decreasing liquid flow rate, i. e. at high phenol conversion. At lower liquid flow rate the wetting efficiency of upflow reactor may be less than unity, and the oxidation of phenol may be enhanced by direct transfer of oxygen to the solid, thereby its performance approaches that of the trickle flow reactor. For kinetic measurements it is thus highly recommended to select the correct flow direction depending on the limiting reactant and operating conditions.

### 6.2.2 Influence of phenol feed concentration

As described in section 4.2.4, CWAO experiments were conducted with sequential variation of phenol inlet concentration to reduce the total operation time of the AC catalyst during kinetic measurement of phenol oxidation in a TBR. In order to exclude any catalyst deactivation effect during the experiment, phenol conversion was also assessed at the end of each sequence (after ca. 80 h time on stream) for the standard phenol inlet concentration of 5 g/L. A typical conversion-time profile showing the sequential variation of inlet phenol concentration has been plotted in Figure 6.9a). As it can be seen there, first steady state of adsorption and reaction is reached after 20 h for the standard feed phenol concentration of 5 g/L, but then the time to reach steady state becomes smaller for the subsequent change in phenol feed concentration, i.e. for a change of feed concentration from 1 to 0.5 g/L it took only 3 to 4 h to reach steady state.

Table 6.2 compares the steady state phenol conversion at 5 g/L after 20 h and ca. 80 h of operating time. As it can be seen, for all space-times tested, the differences ranges between -3 and +7% suggesting that the initial activity of the catalyst was not influenced by sequential dilution strategy during operating times

Table 6.2: Phenol conversion obtained after 20 h and 80 h of operation:  $P_{O_2} = 2$  bar,  $T = 140^\circ\text{C}$ ,  $F_G = 9$  NL/h,  $C_{Ph} = 5$  g/L,  $W_{cat} = 7$  g .

$\tau$ (h)	$X_{Ph}$ ( 24 h)	$X_{Ph}$ ( 80 h)	diff (%)
0.07	0.29	0.31	+7
0.12	0.46	0.58	+ 6
0.18	0.58	0.61	+5
0.24	0.75	0.73	-2.7

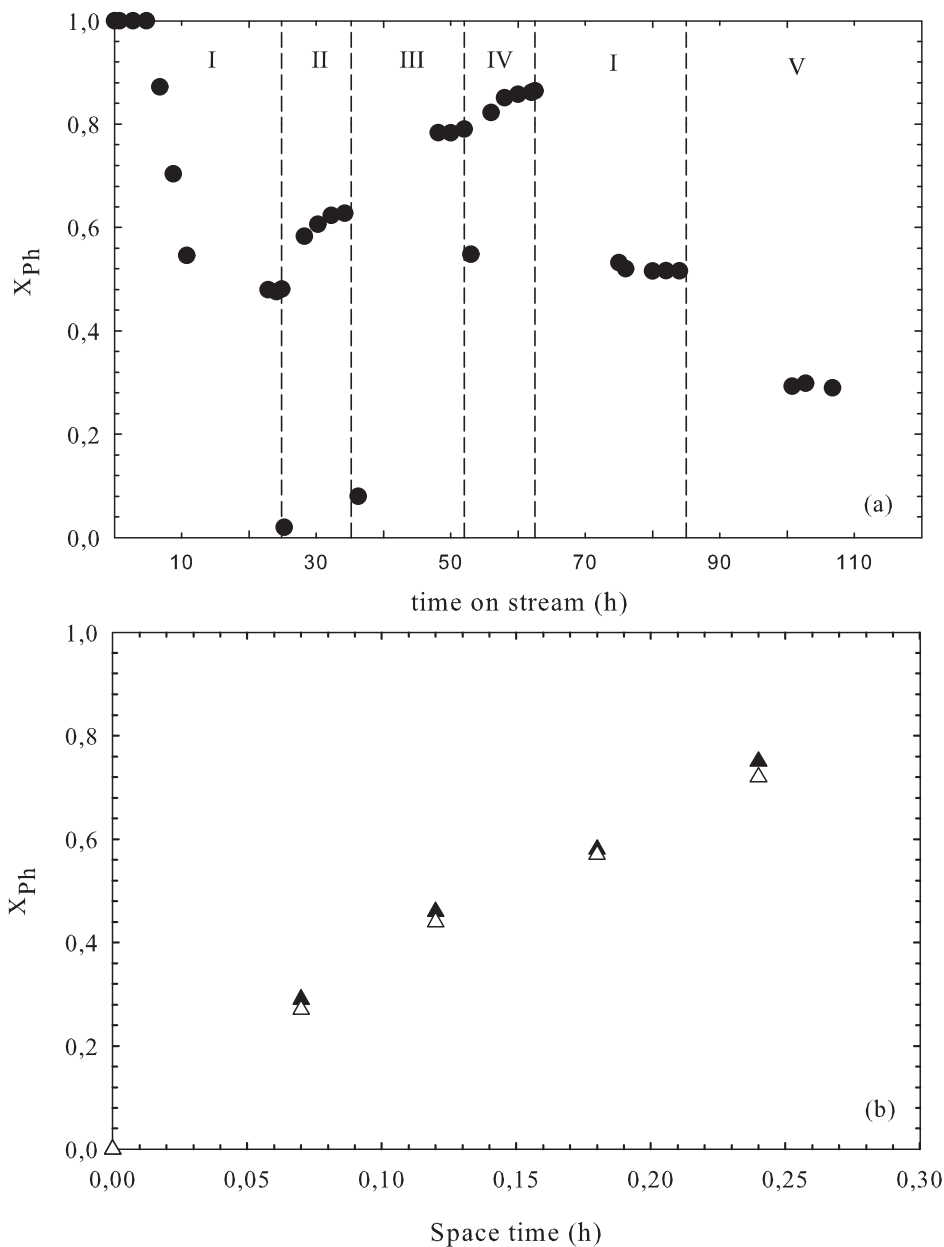


Figure 6.9: (a) Phenol conversion for sequentially dilution of phenol feed concentration: (I) 5 g/L, (II) 2.5 g/L, (III) 1 g/L, (IV) 0.5 g/L, (I) 5 g/L, (V) 10 g/L: (b) Comparison of sequential dilution of phenol feed concentration and variation of liquid flow rates:  $P_{O_2} = 2$  bar,  $T = 140^\circ\text{C}$ ,  $\tau = 0.12$  h,  $F_G = 9$  NL/h,  $W_{cat} = 7$  g.

of ca. 100 h. The sequential dilution experiment was also cross checked through varying the liquid flow rate (liquid space time of 0.07 - 0.24 h) for the standard phenol concentration of 5 g/L and otherwise same conditions. The conversion-space time profiles of the two strategies are compared in Figure 6.9 b). Both methods gave very similar phenol conversion confirming that the sequential strategy is adequate to obtain kinetic data with confidence.

Steady state phenol and TOC conversions were then assessed for liquid space times of 0.07, 0.12 h, 0.18 h and 0.24 h at 140 °C and 2 bar of oxygen partial pressure. Figure 6.10 illustrates the results, which reveal a remarkable increase of phenol and TOC conversion with decreasing phenol inlet concentration. For example, almost total destruction of phenol (100%) was achieved at low feed concentration of 0.5 g/L and liquid space-time of 0.24 h as compared to only 55% phenol conversion for 10 g/L feed concentration. A similar, but less pronounced trend was observed for TOC conversion. These results point towards the assumption that catalytic wet air oxidation of phenol over AC catalyst may not follow a first order kinetics with respect to phenol concentration contrary to what has been mostly reported in literature for AC and Fe/AC catalysts [79, 185]. Adsorption and reaction of phenol in adsorbed state (Langmuir-Hinshelwood surface reaction mechanism) were also used to explain the non liner increase in reaction rates for higher phenol surface coverage [183]. However, adsorption capacity of diverse carbons can not be related at all with their activity [32]. The role that may play active carbon in the oxidation of phenol is yet not clear, but AC can also adsorb and dissociate molecular oxygen on its surface thereby generating reactive oxygenated free radicals. As it has been pointed out in the literature review, several authors proposed that activated carbon accelerates the decomposition rate of oxygen molecule to generate  $H_2O_2$  in aqueous solution, through formation of  $OH^\bullet$  radical [91, 120, 121]. These authors underline that both textural and surface chemical properties of AC affect the decomposition rate, being the delocalized  $\pi$  electron system or the oxygenated basic surface groups such as chromene and pyrone, identified as the active center for oxygen decomposition. Further research at molecular level is required to better understand the catalytic actuation of activated carbon in the field of catalytic wet air oxidation.

### 6.2.3 Influence of oxygen partial pressure

Sequential CWAO experiments have been conducted at total pressure of 6, 9, 14 and 21 bar, which correspond to oxygen partial pressures of 0.5, 1, 2 and 3.6 bar, respectively. The variation of the activity of the carbon catalyst during each sequence was also checked by conducting a CWAO experiment at standard pressure (2 bar

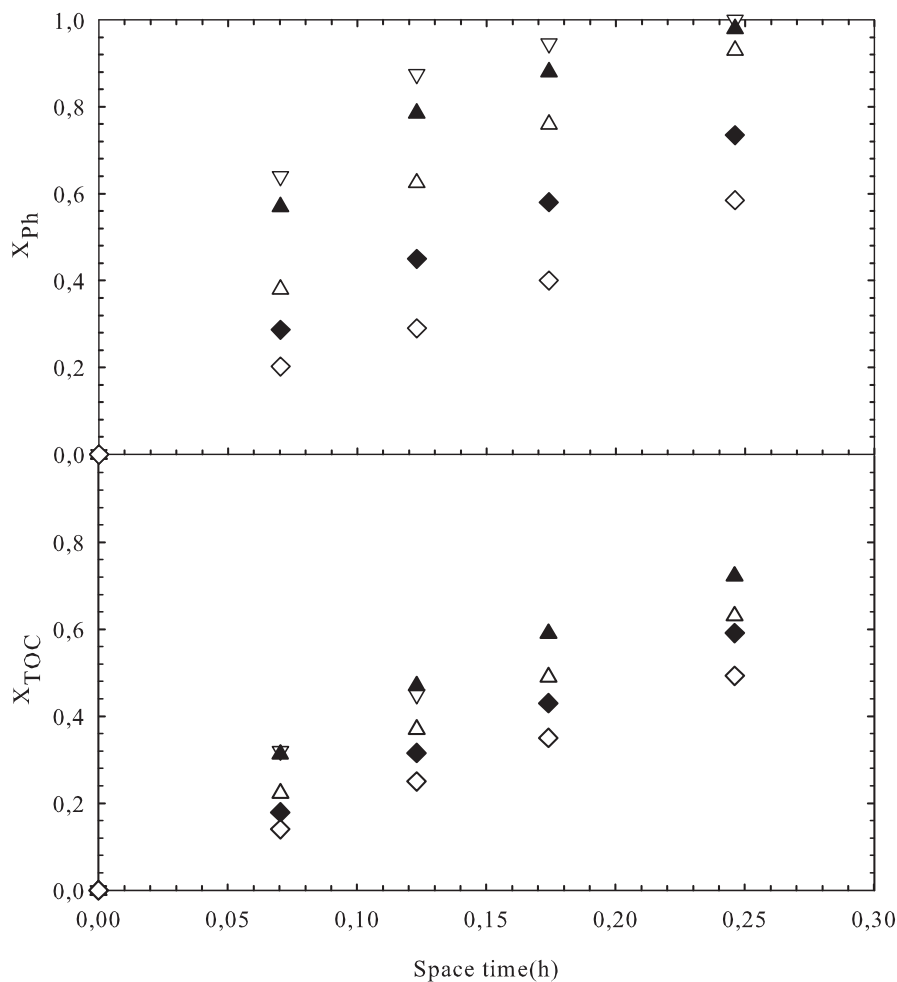


Figure 6.10: Phenol and TOC conversion as a function of space time and different feed concentration: ( $\nabla$ ) 0.5 g/L; ( $\blacktriangle$ ) 1 g/L; ( $\triangle$ ) 2.5 g/L; ( $\blacklozenge$ ) 5 g/L; ( $\diamond$ ) 10 g/L:  $P_{O_2} = 2$  bar,  $T = 140^\circ\text{C}$ ,  $F_G = 9$  NL/h,  $W_{\text{cat}} = 7.5$  g.

oxygen pressure) at the end of each sequential oxidation run. Figure 6.11 plots the steady state phenol and TOC conversion against the oxygen partial pressure. As it can be seen there, both phenol and TOC conversion increase almost linearly with oxygen partial pressure (up to 1 bar), but then level off. Increasing of oxygen pressure improves the amount of dissolved oxygen in the liquid phase [186] and thereby the mass transfer driving force for the gaseous reactant. Nevertheless, conversion

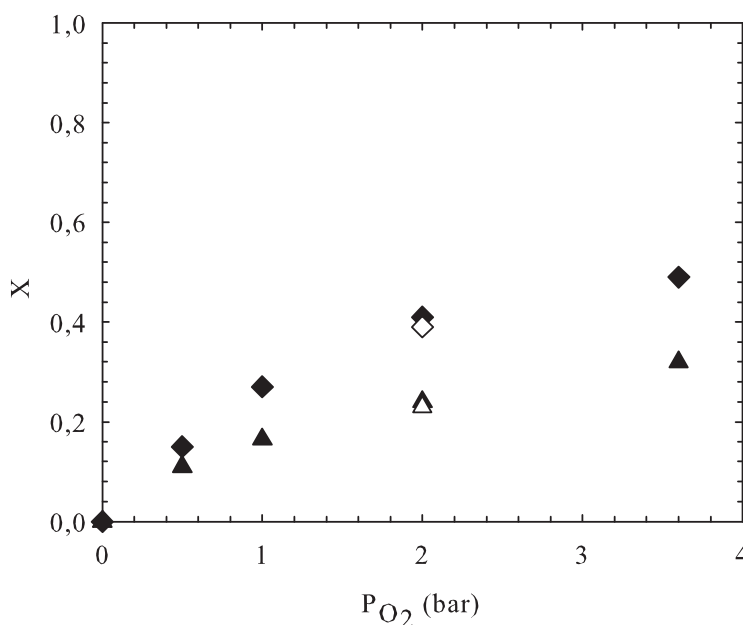


Figure 6.11: Phenol and TOC conversion as function of oxygen partial pressure: (◆)  $X_{Ph}$ , (▲)  $X_{TOC}$ :  $T = 140^{\circ}C$ ,  $\tau = 0.12$  h,  $F_G = 9$  NL/L,  $W_{cat} = 7$  g,  $C_{Ph} = 5$  g/L.

enhancement is leveling off when pressure becomes higher, hence, working pressures for the oxidation of phenol in TBR should not exceed 10 to 15 bar (1 to 2 bar of oxygen pressure) because a higher system pressure would not significantly enhance phenol conversion but increase the difference between phenol and TOC removal. The non linear dependency of phenol and TOC conversion on oxygen pressure observed supports the hypothesis that for the oxidation of phenol to occur molecular oxygen has to adsorb and dissociate first on the active carbon surface to form free radicals that subsequently attack phenol molecules in the liquid phase near to the catalyst surface. Finally, the activity of the catalyst was also not significantly affected by the sequential variation of oxygen pressure as almost similar conversions were achieved at standard conditions (see Figure 6.11) at the end of the sequential experiment.

#### 6.2.4 Influence of temperature

The performance of AC catalyst for phenol oxidation was assessed at 120, 140 and 160 °C, 2 bar of oxygen partial pressure and liquid space time of 0.07 to 0.25 h. Sequential variation of reactor inlet temperature was applied to obtain the transient

conversion profiles. The evolution of conversion for a two temperatures sequence

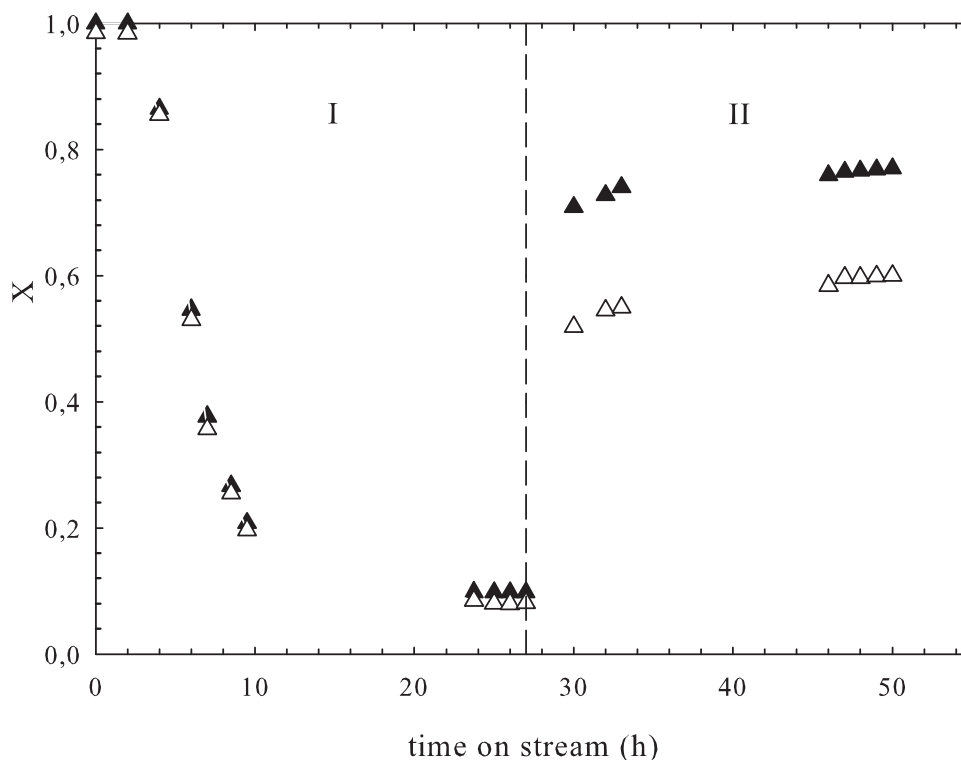


Figure 6.12: Phenol (▲) and TOC (△) conversion as function of time on stream for sequential temperature variation: (I) 120°C, 160°C:  $P_{O_2} = 2$  bar,  $\tau = 0.07$  h,  $F_G = 9$  NL/h,  $W_{cat} = 7$  g,  $C_{Ph} = 5$  g/L.

is exemplarily illustrated in Figure 6.12 for a transition from 120 to 160°C for a liquid space time of 0.07 h. It can be seen that the system needed a relatively large period of 10 h to reach a new steady state at 160°C. However, this time interval becomes smaller at higher liquid space time. Also, Figure 6.12 indicates that temperature has a strong effect (kinetic control) on phenol oxidation rate; temperature increment of 40°C resulted in a remarkable enhancement (up to 85%) of phenol and TOC conversion suggesting that temperature is one key factor for controlling the reaction rate in CWAO of phenol over AC catalyst.

The steady state conversions-space time profiles obtained by sequential reactor inlet temperature variation are given in Figure 6.13. As expected, increasing of temperature or liquid space time has a positive effect on phenol conversion and TOC

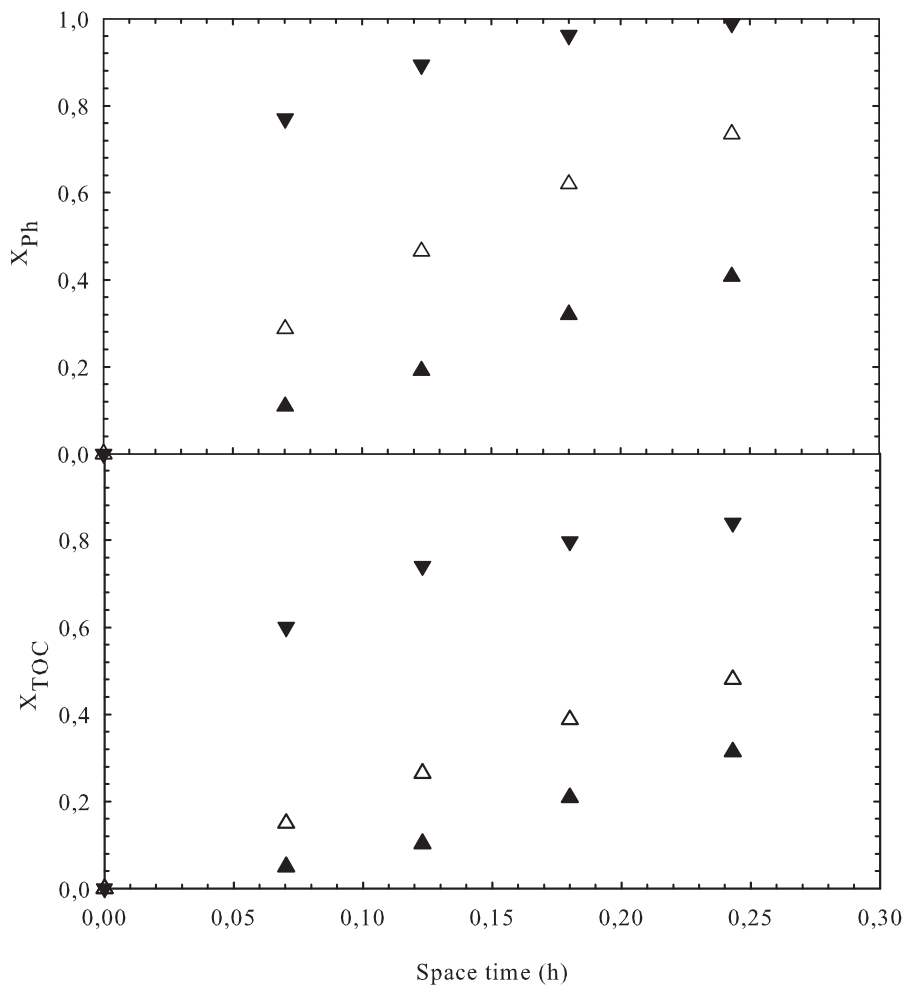


Figure 6.13: Phenol and TOC conversion as function of space time for different temperatures: ( $\blacktriangledown$ ) 120°C ( $\triangle$ ) 140°C, ( $\blacktriangle$ ) 160°C:  $P_{O_2} = 2$  bar,  $\tau = 0.12$  h,  $F_G = 9$  NL/h,  $W_{cat} = 7$  g,  $C_{Ph} = 5$  g/L.

destruction. It can be noted that mineralization of the reacted phenol to  $CO_2$  and  $H_2O$  is almost complete at lower conversion of phenol, while the difference between the phenol and TOC conversion becomes larger as the phenol conversion increases. At 160°C and 0.2 MPa of oxygen pressure, almost complete phenol conversion ( $> 99\%$ ) and more than 85 % of TOC conversion were achieved for liquid space times greater than 0.24 h. The difference between phenol and TOC conversion is due to the accumulation of refractory lower molecular acids, mainly acetic acid.

The observed sensibility of phenol and TOC conversion to temperature indicates

that phenol oxidation in TBR should proceed in the kinetic controlled regime with the standard activated carbon (Merck carbon). Kinetic analysis (data fitting) of the resulting conversion profiles is currently started to obtain specific rate expression based on free radical mechanism. However, the kinetic study is yet not matured to present the results.

### 6.2.5 Influence of solution pH

The influence of solution pH on CWAO of phenol over AC catalyst was investigated at 140°C, 2 bar of oxygen partial pressure and liquid space time of 0.12 h. Constant pH during CWAO was achieved by adding a buffer solution (see section 4.2.4) to the feed tank. The steady state phenol conversion as a function of for different solution pH tested is shown in Figure 6.14. As can be seen there, phenol conversion

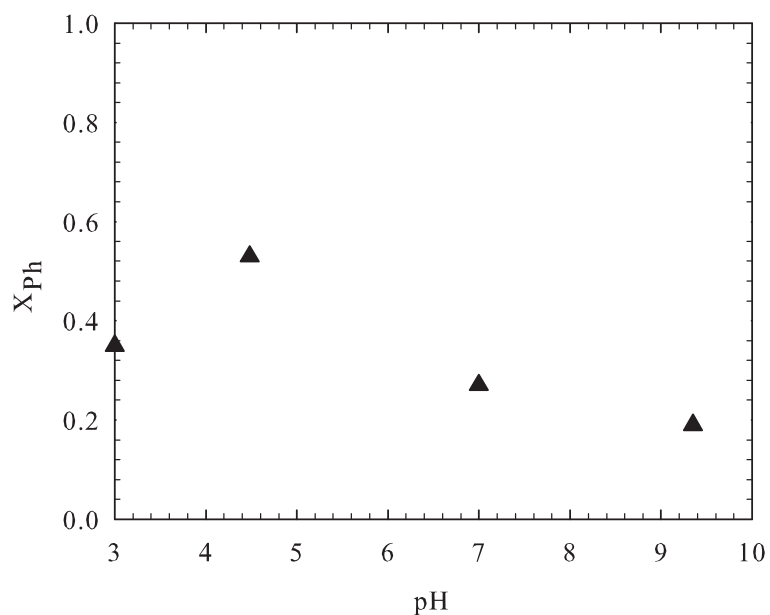


Figure 6.14: Phenol conversion as function of pH during CWAO of phenol over:  $P_{O_2} = 2$  bar,  $T = 140^\circ\text{C}$ ,  $\tau = 0.12$  h,  $F_G = 9$  NL/h,  $W_{\text{cat}} = 7$  g,  $C_{\text{Ph}} = 5$  g/L.

is markedly influenced by pH, having a maximum conversion at a pH value of 4 - 4.5 as for heterogeneous catalysis of CWAO [187, 188].

The observed dependency of phenol conversion on pH may indicate that phenol oxidation over AC catalyst involves a free radical mechanism. The influence of pH

could be mainly by altering the oxidation initiation steps near to the liquid phase. And, the surface chemistry of AC may be influenced by pH affecting thereby the adsorption of phenol and dissociation of molecular oxygen on the carbon surface.

### 6.2.6 Influence of WAO and free radical scavengers

**Non-catalytic wet oxidation:** The contribution of non-catalytic homogeneous wet air oxidation was examined in our TBR for 120, 140 and 160°C. Same reactor bed height and packing procedure as in the CWAO experiment using inert particle have been used to provide the same hydrodynamic characteristics. The resulting conversion-space time profiles are illustrated in Figure 6.15. As expected, phenol

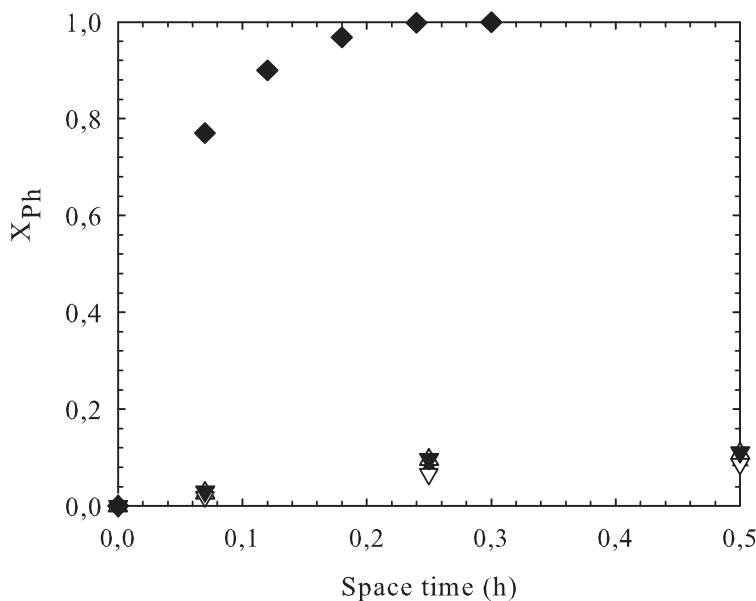


Figure 6.15: Phenol conversion as function of space time during WAO/CWAO in TBR: ( $\blacktriangledown$ ) 160°C (with 3 ppm of  $Fe^{2+}$ ), ( $\triangle$ ) 160°C, ( $\blacktriangle$ ) 140°C, ( $\nabla$ ) 120°C:  $P_{O_2} = 2$  bar,  $F_G = 9$  NL/h,  $W_{inert} = 27$  g,  $C_{Ph} = 5$  g/L.

conversion increased in WAO with both temperature and liquid space time. Nevertheless, the homogeneous WAO phenol conversion was always below 8% at  $\tau = 0.24$  h compared to complete phenol conversion in CWAO over AC catalyst. Also, wet air oxidation run has been conducted in the presence of  $Fe^{2+}$  (3 ppm) in the feed solution to examine a possible homogeneous catalytic contribution of Fe leached

from AC during CWAO of phenol. The specified amount of Fe corresponds to that detected in the CWAO effluent at 160 °C and 2 bar of oxygen partial pressure. As shown in Figure 6.15, addition of Fe did not improved the non-catalytic homogeneous phenol conversion.

Comparison of catalytic and non-catalytic WAO of phenol conversion at the same experimental conditions (160 °C and 2 bar oxygen partial pressure) confirms that the contribution of non-catalytic homogeneous oxidation reaction is minor in the range of temperature and liquid space studied and might be neglected in the kinetic fitting of TBR data.

**Effect of free radical scavenger:** Humade et al [121] and Santiago et al [95] reported on the ability of AC to yield  $H_2O_2$ , through formation of  $OH^\bullet$  radicals, in the presence of molecular oxygen in acidified aqueous solution. Moreover, CWAO of phenol is believed to proceed through homogeneous-heterogeneous free radical mechanisms. Therefore, a few CWAO experiments were carried out at 140 °C, 2 bar of oxygen partial pressure and liquid space time of 0.12 h in the presence of methanol, tert-butanol and bicarbonate, which are know as ( $OH^\bullet$ ) radical scavengers [19, 123, 189]. The steady state phenol conversions are illustrated in Figure 6.16 for each scavengers as a function of its inlet concentration. Results (no influence of scavenger) are not as expected for methanol as its strong scavenging effect has been already reported in literature [123]. Similarly, only a very mild scavenging effect has been observed in case of tert-butanol (Figure 6.16) [19]. This may be attributed to their relative high vapor pressure at the tested condition. Nevertheless, at a total system pressure of 15 bar, 140°C and for the lowest scavenger concentration, the estimated molar flow rate of methanol to saturate the gas phase is not higher than ca.10% of the methanol entering with the liquid flow. In that case, the formation of free radicals that will initiate the oxidation reaction seems to predominantly occur on the AC surface, although the subsequent attack of these radicals on phenol molecule may proceed in the liquid phase in the closest vicinity of the catalyst surface.

Additional CWAO experiment was conducted in the presence of a nonvolatile bicarbonate ( $NaHCO_3$ ) as free radical scavenger. In this case, phenol conversion is significantly affected in the presence of bicarbonates (see Figure 6.16). Conversion decreased from 45% to 12% suggesting that sodium bicarbonate is a strong competitor of hydroxyl radicals with organic contaminants. Assuming that bicarbonate is adsorbed on different active site of the AC surface, it may be concluded that CWAO of phenol over AC occurs mainly via heterogeneous surface mechanism initiated by free radicals very close to the liquid interface [33, 190]. Hence, the role of AC during

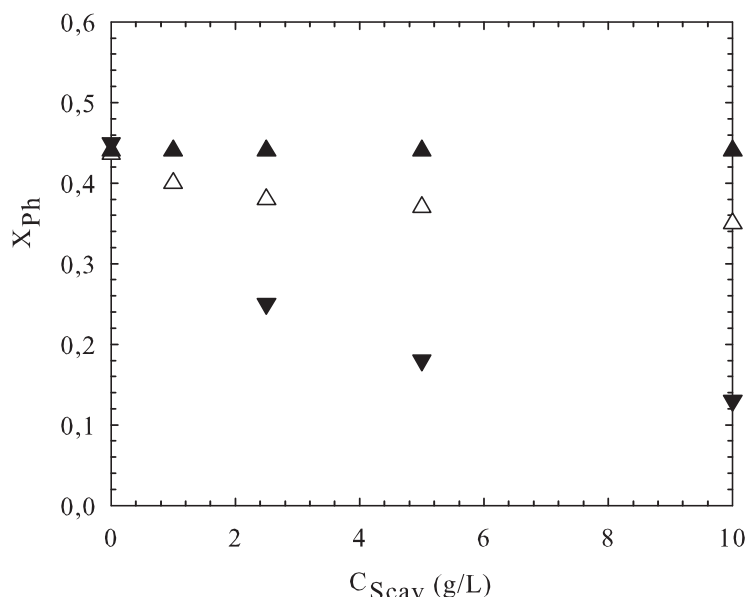


Figure 6.16: Phenol conversion as function of feed concentration of different free radical scavenger: (▲) methanol, (△) tert-butanol, (▼) sodium bicarbonate:  $P_{O_2} = 2$  bar,  $T = 140^\circ\text{C}$ ,  $\tau = 0.12$  h,  $F_G = 9$  NL/h,  $W_{cat} = 7$  g,  $C_{Ph} = 5$  g/L.

CWAO of phenol may be to accelerate the generation of oxygenated free radicals such as  $O_2H$ , which subsequently attack the phenol molecule.

## 6.2.7 Conclusion

Kinetic measurement in trickle bed reactor requires previous determination of kinetic regime and flow hydrodynamics to minimize their effect on the intrinsic reaction rate. It can be said that for the selected operations conditions of this work internal and external mass transfer limitation were found insignificant during phenol oxidation in TBR. Moreover, results from variation of catalyst bed height in the presence or absence of inert fines diagnoses that flow hydrodynamic only affect marginally our laboratory TBR.

In conditions of kinetic control almost complete phenol conversion (>99%) and 85% of TOC removal were achieved in our TBR using a commercial Merck carbon and initial oxidic bed saturation at  $160^\circ\text{C}$ , 2 bar of oxygen pressure and liquid space times of ca. 0.24 h. The observed sensibility on phenol conversion to the operating

temperature further confirmed that the oxidation reaction should proceed in the kinetic controlled regime in the range of liquid space time tested. With respect to the strong non linear influence of feed concentration on phenol and TOC conversions, it can be said that the performance of the AC catalyst may not be explained by first order kinetics. In that case heterogeneous surface kinetics expression accounting for oxygen dissociation may better explain the observed results. With respect to the effect of radical scavengers and solution pH, it can be said that phenol oxidation over AC catalyst should follow a heterogeneous surface free radical mechanism in agreement with what has been reported for metal based heterogeneous catalysts.

However, a temperature of 160°C is seen too severe to maintain long term activity in steady state TBR operation. Burn-off of active carbon became influent at 2 bar of oxygen partial pressure ; phenol conversion decreased progressively after 50 h of operating time. Improvement of long term stability may be performed by periodic fixed bed reactor operation conditions, and the results obtained with this operation concept will be discussed in the following chapters.



## Chapter 7

# CWAO of Phenol in Periodically operated Fixed Bed Reactor

It has been shown that continuous CWAO of phenol over AC in a TBR can achieve high phenol and TOC conversion and biodegradability enhancement using oxidic AC bed saturation, 160°C, 2 bar of oxygen partial pressure and liquid space times of 0.2 to 0.3 h. Successful industrial application however, is linked to stable activity of the AC catalyst. It has been also reported that, AC can undergo self oxidation (combustion) at higher temperature and oxygen pressure during CWAO processes [43]. Stable but too low phenol conversion of ~50% are only achieved at 140°C and 2 bar of oxygen pressure. Incrementing the temperature to 160°C resulted in a strong increase of phenol conversion and simultaneously AC burn-off enhancement. This clearly evidences that carbon burn off limits the overall performance of CWAO in steady state TBR operation. Performing high and stable phenol and TOC conversions at 140°C is possible with AC catalyst, but would require large liquid space times, i.e. undesired large reactor volume and amounts of catalyst. It has been demonstrated improvement of AC stability can be achieved by the application of periodic changes in gas flow and gas feed composition [114]. Despite the improvement observed in terms of phenol conversion compared to steady state operation, reduced but slow AC burn-off seems still unavoidable. Temperature feed and liquid flow modulation could be an alternative option to further reduce the undesired self oxidation of AC. This work should also provide data required for the modelling of TBR operated under feed temperature or gas feed flow modulations during CWAO of phenol over AC catalyst. For this reason, the first part of this work (section 7.1) is dedicated to the heat transfer experiments conducted in our trickle bed column under steady and nonsteady state conditions and its modelling.

## 7.1 Heat Transfer in Trickle Bed

### 7.1.1 Influence of insulation materials

In the first experimental series the effect of insulation materials on trickle bed column axial temperature profile was studied using a fixed bed of active carbon and water-nitrogen two phase flow. The experiments were conducted at operation conditions of  $P_T = 15$  bar,  $T_{oven} = 170^\circ\text{C}$ ,  $F_L = 100$  mL/h,  $F_G = 18$  NL/h. Figure 7.1 shows the

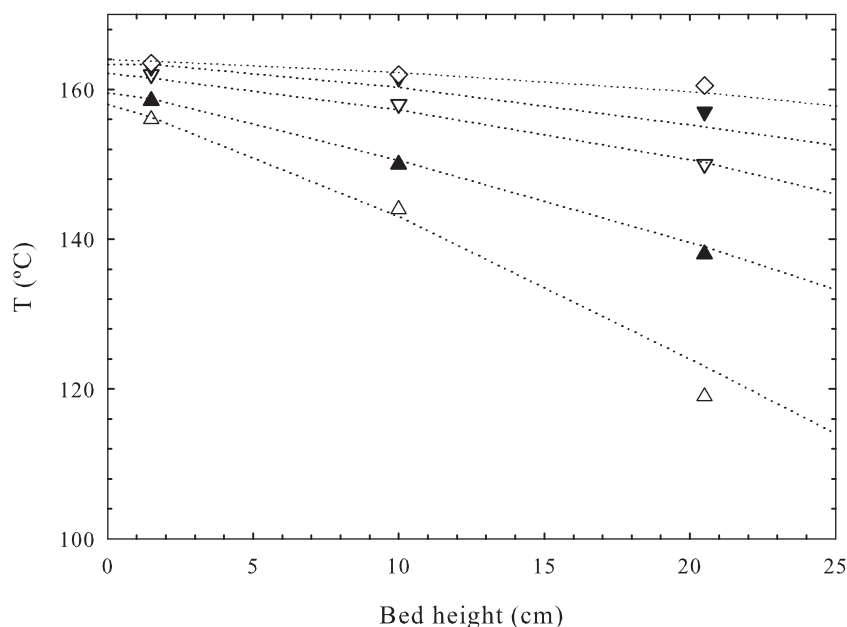


Figure 7.1: Influence of different insulating material on axial temperature profile in a trickle bed column: ( $\diamond$ ) Polyurethane, ( $\blacktriangledown$ ) Rock wool, ( $\nabla$ ) glass fiber, ( $\blacktriangle$ ) ceramic fiber, ( $\triangle$ ) without isolation, discontinuous lines represent model predictions:  $P_T = 15$  bar,  $T_{Oven} = 170^\circ\text{C}$ ,  $F_L = 100$  mL/h,  $F_G = 18$  NL/h,  $W_{cat} = 7.5$  g.

axial temperature profiles that establish for the different heat insulating materials tested. A significant heat losses was occurred in the trickle column without thermal insulation leading to a bed gradient of ca.  $-2$  K/cm. Accordingly, improvement was found in case of the insulated column, the cylindrical rockwool foam configuration revealing better insulating properties, i.e. a five times smaller bed gradient of only  $-0.4$  K/cm. Adiabatic conditions were not accomplished with this material as it is desirable for experiments with temperature feed modulated CWAO of phenol over

AC. It is noteworthy to state that the experimental axial profiles exhibit a convex curving as the bed temperature gradient increases. A stronger gradient favors condensation of water vapor from the saturated gas phase and condensation effects may be at the origin of the observed trend.

Figure 7.1 also confirms the good match achieved between experimental axial temperature profiles and those predicted from Eq.5.1. Further evidence for the overall quality of the experiments and the fitting of the overall heat transfer coefficient  $U$  are the thermal conductivities of the insulating materials deduced from Eq.5.5, which fall within the range of values extracted from literature or manufacturer data sheets.

### 7.1.2 Axial temperature profiles

The effect of operating variables ( $P_T$ ,  $T_{oven}$ ,  $F_L$  and  $F_G$ ) on the heat transfer of trickle column packed with AC was investigated at steady state conditions using rock wool foam as insulation material to establish a non-adiabatic temperature profile across the trickle column. In a standard experiment, a liquid flow rate of 100 mL/h was fixed for a given total pressure and gas flow rate to warm up the reactor until reaching stable steady state temperatures. Subsequently, the liquid flow rate was decreased to 60 mL/h to establish a new steady state temperature and then to 30 mL/h fixing the other parameters constant. Figure 7.2 exemplarily illustrates the temperatures recorded in such a standard experiment. As it can be seen, the temperatures inside the bed shows a certain delay with respect to the oven temperature. The difference of 10 to 15 K between the oven and the trickle column inlet temperatures is essentially due to the insufficient insulation of the tubing section between the oven outlet and the column inlet. Nevertheless, the first steady state establishes after ca. 100 min for a liquid flow rate of 100 mL/h. For a subsequent decrease in the liquid flow rate to 60 mL/h and 30 mL/h, only it took respectively 15 min and 30 min to reach stable temperatures (see Figure 7.2 ).

Representative axial temperature profiles and corresponding steady state predictions are depicted in Figure 7.3 for total pressures of 9, 15 and 25 bar, respectively, the three liquid flow rates studied and a gas flow rate of 9 NL/h. As it can be seen in the figure, a good agreement was obtained between the experimental values and the theoretical values for all conditions investigated. An interesting observation to point out is the strong influence that has pressure on the shape of the temperature profiles. The flat and straight profiles that establish at 9 bar become more steep and curved for intermediate pressure of 15 bar and decreasing liquid flow rate. A further increase to 25 bar results in steeper profiles, which however show no longer convex

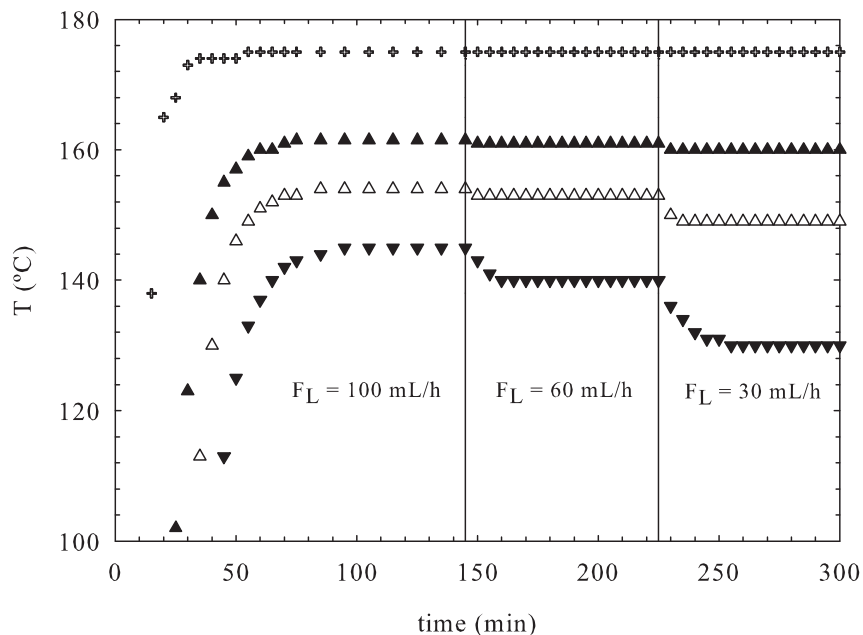


Figure 7.2: Evolution of axial temperature during a standard heating experiment: (+) oven temperature, (▲) axial temperature at  $z = 1.5$  cm, (△) axial temperature at  $z = 10$  cm, (▼) axial temperature at  $z = 20.5$  cm;  $T_{\text{Oven}} = 175^\circ\text{C}$ ,  $F_G = 9$  NL/h.

curving. The curving of the profiles with pressure may be related to condensation effects as already suggested above. At a total system pressure of 9 bar and  $160^\circ\text{C}$ , the saturated nitrogen phase flowing through the fixed bed contains a high fraction (ca. 70%) of water vapor. However, the axial temperature gradients establishing at this pressure are very small (see Figure 7.3a) and condensation of water vapor is not important. Increasing the pressure to 15 bar reduces the water vapor fraction (ca. 40%) of the flowing gas phase, but 10 to 20 times higher temperature differences develop now in axial direction (see Figure 7.3 b). Hence, condensation will occur along the packed bed what may explain the curved shape of the axial temperature profile. This influence should become more visible at lower liquid flow rate as Figure 7.3 b suggests by the increase in curving of the profiles occurring in the transition from 60 mL/h to 30 mL/h. At 25 bar of total pressure the (condensable) water vapor fraction of the flowing gas is probably becoming then small enough (ca. 15%) to mask any effect of condensation (on the profiles) although the higher temperature gradients observed at 25 bar actually enhance condensation through a stronger decrease in the water vapor pressure. The model strongly supports the aforementioned

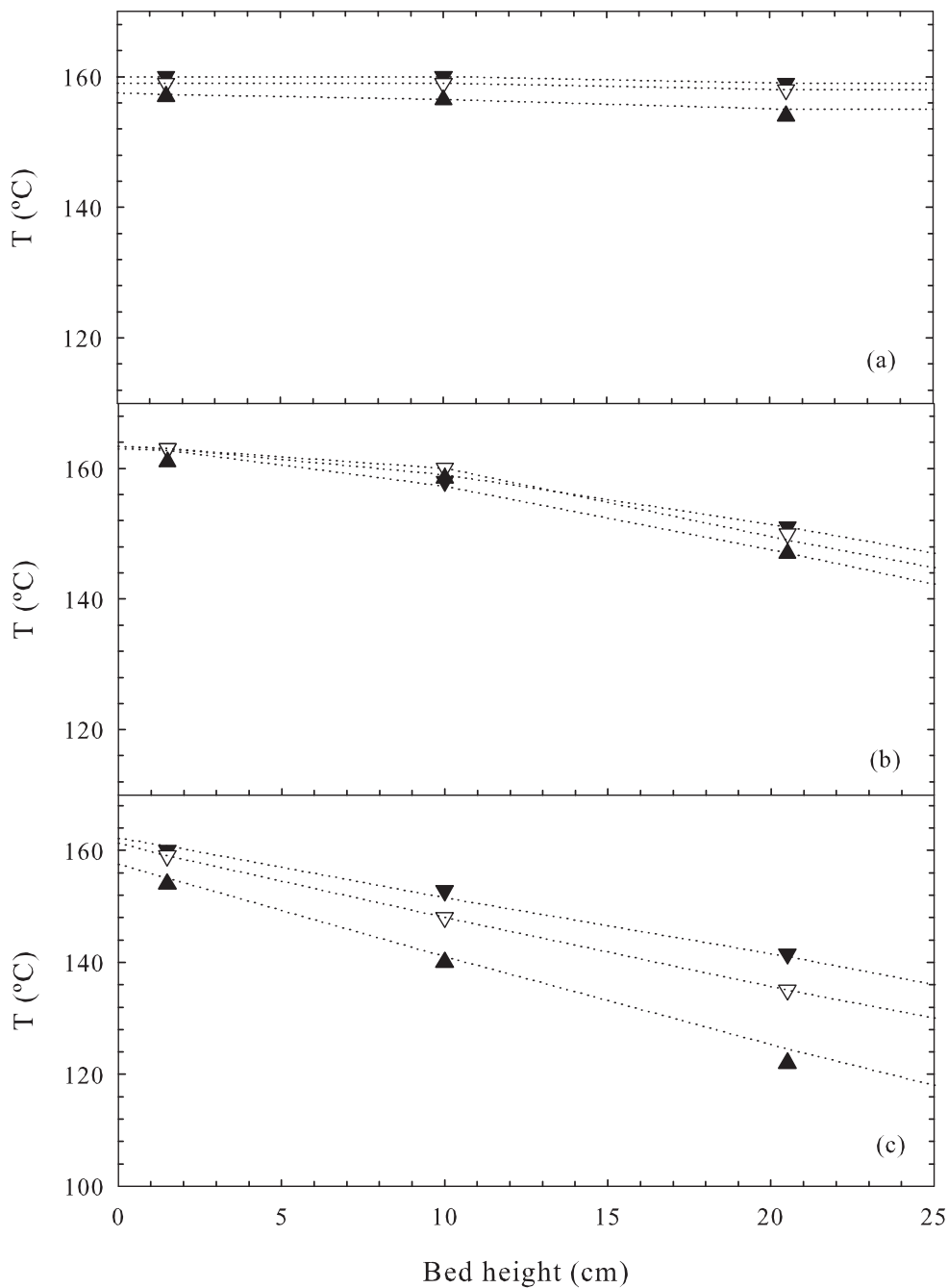


Figure 7.3: Axial temperature profile for different liquid flow rates and pressures: (a) 9 bar, (b) 15 bar, (c) 25 bar: ( $\nabla$ )  $F_L = 100$  mL/h, ( $\nabla$ )  $F_L = 60$  mL/h, ( $\blacktriangle$ )  $F_L = 30$  mL/h, discontinuous lines represent model predictions:  $T_{Oven} = 170^\circ\text{C}$ ,  $F_G = 9$  NL/h.

effect of condensation on heat transfer as curving of the model profiles could be only achieved when accounting for the contribution of water vapor condensation to the heat balance (eq.5.1).

### 7.1.3 Influence of operating conditions

To discuss the effect of operating variables on heat transfer, all raw axial profiles were converted to axial temperature differences ( $\Delta T$ ) defined as the difference between the temperatures measured at axial positions of 1.5 cm and 20.5 cm, respectively. Figure 7.4 plots the so obtained axial temperature gradient data against total pressure and the gas and liquid flow rates studied.

Total pressure, liquid flow rate and gas flow rate all seem to affect the axial temperature gradient. However, the influence of parameters is found to decrease in the aforementioned order. At lower pressures (from 9 bar to 12 bar) and independently of the liquid and gas flow rates applied, flat axial temperature profiles establish in the column (see small  $\Delta T$  in Figure 7.4) indicating a poor heat transfer inside the bed and from the bed to the wall. A further increase in total pressure goes in hand with a strong augmentation of the axial temperature differences before the  $\Delta T$  reach a plateau at 25 bar (see Figure 7.4). Incrementing the pressure at constant liquid and gas flow rate leads to gradually smaller superficial gas velocities that must provide better heat transfer conditions in the bed.

For increasing liquid flow rates, the  $\Delta T$  decrease (Figure 7.4) what apparently seems contradictory as smaller  $\Delta T$  could be wrongly interpreted as a sign of worse heat transfer. The axial temperature profiles that establish in the column are the consequence of heat input by the flowing liquid and radial heat loss through the column wall. In case of higher liquid flow rates, the heat input due to forced convection proportionally increase with the product  $\rho_L \times cp_L \times u_L$  (neglecting the contribution of the gas phase), whereas the radial heat losses ( $U \frac{4}{DI} (T - T_{ext})$ ) are not enhanced in the same proportions due to a smaller effect of liquid flow rate (or velocity) on the overall heat transfer coefficient  $U$ .

### 7.1.4 Determination of overall heat transfer coefficient ( $U$ )

The result of  $U$  obtained by fitting the model predications to the experimental data are plotted in Figure 7.5 and 7.6 for all experimental conditions studied. Both figures clearly reflect the influence of the operating parameters on the heat transfer as previously established in section 7.1.3. The effect of the gas flow rate on heat transfer ( $U$ ) is not very relevant (see Figure 7.6) in trickle flow regime as reported in

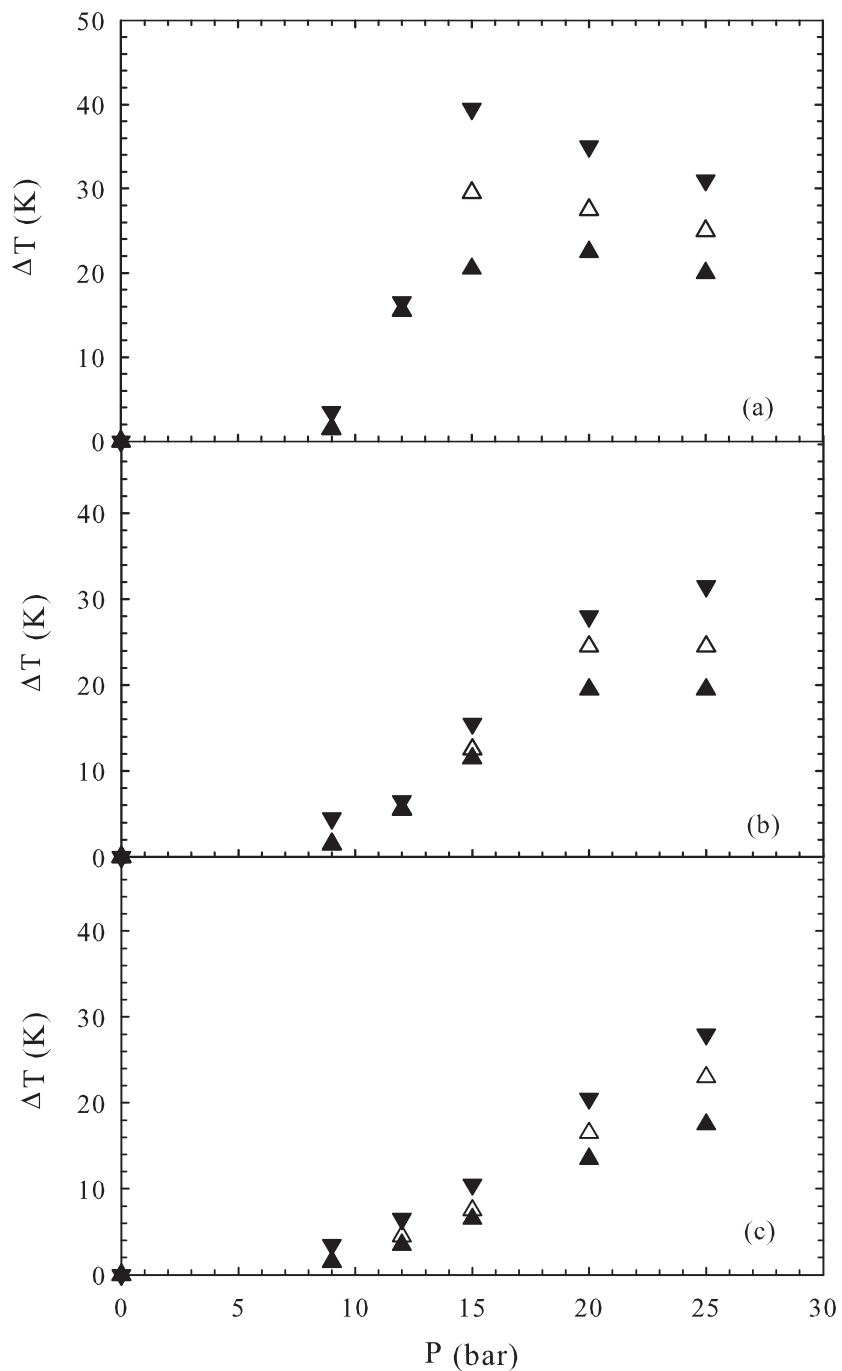


Figure 7.4: Axial temperature gradient as function of system pressure for different liquid and gas flow rates; (a) 3 NL/h, (b) 9 NL/h, (c) 18 NL/h: (▲)  $F_L = 100$  mL/h, (△)  $F_L = 60$  mL/h, (▼)  $F_L = 30$  mL/h:  $T_{\text{Oven}} = 170^\circ\text{C}$ ,  $W_{\text{cat}} = 7.5$  g.

literature [166, 171, 171]. It is noteworthy that the study of Mariani et al. [171] was conducted for trickle beds with:  $DI/d_p > 4.7$  and  $5.4 < Re_L < 119.6$  and  $2 < Re_G < 158.5$ . The condition of our work coincides in the aspect ratio, but our liquid and gas Reynolds numbers are outside at the inferior limits of the validity range of Mariani et al. [171].

A positive effect of liquid flow rate on heat transfer is deduced from Figure 7.5. Its dependency on the liquid Reynolds number is ca. 0.3 (see exponent of  $Re_L$  in correlation of  $h_W$  in section 7.1.5). This generally agrees with the findings of other authors [166, 171]. The trend in these works is that the dependency (of  $Nu_W$  or  $Nu_T$ ) on the liquid Reynolds number decreases with decreasing liquid and gas Reynolds number. Mariani et al. [171] report an exponent of 0.65 of  $Re_L$  for their conditions, whereas Sokolow et al. [191] (as cited in Table 2 in Lamine et al. [166]) obtained a smaller  $Re_L$  0.43 dependency of  $Nu_W$  for the following conditions:  $DI/d_p > 54-93$  and  $0.2 < Re_L < 60$  and  $0 < Re_G < 43$ .

The strongest effect on heat transfer exerts the system pressure. From 9 bar to 20 bar the overall heat transfer coefficient is a quasi linear function of pressure before becoming independent of pressure at 25 bar (see Figures 6 and 7). This finding is interesting, but cannot be contrasted with other data due to the lack of studies that deal with the effect of pressure on heat transfer. Increasing pressure can enhance the heat transfer indirectly (since it seems to be independent on  $Re_G$ ) if the related decrease in gas velocity leads to a higher liquid holdup. However, this effect alone can not explain the strong influence of pressure observed in our study. For our particular nitrogen-water system and high temperatures, condensation of water vapor from the gas phase was identified to have a positive role on heat transfer. One can speculate that condensation may lead to the formation of a thin slowly moving liquid water layer in the column, thereby enhancing the heat transfer.

Finally, the precision of the fitted overall heat transfer coefficients has to be analyzed. The uncertainty in the fitting procedure is caused by the precision of the temperature measurement ( $\pm 0.5$ ) and the quality of the fit particularly in case of curved profiles. All thermocouples used were calibrated against ambient and boiling water to determine and eliminate eventual differences due to the manufacturing. At the lowest system pressure of 9 bar the axial temperature differences recorded during the experiments ranged between 2 and 5 K depending on the liquid flow rates. Assuming a maximum possible error in the temperature measurements of 1 K, uncertainties of 20 to 50% in the worst case could be propagated to the fitting of  $U$  by eq. 5.1. For higher system pressures, the  $\Delta T$ s measured sharply increased and at 15 bar the maximum uncertainty in  $U$  due to errors in the temperature measurements reduces now to 2.5-10%. On the other, at intermediate system pressures of 12 and 15

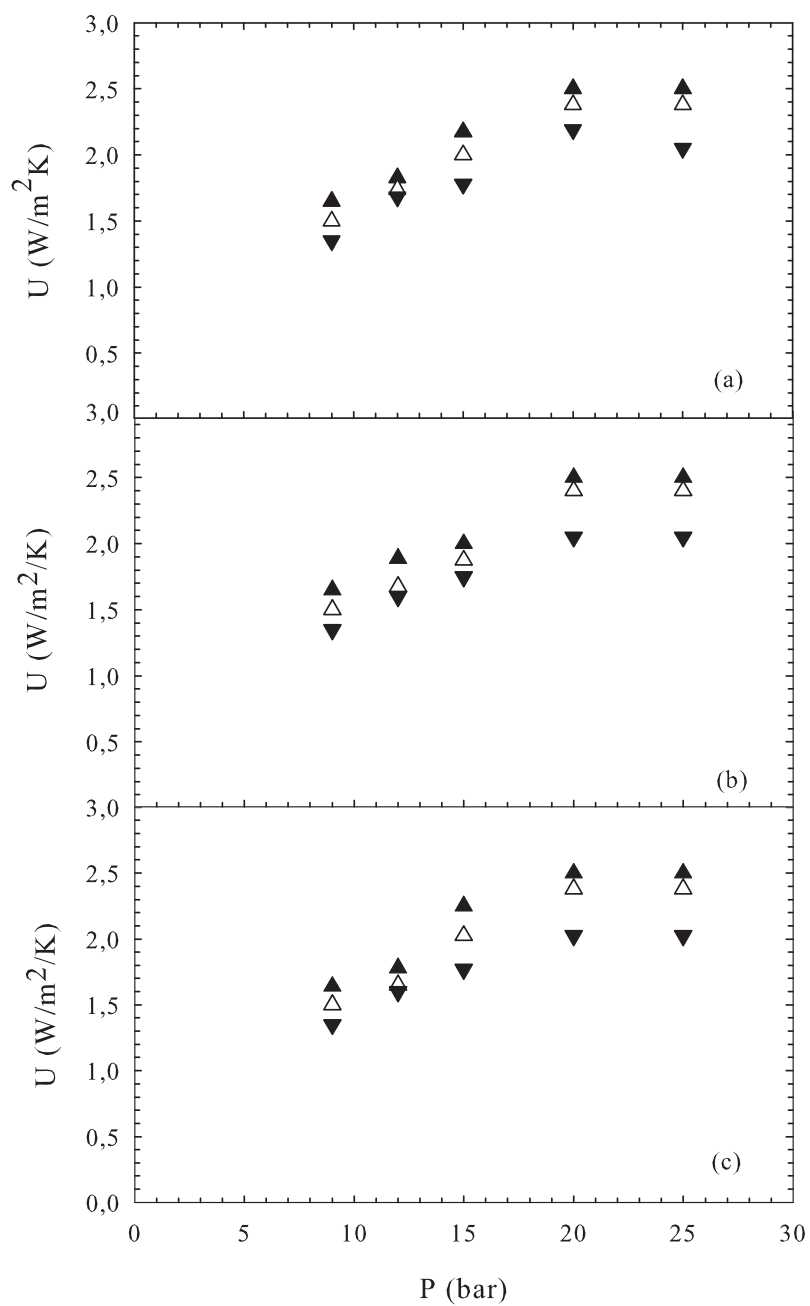


Figure 7.5: Overall heat transfer coefficient as a function of system pressure for different liquid at constant gas flow rates: (a) 3 NL/h, (b) 9 NL/h, (c) 18 NL/h: (▲)  $F_L = 100$  mL/h, (△)  $F_L = 60$  mL/h, (▼):  $F_L = 30$  mL/h:  $T_{Oven} = 170^\circ\text{C}$ ,  $W_{cat} = 7.5$  g.

bar, curved profiles occurred in particular at the lowest liquid velocity of 30 mL/h. The fit of these profiles although acceptable showed a higher deviation than that of straight profiles, which are very easy to match. The highest precision should therefore result for the values of  $U$  fitted at 20 and 25 bar. The convex curving of the temperature profiles disappeared at these pressures and the highest deviation introduced by the error of the thermocouples was between 2.5 and 5%.

### 7.1.5 Determination of bed to wall heat transfer coefficient ( $h_w$ )

With the help of eq.5.5 and the fitted overall heat transfer coefficients, the bed to wall heat transfer coefficient  $h_w$  was evaluated for all experimental conditions used. Obtained values of  $h_w$  vary between 2 and 8 W/m<sup>2</sup>K, hence being close but always superior to the coefficients of  $h_w$  calculated with the correlation proposed by Specchia et al. [192] for the limiting case of gas solid heat transfer. This result may not surprise since the liquid flow rates used in our work are very small and conditions that arise for bed to wall heat transfer could be quite similar to those of a gas-solid system. The precision of the  $h_w$  coefficients not only depends on the quality of the fitting of  $U$ , but also on to what extent the bed to wall heat transfer is the controlling resistance of the process. For our system, the corresponding thermal resistances of the natural convection, heat conduction in the insulating material and bed to wall heat transfer are calculated to 0.027 m<sup>2</sup>K/W, 0.22 m<sup>2</sup>K/W and 0.125-0.5 m<sup>2</sup>K/W. As expected, natural convection outside the insulating material is not controlling its resistance typically being ten times smaller than the other two resistances. Accordingly, both the bed to wall heat transfer and the insulating heat conduction are controlling steps in the overall heat transfer. For pressures up to 15 bar,  $h_w$  exerts a stronger control than heat conduction, but then the resistances become similar. This means that the uncertainty in  $h_w$  is a function of its absolute value being smaller for low  $h_w$ . Overall,  $h_w$  is found to exactly follow the trends as observed for  $U$  providing thus confidence to the estimated values of  $h_w$ .

The values of  $h_w$  were correlated with operating conditions employing the following expression assuming the usual Chilton-Coburn dependency for the Prandtl number:

$$h_w = Re_L^{0.305} Pr_L^{1/3} Re_G^{0.0475} P_T^{0.98} \quad (7.1)$$

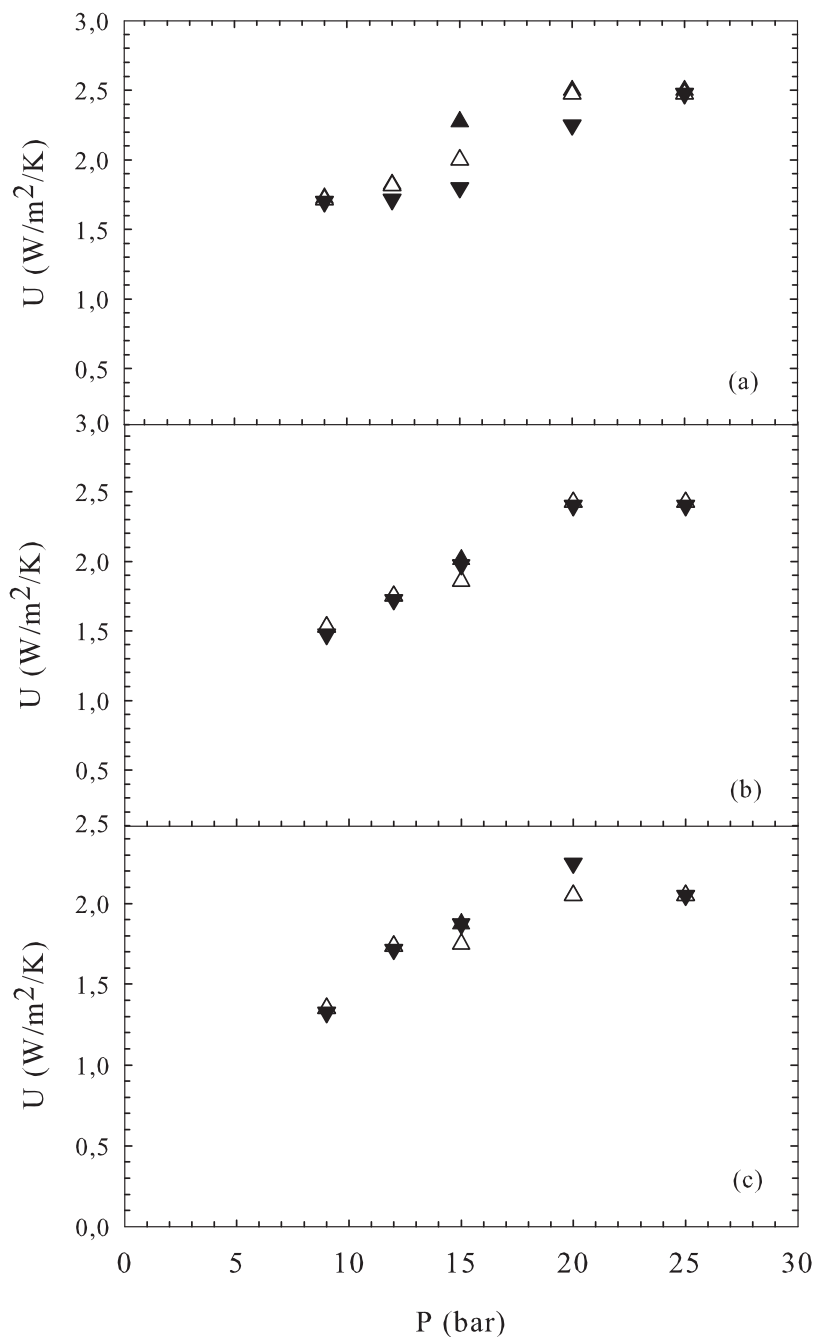


Figure 7.6: Overall heat transfer coefficient as a function of system pressure for different gas flow rates at constant liquid flow rate: (a) 100 mL/h, (b) 60 mL/h, (c) 30 mL/h; (▲)  $F_G = 18$  NL/h, (△)  $F_G = 9$  NL/h, (▼):  $F_G = 3$  NL/h;  $T_{Oven} = 170^\circ\text{C}$ ,  $W_{cat} = 7.5$  g.

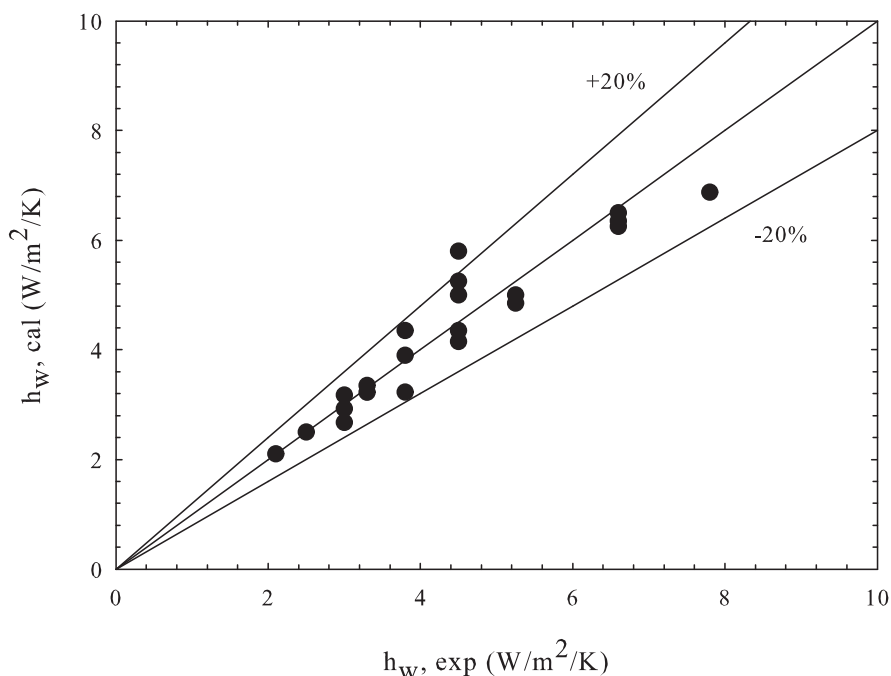


Figure 7.7: Parity plot for experimentally determined  $h_W$  and values calculated from the correlation proposed in equ. 7.1.

for  $DI/dp = 18.6$ ,  $0.16 < Re_L' < 1.0$ ,  $0.35 < Re_G' < 4.5$  and  $9 \text{ bar} < P_T < 20 \text{ bar}$ .

The optimized exponents for the gas and liquid Reynolds number and total pressure clearly reflects the experimental trends outlined in the previous sections. The calculated average error of the correlation proposed is small (ca. 7%) with 12 data points with a negative deviation and 24 data points with a positive deviation. The overall quality of the fit can be appreciated in Figure 7.7, which shows a parity plot of experimentally determined  $h_W$  values and  $h_W$  values predicted by the correlation of eq. 7.1. It can be concluded that the correlation suitably represents the experimental data, although its use is restricted to a narrow range of operating conditions that includes a variation of the system pressure.

### 7.1.6 Conclusion

Steady state axial temperature profiles have been measured in a rock wool insulated packed bed column with co-current downflow of nitrogen and water phases for dif-

ferent column pressures and very small gas and liquid flow rates corresponding to the low interaction regime. It has been observed that gas flow rate only marginally affects the heat transfer, whereas increasing the liquid flow rate enhances the heat transfer from the bed to wall. Moreover, a linear pressure dependency of heat transfer is observed from 9 bar to 20 bar before it levels off at 25 bar. At intermediate pressures, convex curving of the profiles occurred suggesting that condensation of water vapor from the gas phase impact on the heat transfer conditions inside the packed bed.

The whole data set was interpreted with a pseudo homogeneous one parameter model confirming the influence of condensation of water vapor on heat transfer. Curving of the profiles as observed in the experiments could be only reproduced by the model when accounting for the contribution of condensation to the heat balance.

Overall heat transfer coefficients  $U$  based on the inside column area were evaluated by fitting the model predictions to the experimental data. The values of  $U$  obtained (1.25 to 2.5 W/m<sup>2</sup>K) quantitatively reflect the aforementioned influences of operating variables on heat transfer. The uncertainty in  $U$  is pressure dependant because at low system pressure the bed gradients are small and the error of the thermocouples can become important (only at 9 bar). Curving of the profiles (essentially occurring at pressures of 15 bar) is a second contribution that can moderately increase the uncertainty since fitting of curved profiles is acceptable but not as precise as fitting of straight profiles. In agreement with the very small liquid flow rates employed in the experiments, the values of  $h_w$  (between 2 and 8 W/m<sup>2</sup>K) are close to the limiting case of gas solid heat transfer. The average error in  $h_w$  calculated from the correlation is less than 7%. As in our work the use of an insulating material was mandatory, a mixed control of heat transfer resulted, although the bed to wall heat transfer is the larger resistance at least for pressures up to 15 bar. Overall, it can be concluded that the correlation developed suitably represents the experimental temperature data. The overall performance of the model developed (including the fitting of  $U$ ) gives confidence for its ultimate application in the investigation of the catalytic wet air oxidation of phenol over active carbon conducted in a trickle bed reactor under temperature feed modulation.

## 7.2 Feed Temperature Modulated CWAO in Trickle Bed Reactor

### 7.2.1 Temperature feed modulation without reaction

Two series of temperature feed modulation experiments without reaction have been conducted: 1) using a nitrogen-water-AC system to study the heat dynamics of a packed bed column and 2) using a nitrogen-phenol solution-AC system to study the adsorption/desorption dynamics induced by temperature feed modulation.

**Dynamic heat transfer:** The dynamic heat transfer results with imposed temperature feed modulation are illustrated in Figure 7.8 for a total pressure of 15 bar, gas flow rate of 9 NL/h and three different liquid flow rates. The cycle period and split for these experiments were set to 108 min and 5/6 respectively, i.e. feed temperature of the column inlet was periodically changed to 25 °C during 18 min and then to 160 °C during 90 min. However, the arrangement of the tubing and inlet column connections originated a distortion of the ideal square wave for the feed temperature and generated instead a V shaped temperature distribution at the column inlet similar to the measured profiles at  $z = 1.5$  cm (see Figure 7.8). In all cases the liquid flow rate was not high enough to cool the hot reactor inlet to ambient temperature within 18 min of cold cycle. A longer time interval with cold flow would be needed, i.e. a smaller split or a higher cycle period, to achieve the aforementioned goal. When switching back to hot feed flow, the column inlet temperature raised rapidly to reach a pseudo steady state temperature of 160 °C. Thus, a temperature wave established in the reactor inlet and propagated downstream to the column exit.

Simulated temperature profiles using the values of  $U$  fitted in section 7.1.4 are also plotted in Figure 7.8. The model predicts very well all the experimental dynamic temperature profiles close to the inlet zone, although a slight but progressive deviation is observed in the simulations of the temperatures towards the column outlet. The dynamics of heat transfer predicted by the model is slightly slower than experimentally observed. Parametric analysis (not shown here) allowed identifying the relevance of the liquid holdup as a key parameter that defines the temperature wave propagation speed along the trickle bed column length. This highlights the need of an accurate estimation of liquid holdup to succeed in modeling of non steady state operation of trickle bed reactors. Moreover, the thermal dynamics of the insulated column, which is not considered in the model formulation, could influence the temperature profiles inside the bed and partly be responsible for the deviation observed.

**Adsorption/desorption dynamics:** the dynamic experiments with phenol so-

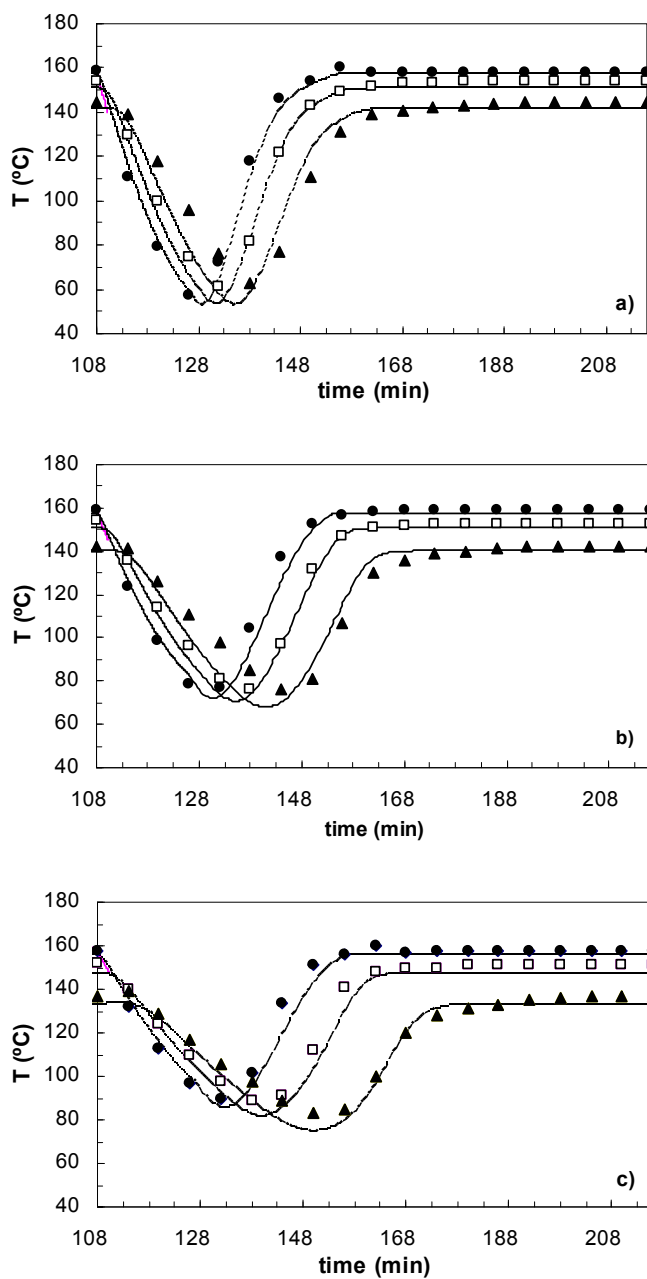


Figure 7.8: Evolution of axial temperatures during operation with imposed feed temperature modulation: ( $\bullet$ )  $T(1.5 \text{ cm})$ , ( $\square$ )  $T(10 \text{ cm})$ , ( $\blacktriangle$ )  $T(20.5 \text{ cm})$ , lines represent model predictions: (a) 100 mL/h, (b) 60 mL/h, (c) 30 mL/h;  $P_T = 15 \text{ bar}$ ,  $T_{\text{Oven}} = 170^\circ\text{C}$ ,  $F_G = 9 \text{ NL/h}$ .

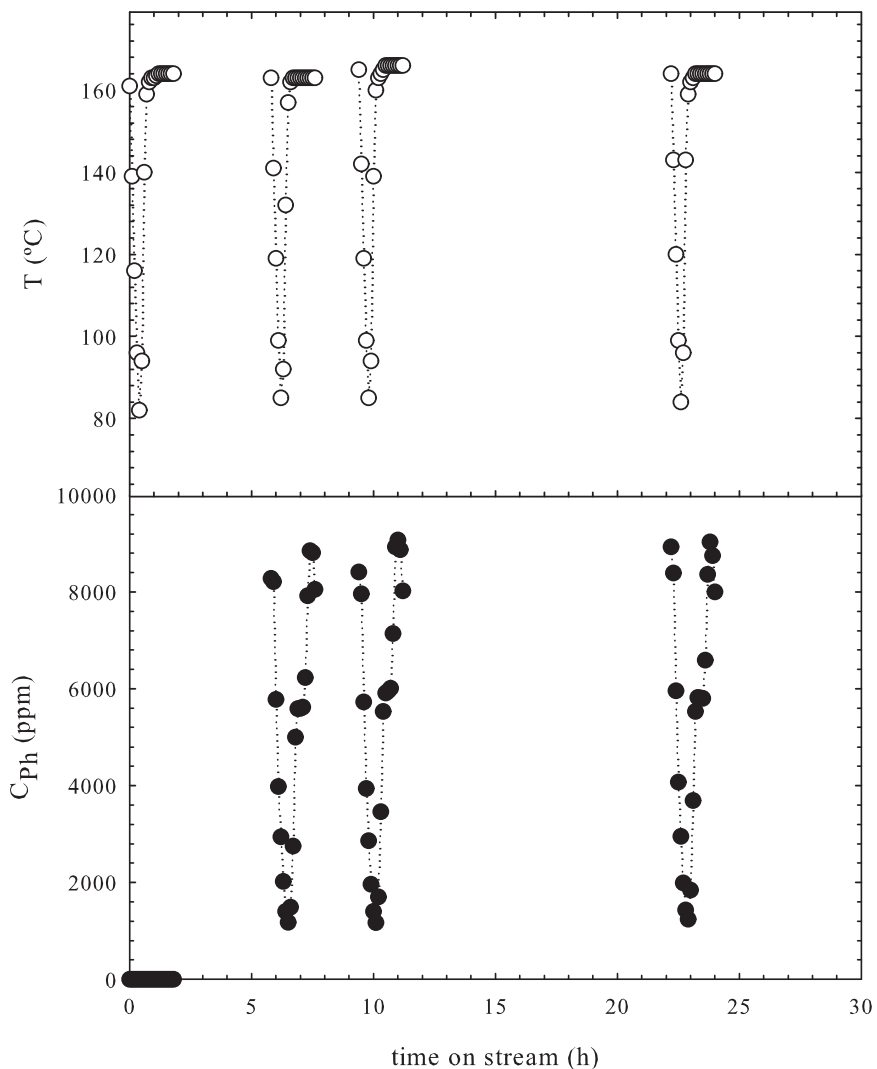


Figure 7.9: Adsorption-desorption dynamics of phenol concentration under temperature feed modulation without reaction:  $P_T = 15$  bar,  $T_{\text{inlet}} = 163^\circ\text{C}$ ,  $F_L = 63$  mL/h,  $F_G = 9$  NL/h,  $C_{\text{Ph}} = 5$  g/L,  $W_{\text{cat}} = 7.5$  g.

lution were conducted to highlight the temperature driven adsorption/desorption dynamics of phenol over AC in the absence of reaction. The resulting temperature and concentration profiles are illustrated in Figure 7.9. Except for the first cycle, periodic oscillation of temperature induces a similar phenol concentration cycle at the fixed-bed column outlet due to periodic adsorption-desorption of phenol on the

AC surface. The phenol concentration wave oscillated between 9000 ppm and 1200 ppm corresponding roughly to ca. 5000 ppm (feed concentration) as a mean of oscillation. Thus, for phenol oxidation under feed temperature modulation, it can be deduced that as soon as the temperature falls below 120 °C, the oxidation is going to halt while phenol re-adsorption is favored leading to 100% apparent phenol conversion. When the hot liquid stream is switched on again, the temperature rapidly comes back to the oven temperature set of 160 °C, and desorption start to dominate leading to higher phenol concentration in the liquid phase. This cyclic surface renewal of phenol could protect the AC surface from being directly attacked by dissolved molecular oxygen. Hence, the adequate choice of period and split will be crucial for achieving high mean phenol conversion during CWAO of phenol over AC in TBR under feed temperature modulation.

## 7.2.2 Temperature feed modulation with reaction

### 7.2.2.1 Adiabatic operation

As it has been already commented in the previous section (7.1.1), keeping the reactor close to adiabatic operation may be beneficial to feed temperature modulated CWAO of phenol over AC catalysts. To check this, steady state CWAO experiments under isothermal and close to adiabatic conditions were thus conducted in the TBR using the polyurethane insulation to achieved adiabatic operation. The corresponding temperature and phenol conversion profiles are illustrated in Figure 7.10. With respect to the phenol conversion a significant 5% conversion improvement from 90 to 95% is observed when the reactor was operated adiabatically. However, the observed adiabatic temperature rise ( $\Delta T = 5 - 6$  K) for  $X_{Ph}$  of 0.95. is small compared to the maximum  $\Delta T_{Adi}$  of 40 K for 5 g/L of phenol solution reported in the previous studies [124]. Heat loss and particularly water evaporation must greatly reduce the maximum adiabatic temperature rise inside the bed in our experimental condition.

### 7.2.2.2 Influence of period and split on phenol conversion

In the first series, temperature feed modulated CWAO experiments were conducted over 50 h of time on stream for different period and split combinations to select appropriate cycle values for long run CWAO experiments. Figure 7.11 shows typical temperature and phenol conversion profiles obtained for  $T_{inlet} = 163$  °C,  $F_L = 63$  mL/h and  $F_G = 9$  NL/h. Cycling of temperature in each experiment was only started after ca. 24 h of continuous catalytic wet oxidation to reach first steady state of adsorption and reaction. The cycle was always initiated by injecting cold gas-

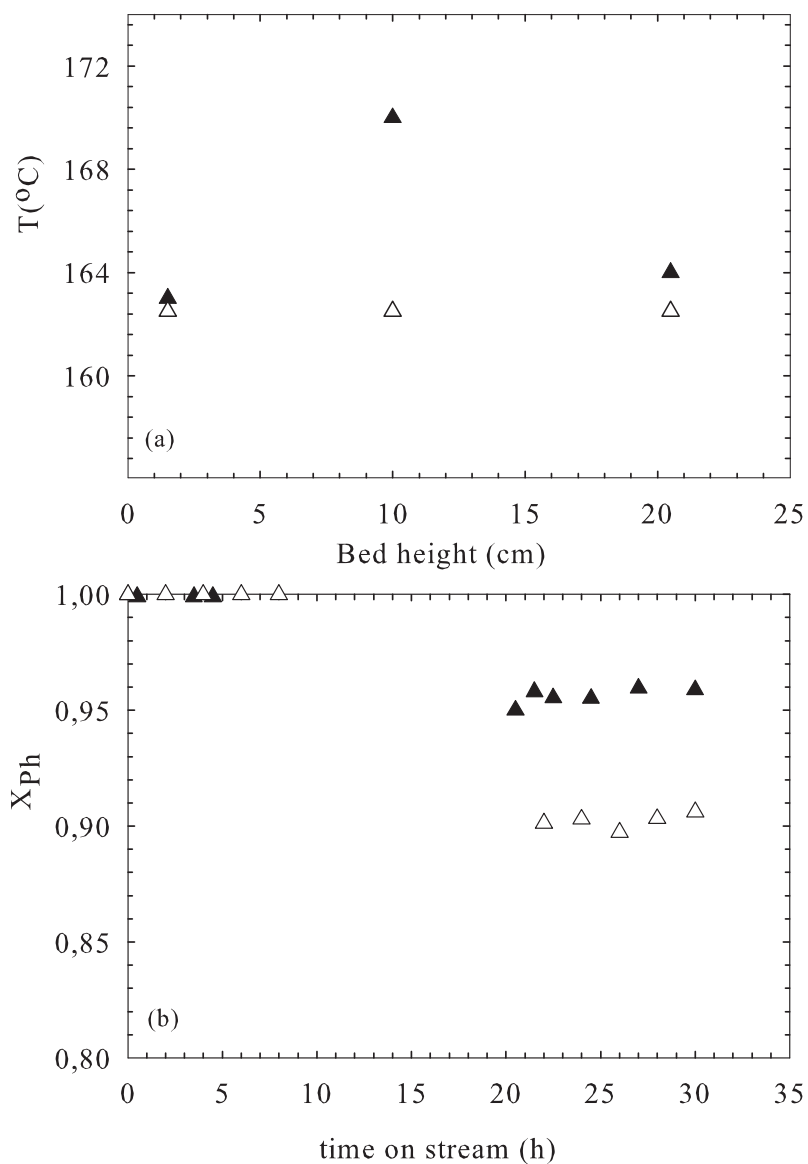


Figure 7.10: Phenol conversion and temperature profiles for (▲) adiabatic and (△) isothermal steady state TBR operation:  $P_{O_2} = 2$  bar,  $T_{inlet} = 163^\circ\text{C}$ ,  $F_L = 63$  mL/h,  $F_G = 9$  NL/h,  $C_{Ph} = 5$  g/L,  $W_{cat} = 7.5$  g.

liquid mixture into the hot catalyst bed via the timer controlled three-way solenoid valve. Analysis of the dynamic profiles in Figure 7.11 highlights the strong influence

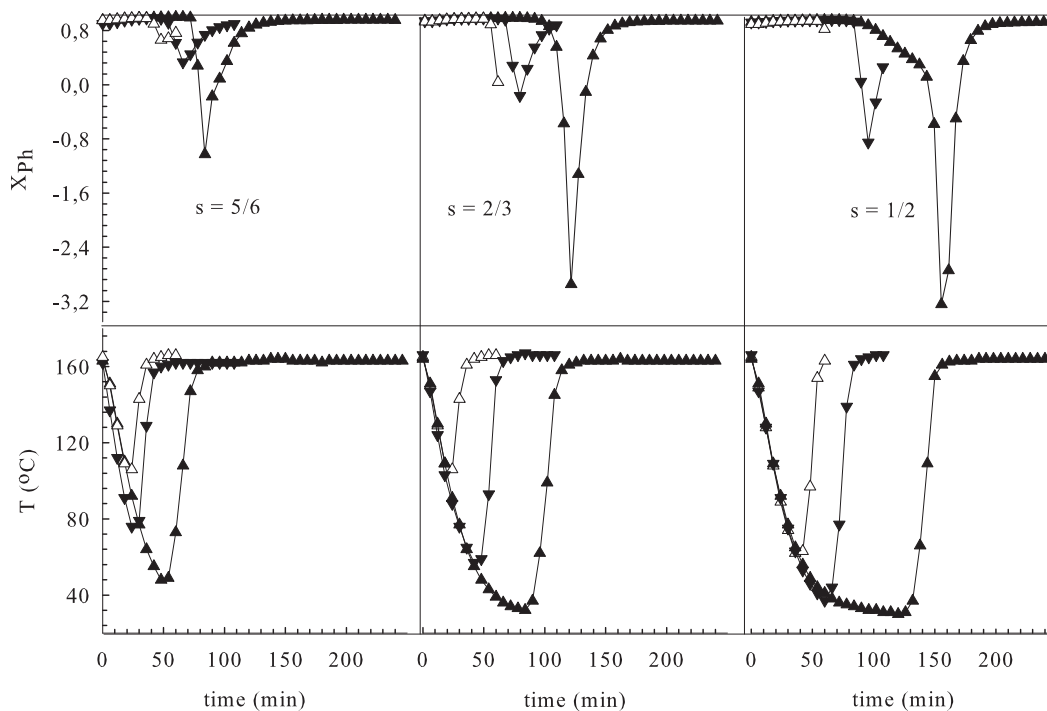


Figure 7.11: Effect of period and split on phenol conversion and temperature observed during modulated CWAO of phenol over AC: ( $\Delta$ )  $p = 1$  h, ( $\nabla$ )  $p = 1.8$  h, ( $\blacktriangle$ )  $p = 4$  h;  $P_{O_2} = 2$  bar,  $T_{inlet} = 163^\circ\text{C}$ ,  $F_L = 63$  mL/h,  $F_G = 9$  NL/h,  $C_{Ph} = 5$  g/L,  $W_{cat} = 7.5$  g.

that has temperature feed modulation on adsorption-desorption dynamics and reaction. Depending on the split and period used, the reactor temperature could drop to ambient conditions ( $\sim 35^\circ\text{C}$  for the lower split and higher period of 0.5 and 4 h, respectively) during the cold cycle and then normally propagates back to the oven temperature during the hot cycle. During the bed temperature is approaching to ambient conditions (cold cycle), the AC bed is re-saturated with phenol and therefore the apparent phenol conversion goes up to ca. 100%. When the bed is flushed again with the hot gas-liquid mixture during the hot cycle, the reactor temperature rapidly rises to the oven temperature and most of the re-adsorbed phenol on the AC surface is instantaneously desorbed thereby leading to apparently negative phenol

conversions. Nevertheless, phenol oxidation (exothermic reaction) dominates within a short time causing a rapid increase in phenol conversion to the steady state conversion ( $X_{Ph} = 0.93$ ). In general, phenol conversion and bed temperature come back to steady state irrespective of the split used in case of longer periods. This is not so for phenol conversion at splits and periods of smaller than 0.8 and 2 h, respectively, whereas temperature always reaches steady state.

Regarding the dynamic response of temperature and concentration, Figure 7.11 indicates that heat transfer dynamics are fast. On the other hand, there is a delay of ca. 25-30 minutes in the concentration profile with respect to the temperature profiles suggesting that the response of adsorption/desorption coupled with reaction is slower than that of heat transfer. It has to be mentioned, however, that temperature readings are taken instantaneously very close to the reactor outlet, while liquid samples are taken at , approximately 2 m down stream of the reactor outlet.

To determine the split and cycle period combinations that may provide maxi-

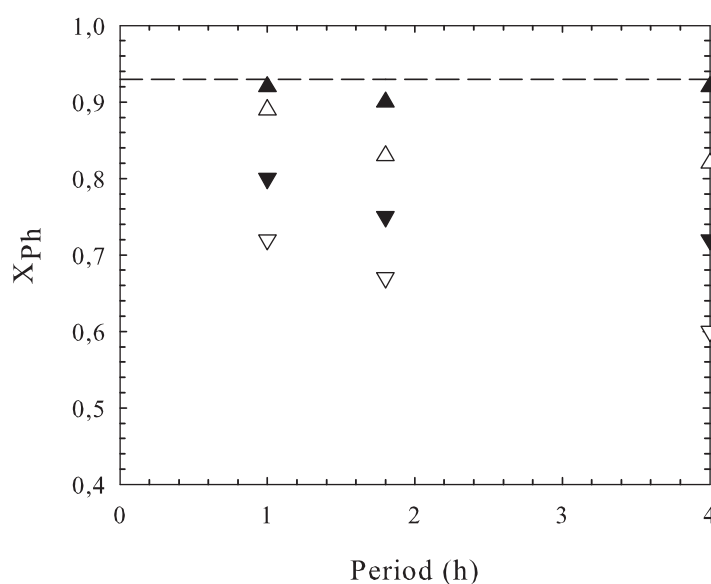


Figure 7.12: Mean cycle phenol conversion after 50 h of CWAO operation as function of cycle period : (▲)  $s = 0.9$ , (△)  $s = 0.83$ , (▼)  $s = 0.67$ , (▽)  $s = 0.5$ :  $P_{O_2} = 2$  bar,  $T_{inlet} = 163$  °C,  $F_L = 63$  mL/h,  $F_G = 9$  NL/h,  $C_{Ph} = 5$  g/L,  $W_{cat} = 7.5$  g.

mum phenol conversion and minimum AC burn-off in the long run phenol oxidation experiments, short term cycling results should be compared with those performed

at same steady state conditions. The mean cycle phenol conversions of 50 h were thus calculated and compared in Figure 7.12 with the corresponding steady state conversion obtained after 50 h of reactor operation. Depending on the split-period combinations used, the mean cycle phenol conversion was calculated from one or two consecutive cycles because at shorter periods complete cycle did not establish during the first cycle. As it can be seen in Figure 7.12, the mean cycle phenol conversions always fall below the corresponding steady state conversion. For a given cycle period, as the split increases, the cycle time fraction of the hot liquid stream to flush the reactor bed is increased and thus the level of conversion approaches the steady state value. Similarly, for constant split, when relatively short cycle periods are employed, the mean cycle phenol conversion also tends to the steady state conversion. On the other hand, for longer cycle period, the mean cycle conversion profile asymptotically approaches the split times the steady state phenol conversion ( $X_{Ph,cy} = s X_{Ph,ss}$ ). A similar trend has been reported for gas feed composition and gas feed flow modulation studied in an isothermal trickle bed reactor [114, 115]. It appears from Figure 7.12 that, operating the reactor at higher split and longer period (i.e. close to steady state) becomes advantageous because it avoids phenol conversion to drop zero. However, the exposure of AC to the hot fluid stream is comparable with steady state operation and consequently AC burn-off could be significant. At longer period and short split, phenol desorption becomes important (see Figure 7.11) due to bed saturation during the cold cycle leading to too low mean cycle conversions. Thus, a balance between the adsorption, activity and stability should be considered for the overall performance of the process. This will be tested in the long term CWAO experiments carried out at a fixed split and different cycle periods.

### 7.2.2.3 Influence of cycle parameters on catalyst stability

Based on the mean cycle conversion obtained in the short term experiment, several long term experiments (ca. 150) were performed for different cycle periods at fixed cycle split of 0.8 and for two different reactor inlet temperatures. A continuous steady state long term experiment at otherwise same operating condition was also conducted for purpose of comparison. Moreover, the weight and phenol adsorption capacity of the spent ACs were determined after each long run CWAO experiment.

An example of the conversion and temperature-time profiles obtained in a long term CWAO is illustrated in Figure 7.13 ( $p = 1$  h and split of 0.8). Conversion and temperature profiles for the other periods are given in appendices D.1. During the first 8 to 10 h, conversion remained at apparent 100% due to the AC bed saturation. After ca. 10 h TOS, phenol conversion gradually decreases to reaches a pseudo-steady state conversion of 93% at ca. 24 h. At this point feed tempera-

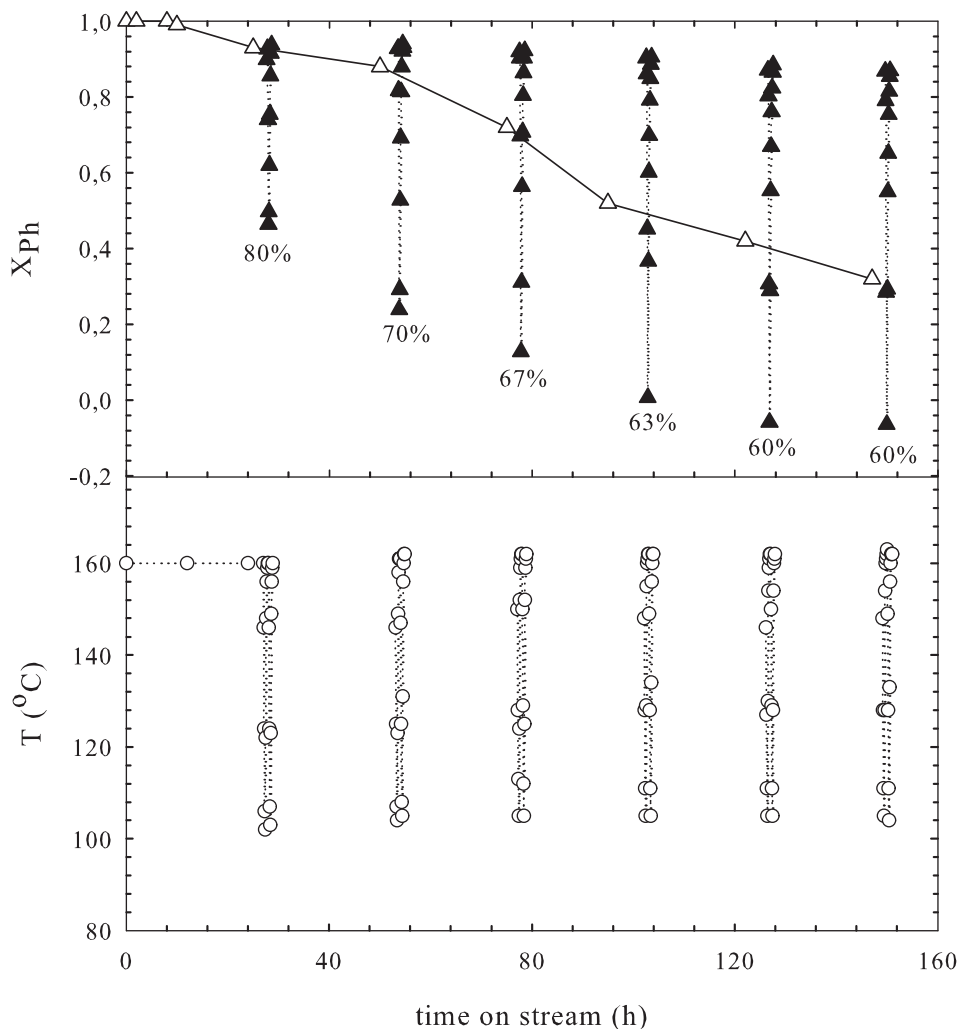


Figure 7.13: Unsteady state phenol conversion and temperature profile as function of time on stream for ca. 150 h : ( $\Delta$ ) steady state conversion, ( $\blacktriangle$ ) periodic conversion, line represents trends:  $P_{O_2} = 2$  bar,  $T_{inlet} = 163$  °C,  $F_L = 63$  mL/h,  $F_G = 9$  NL/h,  $C_{Ph} = 5$  g/L,  $W_{cat} = 7.5$  g,  $p = 1$  h,  $s = 0.8$ .

ture modulation was started to induce a temperature wave down stream the reactor length (bed). As a consequence, temperature and concentration start to oscillate between their maximum and minimum values. Figure 7.13 further shows that the oscillation amplitude remains nearly constant for temperature wave, whereas the amplitude of the concentration wave varies with operating time. The minimum

peak point for phenol conversion is progressively diminished over 100-120 h before stabilizes at a low value of 10%. This suggests that a progressive loss of the AC sorption capacity occurred during the oxidation run. On the other hand, phenol conversion always comes back to the reference steady state conversion during the hot cycle indicating that the activity of the catalyst is rather unaffected by the loss of its adsorption capacity.

To check this assumption, phenol adsorption isotherms were determined for the

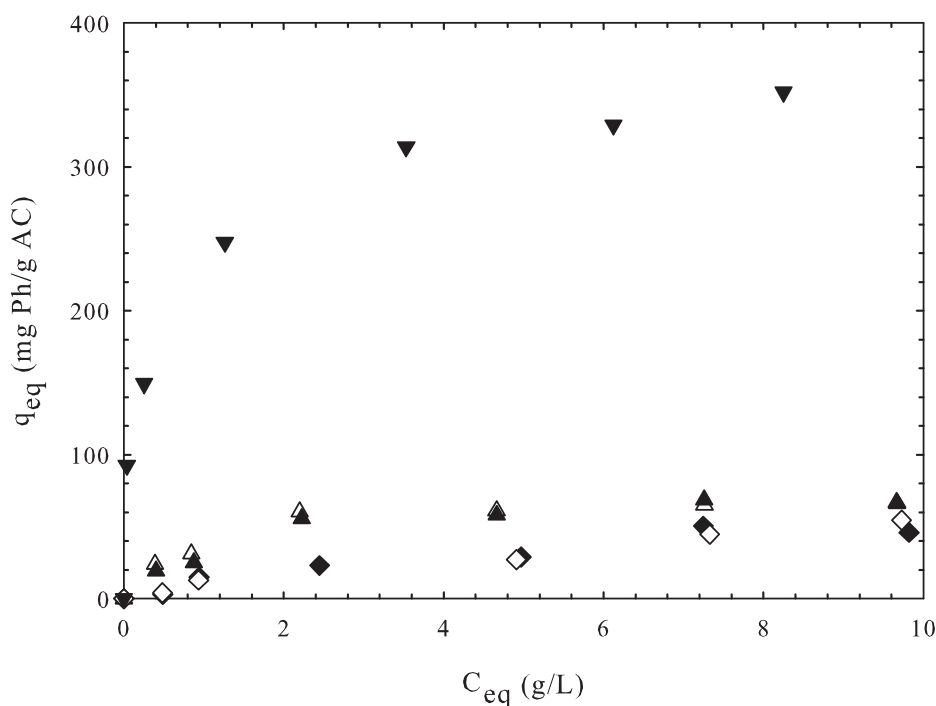


Figure 7.14: Phenol adsorption isotherm of fresh and CWAO spent AC samples obtained at  $22 \pm 1$  °C: ( $\nabla$ ) Fresh AC, ( $\triangle$ ) after 50 h of continuous operation, ( $\blacktriangle$ ) after 50 h of periodic operation  $s = 0.83$  and  $p = 4$  h, ( $\diamond$ ) after ca. 150 h of periodic operation  $s = 0.83$  and  $p = 1.8$  h, ( $\blacklozenge$ ) after ca. 150 h of periodic operation,  $s = 0.83$  and  $p = 0.5$  h.

fresh and CWAO spent ACs. Figure 7.14 illustrates the corresponding isotherms obtained at  $22 \pm 1$  °C under oxic conditions. The result in Figure 7.14 clearly confirms the significant reduction in adsorption capacity produced during continuous or dynamic CWAO experiments. It also appears that the AC must lose most of its

adsorption capacity in the early stage of the CWAO experiments since more than 80% of its original adsorptive capacity is lost within the first 50 h operating time. Then, the loss of adsorption capacity slowed down and adsorption capacities after 50 and 145 h only differ by 20%.

Figure 7.15 compares the cycle mean phenol and TOC conversion of the three

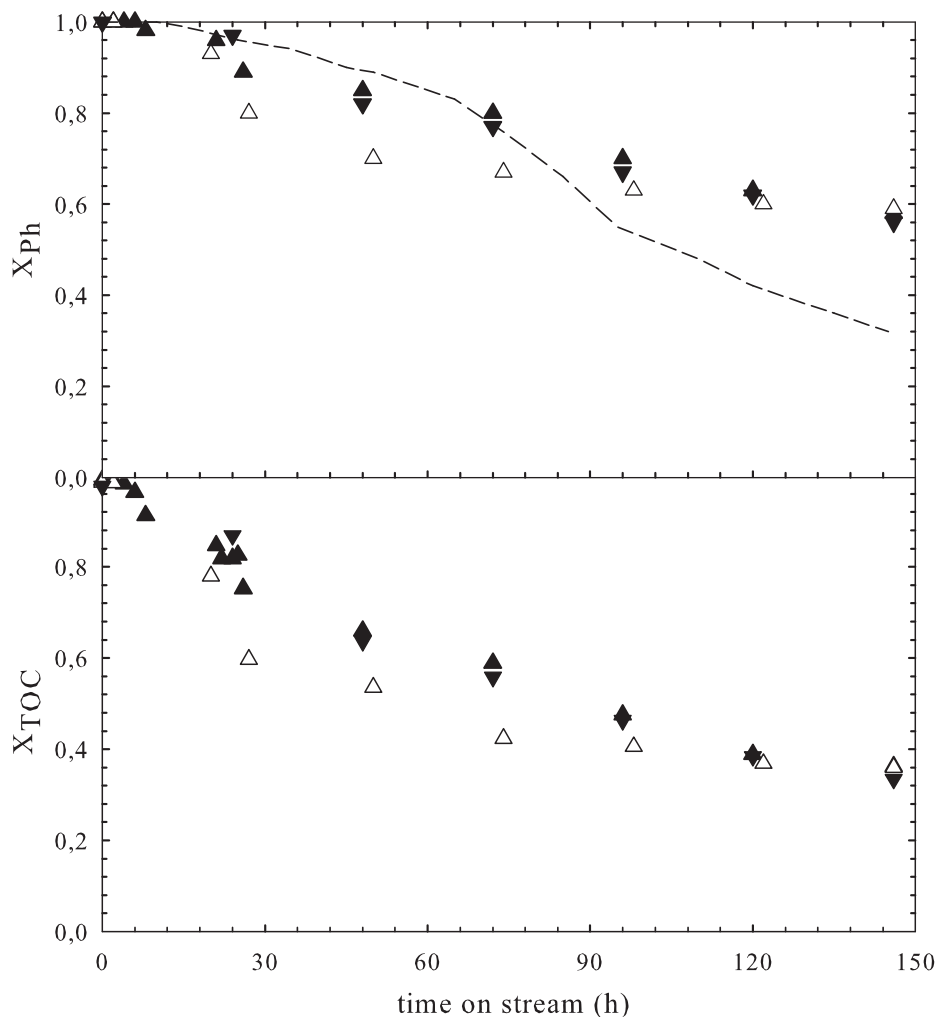


Figure 7.15: Mean cycle phenol and TOC conversion as function of time on steam for different period: ( $\blacktriangle$ )  $p = 1.8$  h, ( $\triangle$ )  $p = 1$  h, ( $\blacktriangledown$ )  $p = 0.5$ , discontinues line represents steady state conversion:  $P_{O_2} = 2$  bar,  $T_{i,nlet} = 163$  °C,  $F_L = 63$  mL/h,  $F_G = 9$  NL/h,  $C_{Ph} = 5$  g/L,  $W_{cat} = 7.5$  g, split = 0.8.

long term CWAO experiments with the reference steady state experiment. It is seen that a higher initial phenol conversion was obtained at large (1.8 h) and small (0.5 h) periods for a given split of 0.8. This is because for a fixed split, the larger the period, the longer the hot stream flushes the cold catalyst bed, thus the reaction has enough time to oxidize the adsorbed phenol and possible oxidation products. With respect to shorter period, the system is always close to the steady state conditions for a high split of 0.8. However, at about ca. 110 h the cycle mean conversions for all periods are merging to the same values of TOS; although phenol conversion seems more stable after three consecutive days in case of  $p = 1$  h. Thus, an intermediate cycle period appears to be optimal with respect to activity and stability of the AC. On the other hand, when we compare steady state with periodic operation, the former provides an initially higher phenol conversion. After about 70 h however, both operation modes result in the same phenol conversion. Then, feed temperature modulation outperforms steady state operation yielding 60 and 32% phenol conversion respectively after ca. 150 h of TOS. The better long term performance of the catalyst in case of temperature feed modulation should be mainly attributed to a substantial delay in AC burn-off (as will be shown later) achieved by the temperature induced dynamics of adsorption and reaction.

Additional phenol oxidation experiments were conducted for a different reactor inlet temperature of 152°C at otherwise same periodic operating conditions. The resulting cycle mean conversion-time profiles are illustrated in Figure 7.16 and compared with the results obtained at 163°C ( $p = 1$  h,  $s = 0.8$ ). As it can be seen in the figure, stable phenol conversion was achieved even for higher split of 0.9 but the cycle mean conversion is lower than that performed at 163 °C and same split of 0.8. Also, the cycle mean conversions obtained at 152°C are comparable with the steady state conversion achieved at 140 °C, where AC burn-off was not significant at the end of a 10 day oxidation run [43]. Therefore, feed temperature modulation is only beneficial to CWAO at higher temperature, where AC burn-off is significant during steady state TBR operation.

Table 7.1 summarizes the result of weight and BET surface area measurement of the spent ACs obtained after each long run CWAO experiments and the main results. As it can be seen in Table 7.1, there exists a considerable reduction in AC burn-off during CWAO when its surface was subjected to a periodic variation of phenol coverage induced by feed temperature modulation. At 152°C a weight gain of 2.6 and 3.2 was observed for splits of 0.8 and 0.9, respectively. Temperature feed modulation enables to achieve catalyst stability, however with too small phenol and TOC conversion removal. At 163°C, the situation is different, only the period/split combinations of 1 h/0.8 seems to balance AC burn-off and formation/destruction of

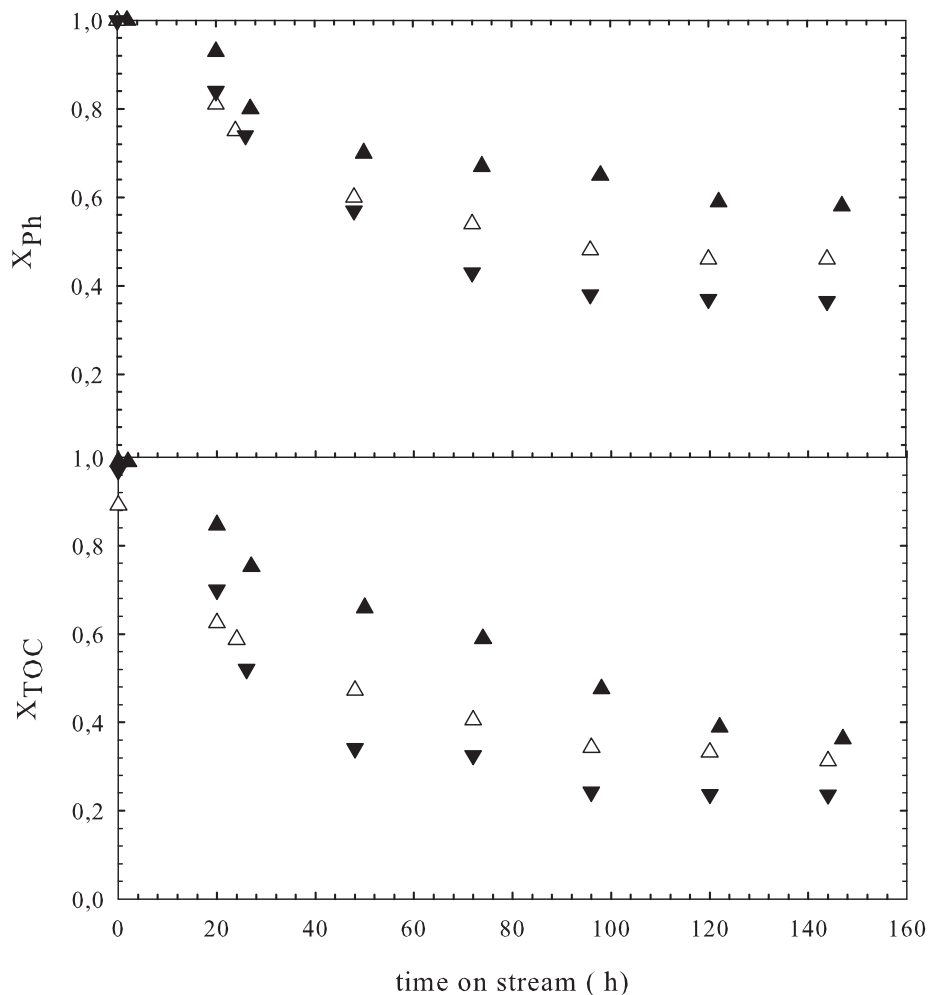


Figure 7.16: Mean cycle phenol and TOC conversion with time on steam for different temperature: (▲) 163°C (s = 0.8), (△) 152°C (s = 0.9), (▼) 152°C (s = 0.8):  $P_{O_2} = 2$  bar,  $F_L = 63$  mL/h,  $F_G = 9$  NL/h,  $p = 1$  h,  $C_{Ph} = 5$  g/L,  $W_{cat} = 7.5$  g.

oxidative coupling products. For the other periods some degree of AC combustion is observed in agreement with their smaller final conversion achieved. However, it is clearly demonstrated that temperature feed modulation can completely avoid AC burn-off, whereas the consumption of AC reached ca. 75% of the initial amount of AC loaded at steady state operation.

Table 7.1: Phenol conversion and AC weight difference measured after ca. 150 h TOS under feed temperature modulation:  $P_{O_2} = 2$  bar,  $F_L = 63$  mL/h;  $F_G = 9$  NL/h,  $C_{Ph} = 5$  g/L,  $W_{AC} = 7.5$  g.

T (°C)	p (h)	s	$\Delta W_{AC}$ (g)	$S_{BET}$ (m <sup>2</sup> /g)	$X_{ph}$	$X_{TOC}$
152	1	0.8	3.2	-	0.37	0.24
152	1	0.9	2.6	-	0.46	0.31
163	0.5	0.8	-0.8	321	0.56	0.34
163	1	0.8	1	355	0.60	0.35
163	1.8	0.83	-3	292	0.58	0.36
163	-	-	-5.2	-	0.32	-

### 7.2.3 Conclusion

The experiments conducted with imposed temperature feed modulation under non-reactive conditions revealed the formation of V-shaped temperature profiles in the column packed with AC. The deviation from the ideal square wave is mainly due to the experimental arrangement of tubing and column inlet connections. The accurate modeling of these temperature waves was achieved with a dynamic model using the previously fitted values of the overall heat transfer coefficient (U). Parametric analysis indicated that the dynamics of heat transfer is particularly sensitive to the value of the liquid flow rate (dynamic liquid hold up). The model developed gives confidence for its ultimate application in the investigation of the catalytic wet air oxidation of phenol over active carbon conducted in a trickle bed reactor under temperature feed modulation.

CWAO of phenol in steady state operation confirmed that the stability of activated carbon catalyst largely depends on the operating conditions employed and the way how the carbon is contacted with phenol. At 163°C, 2 bar of oxygen partial pressure, space time of 0.12 h and oxic TBR start up, the conversion performed is high (over 93%), but the AC burn-off is also enhanced leading to a remarkable loss of catalyst activity with time on stream. Temperature feed modulated CWAO of phenol proved to be an effective operating strategy to minimize AC burn-off. Stable activity during modulated CWAO of phenol over AC was achieved in our TBR at period of 1 h, split of 0.8, 163°C, 2 bar of oxygen pressure and low liquid space time of 0.12 h. At these conditions, it has been observed that AC burn-off was completely avoided, accordingly improving the final phenol conversion from 32%

(steady state) to 60-65% (periodic operation). The improvement is mainly due to adsorption/reaction cycle induced by temperature on the AC surface during CWAO. Nevertheless, a significant adsorption capacity loss of AC has been observed which ultimately limited the mean cycle phenol conversion to 60-65% and thereby its industrial application.

### **7.3 Liquid Flow Modulated CWAO in Fixed Bed Upflow Reactor**

Continuous CWAO of phenol over AC conducted in upflow mode at 160 °C and 2 bar of oxygen pressure revealed that no apparent carbon weight loss was detected after ca. 150 h operation time contrary to what has been observed in downflow operation mode. The carbon weight loss in downflow mode can be related to the combustion of AC during the oxidation process (see section 7.2). In the upflow operation mode, the carbon particles seem protected against combustion by a liquid film that completely covers the carbon surface, thus AC combustion may not be a dominant factor. However, a similar phenol conversion decline with operating time at apparently invariable AC weight was observed for upflow operation mode. Probably, the dominant deactivation mechanism in upflow reactor could be due to blockage of the active site of AC by irreversible adsorbed oxidative coupling products. Moreover, the liquid film covered the catalyst surface may induce mass transfer resistance for the gaseous reactant. Periodic variation of liquid flow may overcome the aforementioned drawbacks of upflow mode. Thus, a series of on-off liquid flow modulation catalytic wet oxidation experiments have been conducted in upflow mode.

#### **7.3.1 Influence of period and split on phenol conversion**

Liquid flow modulated CWAO experiments with different cycle period and split combinations were performed at 160 °C and 2 bar of oxygen partial pressure. Liquid flow rate was adjusted depending on the split used so as to provide the same liquid velocity (liquid flow rate) as that of steady state operations. Cycle conversion-time profiles typically obtained with on-off liquid flow modulation are illustrated in Figure 7.17 for different splits and period. As can be seen in Figure 7.17, there is evidence for a certain cycle conversion enhancement beyond the steady state conversion due to periodic variation of liquid flow on the AC surface. The enhancement becomes more visible for shorter splits irrespective of the cycle period studied (see Figure 7.17).

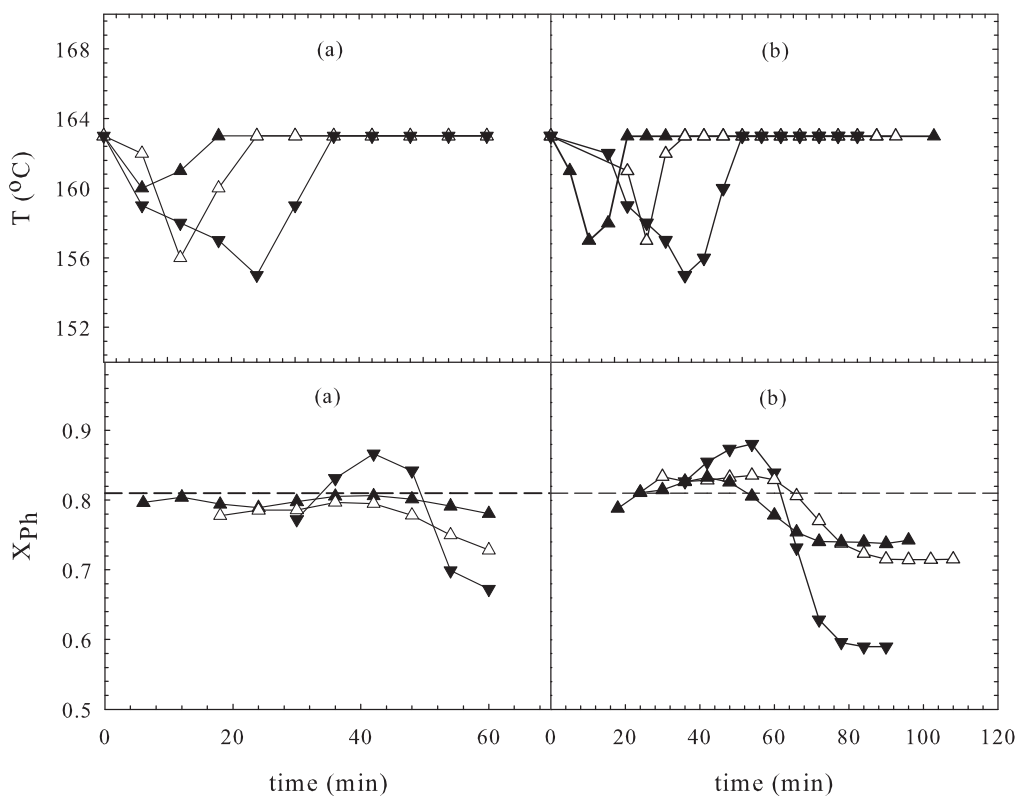


Figure 7.17: Effect of periodic parameters on phenol conversion under liquid flow modulation: (a)  $p = 1$  h, (b)  $p = 1.8$  h: (▲)  $s = 0.9$ , (△)  $s = 0.8$ , (▼)  $s = 0.6$ , discontinuous line represents steady state conversion:  $P_{O_2} = 2$  bar,  $T = 160$  °C,  $F_L = 60$  mL/h,  $F_G = 9$  NL/h,  $C_{Ph} = 5$  g/L,  $W_{cat} = 7$  g.

Periodic variation of liquid flow provides also periodic and direct oxygen transfer through unwetted catalyst surface during the dry cycle and renewal of phenol to the catalyst surface during the wet cycle. During the off cycle the bed is partially drained and the catalytic reaction proceeds only between the gaseous reactant and the liquid reactant entrapped inside the catalyst pore. Higher reaction rates are expected due to the direct transfer of the gaseous reactant to the catalyst site and outlet conversion at the beginning of the hot cycle may increase because all the phenol inside the AC pore may have reacted. This is reflected in Figure 7.17 for both periods. Nevertheless, care should be taken to avoid liquid reactant starvation at prolonged off cycle, which at the same time may lead to a substantial AC weight loss due to enhanced combustion of the catalyst by excess dissolved oxygen. Moreover,

since the liquid flow rate is increased due to split adjustment, the slight conversion enhancement can be compensated by too low reactant contact times. This situation is more pronounced at longer period and shorter split, where the bed is exposed to high liquid flow rate for prolonged periods.

Unlike temperature feed modulated CWAO, temperature induced adsorption-desorption in liquid flow modulations is not important since the oscillation in reaction temperature is very small ( $\Delta T \sim 8$  K)(see Figure 7.17).

Short term experiments of liquid flow modulation were first done to find out optimal cycle parameters that will provide stable activity as well as reasonable phenol conversion in the long run CWAO experiments. To this purpose, the mean

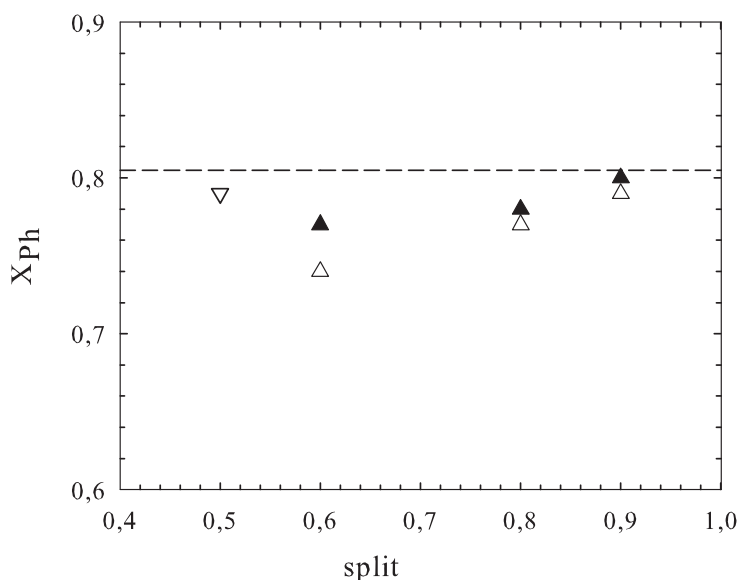


Figure 7.18: Mean cycle phenol conversion as function of split for different periods during liquid flow modulated CWAO: ( $\nabla$ )  $p = 0.2$  h, ( $\blacktriangle$ )  $p = 1$  h, ( $\triangle$ )  $p = 1.8$  h,  $P_{O_2} = 2$  bar,  $T = 160$  °C,  $F_L = 58$  mL/h,  $F_G = 9$  NL/h,  $C_{Ph} = 5$  g/L,  $W_{cat} = 7$  g.

cycle conversions for different split and period length are calculated from the raw data and compared with corresponding steady state conversion. The obtained results are illustrated in Figure 7.18. Although phenol conversion higher than the steady state were observed during the cycle, the mean cycle conversions are always below the steady state conversion indicating that liquid flow modulation does not help the reaction to improve outlet mean phenol conversion. However, it is seen that as the modulation frequency increases (decreasing the period) the mean cycle conversion

approaches the steady state conversion. With respect to the influence of split, the mean cycle conversion approaches the steady state values with increasing cycle split. It is seen that liquid flow modulation working at higher modulation frequency could be a more beneficial to achieve higher conversion during CWAO.

### 7.3.2 Influence of cycle parameters on AC stability

Several long term phenol oxidation experiments at steady state and on-off liquid flow modulation were finally carried out at 160°C and 2 bar of oxygen partial pressure to explore the potential of periodic liquid flow modulation of upflow reactor with respect to catalyst stability enhancement. The obtained results including steady state data are illustrated in Figure 7.19 in terms of mean cycle conversion as function of time on stream. In addition, the weight and BET surface area changes for the spent ACs were determined after each oxidation run (see Table 7.2). It appears from Figure 7.19 that both steady state upflow and down flow operations and liquid flow modulation yield a very similar phenol conversion for the first 40 h. Then liquid flow modulation with a period of 0.2 h and split of 0.5 outperforms both steady state upflow and down flow operation stabilizing at 65% of phenol conversion after 80-90 h of operating time. However, after 100 h of CWAO phenol conversion progressively dropped again to yield mean cycle conversion lower than 30%. This drop must be related to catalyst attrition and subsequent tube clogging occurred at the given liquid flow rate of 110 mL/h used in upflow mode. In agreement with the short run experiments, periodic operation close to fast modulation regime displays a better conversion improvement in the long run CWAO experiments if tube clogging can be avoided.

Conversion enhancement achieved in the long run oxidation experiment should be attributed to the suppression of oxidative coupling product that causes AC deactivation in steady state upflow reactor operation. In liquid flow modulation at relatively short period operation mode, since the catalyst bed is exposed to alternative variation of dry and wet period (liquid on-off), the liquid to solid ratio decreases and hence liquid phase homogeneous reaction should be minimized. Moreover, when the liquid flow is halted (dry period) the adsorbed oxidative coupling products could be oxidized by dissolved molecular oxygen in excess, hence partly recovering the textural structure as well as surface properties of AC for the next liquid on-cycle.

Table 7.2 summarizes the result of weight measurement of the spent ACs obtained after each long run CWAO experiments in upflow operation mode. As it can be seen in Table 7.2, in general the AC weight is more or less constant when the AC bed was subjected to variation of liquid flow (on-off liquid flow modulation) during

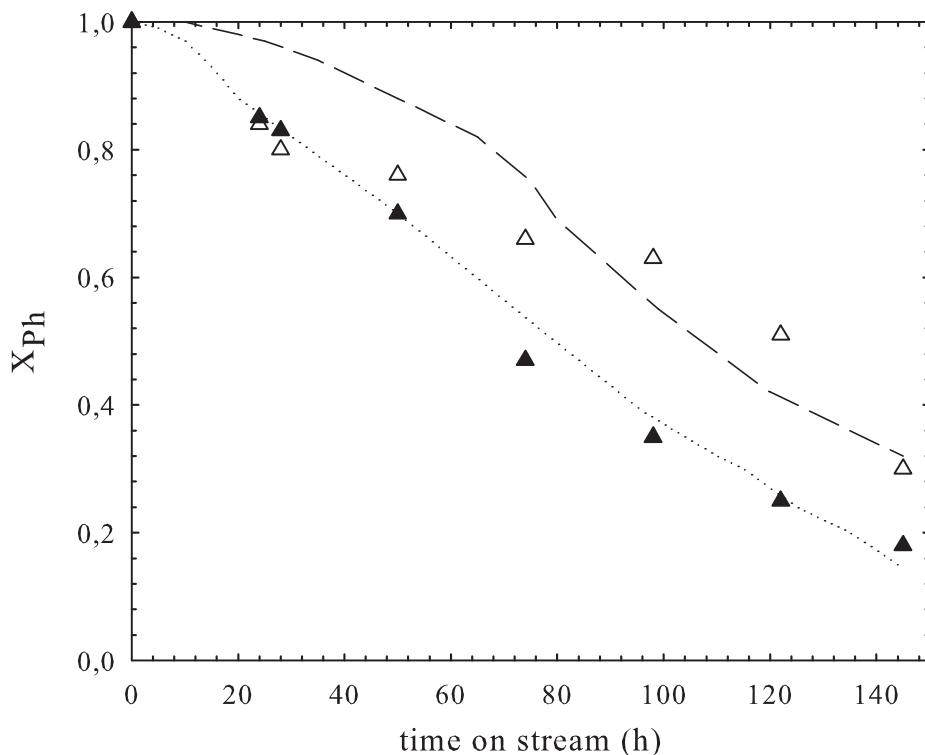


Figure 7.19: Mean cycle phenol conversion as function of time on steam for different periods: ( $\Delta$ )  $p = 0.2$  h, ( $\blacktriangle$ )  $p = 1$  h, line shows steady state trends: (dotted line) upflow, (dash line) downflow:  $P_{O_2} = 2$  bar,  $T = 160$  °C,  $F_L = 58$  mL/h,  $F_G = 9$  NL/h,  $C_{Ph} = 5$  g/L,  $W_{cat} = 7$  g.

Table 7.2: Phenol conversion, AC weight and  $S_{BET}$  measured after ca.150 h of liquid flow modulation:  $P_{O_2}=2$  bar,  $T=160^\circ\text{C}$ ,  $F_G=9$  NL/h,  $C_{Ph}=5$  g/L,  $W_{AC}=7$  g.

p (h)	s	$F_L$ (mL/h)	$\Delta W_{AC}$ (g)	$S_{BET}$ ( $\text{m}^2/\text{g}$ )	$X_{ph}$ (100 h)	$X_{ph}$ (ca. 150 h)
0.2	0.5	110	-0.5	371	0.63	0.27
1	0.83	70	1.1	363	0.47	0.18
UFBR	-	58	1	n.m		0.17*
TBR	-	58	-5.2	n.m		0.32*

\* Steady state values

CWAO of phenol. For example, at shorter periods of 0.2 h (12 min) and split of 0.5 a weight loss of 0.5 g was observed. It appears from Table 7.2 at a certain conditions liquid flow modulation in upflow mode provide similar values of phenol conversion, AC weight change and textural properties with feed temperature modulation.

### 7.3.3 Conclusion

Short term CWAO experiments showed that liquid flow modulation has only a mild although negative influence on phenol conversion as the cycle mean conversions are always lower than the corresponding steady state conversions. Nevertheless, the long term AC stability is largely improved during liquid flow modulated CWAO specially when operated with shorter periods and splits. For example, phenol conversion was improved to 65% for period of 0.2 h and a split of 0.5. It seems that the balance between formation, adsorption and destruction of coupling products on the AC surface during the dry period (liquid off mode) is responsible for obtained improved long term AC stability. Nevertheless, further investigation is required to minimize the unacceptable catalyst attrition, preventing so far the safe application of liquid flow modulation to CWAO over AC.



# Part IV

## Concluding Remarks

UNIVERSITAT ROVIRA I VIRGLI

CATALYTIC WET AIR OXIDATION OF PHENOL OVER ACTIVE CARBON IN FIXED BED REACTOR: STEADY STATE  
AND PERIODIC OPERATION

Nigus Gabbiye Habtu

ISBN:/DL:T.1262-2011

# Chapter 8

## Conclusions and Outlook

### 8.1 Conclusions

The application of cheap and non hazardous active carbon as an alternative catalyst for organic wastewater remediation has been thoroughly explored in continuous and periodically operated downflow and upflow fixed-bed reactors. The outcomings generated in this work allow defining appropriate operation mode and conditions of a fixed bed reactor, for which a better catalyst stability can be achieved in the wet air oxidation of phenol over activated carbon. It has been shown that the performance of AC in a steady state laboratory packed bed reactor is largely affected by reaction temperature, phenol feed concentration, oxygen partial pressure, the flow direction of gas and liquid phases and the way how active carbon is initially saturated with phenol. At typical CWAO conditions, active carbon does not only promote the oxidation of phenolic compounds but also its self combustion and the formation and irreversible adsorption of condensation products. Thus, the key for obtaining a high and stable activity is to balance the formation, destruction and adsorption of condensation products through the selection of adequate operating conditions ( $T$ ,  $P_{O_2}$ ,  $C_{Ph}$ ) and proper start up procedure, which at the same time prevent the AC from being burned off. Almost complete phenol conversion ( $>99\%$ ) and 85% of TOC removal were achieved in trickle bed operation with "oxic" bed saturation at  $160^\circ\text{C}$ , 2 bar of oxygen pressure and liquid space times in the range of 0.25 h. Activated carbon is seen to favor the formation of refractory but biodegradable acetic acid, which accumulates in the reactor outlet effluent. Consequently, an effluent pH as low as 2.5 established during CWAO of a 5 g/L phenol solution requiring the use of corrosion resistant reactor materials like stainless steel. However, a temperature of  $160^\circ\text{C}$  is found too severe to maintain a stable activity in the long term CWAO

experiments since burn-off of active carbon became influent in the course of operation, hence phenol and TOC conversion decreased progressively after 50 h time on stream.

The observed sensibility of phenol conversion to temperature confirmed that the phenol oxidation over AC should proceed in the kinetic controlled regime in our TBR. With respect to the non linear influence of feed phenol concentration and oxygen pressure on both phenol and TOC conversions, it can be said that the oxidation of phenol over AC may not follow simple first order kinetics. In that case, heterogeneous surface kinetics accounting for oxygen dissociation may better explain the observed results. The promoting effect of AC in CWAO of phenol can be related to the generation of oxygenated free radicals that initiate the oxidation reaction as also suggested by the observed influence of both radical scavengers and feed solution pH on phenol conversion. Detailed kinetic modelling of the acquired data is necessary to discriminate the possible reaction mechanism.

Periodic operation as a novel concept for conducting CWAO of phenol has been investigated in gas-liquid down and upflow fixed bed reactors. In particular, feed temperature modulation was applied to trickle flow to induce temperature driven adsorption-reaction cycle at the AC surface. Numerous short and long term experiments were thus done at variable cycle periods and splits. It has been observed in 7 days run of CWAO that periodic temperature feed modulation can be an effective operating mode to completely suppress AC burn-off under certain conditions, i.e. high splits ( $>0.8$ ) and cycle periods around 1 h. Accordingly, the conversion level was improved from 32% obtained in steady state conditions to 60-65%. Nevertheless, the temperature induced adsorption/desorption-reaction cycles are accompanied by a significant loss of AC adsorption capacity representing a main barrier for performing higher phenol conversion ( $X_{Ph} > 80$ ).

Similarly, an important catalyst stability improvement has been achieved with liquid flow modulation when working close to the fast modulation regime. Phenol conversion was thus improved to 65% for short period of 0.2 h and split of 0.5 with stable AC weight. Yet, enhanced catalyst attrition must occur during liquid flow modulation leading to clogging down stream of the reactor outlet and ultimately to the shutdown of the experiment.

For the modelling of dynamic CWAO, trickle bed heat transfer has been also explored in the absence of reaction for a given range of operating conditions ( $P_T$ ,  $T$ ,  $F_L$ ,  $F_G$ ) under steady and nonsteady state conditions. It has been observed that gas flow rate only marginally affects the bed to wall heat transfer ( $h_w$ ), whereas increasing the liquid flow rate enhances  $h_w$ . With respect to pressure, a linear dependency of the heat transfer coefficients ( $U$  and  $h_w$ ) is observed from 9 bar to 20 bar before

it levels off at 25 bar. At intermediate pressures, convex curving of the profiles occurred suggesting that condensation of water vapor from the saturated gas phase impacts on the heat transfer conditions inside the trickle bed column. The analysis of the axial temperature profiles with a pseudo homogeneous one parameter model further confirmed that the influence of condensation of water vapor on heat transfer during CWAO process can not be neglected. The values of the overall heat transfer coefficient ( $U$ ) obtained by fitting the model predictions to the experimental data quantitatively reflect the aforementioned influences of operating variables on heat transfer. An empirical correlation showing the dependency of  $h_w$  on operation pressure, liquid and gas Reynolds number was established for the range of conditions studied in this work. Moreover, accurate modelling of the thermal waves induced by feed temperature modulation was performed using the dynamic model. These results give thus confidence for the application of the model to simulate the CWAO of phenol over AC conducted in a TBR under temperature feed modulation.

## 8.2 Outlook

Understanding of heterogeneous catalytic reaction systems requires a specific knowledge in different areas of chemistry and chemical engineering. It is impossible to treat all of them exhaustively in one PhD thesis. In particular, for CWAO of organic pollutants, several open topics both at molecular and reactor scale are worth to be addressed by future research work in order to successfully apply CWAO to the remediation of organic pollutants at industrial scale.

One important field of study could be to elucidate at molecular level the role of AC in CWAO of organic pollutants. In this context, further experimentation dealing with the effect of radical scavengers on phenol oxidation over AC and detail surface characterization of both spent and fresh ACs are crucial to establish a more realistic free radical based reaction mechanism. In this context, the knowledge on the active sites of AC for both phenol and molecular oxygen adsorption and/or reaction must be extended.

One of the relevant findings of this work is that adsorption-reaction cycles imposed by feed temperature modulation are responsible for achieving stable catalyst. Nevertheless, the adsorption capacity loss of AC observed represents the main barrier to perform higher phenol conversion ( $X_{Ph} > 80$ ). On the other hand, further periodic operation studies should optimize the operating window defined in this work with respect to cycle period and split to provide higher pollutant mineralization. Tailoring the textural structure of AC to have a mesopore carbon, coating of AC with Fe or developing a synergetic hybrid material such as zeolite/carbon composite that have

Fe/Cu based active species could also help to achieve the aforementioned goals. A first step has been done in this direction by synthesizing a synergetic zeolite/carbon hybrid material through hydrothermal synthesis in collaboration with the research group of Prof. dr. ir. Jaap Schouten at Technical University of Eindhoven. A preliminary characterization of the synthesized AC-Zeolite composite material showed that the AC to Zeolite ratio is a key parameter for controlling the crystal growth. Moreover, Fe and Cu were effectively incorporated in the framework of the composite material. Therefore, future research should now focus on the application of these hybrid materials to steady state and periodically operated CWAO processes.

## Bibliography

- [1] G. Busca, S. Berardinelli, C. Resini, and L. Arrighi, *Journal of Hazardous Materials* **160**, 265 (2008).
- [2] W. Simmler, T. M. M. Berger, G. Kern, J. Lemke, D. Klockner, E. Neuber, G. Hebbel, U. Werthmann, G. Klinsmann, J. F. Lawson, et al., *Wastewater*, vol. McGraw-Hill of *Ullmann's Encyclopedia of Industrial Chemistry* (2000), 3<sup>rd</sup> edition ed.
- [3] United and Nations, *Water in a Changing World* (Report 3, 2009).
- [4] METCALF and I. EDDY, *Waste water Engineering: Treatment, Disposal, and Reuse*, revised by: G. Tchobanoglous and F.L. Burton (McGraw-Hill, New York, 1991), 3<sup>rd</sup> edition, p.17 ed.
- [5] W. Jordan, H. van Barneveld, O. Gerlich, M. Kleine-Boymann, and J. Ullrich, *Phenol*, Ullmann's Encyclopedia of Industrial Chemistry (Wiley-VCH Verlag, 2002).
- [6] <http://www.epa.gov/tri/> (2009).
- [7] Wang, *Degradation of phenol and phenolic compounds by a defined denitrifying bacterial culture* (McGraw-Hill, 1992).
- [8] <http://prtr.ec.europa.eu/PollutantReleases.aspx> (2008).
- [9] V. S. Mishra, V. V. Mahajani, and J. B. Joshi, *Industrial and Engineering Chemistry Research* **34**, 2 (1995).
- [10] E. W. Low and H. A. Chase, *Water Research*. **33**, 1119 (1999).
- [11] C. F. Foster, *Biotechnology and Wastewater Treatment* (Cambridge University Press, Cambridge, 1985).

- [12] A. Cybulski, *Industrial and Engineering Chemistry Research* **46**, 4007 (2007).
- [13] P. Gogate and R. Pandit, *Advance in Environmental Research* **8**, 501 (2004).
- [14] H. G. William, K. Joon-Wun, and H. C. Douglas, *Ozone Science Engineering* (1987).
- [15] H. Debellefontaine and J. N. Foussard, *Waste Management* **20**, 15 (2000).
- [16] S. T. Kolaczowski, P. Plucinski, F. J. Beltran, F. J. Rivas, and D. B. McLurgh, *Chemical Engineering Journal* **76**, 143 (1999).
- [17] J. Levec and A. Pintar, *Catalyst Today* **124**, 172 (2007).
- [18] P. J. Crooker, K. S. Ahluwalia, Z. Fan, and J. Prince, *Industrial and Engineering Chemistry Research* **39**, 4865 (2000).
- [19] P. D. Vaidya and V. V. Mahajani, *Advances in Environmental Research* **62**, 429 (2002).
- [20] A. Pintar and J. Levec, *Chemical Engineering Science* **47**, 2395 (1992).
- [21] S. Imamura, *Industrial and Engineering Chemistry Research* **38**, 1743 (1999).
- [22] F. Luck, *Catalysis Today* **53**, 81 (1999).
- [23] S. Yang, W. Zhua, J. Wang, and Z. Chen, *Journal of Hazardous Materials* **153**, 1248 (2008).
- [24] S.-K. Kim, K.-H. Kim, and S.-K. Ihm, *Chemosphere* **68**, 287 (2007).
- [25] A. Santos, P. Yustos, A. Quintanilla, G. Ruiz, and F. Garcia-Ochoa, *Applied Catalysis B: Environmental* **61**, 323 (2005).
- [26] I.-P. Chen, S.-S. Lin, C.-H. Wang, L. Chang, and J.-S. Chang, *Applied Catalysis B: Environmental* **50**, 49 (2004).
- [27] J. Trawczynski, *Carbon* **41**, 1515 (2003).
- [28] Z. Masende, B. Kuster, K. Ptasinski, F. Janssen, J. Katima, and J. Schouten, *Topics in Catalysis* **33**, 87 (2005).
- [29] S. Hamoudi, K. Belkacemi, and F. Larachi, *Chemical Engineering Science* **54**, 3569 (1999).

- [30] S. Cao, G. Chen, X. Hu, and P. L. Yue, *Catalysis Today* **88**, 37 (2003).
- [31] A. Fortuny, J. Font, and A. Fabregat, *Applied Catalysis B: Environmental* **19**, 165 (1998).
- [32] F. Stüber, J. Font, A. Fortuny, C. Bengoa, A. Eftaxias, and A. Fabregat, *Topics in Catalysis* **33** (2005).
- [33] J. Levec and A. Pinter, *Catalysis Today* **24**, 51 (1995).
- [34] A. Santos, P. Yustos, S. Rodriguez, and F. Garcia-Ochoa, *Applied Catalysis B: Environmental* **65**, 269 (2006).
- [35] J. A. Zazo, J. A. Casa, A. F. Motedano, M.A.Gilarranz, and J. J. Rodriguez, *Environmental Science and Technology* **39**, 9295 (2005).
- [36] P. C. C. Faria, J. J. J. Orfao, and M. Pereira, *Applied Catalysis B: Environmental* **79**, 237 (2008).
- [37] M. E. Suarez-Ojeda, A. Guisasola, J. A. Baeza, A. Fabregat, F. Stüber, A. Fortuny, J. Font, and J. Carrera, *Chemosphere* **66**, 2096 (2007).
- [38] A. Santos, P. Yustos, S. Rodriguez, E. Simon, and F. Garcia-Ochoa, *Journal of Hazardous Materials* **146**, 595 (2007).
- [39] I. Polaert, A. M. Wilhelm, and H. Delmas, *Chemical Engineering Science* **57**, 1585 (2002).
- [40] D. Moses and E. Smith, US Patent 2,690 p. 425 (1954).
- [41] A. I. Njiribeako, R. R. Hudgins, and P. L. Silveston, *Industrial and Engineering Chemistry Fundamentals* **17**, 234 (1978).
- [42] A. Quintanilla, J. Casas, A. Mohedano, and J. Rodríguez, *Applied Catalysis B: Environmental* **67**, 206 (2006).
- [43] A. Fortuny, C. Miró, J. Font, and A. Fabregat, *Catalysis Today* **48**, 323 (1999).
- [44] K.-H. Kim, J.-R. Kim, and S.-K. Ihm, *Journal of Hazardous Materials* **167**, 1158 (2009).
- [45] H. Chen, A. Sayari, A. Adnot, and F. Larachi, *Applied Catalysis A: General* **32**, 195 (2001).

- [46] K.-H. Kim and S.-K. Ihm, *Journal of Hazardous Materials* **146**, 610 (2007).
- [47] H. Ohta, S. Goto, and H. Teshlma, *Industrial and Engineering Chemistry Fundamentals*. **19**, 180 (1980).
- [48] A. Fortuny, C. Bengoa, J. Font, and A. Fabregat, *Journal of Hazardous Materials* **64**, 181 (1999).
- [49] J. F. Akyurtlu, A. Akyurtlu, and S. Kovenklioglu, *Catalysis Today* **40**, 343 (1998).
- [50] A. Alejandre, F. Medina, A. Fortuny, P. Salagre, and J. Sueiras, *Applied Catalysis B: Environmental* **16**, 53 (1998).
- [51] Q. Wu, X. Huy, and P. L. Yue, *International Journal of Chemical Reactor Engineering* **3** (2005).
- [52] A. Singh, K. K. Pant, and K. D. P. Nigam, *Chemical Engineering Journal* **103**, 51 (2004).
- [53] F. Arena, R. Giovenco, T. Torre, A. Venuto, and A. Parmaliana, *Applied Catalysis B: Environmental* **45**, 51 (2003).
- [54] I. U. Castro, F. Stüber, A. Fabregat, J. Font, A. Fortuny, and C. Bengoa, *Journal of Hazardous Materials* **163**, 809 (2009).
- [55] A. Pintar and J. Levec, *Journal of Catalysis* **135**, 345 (1992).
- [56] S.-K. Kim and S.-K. Ihm, *Topics in Catalysis* **33** (2005).
- [57] A. Pintar and J. Levec, *Chemical Engineering Science* **49**, 4391 (1994).
- [58] R. J. Fenoglio, P. A. Massa, F. D. Ivorra, and P. M. Haure, *Journal of Chemical Technology and Biotechnology* **82**, 481 (2007).
- [59] P. Massa, F. Ivorra, P. Haure, and R. Fenoglio, *Catalysis Communications* **10**, 1706 (2009).
- [60] Z. P. G. Masende, B. F. M. Kuster, K. J. Ptasinski, F. J. J. G. Janssen, J. . H. Y. Katima, and J. C. Schouten, *Catalysis Today* **79-80**, 357 (2003).
- [61] Z. P. G. Masende, B. F. M. Kuster, K. J. Ptasinski, F. J. J. G. Janssen, J. H. Y. Katima, and J. C. Schouten, *Applied Catalysis B: Environmental* **41**, 247 (2003).

- [62] L. Oliviero, J. Barbier, D. Duprez, A. Guerrero-Ruiz, B. Bachiller-Baeza, and I. Rodríguez-Ramos, *Applied Catalysis B: Environmental* **25**, 267 (2000).
- [63] S. Yang, Y. Feng, J. Wan, W. Zhu, and Z. Jiang, *Applied Surface Science* **246**, 222 (2005).
- [64] D. Duprez, F. Delanoe, J. J. Barbier, P. Isnard, and G. Blanchard, *Catalysis Today* **29**, 317 (1996).
- [65] A. Pintar, M. Besson, and P. Gallezot, *Applied Catalysis B: Environmental* **31**, 275 (2001).
- [66] D.-K. Lee, D.-S. Kim, T.-H. Kim, Y.-K. Lee, S.-E. Jeong, N. T. Le, M.-J. Cho, and S. D. Henam, *Catalysis Today* **154**, 244 (2010).
- [67] S. Hamoudi, F. Larachi, and A. Sayari, *Journal of Catalysis* **177**, 247 (1998).
- [68] C. B. Maugans and A. Akgerman, *Water Research* **31**, 3116 (1998).
- [69] L. Oliviero, J. J. Barbier, D. Duprez, A. Guerrero-Ruiz, B. Bachiller-Baeza, and I. Rodríguez-Ramos, *Applied Catalysis B: Environmental* **25**, 267 (2000).
- [70] S. Keav, A. Martin, J. J. Barbier, and D. Duprez, *Catalysis Today* **151**, 143 (2010).
- [71] P. Massa, F. Ivorra, P. Haure, F. M. Cabello, and R. Fenoglio, *Catalysis Communications* **8**, 424 (2007).
- [72] A. Pintar, J. Batista, and T. Tisler, *Applied Catalysis B: Environmental* **84**, 30 (2008).
- [73] E. Castillejos-Lopez, A. Maroto-Valiente, D. M. Nevskaia, V. Munoz, I. Rodríguez-Ramos, and A. Guerrero-Ruiz, *Catalysis Today* **143**, 355 (1994).
- [74] D. P. Minh, P. Gallezot, and M. Besson, *Applied Catalysis B: Environmental* **75**, 71 (2007).
- [75] R. Kouraichi, J. J. Delgado, J. D. López-Castro, M. Stitou, J. M. Rodríguez-Izquierdo, and M. A. Cauqui, *Catalysis Today* **154**, 195 (2010).
- [76] T. Trawczynski, *Carbon* **41**, 1515 (2003).
- [77] J. Qin, Q. Zhang, and K. T. Chuang, *Applied Catalysis B: Environmental* **29**, 115 (2001).

- [78] J. S. A. R. J. G. C. Díaz, G. O., Proceedings of European Congress of Chemical Engineering (2007).
- [79] A. Quintanilla, J. A. Casasy, J. J. Rodriguez, M. T. Kreutzer, F. Kapteijn, and J. A. Moulijn, International Journal of Chemical Reaction Engineering **5**, A62 (2007).
- [80] P. M. Alvarez, D. McLurgh, and P. Plucinski, Industrial and Engineering Chemistry Research **41**, 2153 (2002).
- [81] J. L. Figueiredo and M. F. R. Pereira, Catalysis Today **150**, 2 (2010).
- [82] R. Coughlin, Industrial and Engineering Chemistry Product Research and development **8**, 12 (1969).
- [83] G. Ertl, *Handbook of Heterogeneous Catalysis* (WILEY VCH, Federal Republic of Germany, 2008), 2<sup>nd</sup> ed.
- [84] E. Schoeffel and F. Zimmermann, US. Patent, 3,386,922 (1968).
- [85] V. Tukac and J. Hanika, Journal of Chemical Technology and Biotechnol **71**, 262 (1998).
- [86] V. Tukac and J. Hanika, Collect of Czechoslovak Chemical Communications **61** (1996).
- [87] C. Aguilar, R. Garcia, G. Soto-Garrido, and R. Arriagada, Topics in Catalysis **33** (2005).
- [88] C. Aguilar, R. Garcia, G. Soto-Garrido, and R. Arriagada, Applied Catalysis B: Environmental **46**, 229 (2003).
- [89] G. Yu, S. Lu, H. Chen, and Z. Zhu, Carbon **43**, 2285 (2005).
- [90] A. Quintanilla, J. Casas, and J. Rodriguez, Applied Catalysis B: Environmental **76**, 135 (2007).
- [91] M. E. Suarez-Ojeda, F. Stüber, A. Fortuny, A. Fabregat, J. Carrera, and J. Font, Applied Catalysis B: Environmental **58**, 105 (2005).
- [92] F. Stüber, J. Font, A. Eftaxias, M. Paradowska, M. E. Suarez-Ojeda, A. Fortuny, C. Bengoa, and A. Fabregat, Process Safety and Environmental Protection **83**, 371 (2005).

- [93] C. Ayrál, C. J. Lebigue, F. Stüber, A.-M. Wilhelm, and H. Delmas, *Industrial and Engineering Chemistry Research* **49**, 10707 (2010).
- [94] V. Tukac, J. Hanika, and V. Chyba, *Catalysis Today* **79/80**, 427 (2003).
- [95] M. Santiago, F. Stüber, A. Fortuny, A. Fabregat, and J. Font, *Carbon* **43**, 2134 (2005).
- [96] R. R. N. Marques, F. Stüber, K. M. Smith, A. Fabregat, C. Bengoa, J. Font, A. Fortuny, S. Pullket, G. D. Fowler, and N. J. D. Graham, *Applied Catalysis B: Environmental* **101** (2010).
- [97] A. Quintanilla, N. Menendez, J. Tornero, J. A. Casas, and J. J. Rodriguez, *Applied Catalysis B: Environmental* **81**, 105 (2008).
- [98] C. Julcour-Lebigue, C. Andriantsiferana, N. Krou, C. Ayrál, E. Mohamed, A.-M. Wilhelm, H. Delmas, L. L. Coq, C. Gerente, K. M. Smith, et al., *Journal of Environmental Management* **91**, 2432 (2010).
- [99] J. F. Gonzalez, J. M. Encinar, A. Ramiro, and E. Sabio, *Industrial and Engineering Chemistry Research* **41**, 1344 (2002).
- [100] H. T. Gomes, B. F. Machado, A. Ribeiro, I. Moreira, M. Rosario, A. M. Silva, J. L. Figueiredo, and J. L. Faria, *Journal of Hazardous Materials* **159**, 420 (2008).
- [101] A. Santos, P. Yustos, S. Rodríguez, F. Garcia-Ochoa, and M. de Gracia, *Industrial and Engineering Chemistry Research* **46** (2007).
- [102] V. Tukac and J. Hanika, *Journal of Chemical Technology and Biotechnology* **71** (1998).
- [103] J. Rivera-Utrilla and M. Sánchez-Polo, *Applied Catalysis B: Environmental* **39**, 319 (2002).
- [104] P. Bautista, A. F. Mohedano, N. Menendez, J. A. Casas, and J. J. Rodriguez, *Catalysis Today* **151**, 148 (2010).
- [105] Y. Sun, Y. Zhang, and X. Quan, *Separation and Purification Technology* **62**, 565 (2008).
- [106] A. Santos, P. Yustos, T. Cordero, S. Gomis, S. Rodriguez, and F. Garcia-Ochoa, *Catalysis Today* **102-103**, 213 (2005).

- [107] M. M. Baricot, Ph.D. thesis, Universitat Rovira i Virgili (2008).
- [108] S. Yang, X. Li, W. Zhu, J. Wang, and C. Descormed, *Carbon* **46**, 445 (2008).
- [109] F. Stüber, I. Polaert, H. Delmas, J. Font, A. Fortuny, and A. Fabregat, *Journal of Chemical Technology and Biotechnology* **76**, 743 (2001).
- [110] A. Santos, P. Yustos, B. Durban, and F. Garcia-Ochoa, *Environ Science Technology* **35**, 2828 (2001).
- [111] M. E. Suarez-Ojeda, A. Fabregat, F. Stüber, A. Fortuny, J. Carrera, and J. Font, *Chemical Engineering Journal* **132**, 105 (2007).
- [112] T. Cordero, J. Rodríguez-Mirasol, J. Bedia, S. Gomis, P. Yustos, F. García-Ochoa, and A. Santos, *Applied Catalysis B: Environmental* **81**, 122 (2008).
- [113] S. Morales-Torres, A. M. T. Silva, A. F. Perez-Cadenas, J. L. Faria, F. J. Maldonado-Hodar, J. L. Figueiredo, and F. Carrasco-Marina, *Applied Catalysis B: Environmental* **100**, 310 (2010).
- [114] A. Ayude, T. Rodriguez, J. Font, A. Fortuny, C. Bengoa, A. Fabregat, and F. Stüber, *Chemical Engineering Science* **62**, 7351 (2007).
- [115] B. Larruy, A. Ayude, J. Font, A. Fortuny, C. Bengoa, A. Fabregat, and F. Stüber, *Chemical Engineering Science* **62**, 5564 (2007).
- [116] T. Nunoura, G. Lee, Y. Matsumura, and K. Yamamoto, *Industrial and Engineering Chemistry Research* **42**, 3718 (2003).
- [117] Y. Matsumura, T. Urase, K. Yamamoto, and T. Nunoura, *Journal of Supercritical Fluids* **22**, 149 (2002).
- [118] M. F. R. Pereira, J. J. M. Órfão, and J. L. Figueiredo, *Applied Catalysis A: General* **218**, 307 (2001).
- [119] M. Pereira, J. Orfao, and J. Figueiredo, *Applied Catalysis A: General* **184**, 153 (1999).
- [120] V. M. Matsis and H. P. Grigoropoulou, *Chemical Engineering Science* **63**, 609 (2008).
- [121] E. Ahumada, H. Lizama, F. Orellana, C. Suarez, A. Huidobrob, A. Sepulveda-Escribanob, and F. Rodríguez-Reinoso, *Carbon* **40**, 2827 (2002).

- [122] X. Quan, Y. Zhang, S. Chen, Y. Zhao, and F. Yang, *Journal of Molecular Catalysis A: Chemical* **263**, 216 (2007).
- [123] A. Georgi and F. D. Kopinke, *Applied Catalysis B: Environmental* **58**, 9 (2005).
- [124] A. Eftaxias, Ph.D. thesis, Universitat Rovira i Virgili (2002).
- [125] A. Santos, P. Yustos, A. Quintanilla, S. Rodriguez, and F. Garcia-Ochoa, *Applied Catalysis B: Environmental* **39**, 97 (2002).
- [126] H. R. Devlin and I. J. Harris, *Industrial and Engineering Chemistry Research* **23**, 387 (1984).
- [127] A. Eftaxias, J. Font, A. Fortuny, A. Fabregat, and F. Stüber, *Applied Catalysis B: Environmental* **67**, 12 (2006).
- [128] S. K. Bhargava, J. Tardio, J. Prasad, K. Folger, D. B. Akolekar, and S. C. Grocott, *Industrial and Engineering Chemistry Research* **45**, 1221 (2006).
- [129] S. Suwanprasop, A. Eftaxias, F. Stüber, I. Polaert, C. Julcour-Lebigue, and H. Delmas, *Industrial and Engineering Chemistry Research* **44**, 9513 (2005).
- [130] A. Santos, P. Yustos, B. Durban, and F. Garcia-Ochoa, *Industrial and Engineering Chemistry Research* **40**, 2773 (2001).
- [131] V. Tukac, J. Vokal, and J. Hanika, *Journal of Chemical Technology and Biotechnology* **76**, 506 (2001).
- [132] J. Guo and M. Al-Dahhan, *Chemical Engineering Science* **60**, 735 (2005).
- [133] M. R. Khadilkar, Y. X. Wu, M. H. Al-Dahhan, and M. P. Dudukovic, *Chemical Engineering Science* **51**, 2139 (1996).
- [134] I. van der Westhuizen, E. D. Toit, and W. Nicol, *Chemical Engineering Research and Design* **85**, 1604 (2007).
- [135] D. Loudon, W. van der Merwe, and W. Nicol, *Chemical Engineering Science* **61**, 7551 (2006).
- [136] L. Baussaron, C. Julcour-Lebigue, A. M. Wilhelm, H. Delmas, and C. Boyer, *American Institute of Chemical Engineers Journal* **53**, 1850 (2007).

- [137] V. Tuka and J. Hanika, *Collection of Czechoslovak Chemical Communications* **1**, 1010 (1996).
- [138] P. R. Shukla, S. Wang, H. Sun, H. M. Ang, and M. Tad, *Applied Catalysis B: Environmental* **100** (2010).
- [139] P. M. Alvarez, D. McLurgh, and P. Plucinski, *Industrial and Engineering Chemistry Research* **41**, 2147 (2002).
- [140] J. Levec and A. Pintar, *Industrial and Engineering Chemistry Research* **33**, 3070 (1994).
- [141] V. Tukac, M. Simickova, V. Chyba, J. Lederer, J. Kolena, J. Hanika, V. Jiricny, V. Stanek, and P. Stavarek, *Chemical Engineering Science* **62**, 4891 (2007).
- [142] P. L. Silveston and J. Hanika, *Chemical Engineering Science* **57**, 3373 (2002).
- [143] M. Khadilkar, M. Al-Dahhan, and M. Dudukovic, *Chemical Engineering Science* **54**, 2585 (1999).
- [144] P. L. Silveston and R. R. Hudgins, *Chemical Engineering Science* **59**, 4043 (2004).
- [145] P. Massa, M. Ayude, F. Ivorra, R. Fenoglio, and P. Haure, *Catalysis Today* **107-108**, 630 (2005).
- [146] B. Aydin, M. C. Cassanello, and F. Larachi, *Chemical Engineering Science* **63**, 141 (2008).
- [147] P. M. Haure, R. R. Hudgins, and P. L. Silveston, *American Institute of Chemical Engineers Journal* **35**, 1437 (1989).
- [148] J. K. Lee, R. R. Hudgins, and P. L. Silveston, *Chemical Engineering Science* **50**, 2523 (1995).
- [149] L. Gabarain, A. T. Castellari, J. Cechini, A. Tobolski, and P. Haure, *American Institute of Chemical Engineers Journal* **43**, 166 (1997).
- [150] G. Liu, X. Zhang, L. Wang, S. Zhang, and Z. Mi, *Chemical Engineering Science* **63**, 4991 (2008).
- [151] A. Ayude, J. Cechini, M. Cassanello, O. Martnez, and P. Haure, *Chemical Engineering Science* **63**, 4969 (2008).

- [152] R. Lange, J. Hanika, D. Stradiotto, R. R. Hudgins, and P. L. Silveston, *Chemical Engineering Science* **49**, 5615 (1994).
- [153] Z. Cai and G. A. Sorial, *Chemical Engineering Journal* **151**, 105 (2009).
- [154] A. T. Castellari and P. M. Haure, *American Institute of Chemical Engineers Journal* **41**, 1593 (1995).
- [155] M. A. Ayude, M. C. Cassanello, P. M. Haure, and O. M. Martinez, *Industrial and Engineering Chemistry Research* **44**, 9594 (2005).
- [156] J. Hanika, R. Lange, and F. Turek, *Chemical Engineering Processing* **28**, 23 (1990).
- [157] M. S. Fraguio, A. Muzen, O. Martinez, P. Bonilli, and M. Cassanello, *Latin America Applied Research* **34**, 11 (2004).
- [158] A. Muzen, M. S. Fraguio, M. C. Cassanello, M. A. Ayude, P. M. Haure, and O. M. Martnez, *Industrial and Engineering Chemistry Research* **44**, 5275 (2005).
- [159] G. Liu, Y. Duan, Y. Wang, L. Wang, and Z. Mi, *Chemical Engineering Science* **60**, 6270 (2005).
- [160] T. Horie and T. Aida, *Chemical Engineering Science* **63**, 64981 (2008).
- [161] F. Turco, R. R. Hudgins, P. L. Silveston, S. Sicardi, L. Manna, and M. Bancharo, *Chemical Engineering Science* **56**, 1429 (2001).
- [162] D. Brzic, M. Schubert, H. Haring, R. Lange, and M. Petkovska, *Chemical Engineering Science* **65**, 4160 (2010).
- [163] D. Na-Ranong, R. Yuangsawad, P. Kitchaiya, and T. Aida, *Chemical Engineering Journal* **146**, 275 (2009).
- [164] M. P. Dudukovic, F. Larachi, and P. L. Mills, *Catalysis Review* **44**, 123 (2002).
- [165] K. Pangarkar, T. J. Schildhauer, J. van Ommen, J. Nijenhuis, J. A. Moulijn, and F. Kapteijn, *Chemical Engineering Science* **65**, 420 (2010).
- [166] A. S. Lamine, L. Gerth, H. L. Gall, and G. Wild, *Chemical Engineering Science* **51**, 3813 (1996).

- [167] M. H. Al-Dahhan and M. P. Dudukovic, *Chemical Engineering Science* **49**, 5681 (1994).
- [168] J. Hanika, K. Sporcka, V. Rucicka, and R. Pistek, *Chemical Engineering Science* **32**, 525 (1977).
- [169] V. Specchia and G. Baldi., *Chemical Engineering Communication* **3**, 483 (1979).
- [170] K. Muroyama, K. Hashimoto, and T. Tomita, *Kagaku Kogaku Ronbunshu* **3**, 612 (1977).
- [171] N. J. Mariani, O. M. Martinez, and G. F. Barreto, *Chemical Engineering Science* **56**, 5995 (2001).
- [172] K. Muroyama, K. Hashimoto, and T. Tomita, *Heat Transfer Japanese Research* **7**, 87 (1978).
- [173] B. V. Babu, K. J. Shah, and V. G. Rao, *Computers and Chemical Engineering* **23**, 327 (1999).
- [174] A. Fortuny, C. Ferrer, C. Bengoa, J. Font, and A. Fabregat, *Catalysis Today* **24**, 79 (1995).
- [175] M. H. Al-Dahhan, Y. Wu, and M. P. Dudukovic, *Industrial and Engineering Chemistry Research* **34**, 741 (1995).
- [176] J. Levec, A. F. Saez, and R. G. Carbonell, *American Institute of Chemical Engineers Journal* **32**, 515523 (1968).
- [177] J. Levec, K. Grosser, and R. G. Carbonell, *American Institute of Chemical Engineers Journal* **34**, 1027 (1988).
- [178] F. S. Mederos, J. Ancheyta, and J. Chen, *Applied Catalysis A: General* **355**, 1 (2009).
- [179] R. Lange, M. Schubert, and T. Bauer, *Industrial and Engineering Chemistry Research* **44**, 6504 (2005).
- [180] S. W. Churchill and H. H. S. Chu, *International Journal of Heat and Mass Transfer* **18**, 1323 (1975).

- [181] T. Grant and J. King, *Industrial and Engineering Chemistry Research* **29**, 264 (1990).
- [182] O. D. Cooney and Z. Xi, *American Institute of Chemical Engineers Journal*, **40**, 361 (1994).
- [183] A. Santos, P. Yustos, S. Gomis, G. Ruiz, and F. Garcia-Ochoa, *Industrial and Engineering Chemistry Research* **44**, 3869 (2005).
- [184] F. Stüber, A. M. Wilhelm, and H. Delmas, *Chemical Engineering Science* **51**, 2161 (1996).
- [185] A. Eftaxias, J. Font, A. Fortuny, A. Fabregat, and F. Stüber, *Applied Catalysis B: Environmental* **67**, 12 (2006).
- [186] D. M. Himmelblau, *Journal of Chemical Engineering Data* **5**, 10 (1960).
- [187] J. Guo and M. Al-Dahhan, *Industrial and Engineering Chemistry Research* **42**, 5473 (2003).
- [188] A. Sadana and J. R. Katzer, *Journal of Catalysis* **35**, 140 (1974).
- [189] M. Mehrvar, W. A. Anderson, and M. Moo-Young, *International Journal of Photoenergy* **3**, 187 (2001).
- [190] F. J. Rivas, S. T. Kolaczkowski, F. J. Beltrant, and D. B. McLurgh, *Chemical Engineering Science* **53**, 2575 (1998).
- [191] V. N. Sokolov and M. Yablokova, *Journal of Applied Chemistry of the USSR* **56**, 551 (1983).
- [192] V. Specchia, G. Baldi, and S. Sicardi, *Chemical Engineering Communications* **4**, 361 (1980).



# Appendix A

## Appendix

Table A.1: Thermo-physical properties of aqueous phenol solution

Property	120 °C	140°C	160°C
Water density $\text{kgm}^{-3}$	943	926	907
Water viscosity $\text{Nsm}^{-2} \times 10^4$	2.41	2.06	1.80
Water surface tension $\text{Nm}^{-1} \times 10^2$	5.86	5.46	5.03
Oxygen diffusion coefficient $\text{m}^2\text{s}^{-1} \times 10^8$	1.10	1.35	1.62
Phenol diffusion coefficient $\text{m}^2\text{s}^{-1} \times 10^9$	5.37	6.60	7.93
Air viscosity $\text{Nsm}^{-2} \times 10^5$	2.30	2.39	2.47
Henry constant $\text{m}^3\text{Pamol}^{-1} \times 10^{-3}$	130	121	110
Henry constant (MPa)	6.83	6.25	5.53
Water vapor pressure (MPa)	1.99	3.61	6.18
Water specific capacity $\text{kJkg}^{-1}\text{K}^{-1}$	4.24	4.28	4.33
Water heat of vaporization $\text{kJkg}^{-1}$	2212	2153	2091

Table A.2: Mineral content of fresh and CWAO spent AC

Sample ID	TOS	Fe (% w/w)	Comment
Fresh AC-1	-	0.40	AC used in standard saturation
Fresh AC-2	-	0.61	AC used in inert saturation)

Table A.3: List of operating conditions and main results for steady state CWAO of phenol over AC in TBR

Experiment	$PO_2$ (bar)	T (°C)	$\tau$ (h)	$F_g$ (NL/h)	$C_{ph}$ (g/L)	TOS (h)	$X_{ph}$	$X_{TOC}$	$\Delta W_{AC}$ (g)
Particle size:									
(mm)									
$d_p = 0.3$	2	140	0.12	150	5	51	0.47	-	2.5
$d_p = 0.5$	2	140	0.12			53	0.46	-	0.8
$d_p = 1.25$	2	140	0.12			53	0.28	-	1.4
$d_p = 2.5$	2	140	0.12			52	0.19	-	3.7
Gas flow rate:									
	2	140	0.12	25	5	75	0.25		2.1
				50			0.38		
				150			0.44		
				200			0.48		
				400			0.40		
Catalyst load :									
2.5	2	140	0.042	150	5	25	0.17		0.6
4.3			0.07			31	0.27	0.16	1.8
4.3 + 3.2(inert)			0.07			50	0.24	0.16	1.8
5			0.08			33	0.33		1.6
5.5			0.09			31	0.38	0.24	2.4
5.5 + 2(inert)			0.09			53	0.36	0.22	2.1
StartUp:									
Standard	2	140	0.12	150	5	51	0.46		0.4
ExternalC						51	0.26		2.9
In-situ						51	0.29		2.1
inert						51	0.54		3
Levec						107	0.46	0.27	2
Batch						49	0.55		1.4
Scavenger:									
Methanol	2	140	0.12	150	5	58	0.36		1.3

Continued on Next Page...

Table A.3 – Continued

Experiment	PO <sub>2</sub> (bar)	T (°C)	$\tau$ (h)	F <sub>g</sub> NL/h	C <sub>ph</sub> (g/L)	TOS (h)	X <sub>ph</sub>	X <sub>TOC</sub>	$\Delta W_{AC}$ (g)
t-Butanol	2					45	0.44		1.3
NaHCO <sub>3</sub>	2					73	0.12		2.8
Initial pH:									
3	2	140	0.12	150	5	125	0.35		2.9
4.5	2						0.53		
7	2						0.27		
9	2						0.19		
Liquid flow rate:									
29	2	140	0.24	150	5	72	0.28	0.15	2.6
39			0.18				0.45	0.27	
58			0.12				0.58	0.39	
99			0.07				0.72	0.48	
Inlet Phenol: Concentration									
	2	140	0.07	150	0.5	72	0.64	0.32	2.2
					1		0.57	0.31	
					2.5		0.38	0.22	
					5		0.29	0.18	
					10		0.22	0.14	
	2	140	0.12	150	0.5	108	0.88	0.31	3.5
					1		0.79		
					2.5		0.63		
					5		0.45		
					10		0.29		
	2	140	0.18	150	0.5	92	0.95	0.55	1
					1		0.88	0.59	
					2.5		0.76	0.49	

Continued on Next Page...

Table A.3 – Continued

<b>Experiment</b>	<b>PO<sub>2</sub></b> (bar)	<b>T</b> (°C)	<b>τ</b> (h)	<b>F<sub>g</sub></b> NL/h)	<b>C<sub>ph</sub></b> (g/L)	<b>TOS</b> (h)	<b>X<sub>ph</sub></b>	<b>X<sub>TOC</sub></b>	<b>ΔW<sub>AC</sub></b> (g)
					5		0.58	0.43	
					10		0.40	0.35	
	2	140	0.24	150	0.5	110	0.99	0.55	1
					1		0.98	0.59	
					2.5		0.95	0.49	
					5		0.84	0.43	
					10		0.77	0.35	
O <sub>2</sub> partial : Pressure	0.5 1 2 3.6	140	0.12	150	5	96	0.15 0.27 0.41 0.49	0.11 0.17 0.24 0.32	2.7
Temperature :	120		0.07 0.12 0.18 0.24	150	5		0.08 0.18 0.31 0.41	0.08 0.09 0.21 0.31	3.2
	160		0.07 0.12 0.18 0.24	150	5		0.77 0.91 0.96 0.99	0.61 0.74 0.8 0.83	-0.3
Upflow reactor:	2	160	0.24	150	5	30	0.97	-	1.1

## **Appendix B**

### **Appendix**

#### **B.1 Experimental Profiles obtained in Adsorption and Kinetic Measurement**

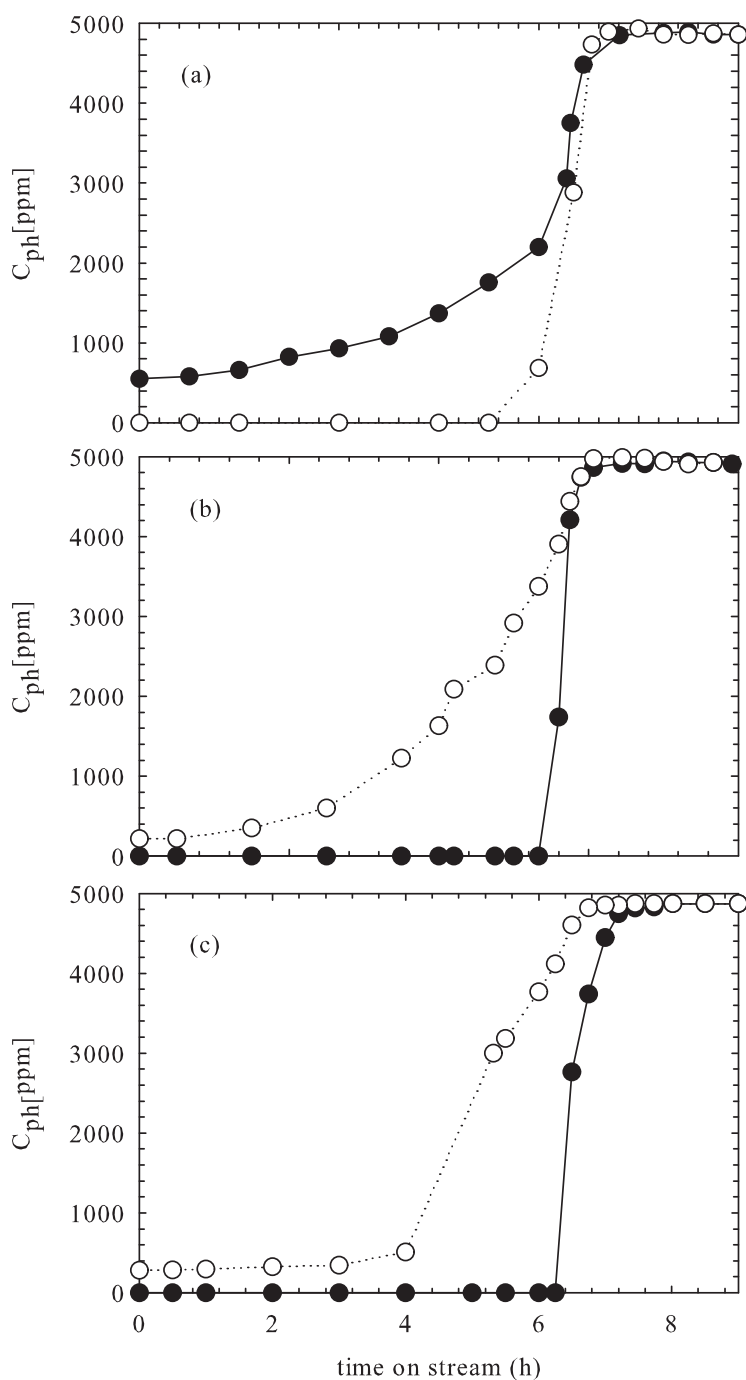


Figure B.1: Phenomena adsorption/desorption over AC for different temperatures under inert conditions: (●) adsorption, (○) desorption:  $P_T = 15$  bar,  $F_L = 60$  mL/h,  $F_G = 9$  NL/h,  $W_{cat} = 7$  g,  $C_{ph} = 5$  g/L.

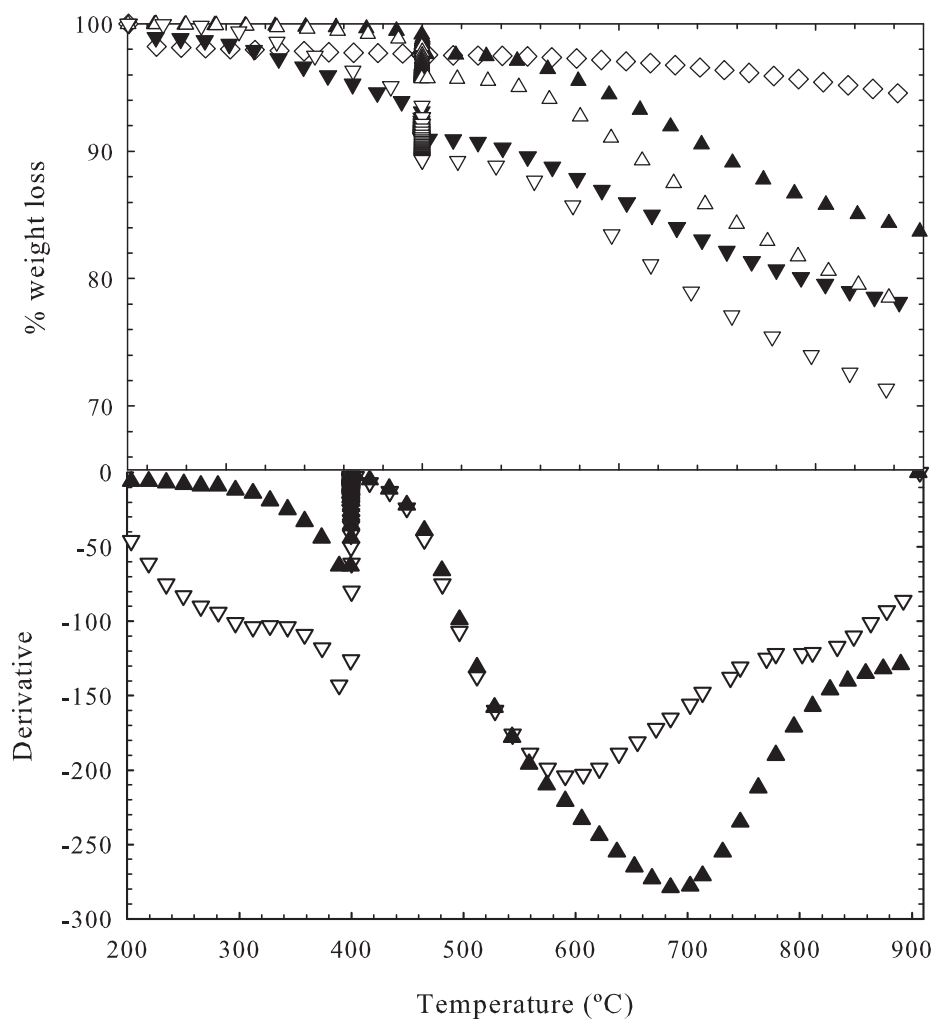


Figure B.2: TGA data of fresh and spent AC for different AC saturation procedures: ( $\diamond$ ) Fresh AC, ( $\blacktriangle$ ) Standard saturation, ( $\triangle$ ) External saturation, ( $\blacktriangledown$ ) Inert saturation, ( $\nabla$ ) Fast in-situ saturation:  $P_{O_2} = 2$  bar,  $T = 140^\circ\text{C}$ ,  $\tau = 0.12$  h,  $F_G = 9$  NL/h,  $W_{\text{cat}} = 7$  g,  $C_{\text{Ph}} = 5$  g/L:

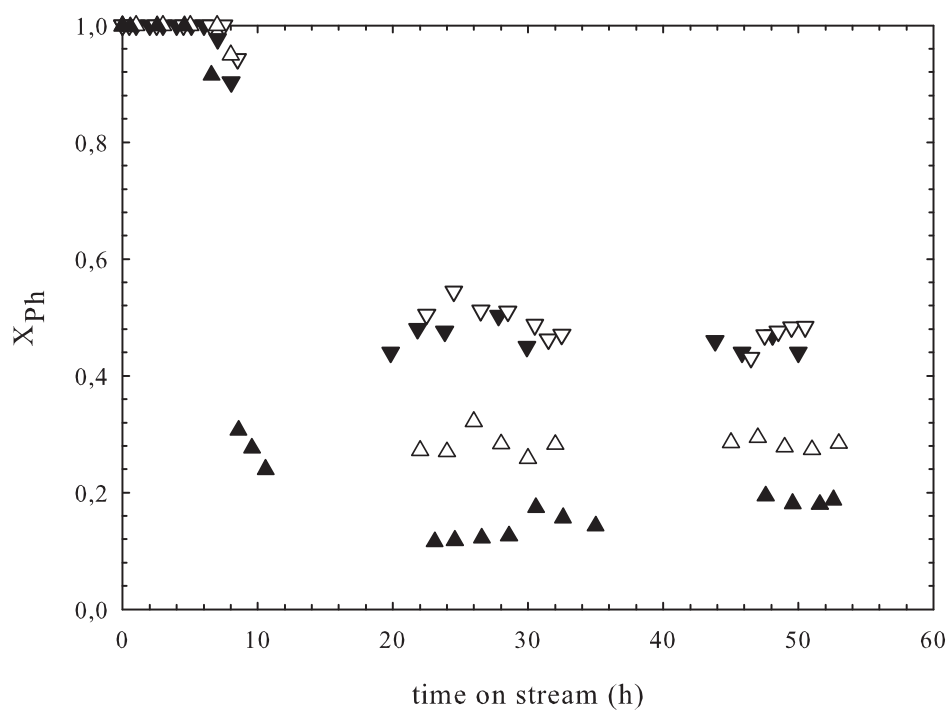


Figure B.3: Phenol conversion as function of time on stream for different AC particle size: ( $\nabla$ )  $d_p = 0.3$  mm, ( $\blacktriangledown$ )  $d_p = 0.5$  mm, ( $\triangle$ )  $d_p = 1$  mm, ( $\blacktriangle$ )  $d_p = 2.5$  mm:  $P_{O_2}$ ,  $T = 140^\circ\text{C}$ ,  $\tau = 0.12$  h,  $F_G = 9$  NL/h,  $W_{cat} = 7$  g,  $C_{Ph} = 5$  g/L.

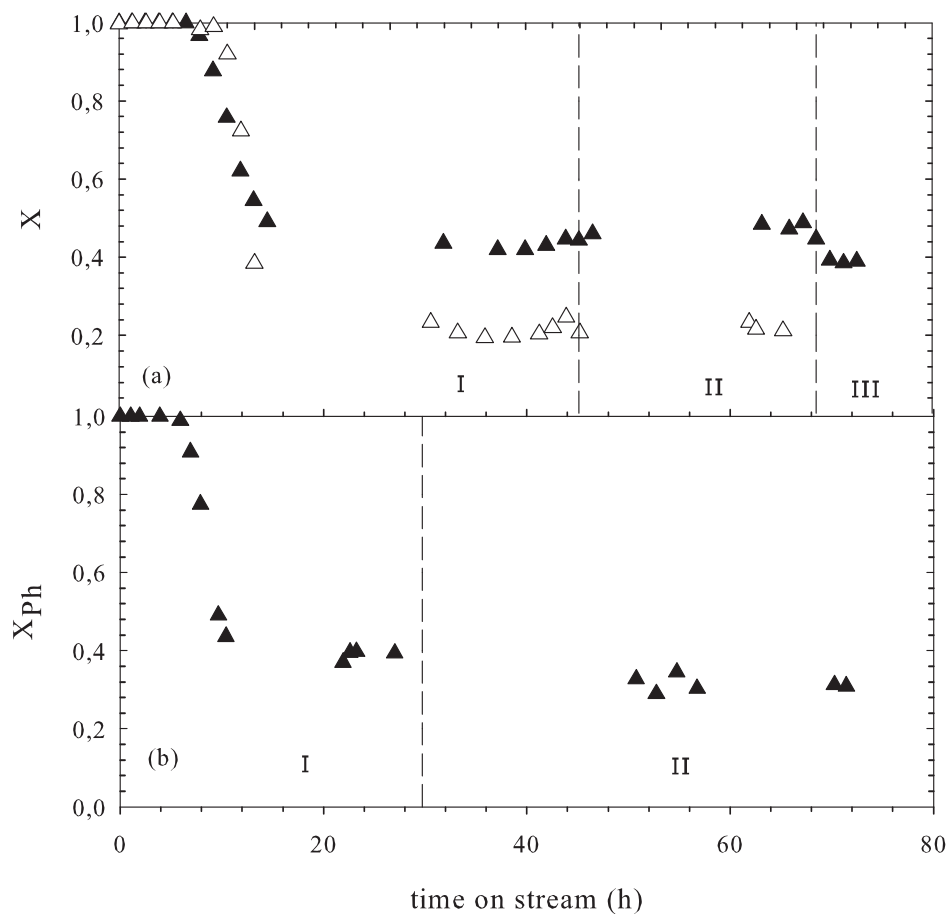


Figure B.4: Phenol (▲) and TOC (△) conversion as function of time on stream for different gas flow rate: (a) (I) → 9 NL/h, (II) → 12 NL/h, (III) → 3 NL/h; (b) (I) → 24 NL/h, (II) → 3 NL/h;  $P_{O_2} = 2$  bar,  $T = 140^\circ\text{C}$ ,  $\tau = 0.12$  h,  $W_{\text{cat}} = 7$  g,  $C_{\text{Ph}} = 5$  g/L.

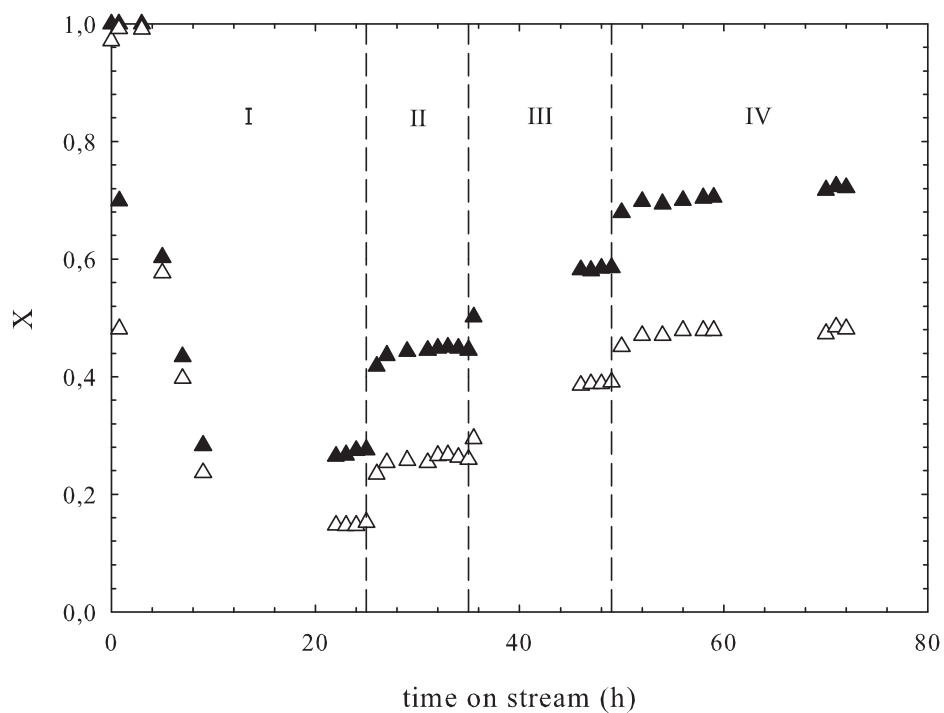


Figure B.5: Time on stream phenol conversion profile for subsequent variation of liquid flow rate (Low to high):(▲) phenol conversion, (△) TOC conversion: (I) → 29 mL/h, (II) → 39 mL/h, (III) → 58 mL/h, (IV) → 83 mL/h, (V) → 99 mL/h:  $P_{O_2} = 2$  bar,  $T = 140^\circ\text{C}$ ,  $F_G = 9$  NL/h,  $W_{\text{cat}} = 7$  g,  $C_{\text{Ph}} = 5$  g/L.

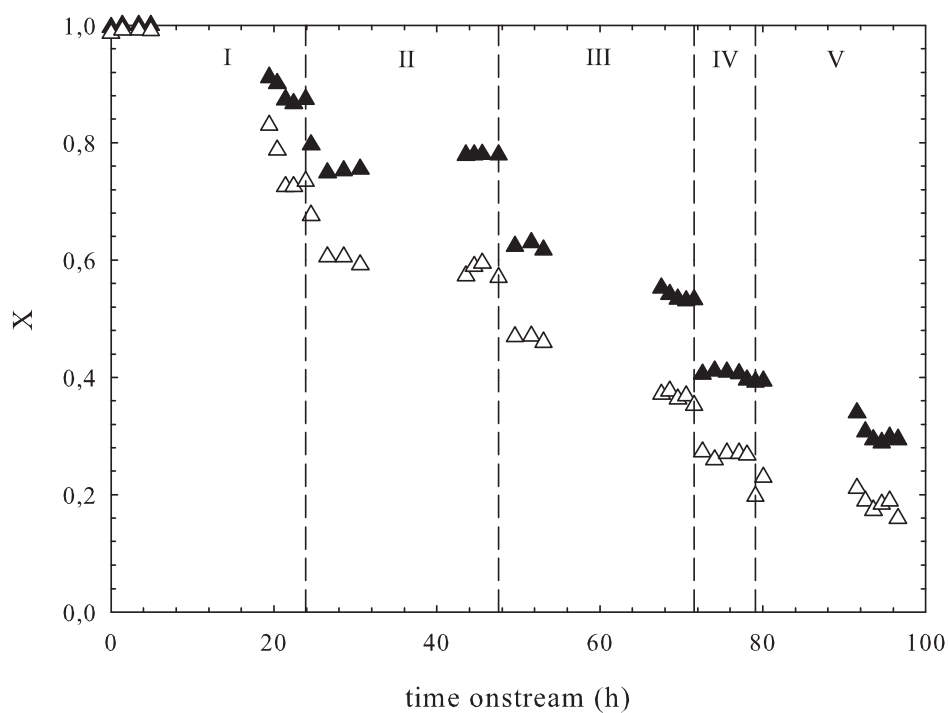


Figure B.6: Time on stream phenol conversion profile for subsequent change of liquid flow rate. (▲) phenol conversion, (△) TOC conversion.  $F_L$ : (I)  $\rightarrow$  99 mL/h, (II)  $\rightarrow$  83 mL/h, (III)  $\rightarrow$  58 mL/h, (IV)  $\rightarrow$  39 mL/h, (V)  $\rightarrow$  29 mL/h:  $P_{O_2} = 2$  bar,  $T = 140^\circ\text{C}$ ,  $W_{\text{cat}} = 7\text{g}$ ,  $C_{\text{ph}} = 5$  g/L.

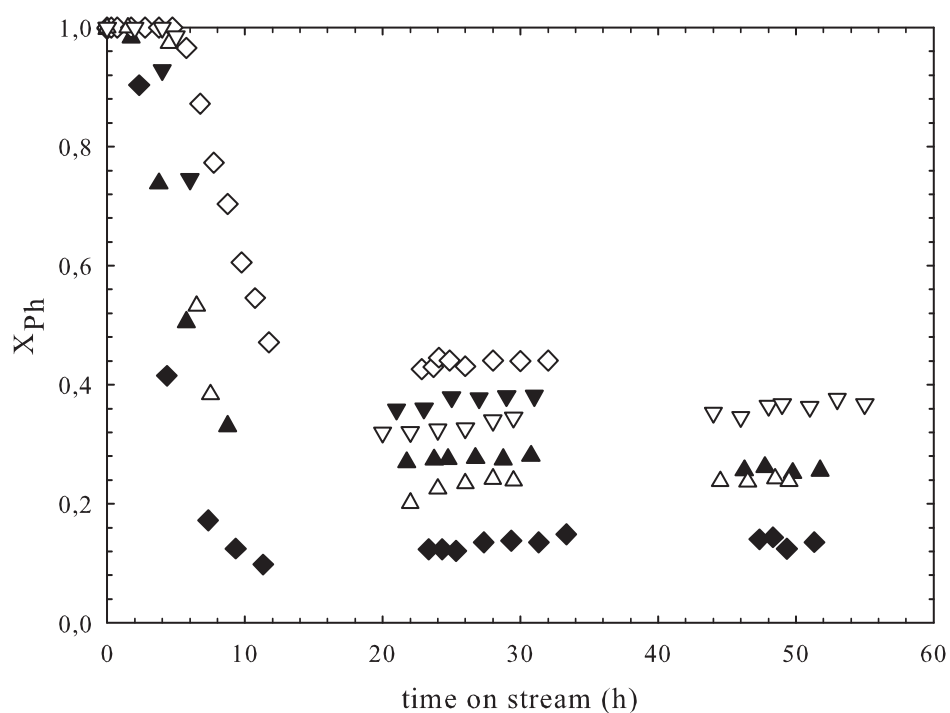


Figure B.7: Phenol conversion versus time on stream for different reactor bed length: (◇) 7 g, (▼) 5.5 g, (▽) 5.5 g (dilated bed), (▲) 4.3 g, (△) 4.3 g (dilated bed), (◆) 2.5 g;  $P_{O_2} = 2$  bar,  $T = 140^\circ\text{C}$ ,  $\tau = 0.12$  h,  $F_G = 9$  NL/h,  $C_{Ph} = 5$  g/L.

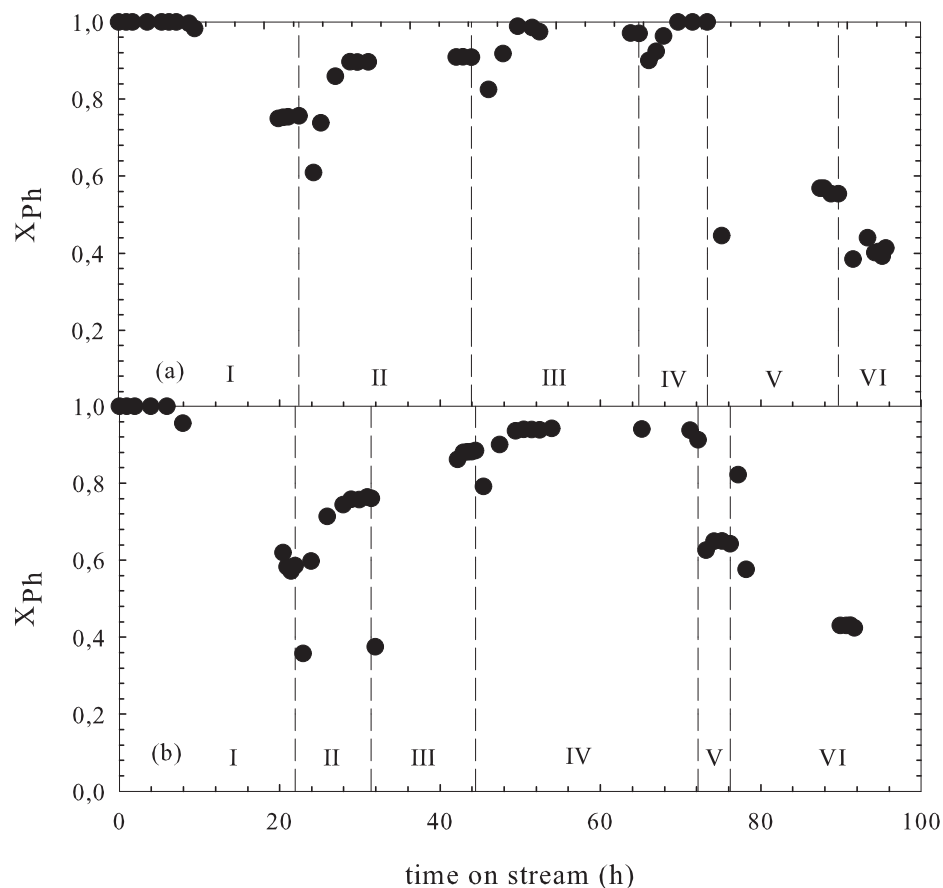


Figure B.8: Time on stream phenol conversion profile for subsequent dilution of feed phenol concentration: (I)  $\rightarrow$  5 g/L, (II)  $\rightarrow$  2.5 g/L, (III)  $\rightarrow$  1 g/L, (IV)  $\rightarrow$  0.5 g/L, (V)  $\rightarrow$  5 g/L, (VI)  $\rightarrow$  10 g/L: (a)  $\tau = 0.24$  h, (b)  $\tau = 0.18$  h:  $P_{O_2} = 2$  bar,  $T = 140^\circ\text{C}$ ,  $W_{cat} = 7$  g,  $F_G = 9$  NL/h.

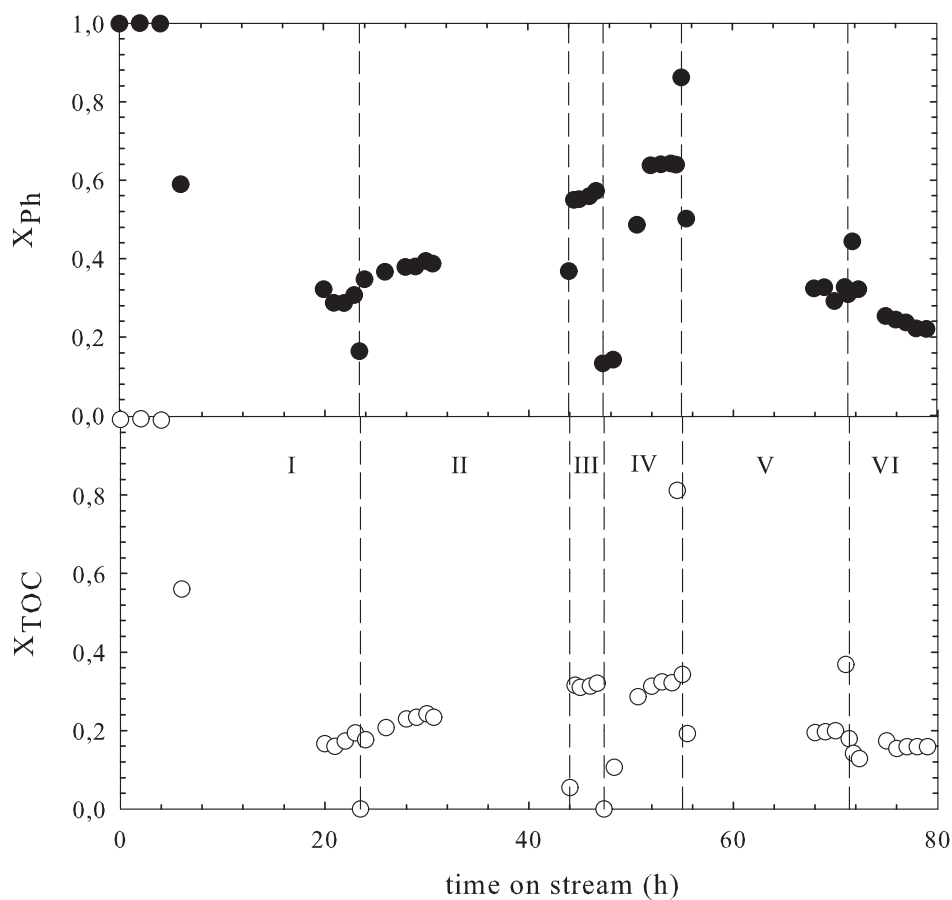


Figure B.9: Time on stream phenol conversion profile for subsequent dilution of feed phenol concentration: (I)  $\rightarrow$  5 g/L, (II)  $\rightarrow$  2.5 g/L, (III)  $\rightarrow$  1 g/L, (IV)  $\rightarrow$  0.5 g/L, (V)  $\rightarrow$  5 g/L, (VI)  $\rightarrow$  10 g/L):  $P_{O_2} = 2$  bar,  $T = 140^\circ\text{C}$ ,  $\tau = 0.07$  h,  $W_{\text{cat}} = 7$  g,  $F_G = 9$  NL/h.

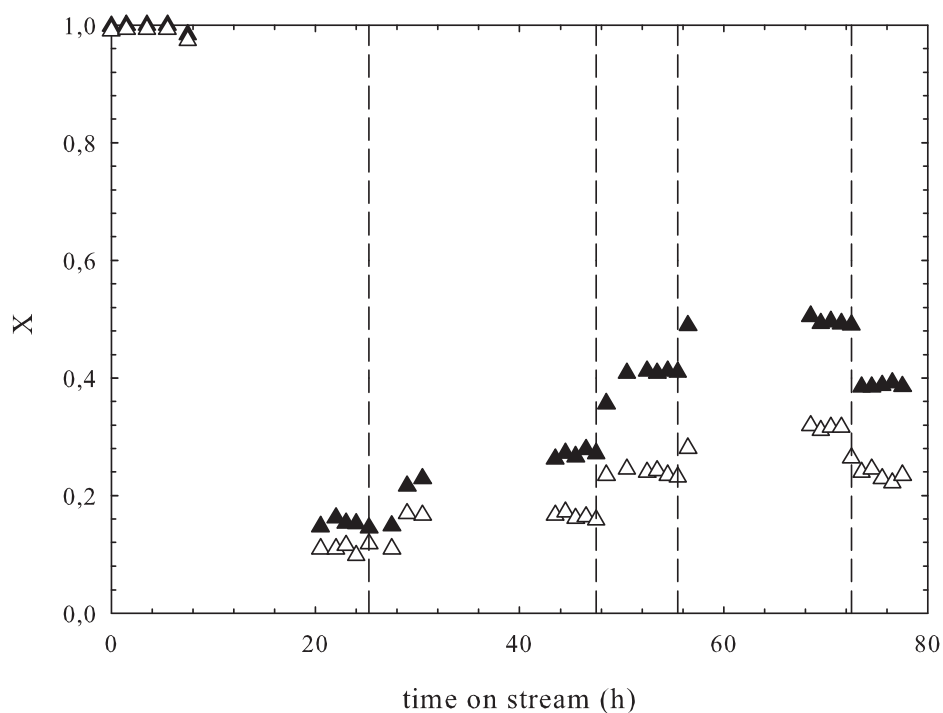


Figure B.10: Phenol conversion as function of time on stream for subsequent variation of oxygen partial pressure. ( $\blacktriangle$ ) phenol conversion, ( $\triangle$ ) TOC conversion: (I)  $\rightarrow$  0.5 bar, (II)  $\rightarrow$  1 bar, (III)  $\rightarrow$  2 bar, (IV)  $\rightarrow$  3.6, (V)  $\rightarrow$  2 bar:  $T = 140^{\circ}\text{C}$ ,  $F_G = 9 \text{ NL/h}$ ,  $\tau = 0.12 \text{ h}$ ,  $W_{\text{cat}} = 7 \text{ g}$ ,  $C_{\text{Ph}} = 5 \text{ g/L}$ .

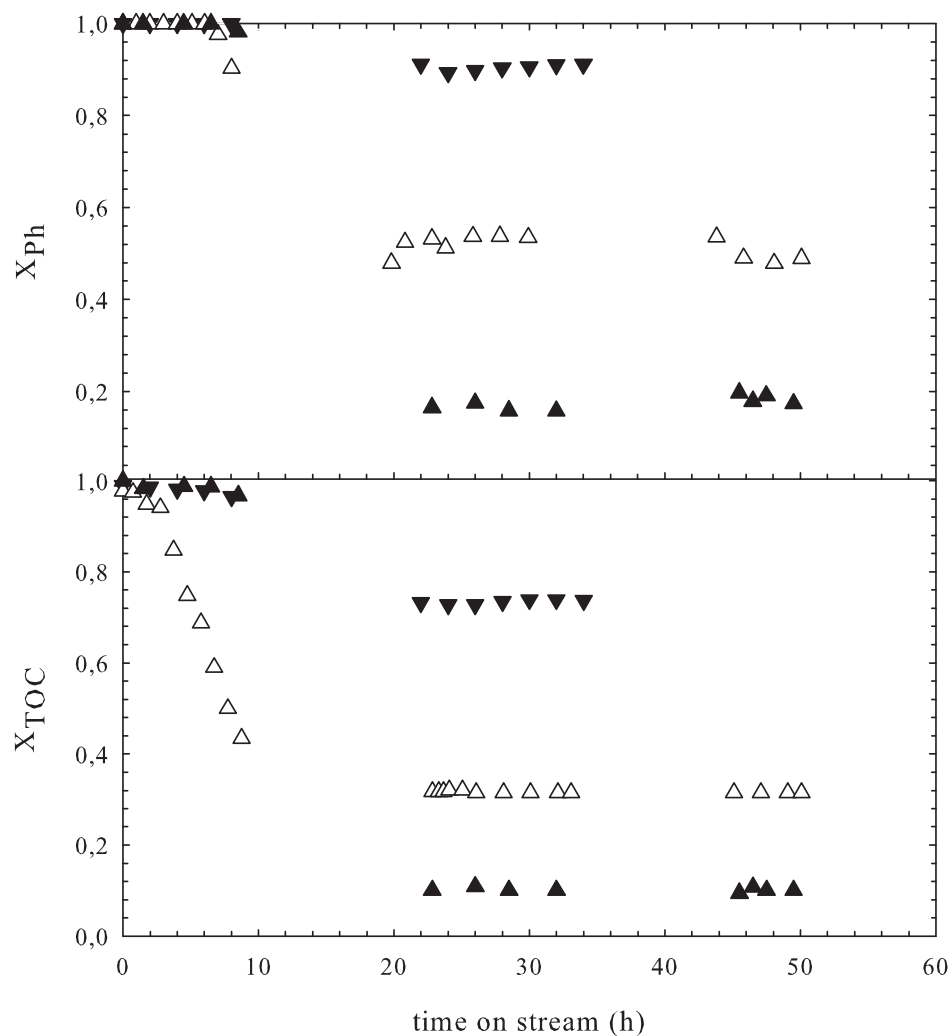


Figure B.11: Phenol conversion as function of time on stream for subsequent variation of reactor inlet temperature ( $\tau = 0.12$  h): (▼) 160°C, (△) 140°C, (▲) 160°C:  $P_{O_2} = 2$  bar,  $F_G = 9$  NL/h,  $\tau = 0.12$  h,  $W_{cat} = 7$  g,  $C_{Ph} = 5$  g/L.

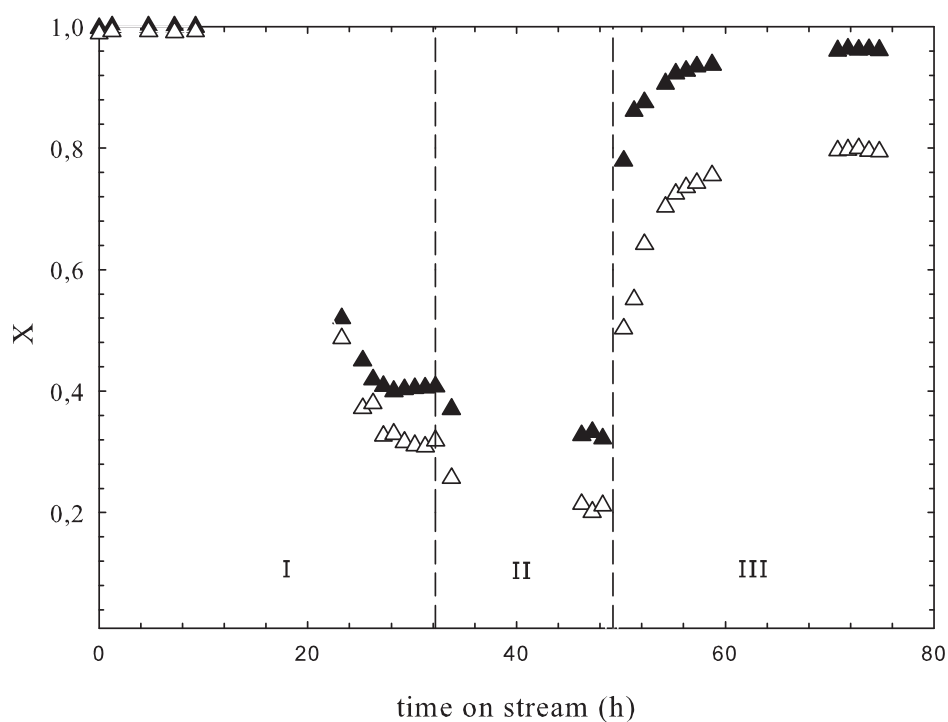


Figure B.12: Phenol conversion as function of time on stream for subsequent variation of reactor inlet temperature ( $\tau = 0.18$  h). (▲) phenol conversion, (△) TOC conversion: (I)  $120^{\circ}\text{C}$  ( $\tau = 0.24$  h), (II)  $120^{\circ}\text{C}$  ( $\tau = 0.18$  h), (III)  $160^{\circ}\text{C}$  ( $\tau = 0.18$  h):  $P_{\text{O}_2} = 2$  bar,  $F_{\text{G}} = 9$  NL/h,  $W_{\text{cat}} = 7$  g,  $C_{\text{Ph}} = 5$  g/L.

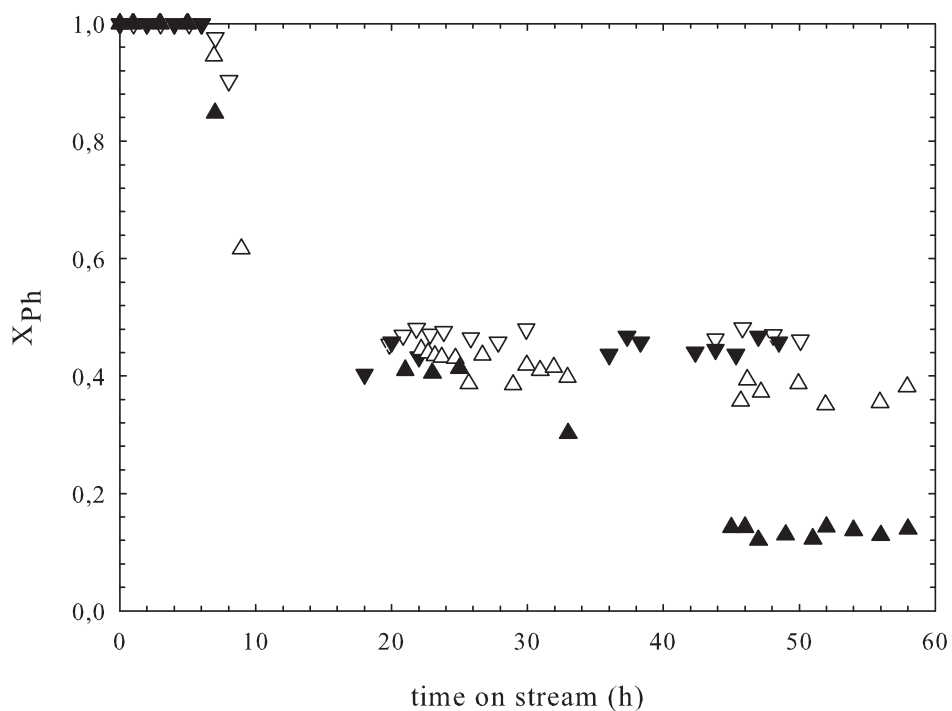


Figure B.13: Phenol conversion versus time on stream for different for different concentration of radical scavengers): (∇) without scavengers, (▼) methanol, (△) t-butanol, (▲) Sodium bi-carbonate:  $P_{O_2} = 2$  bar,  $T = 140^\circ\text{C}$ ,  $\tau = 0.12$  h,  $F_G = 9$  NL/h,  $W_{cat} = 7$  g,  $C_{Ph} = 5$  g/L.

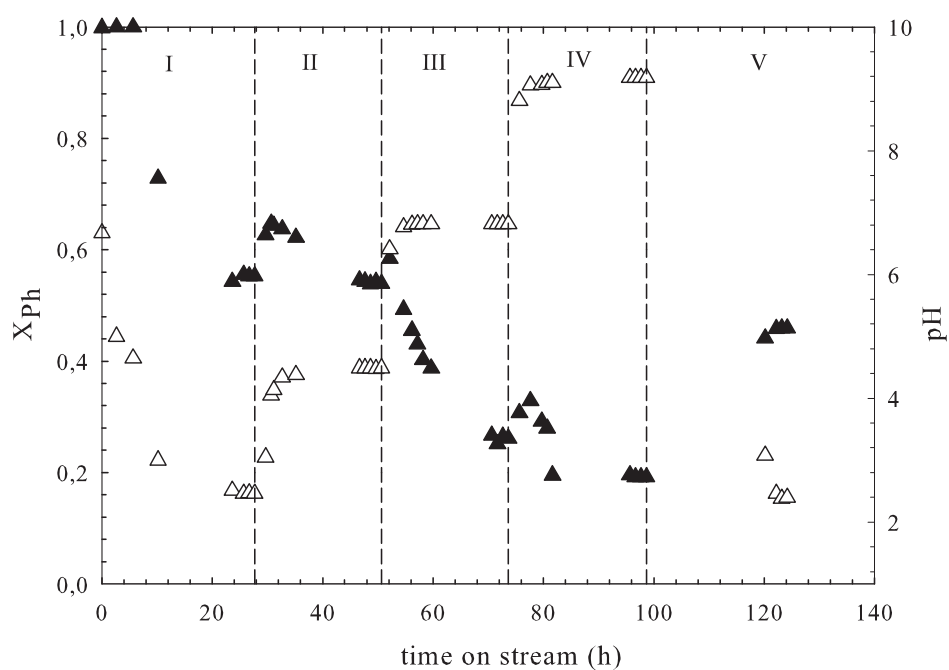


Figure B.14: Evolution of phenol conversion and effluent pH with time on stream during CWAO over AC: ( $\blacktriangle$ ) phenol conversion, ( $\triangle$ ) effluent pH: (I)  $\rightarrow$  2.5, (II)  $\rightarrow$  4.5, (III)  $\rightarrow$  7, (IV)  $\rightarrow$  9.2, (V)  $\rightarrow$  2.5:  $P_{O_2} = 2$  bar,  $T = 140^\circ\text{C}$ ,  $\tau = 0.12$  h,  $F_G = 9$  NL/h,  $W_{\text{cat}} = 7$  g,  $C_{\text{Ph}} = 5$  g/L.



# Appendix C

## Appendix

### C.1 Axial temperature profiles

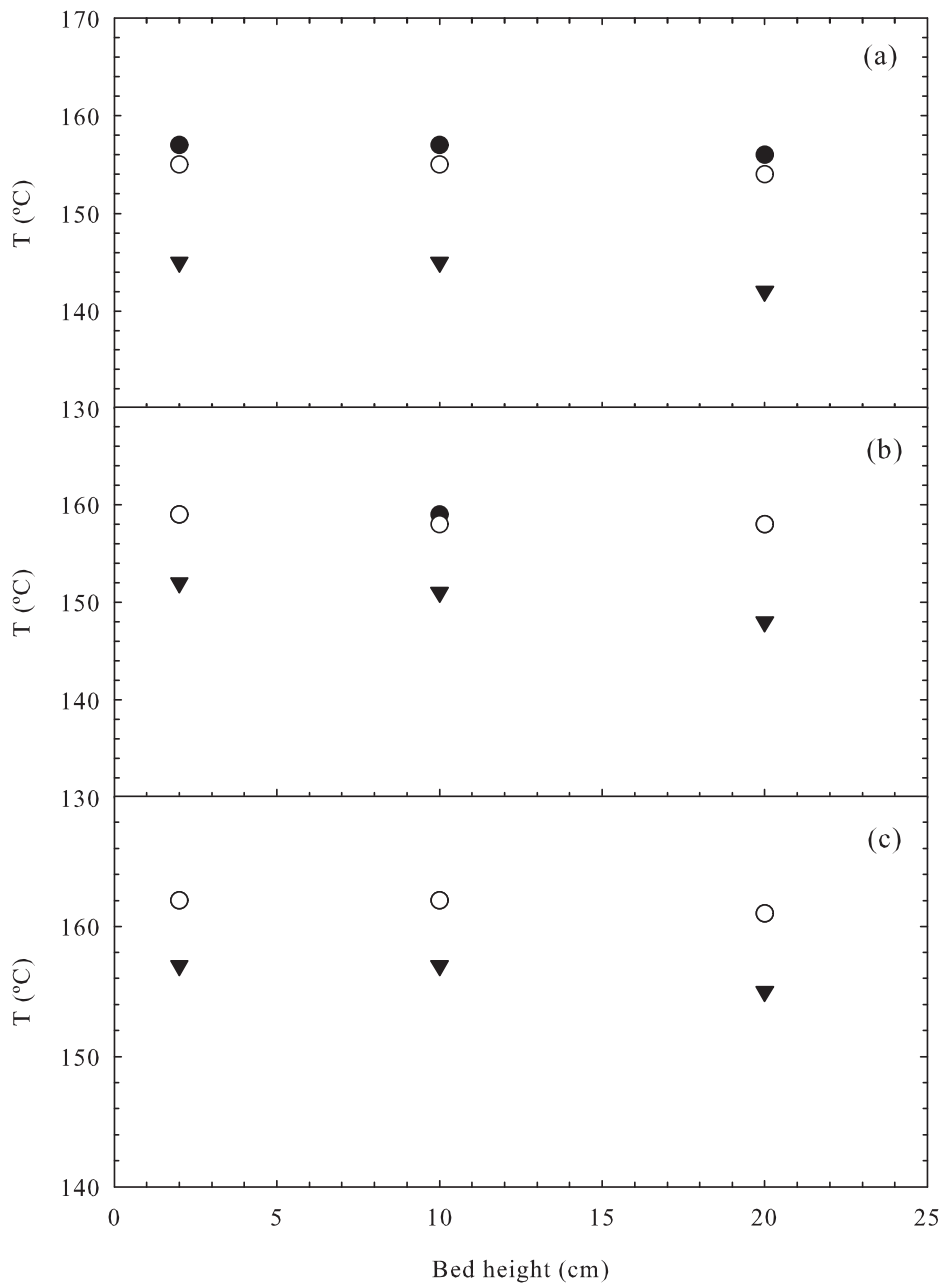


Figure C.1: Trickle column axial temperature profile for different liquid and gas flow rates,  $P_T = 9$  bar, Glass bead packing: (a)  $F_G = 18$  NL/h, (b)  $F_G = 9$  NL/h, (c)  $F_G = 3$  NL/h: (●)  $F_L = 100$  mL/h, (○)  $F_L = 60$  mL/h, (▼)  $F_L = 30$  mL/h:  $T_{oven} = 170$  °C.

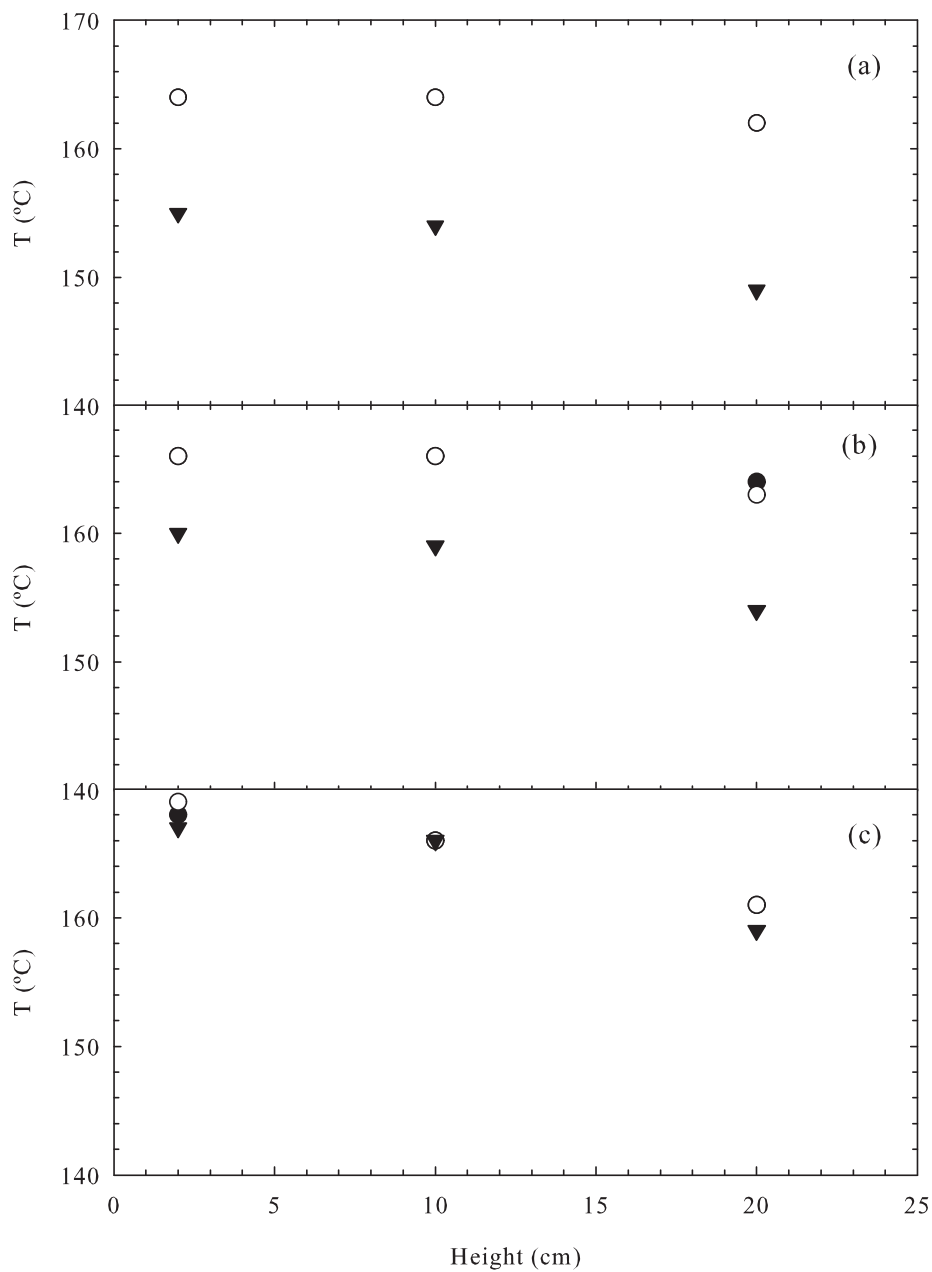


Figure C.2: Trickle column axial temperature profile for different liquid and gas flow rates,  $P_T = 12$  bar, Glass bead packing: (a)  $F_G = 18$  NL/h, (b)  $F_G = 9$  NL/h, (c)  $F_G = 3$  NL/h: (●)  $F_L = 100$  mL/h, (○)  $F_L = 60$  mL/h, (▼)  $F_L = 30$  mL/h:  $T_{oven} = 170$  °C.

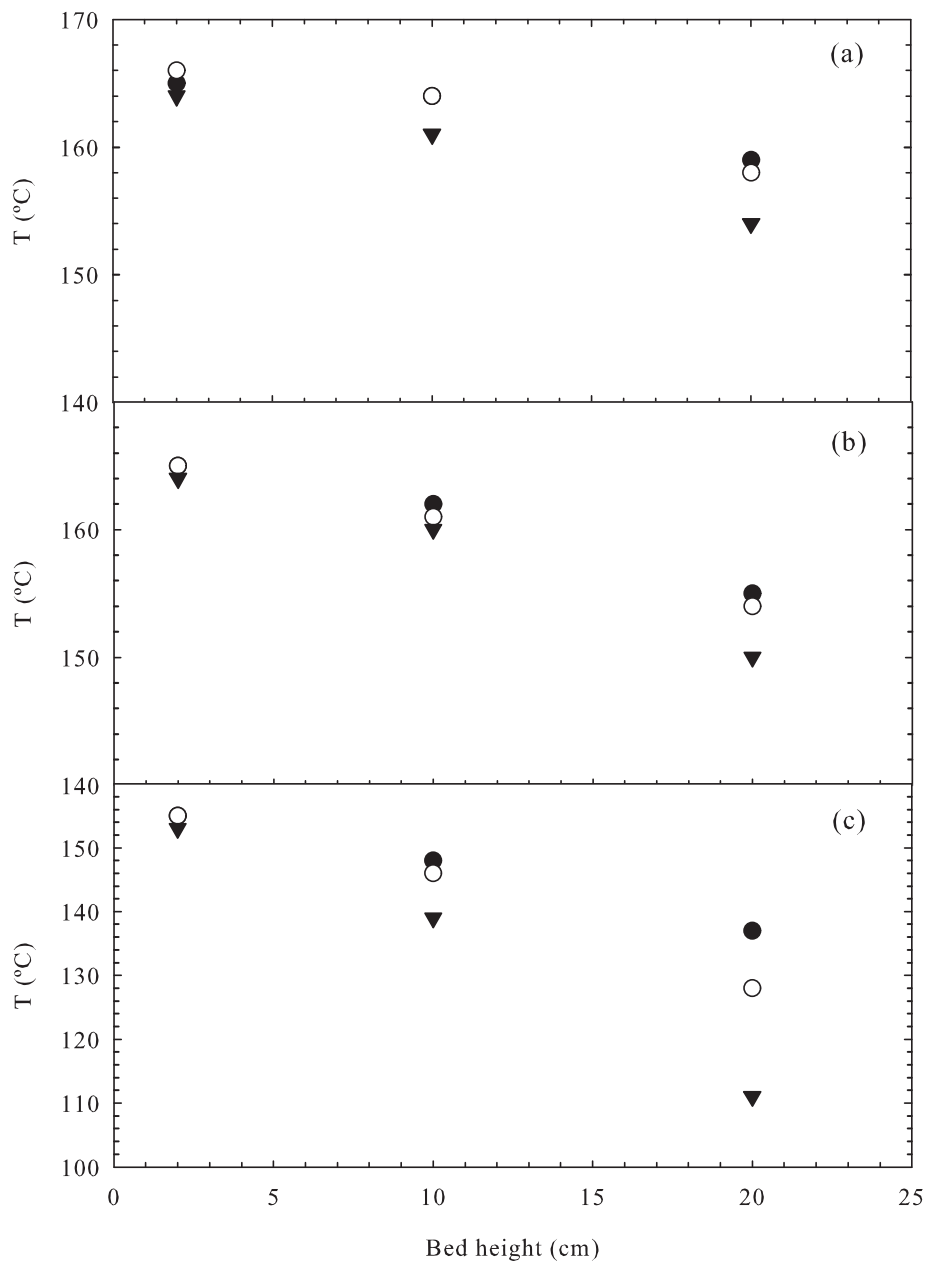


Figure C.3: Trickle column axial temperature profile for different liquid and gas flow rates,  $P_T = 15$  bar, Glass bead packing: (a)  $F_G = 18$  NL/h, (b)  $F_G = 9$  NL/h, (c)  $F_G = 3$  NL/h: (●)  $F_L = 100$  mL/h, (○)  $F_L = 60$  mL/h, (▼)  $F_L = 30$  mL/h :  $T_{oven} = 170$  °C.

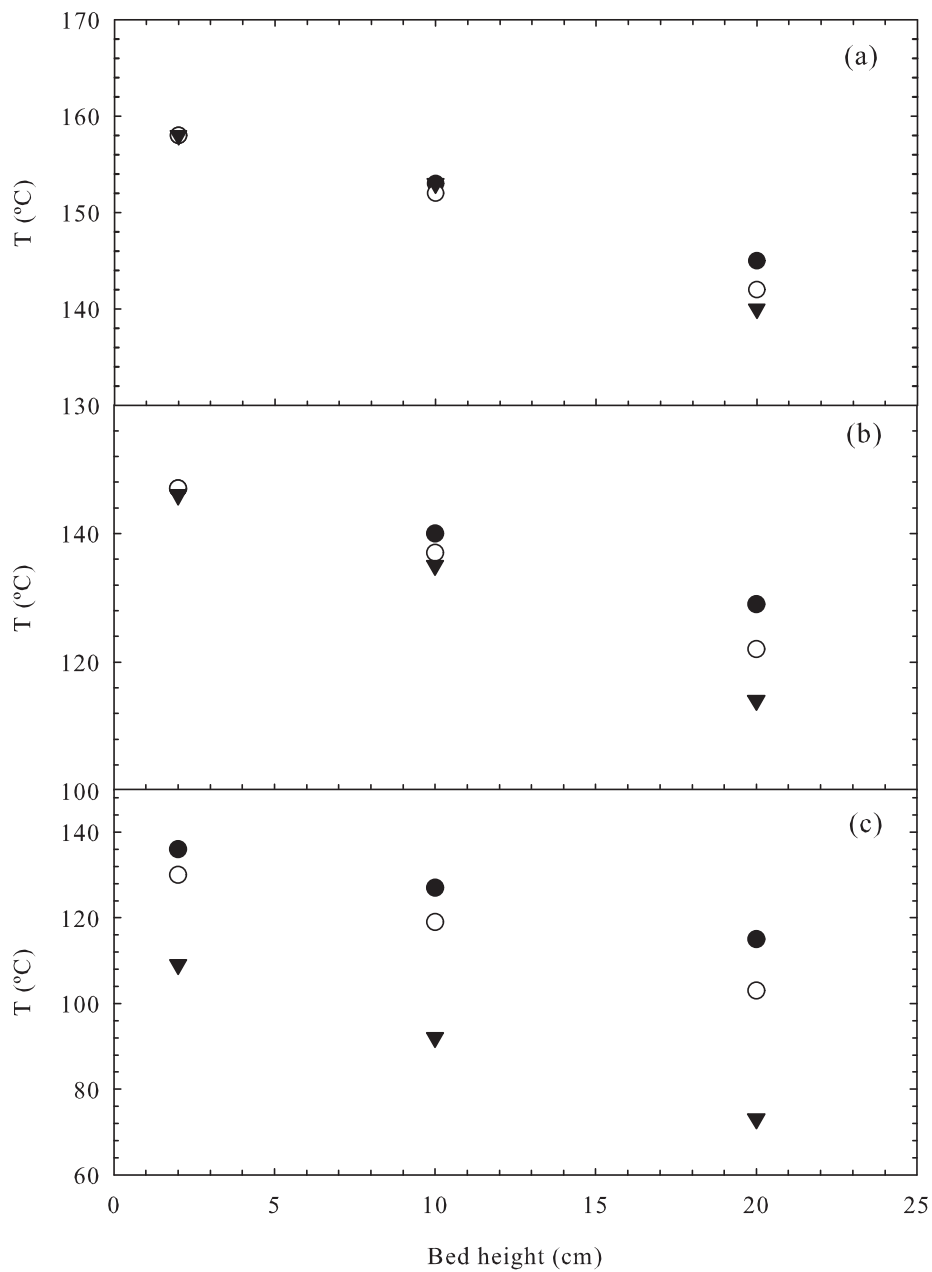


Figure C.4: Trickle column axial temperature profile for different liquid and gas flow rates,  $P_T = 20$  bar, Glass bead packing: (a)  $F_G = 18$  NL/h, (b)  $F_G = 9$  NL/h, (c)  $F_G = 3$  NL/h: (●)  $F_L = 100$  mL/h, (○)  $F_L = 60$  mL/h, (▼)  $F_L = 30$  mL/h:  $T_{oven} = 170$  °C.

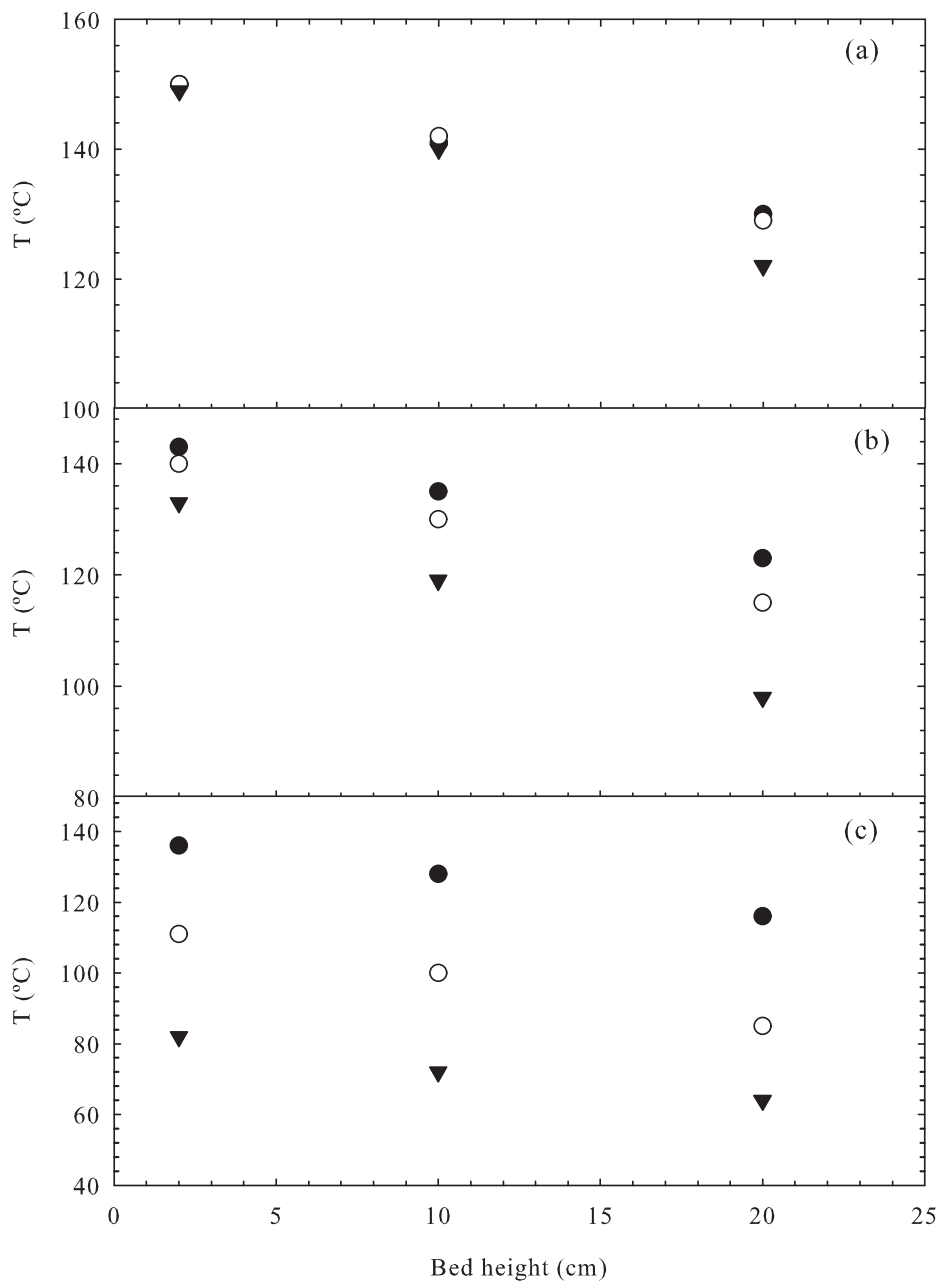


Figure C.5: Trickle column axial temperature profile for different liquid and gas flow rates,  $P_T = 25$  bar, Glass bead packing: (a)  $F_G = 18$  NL/h, (b)  $F_G = 9$  NL/h, (c)  $F_G = 3$  NL/h: (●)  $F_L = 100$  mL/h, (○)  $F_L = 60$  mL/h, (▼)  $F_L = 30$  mL/h :  $T_{oven} = 170$  °C.

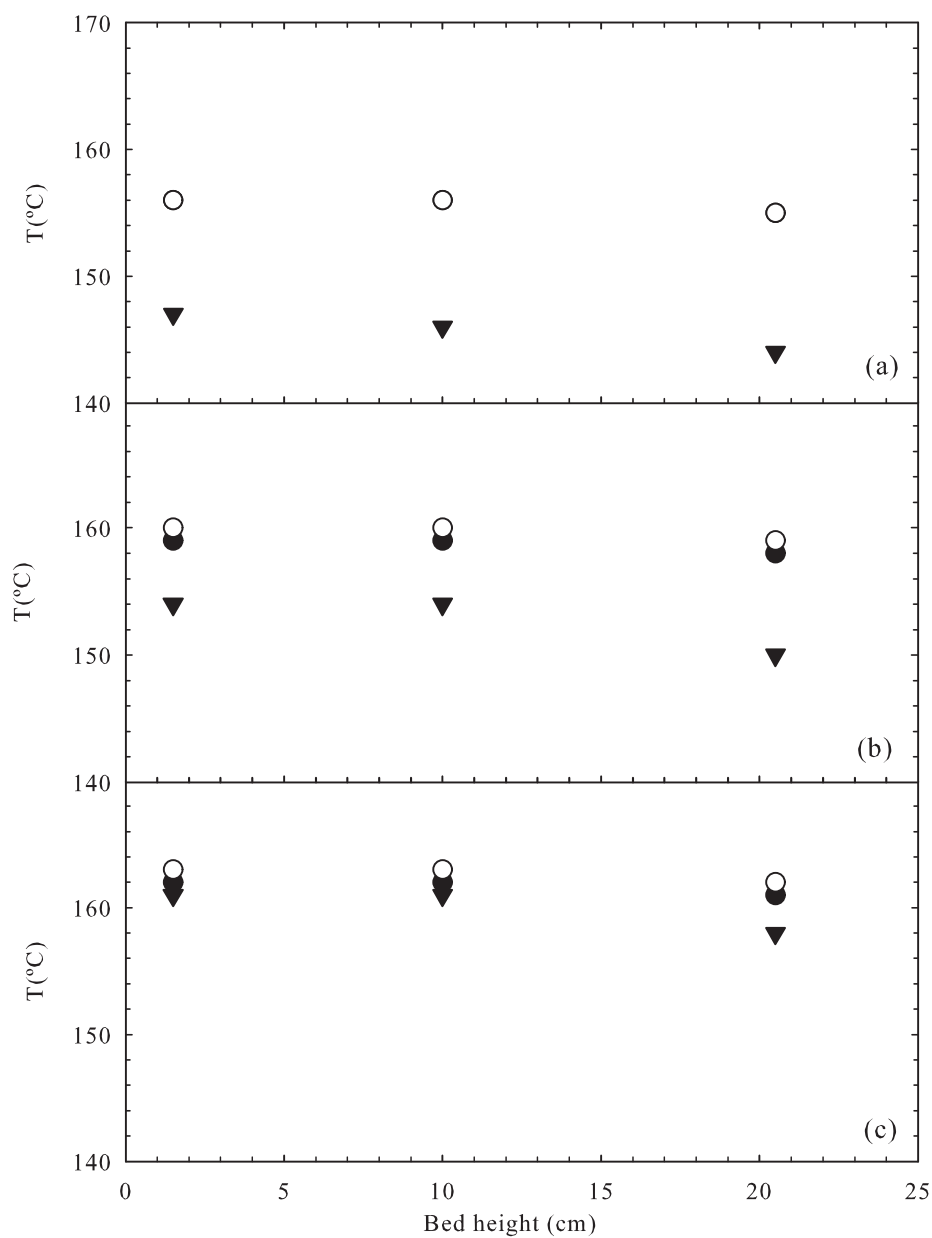


Figure C.6: Trickle column axial temperature profile for different liquid and gas flow rates:  $P_T = 9$  bar, AC packing: (a)  $F_G = 18$  NL/h, (b)  $F_G = 9$  NL/h, (c)  $F_G = 3$  NL/h: (●)  $F_L = 100$  mL/h, (○)  $F_L = 60$  mL/h, (▼)  $F_L = 30$  mL/h:  $T_{oven} = 170$  °C.

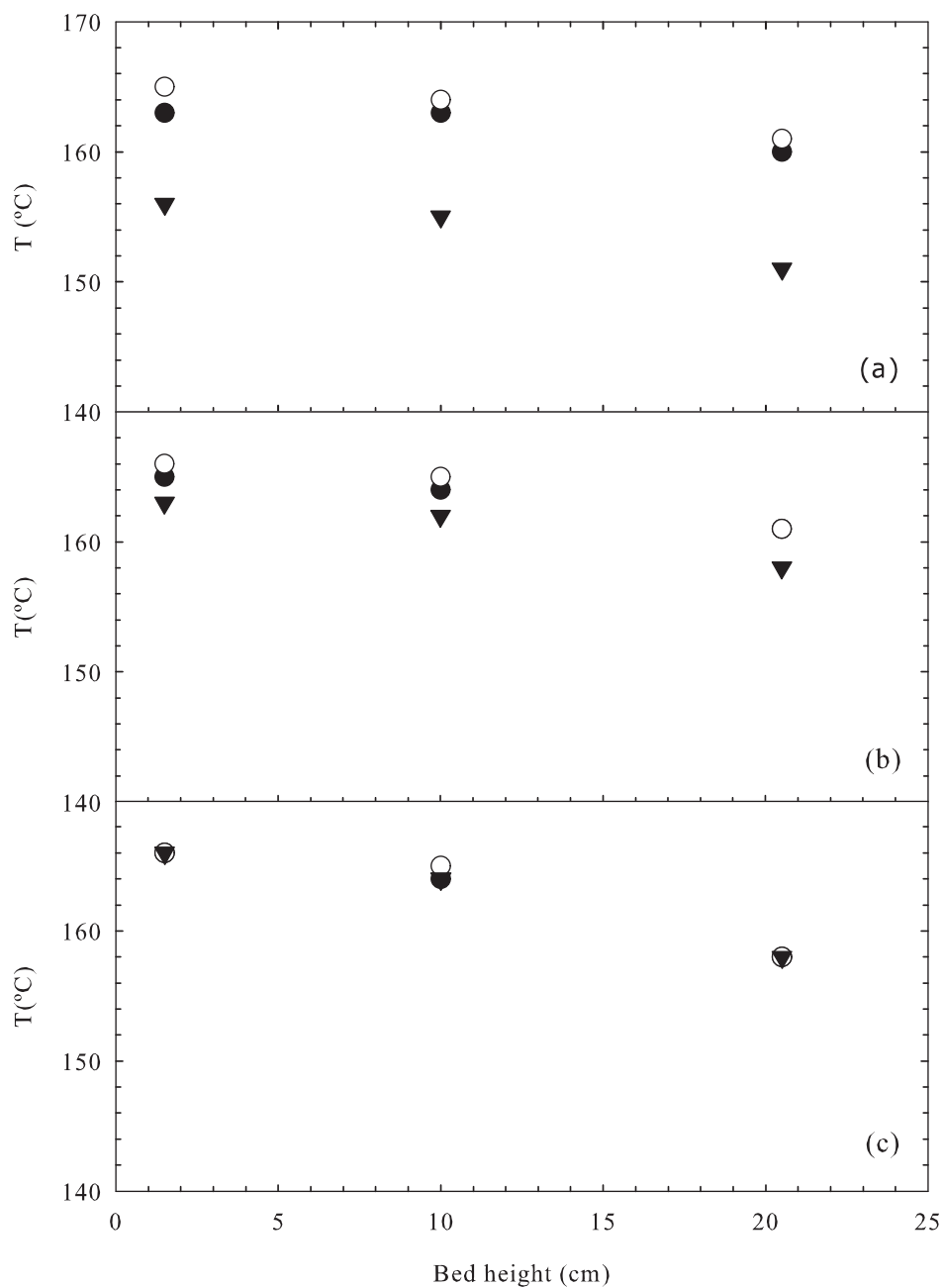


Figure C.7: Tickle column axial temperature profile for different liquid and gas flow rates,  $P_T = 12$  bar, AC packing: (a)  $F_G = 18$  NL/h, (b)  $F_G = 9$  NL/h, (c)  $F_G = 3$  NL/h: (●)  $F_L = 100$  mL/h, (○)  $F_L = 60$  mL/h, (▼)  $F_L = 30$  mL/h:  $P_t = 12$  bar,  $T_{oven} = 170$  °C.

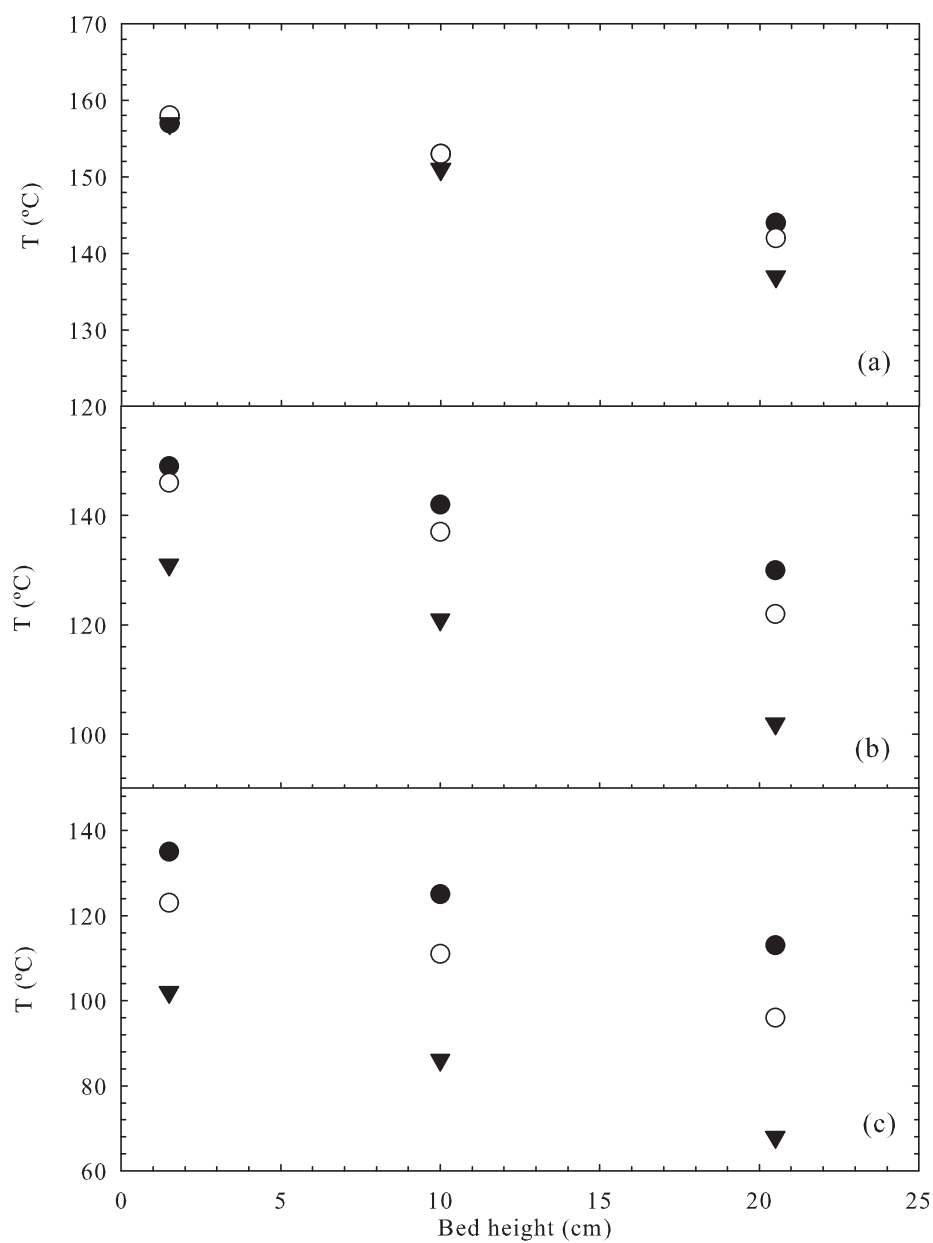


Figure C.8: Trickle column axial temperature profile for different liquid and gas flow rates,  $P_T = 20$  bar, AC packing: (a)  $F_G = 18$  NL/h, (b)  $F_G = 9$  NL/h, (c)  $F_G = 3$  NL/h: (●)  $F_L = 100$  mL/h, (○)  $F_L = 60$  mL/h, (▼)  $F_L = 30$  mL/h:  $T_{oven} = 170$  °C.

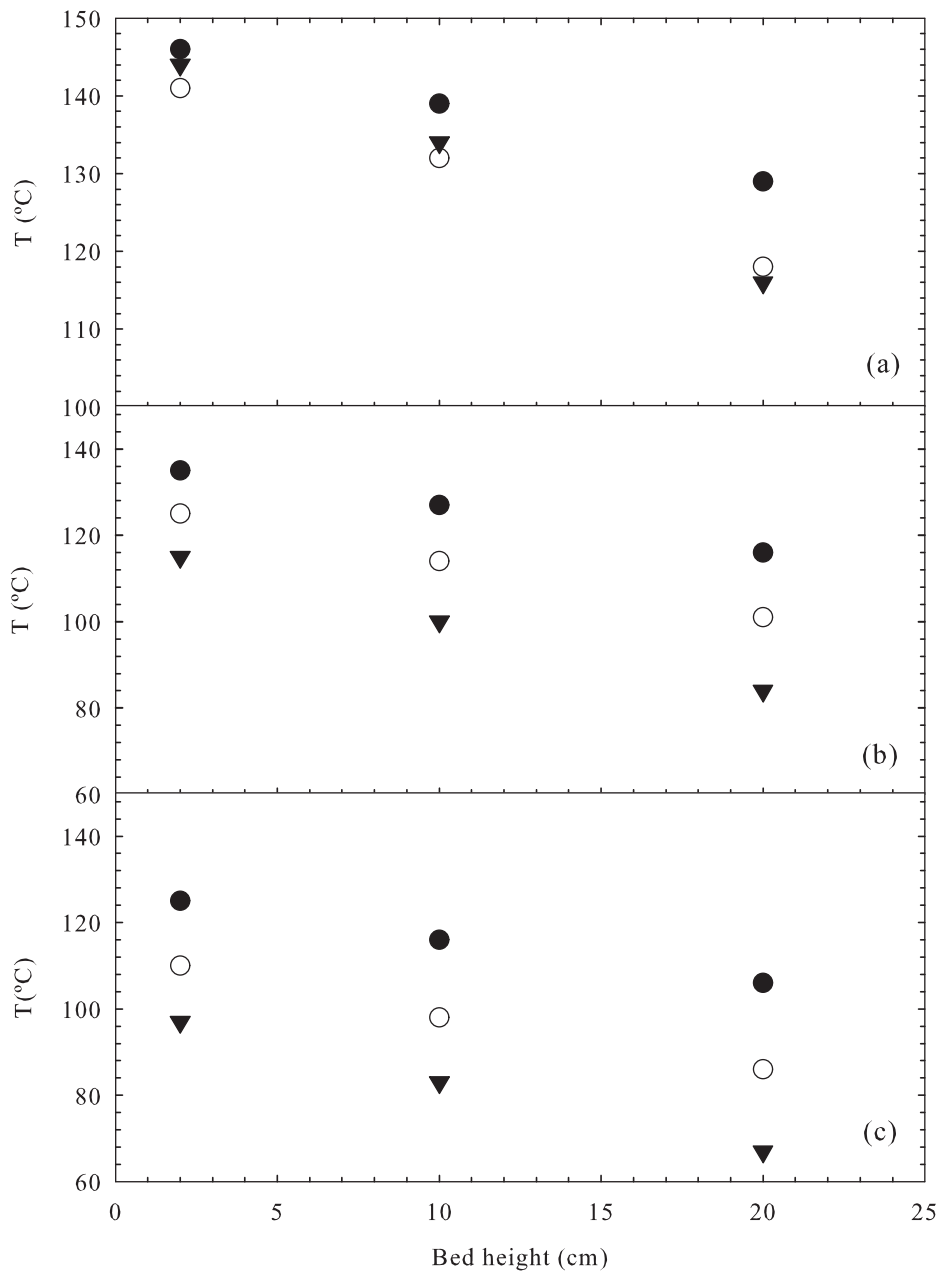


Figure C.9: Trickle column axial temperature profile for different liquid and gas flow rates,  $P_T = 25$  bar, AC packing: (a)  $F_G = 18$  NL/h, (b)  $F_G = 9$  NL/h, (c)  $F_G = 3$  NL/h: (●)  $F_L = 100$  mL/h, (○)  $F_L = 60$  mL/h, (▼)  $F_L = 30$  mL/h:  $T_{oven} = 170$  °C, AC packing.

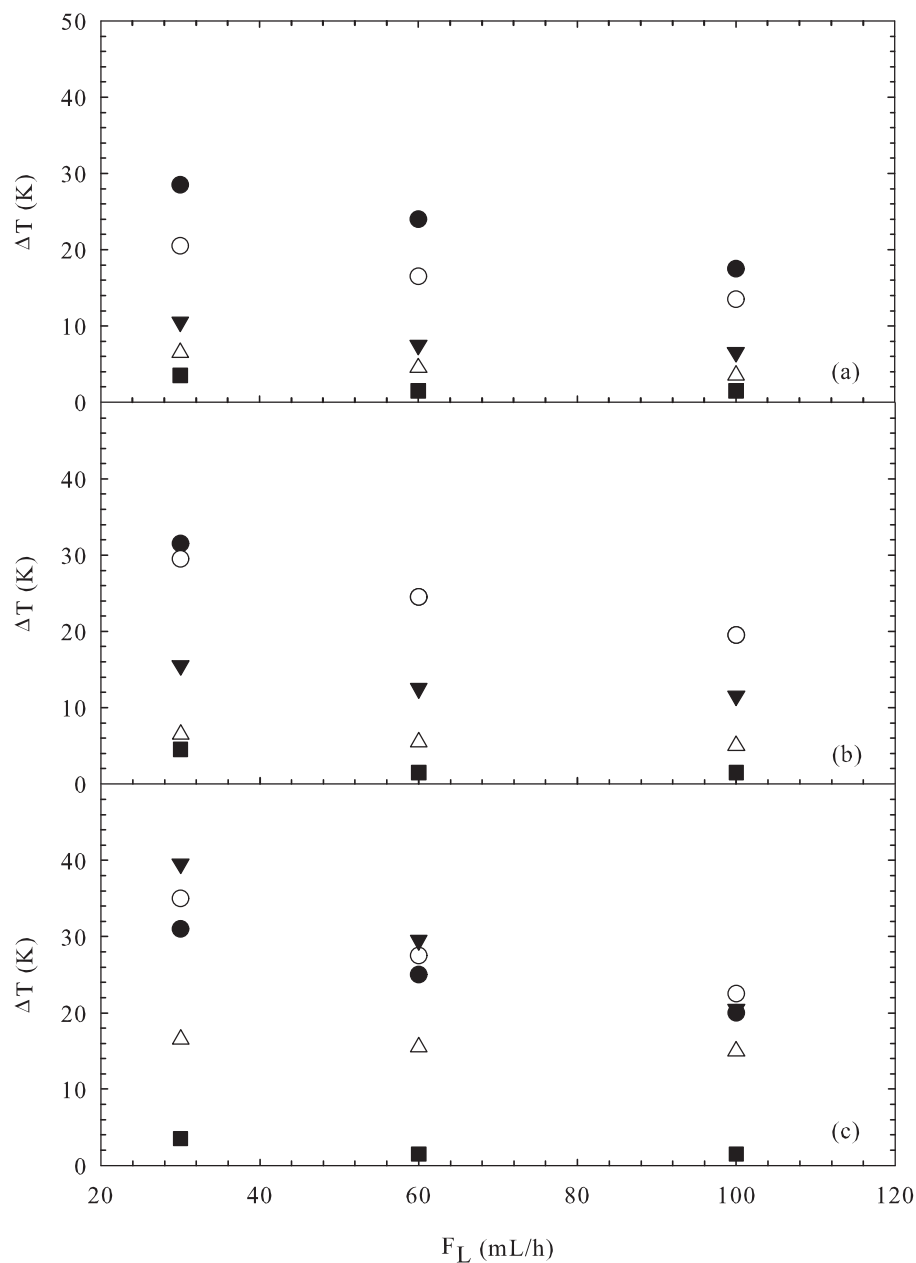


Figure C.10: Axial temperature gradient as function of liquid flow rate for different system pressure and gas flow rates (AC, Rockwool): (a)  $F_G = 18$  NL/h, (b)  $F_G = 9$  NL/h, (c)  $F_G = 3$  NL/h: (●)  $P_T = 25$  bar, (○)  $P_T = 20$  bar, (▼)  $P_T = 15$  bar, (△)  $P_T = 12$  bar, (■):  $P_T = 9$  bar,  $T_{Oven} = 170^\circ\text{C}$ ,  $W_{cat} = 7.5$  g.

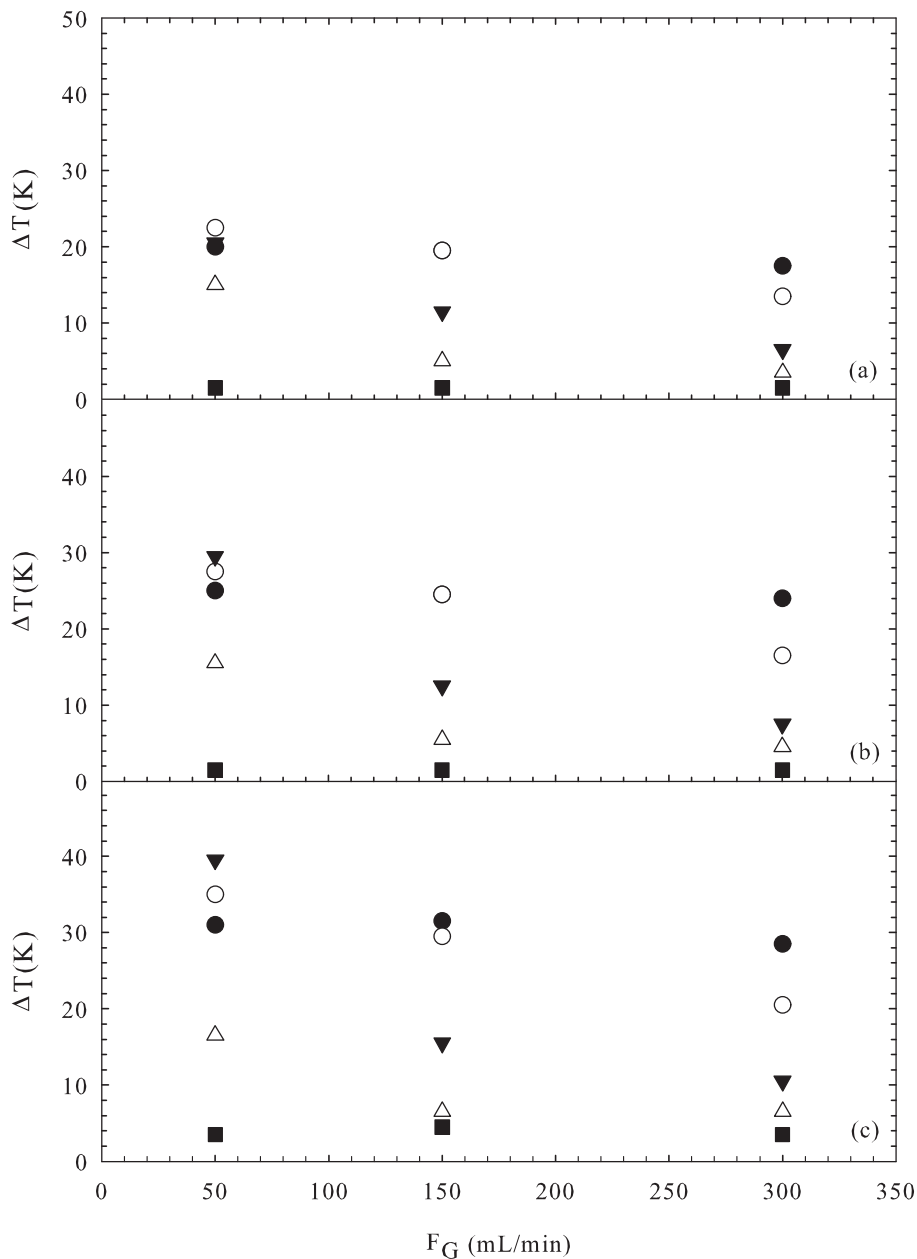


Figure C.11: Axial temperature gradient as function of gas flow rate for different system pressure and liquid flow rates (AC, Rockwool): (a)  $F_L = 100$  mL/h, (b)  $F_L = 60$  mL/h, (c)  $F_L = 30$  mL/h: (●)  $P_T = 25$  bar, (○)  $P_T = 20$  bar, (▼)  $P_T = 15$  bar, (△)  $P_T = 12$  bar, (■):  $P_T = 9$  bar,  $T_{Oven} = 170^\circ\text{C}$ ,  $W_{cat} = 7.5$  g.

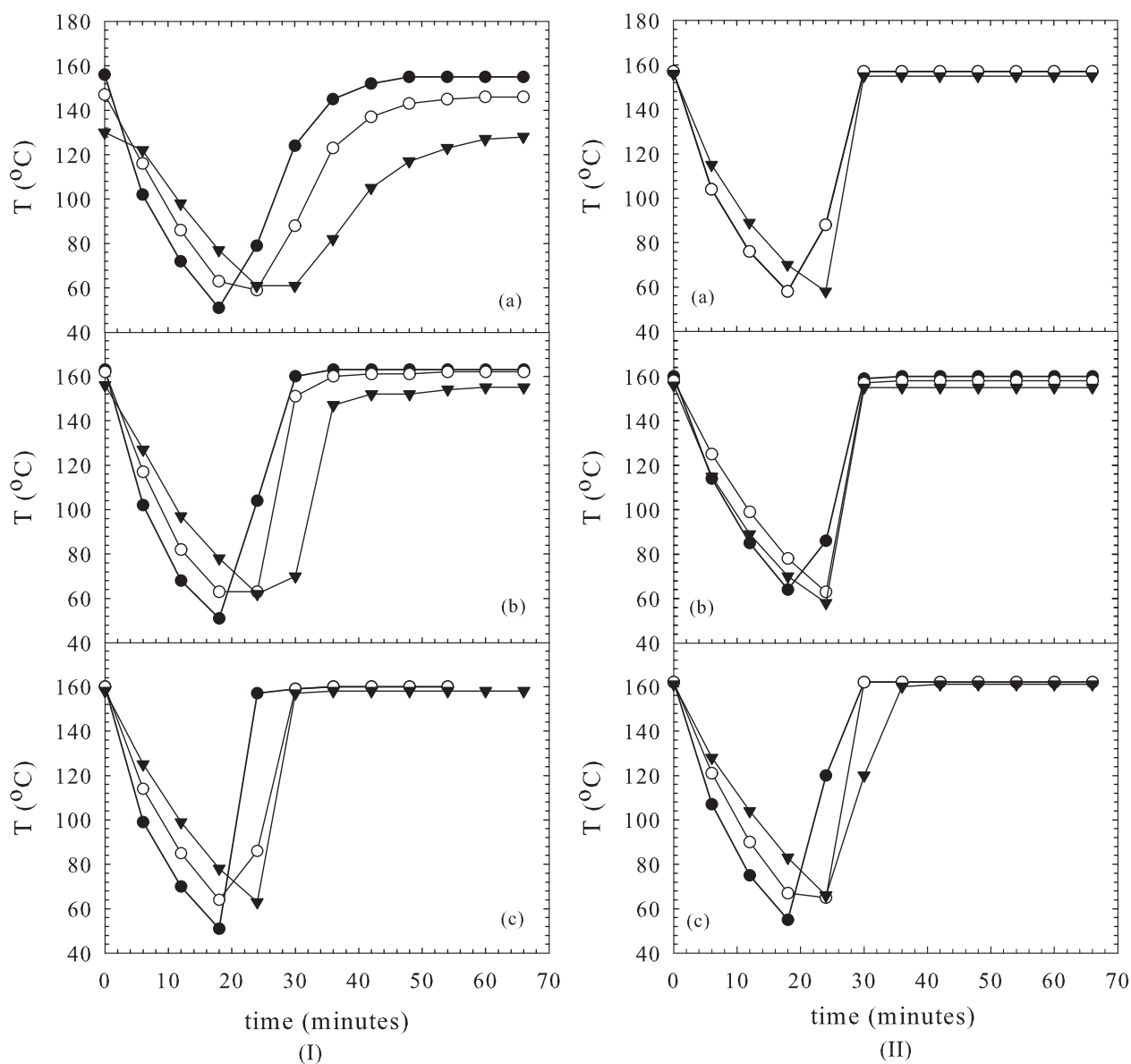


Figure C.12: Dynamic temperature profile in trickle column for different system pressure and gas flow rates: I ( $F_L = 100$  mL/h,  $F_G = 18$  NL/h)  $\rightarrow$  (a) 15 bar, (b) 12 bar, (c) 9 bar; II ( $F_L = 100$  mL/h,  $P_t = 9$  bar)  $\rightarrow$  (a)  $F_G = 18$  NL/h, (b)  $F_G = 9$  NL/h, (c) 3 bar: ( $\bullet$ ) 1,5 cm, ( $\circ$ ) 10 cm, ( $\blacktriangledown$ ) 20,5 cm:  $T_{oven} = 170$  °C, Glass bead, Rigid Board.

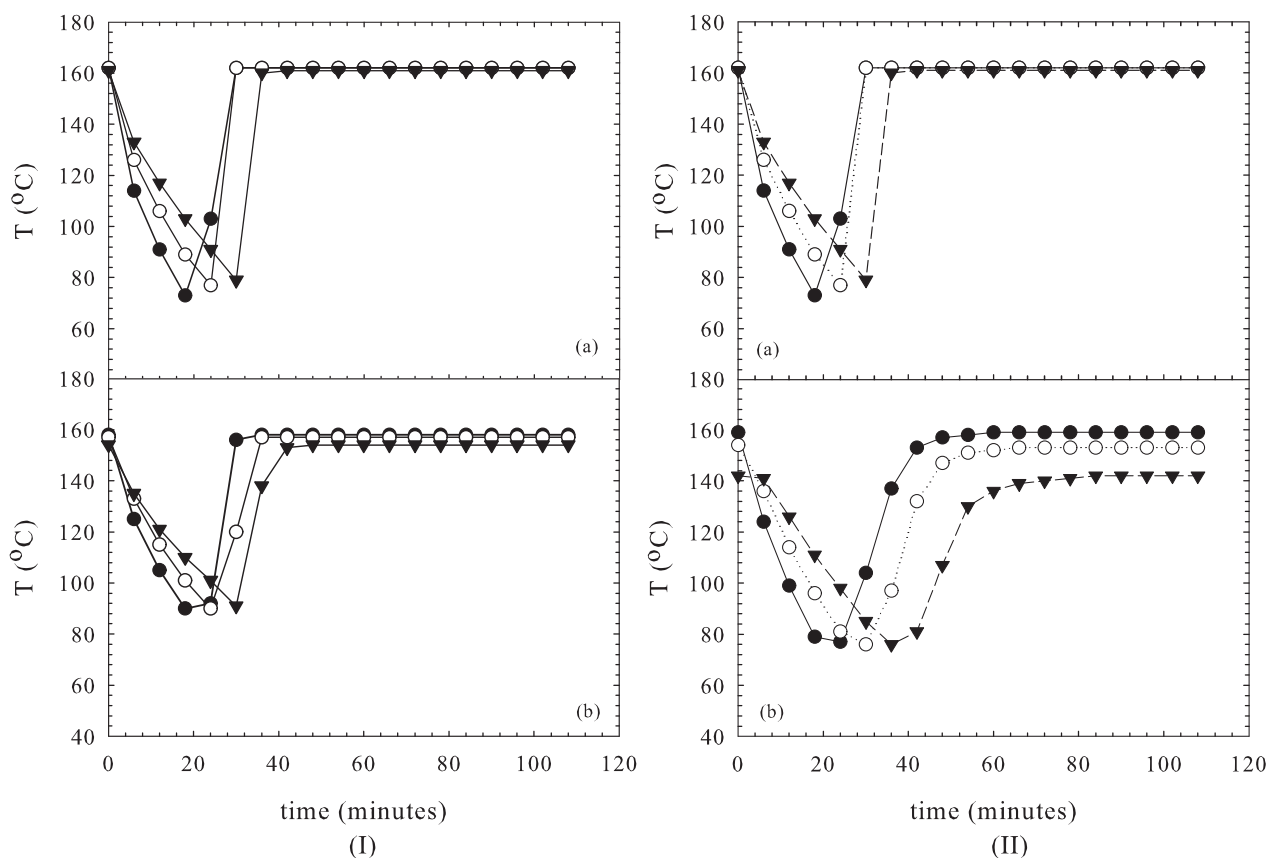


Figure C.13: Dynamic temperature profile in trickle column for different system pressure and liquid flow rates: I ( $P_T = 9$  bar,  $F_G = 9$  NL/h)  $\rightarrow$  (a)  $F_L = 60$  mL/h, (b)  $F_L = 30$  mL/h; II ( $F_L = 60$  mL/h,  $F_G = 9$  NL/h)  $\rightarrow$  (a) 15 bar, (b) 9 bar: ( $\bullet$ ) 1,5 cm, ( $\circ$ ) 10 cm, ( $\blacktriangledown$ ) 20,5 cm:  $T_{oven} = 170$  °C, Active carbon, Rockwool.

## Appendix D

### Appendix

#### D.1 Conversion and temperature profiles for feed temperature modulation

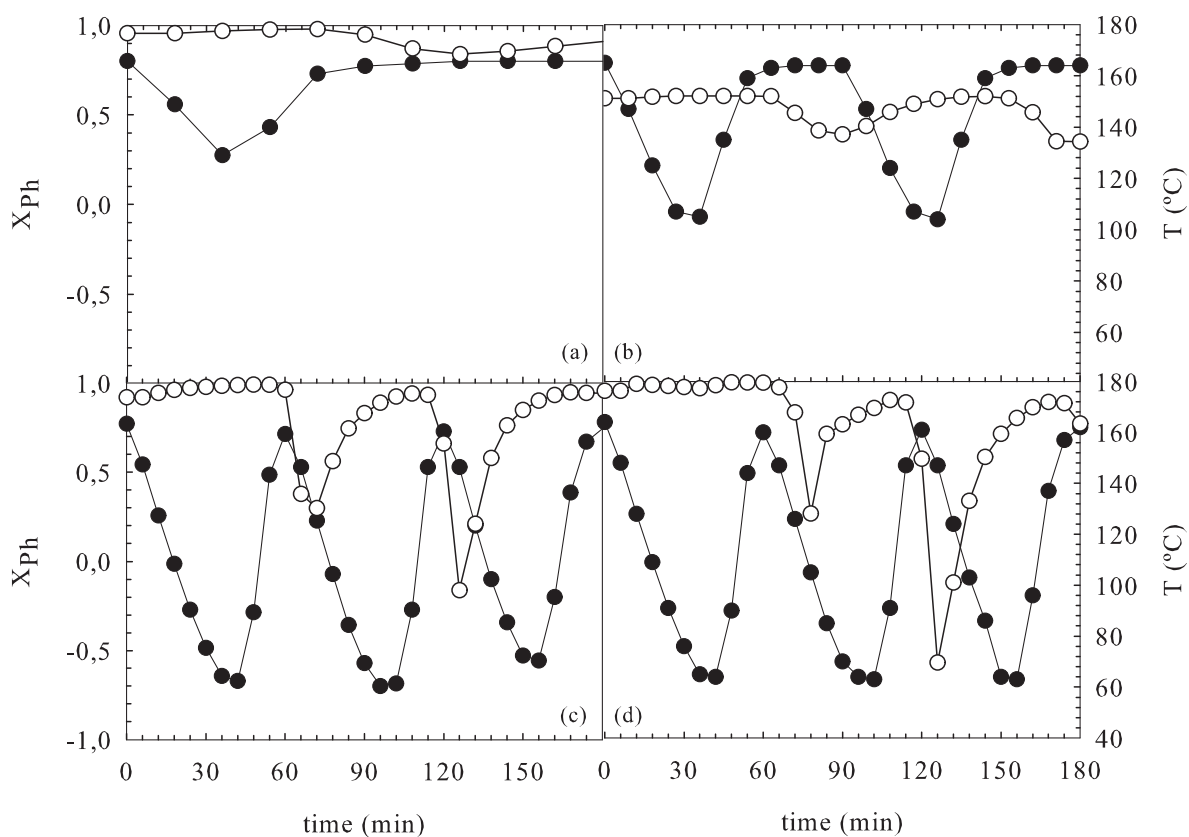


Figure D.1: Dynamic phenol conversion and temperature profile as function of time for different split and cycle period of 1 h: (a)  $s = 0.9$ , (b)  $s = 0.8$ , (c)  $s = 0.6$ , (d)  $s = 0.5$ : (○) phenol conversion, (●) temperature:  $P_{O_2}$ ,  $T_{inlet} = 163^\circ\text{C}$ ,  $F_L = 63 \text{ mL/h}$ ,  $W_{cat} = 7.5 \text{ g}$ ,  $F_G = 9 \text{ N/h}$ ,  $C_{Ph} = 5 \text{ g/L}$ .

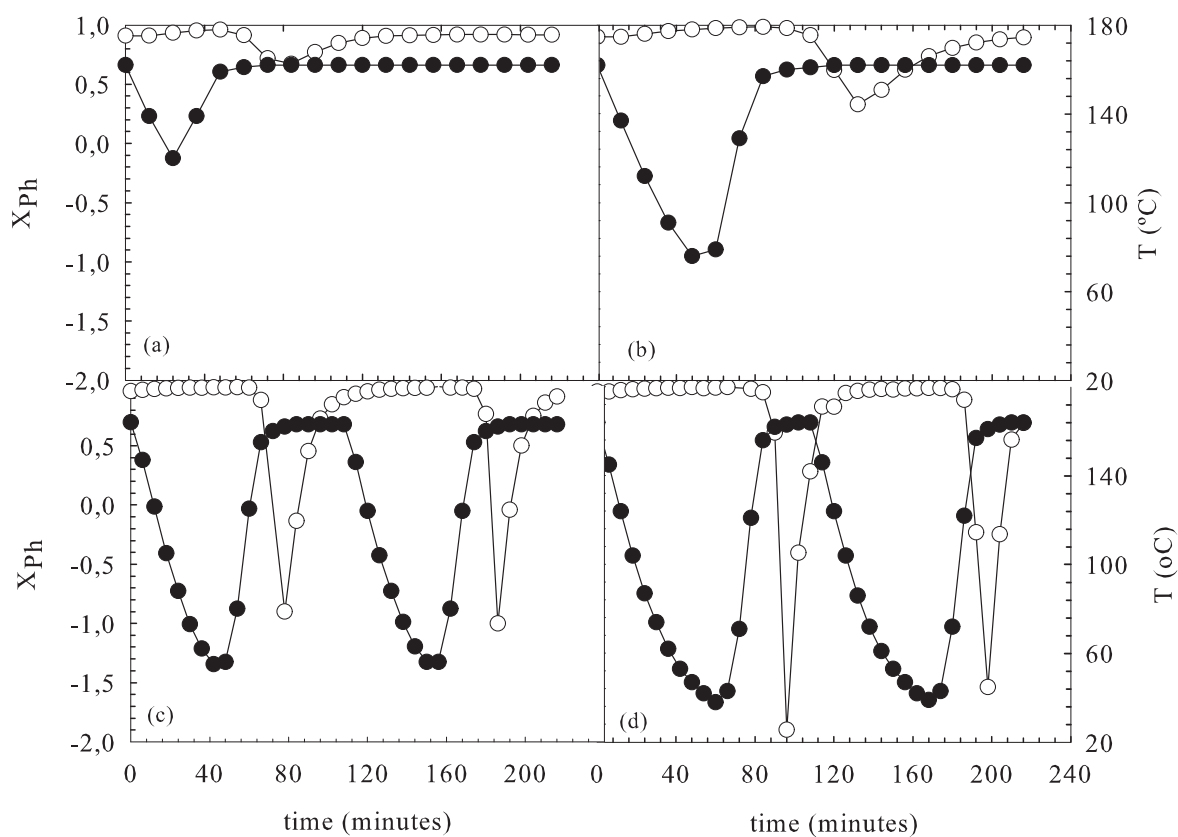


Figure D.2: Dynamic phenol conversion and temperature profile as function of time for different split and cycle period of 1.8 h: (a)  $s = 0.9$ , (b)  $s = 0.83$ , (c)  $s = 0.67$ , (d)  $s = 0.5$ : (○) phenol conversion, (●) temperature:  $P_{O_2}$ ,  $T_{inlet} = 163^\circ\text{C}$ ,  $F_L = 63$  mL/h,  $W_{cat} = 7.5$  g,  $F_G = 9$  N/h,  $C_{Ph} = 5$  g/L.

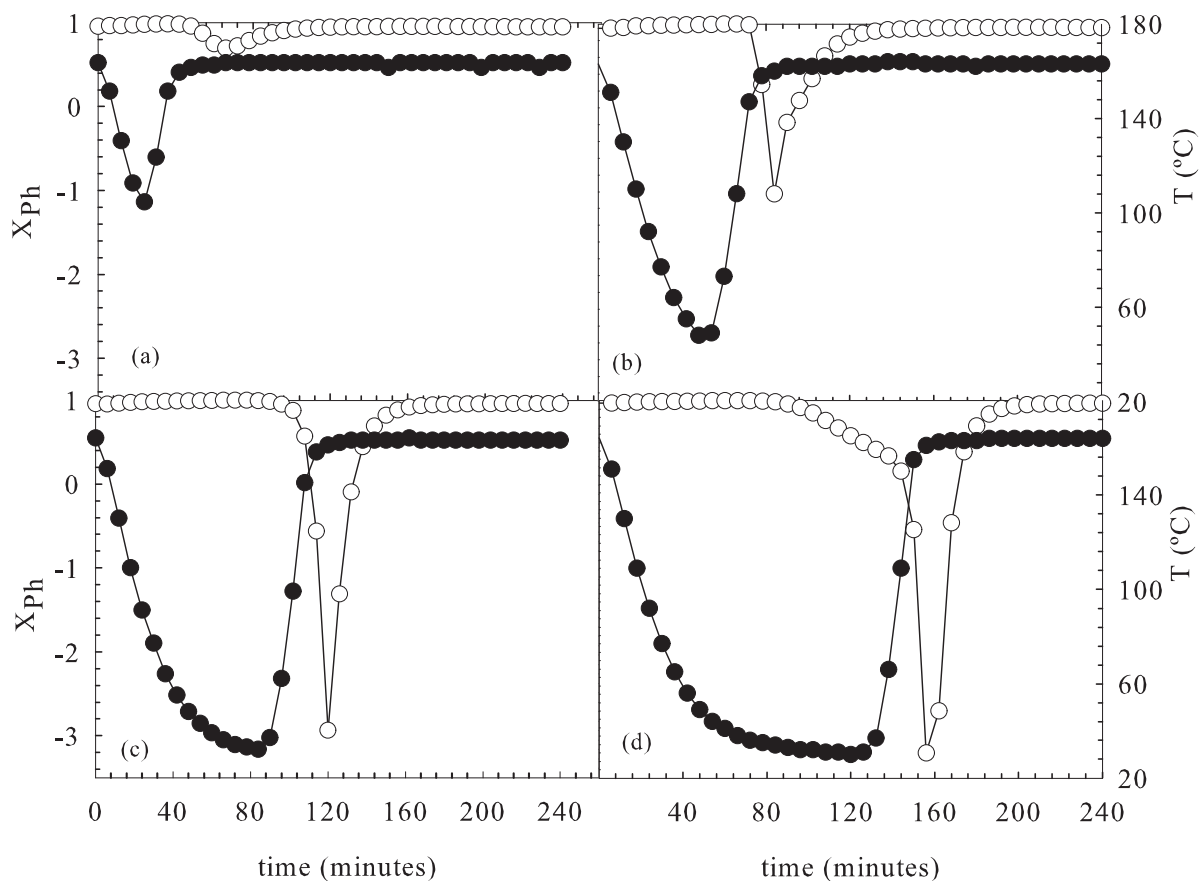


Figure D.3: Dynamic phenol conversion and temperature profile as function of time for different split and cycle period of 4 h: (a)  $s = 0.9$ , (b)  $s = 0.83$ , (c)  $s = 0.67$ , (d)  $s = 0.5$ : (o) phenol conversion, (●) temperature:  $P_{O_2}$ ,  $T_{inlet} = 163^\circ\text{C}$ ,  $F_L = 63$  mL/h,  $W_{cat} = 7.5$  g,  $F_G = 9$  N/h,  $C_{Ph} = 5$  g/L.

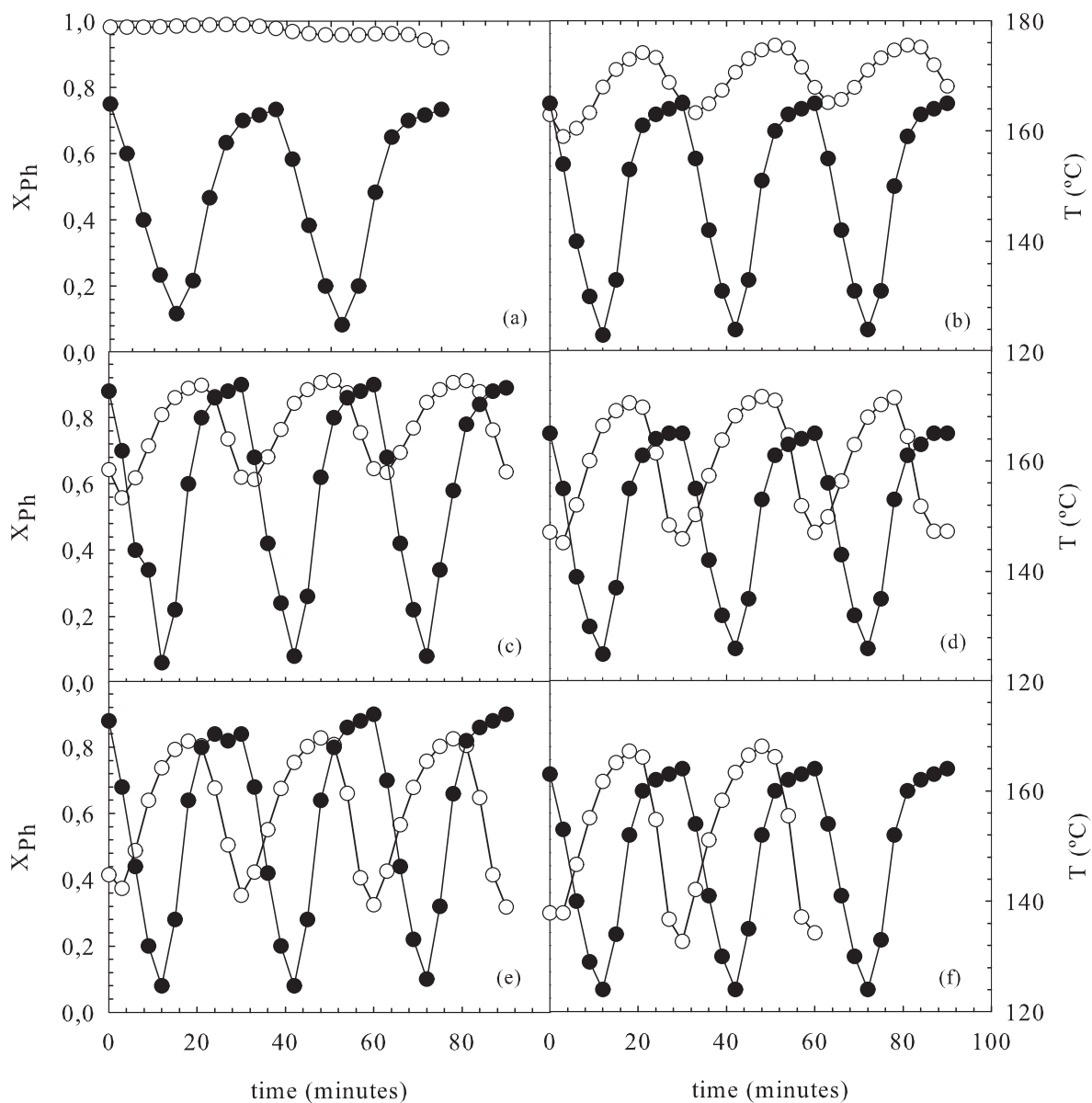


Figure D.4: Cycle phenol conversion and temperature profile as function of time on for long run dynamic experiments at time on stream for: (a) TOS = 24 h, (b) TOS = 48 h, (c) TOS = 72 h, (d) TOS = 96 h, (e) TOS = 120 h, (f) TOS = 150 h: ( $\circ$ ) phenol conversion, ( $\bullet$ ) temperature:  $p = 0.5$  h,  $s = 0.8$ :  $P_{O_2}$ ,  $T_{inlet} = 163^{\circ}C$ ,  $F_L = 63$  mL/h,  $W_{cat} = 7.5$  g,  $F_G = 9$  N/h,  $C_{Ph} = 5$  g/L.

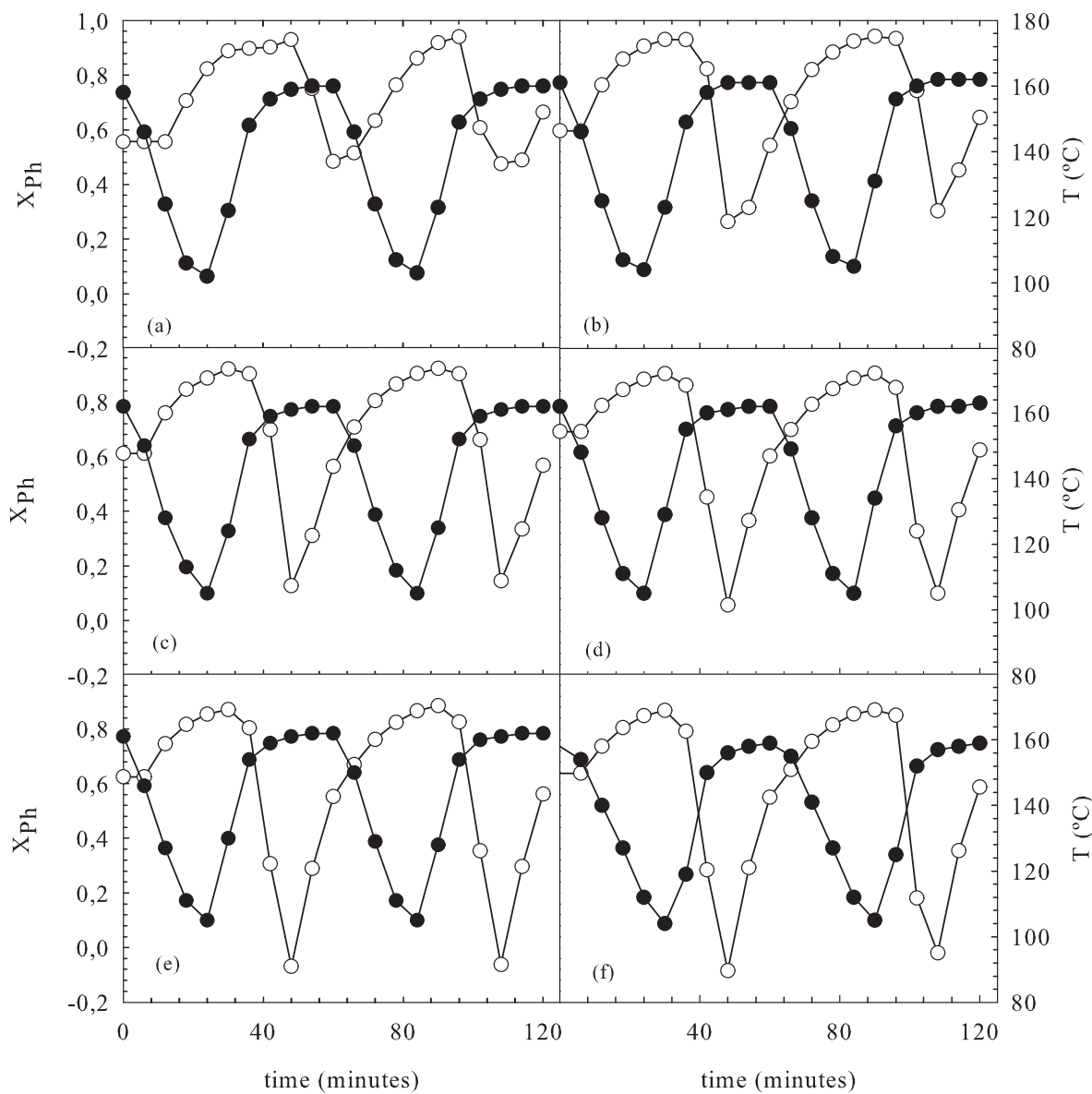


Figure D.5: Cycle phenol conversion and temperature profile as function of time at different time on stream for long run dynamic experiments: (a) TOS = 24 h, (b) TOS = 48 h, (c) TOS = 72 h, (d) TOS = 96 h, (e) TOS = 120 h, (f) TOS = 150 h: (o) phenol conversion, (●) temperature:  $p = 1$  h,  $s = 0.8$ :  $P_{O_2}$ ,  $T_{inlet} = 163^{\circ}C$ ,  $F_L = 63$  mL/h,  $W_{cat} = 7.5$  g,  $F_G = 9$  N/h,  $C_{Ph} = 5$  g/L.

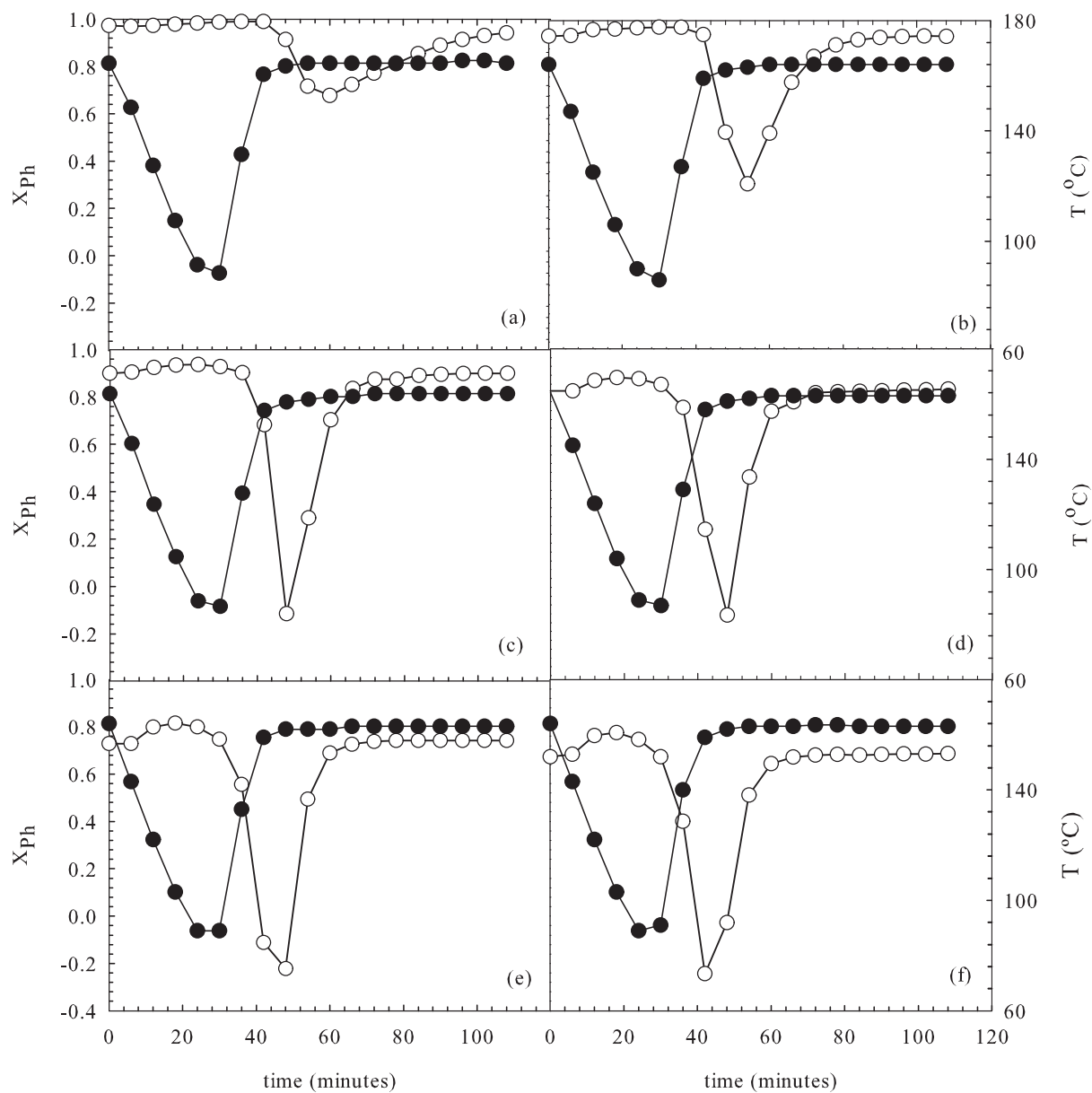


Figure D.6: Cycle phenol conversion and temperature profile as function of time at different time on stream for long run dynamic experiments at different split: (a) TOS = 24 h, (b) TOS = 48 h, (c) TOS = 72 h, (d) TOS = 96 h, (e) TOS = 120 h, (f) TOS = 150 h: (o) phenol conversion, (●) temperature:  $p = 1$  h,  $s = 0.83$ :  $P_{O_2}$ ,  $T_{inlet} = 163^\circ\text{C}$ ,  $F_L = 63$  mL/h,  $W_{cat} = 7.5$  g,  $F_G = 9$  N/h,  $C_{Ph} = 5$  g/L.

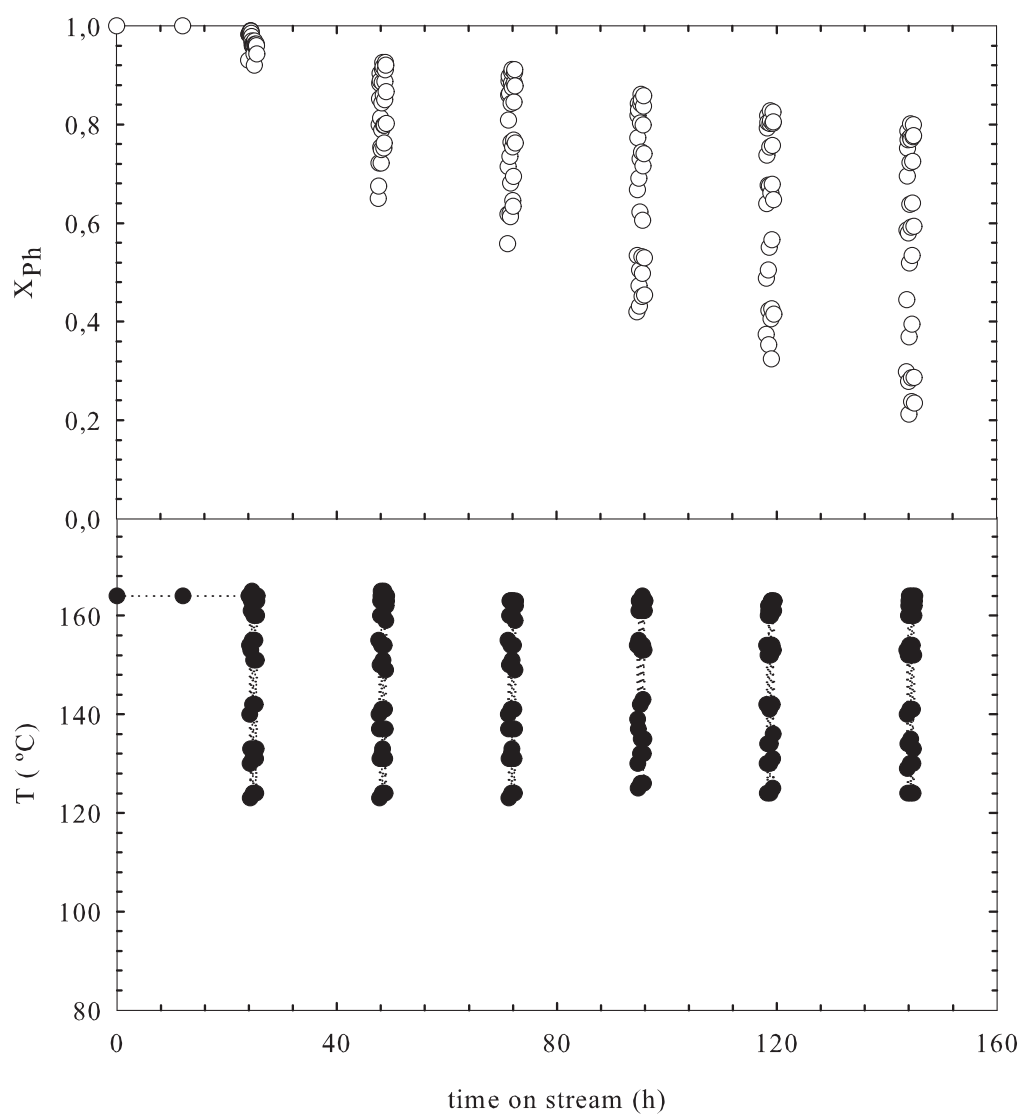


Figure D.7: Mean cycle phenol conversion and temperature profile as function of time on stream for long run dynamic experiments:  $p = 0.5$  h,  $s = 0.8$ :  $P_{O_2}$ ,  $T_{inlet} = 163^\circ\text{C}$ ,  $F_L = 63$  mL/h,  $W_{cat} = 7.5$  g,  $F_G = 9$  N/h,  $C_{Ph} = 5$  g/L.

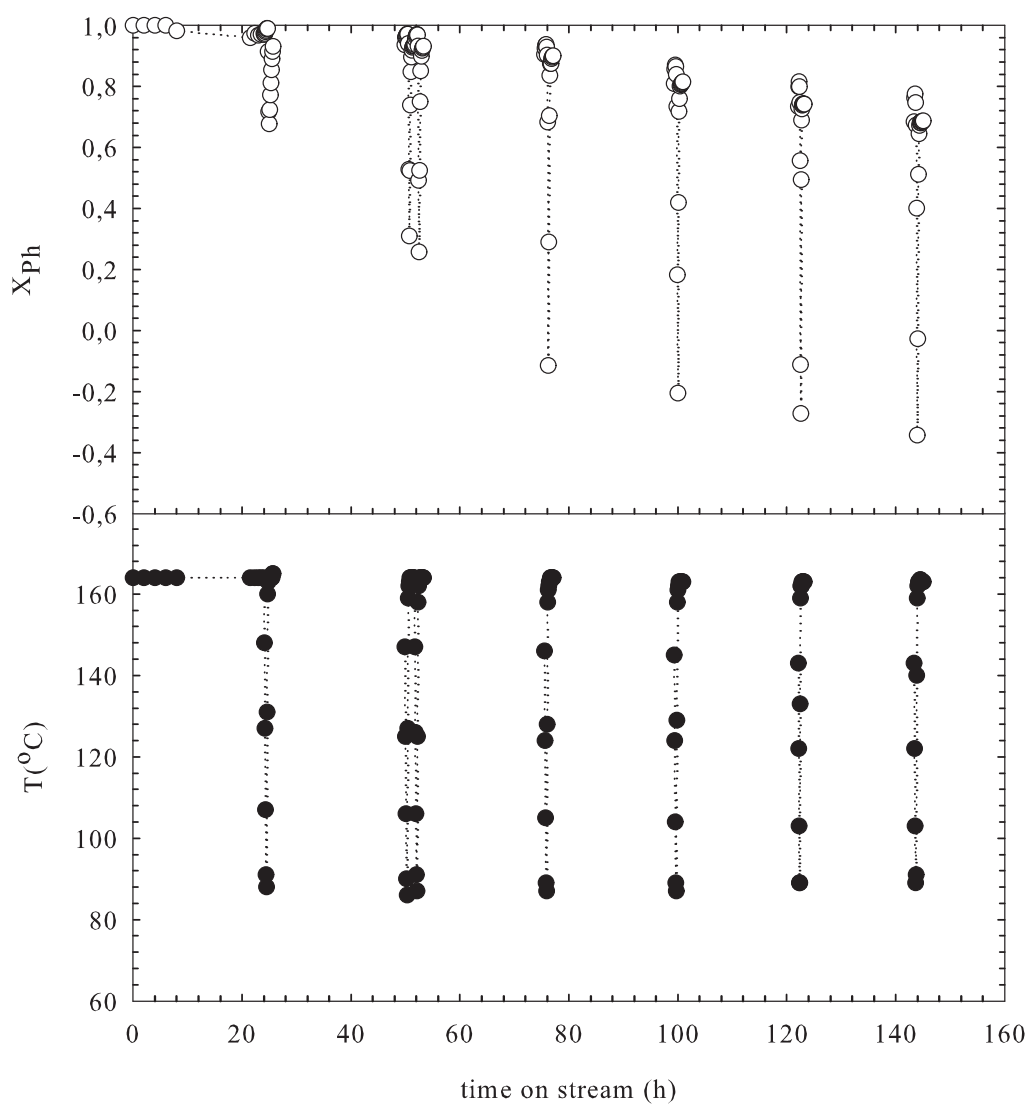


Figure D.8: Mean phenol conversion and temperature profile as function of time on stream for long run dynamic experiments:  $p = 1.8$  h,  $s = 0.8$ :  $P_{O_2}$ ,  $T_{inlet} = 163^{\circ}C$ ,  $F_L = 63$  mL/h,  $W_{cat} = 7.5$  g,  $F_G = 9$  N/h,  $C_{Ph} = 5$  g/L.

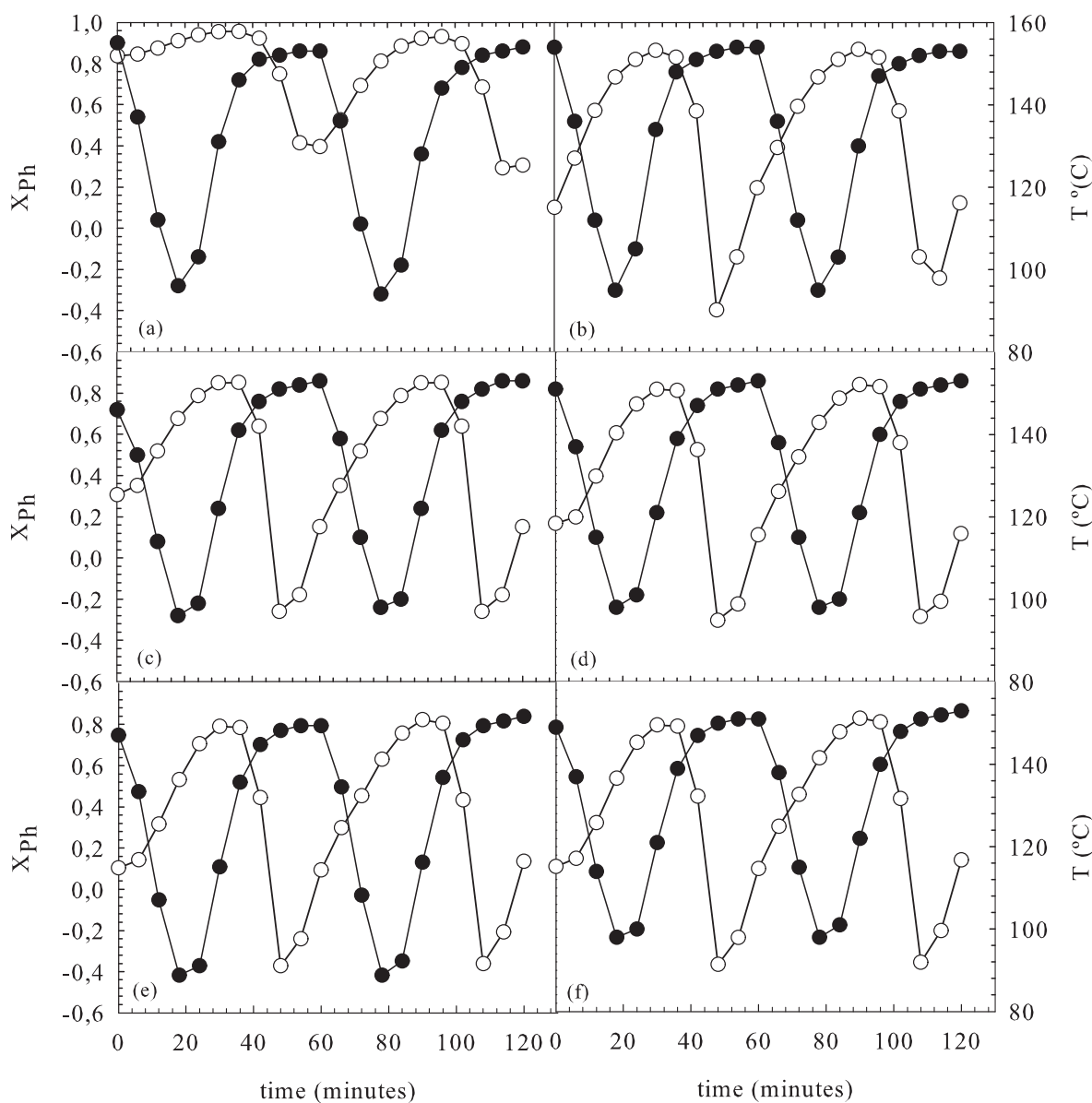


Figure D.9: Cycle phenol conversion and temperature profile as function of time for long run dynamic experiments at different time on stream :  $p = 1$  h,  $s = 0.8$ : (a) TOS = 24 h, (b) TOS = 48 h, (c) TOS = 72 h, (d) TOS = 96 h, (e) TOS = 120 h, (f) TOS = 150 h: (○) phenol conversion, (●) temperature:  $P_{O_2}$ ,  $T_{inlet} = 153^\circ\text{C}$ ,  $F_L = 63$  mL/h,  $W_{cat} = 7.5$  g,  $F_G = 9$  N/h,  $C_{Ph} = 5$  g/L.

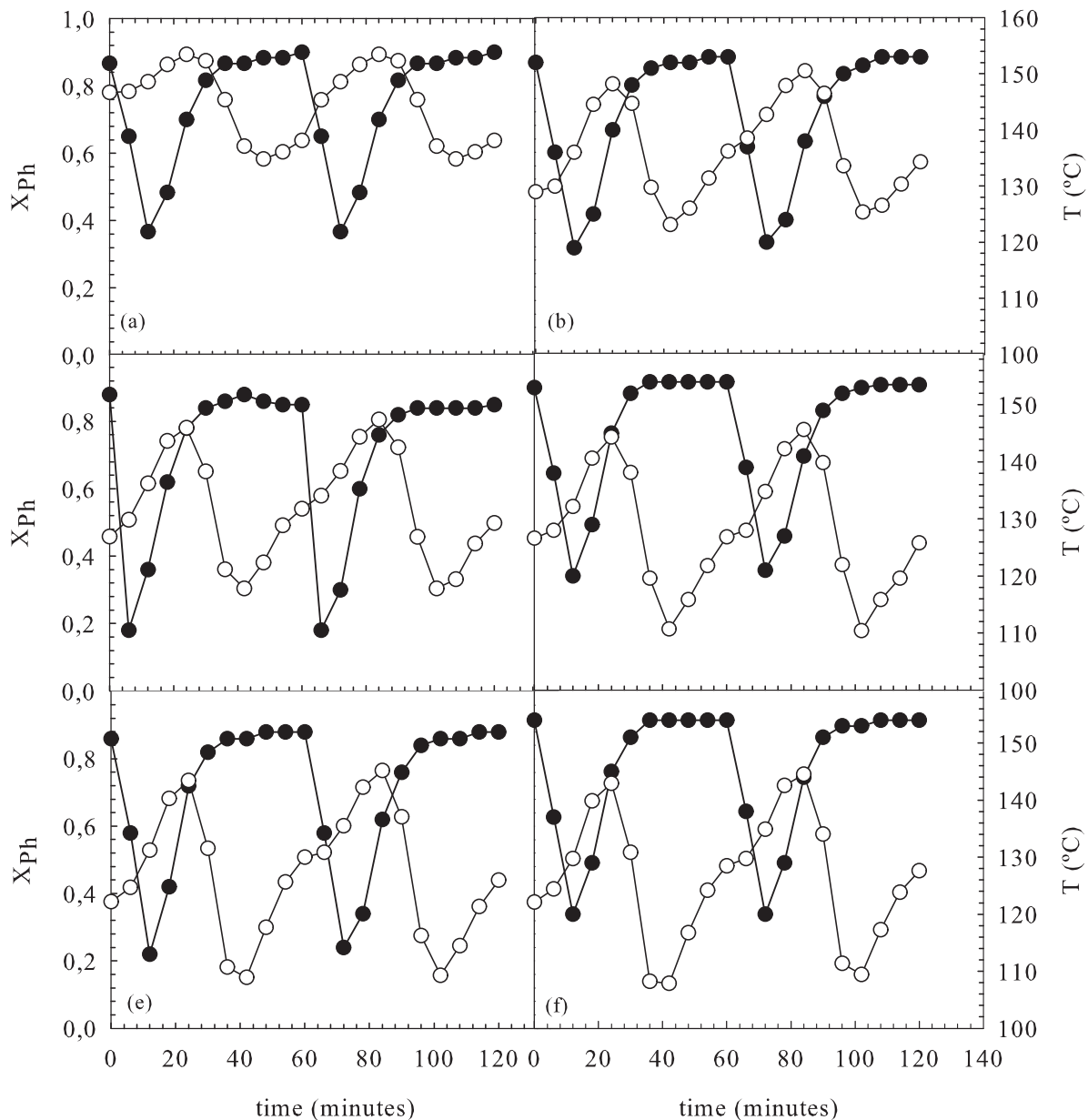


Figure D.10: Cycle phenol conversion and temperature profile as function of time for long run dynamic experiments at different time on stream :  $p = 1$  h,  $s = 0.9$ : (a) TOS = 24 h, (b) TOS = 48 h, (c) TOS = 72 h, (d) TOS = 96 h, (e) TOS = 120 h, (f) TOS = 150 h: (○) phenol conversion, (●) temperature:  $P_{O_2}$ ,  $T_{inlet} = 153^\circ\text{C}$ ,  $F_L = 63$  mL/h,  $W_{cat} = 7.5$  g,  $F_G = 9$  N/h,  $C_{Ph} = 5$  g/L.

## **D.2 Conversion and temperature profiles for liquid flow modulation**

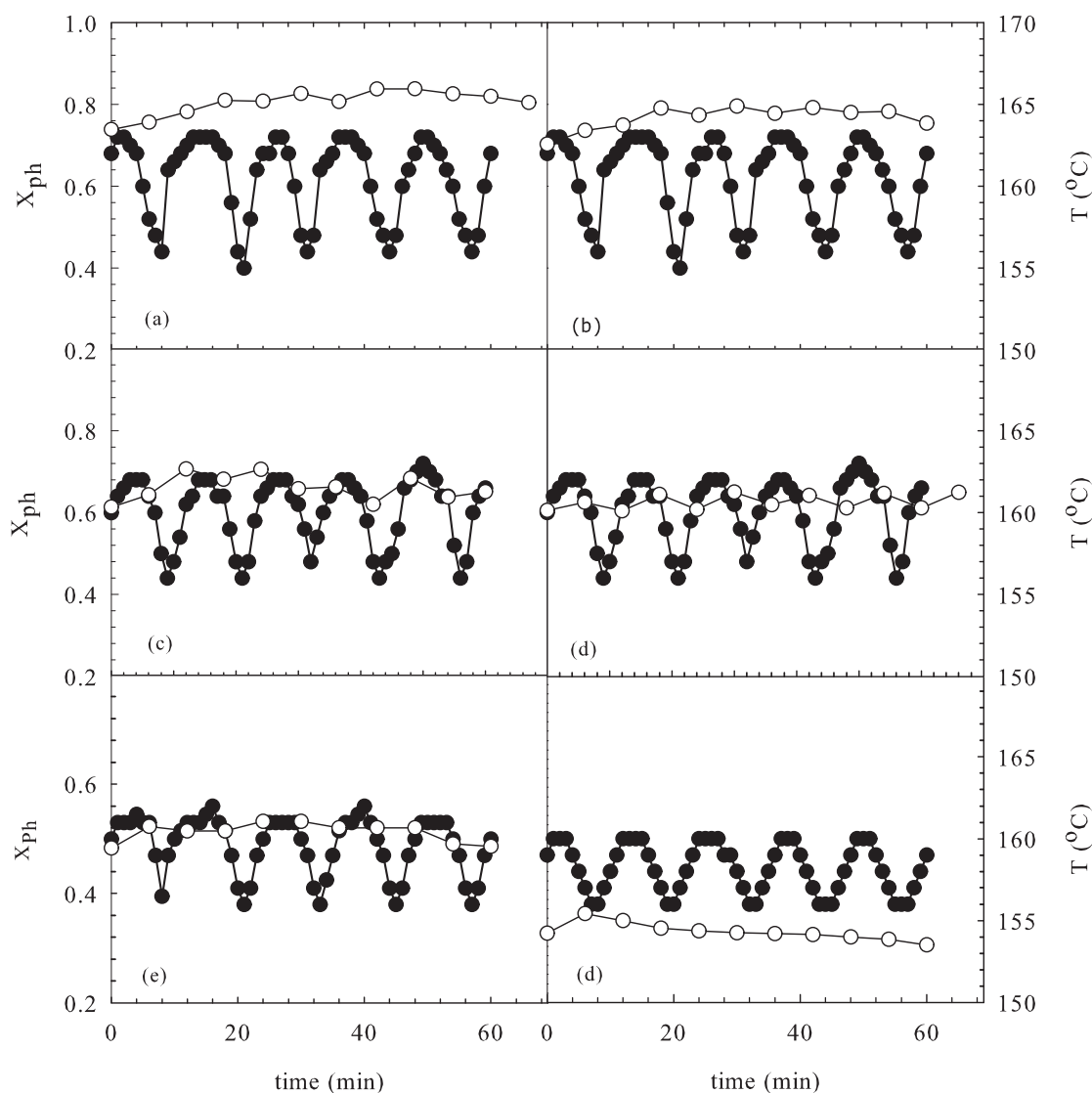


Figure D.11: Cycle phenol conversion and temperature profile with time at different time on stream for long run dynamic experiments:  $p = 0.2$  h,  $s = 0.5$ : (a) TOS = 26 h, (b) TOS = 48 h, (c) TOS = 72 h, (d) TOS = 96 h, (e) TOS = 120 h, (f) TOS = 150 h: (○) phenol conversion, (●) temperature:  $p = 0.2$  h,  $s = 0.5$ :  $P_{O_2}$ ,  $T_{inlet} = 162^\circ\text{C}$ ,  $F_L = 58$  h,  $W_{cat} = 7$  g,  $F_G = 9$  NL/h,  $C_{Ph} = 5$  g/L.

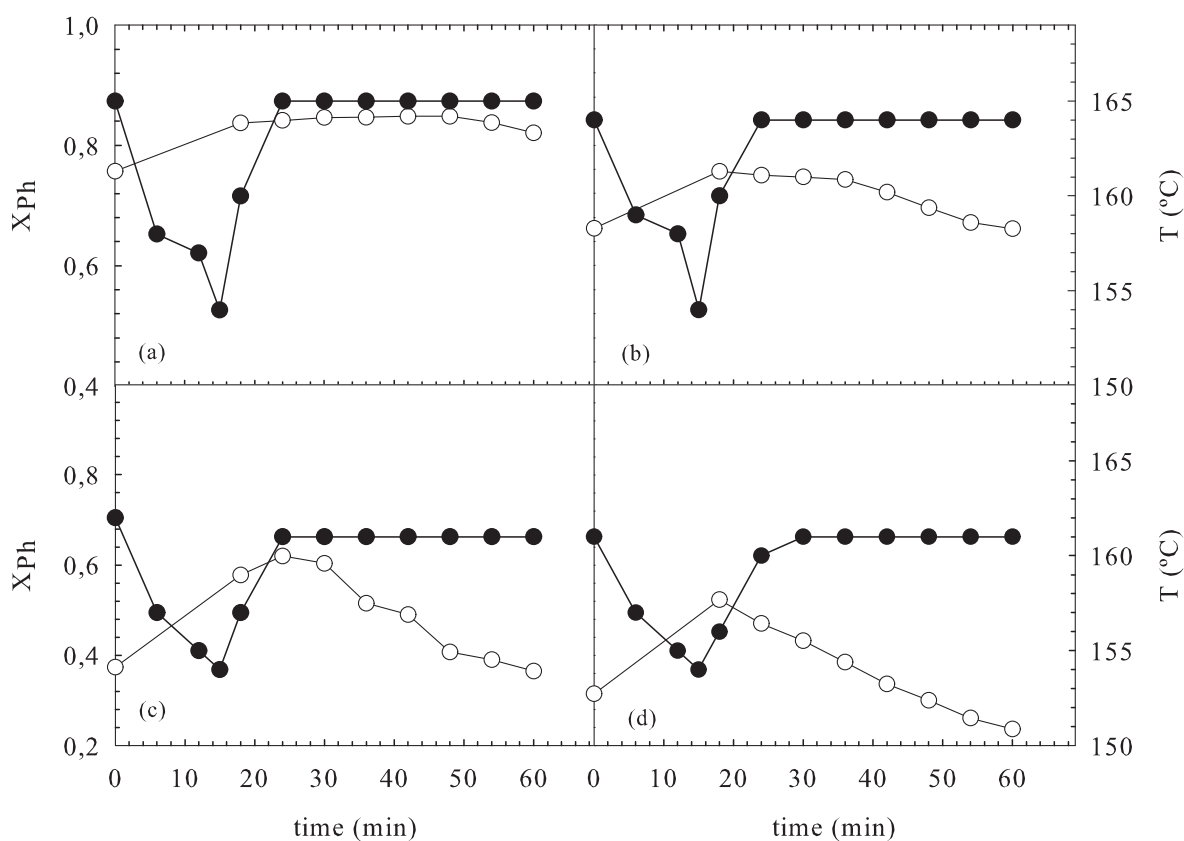


Figure D.12: Cycle phenol conversion and temperature profile with time at different time on stream for long run dynamic experiments for p 1 h and 0.5 split: (a) TOS = 26 h, (b) TOS = 48 h, (c) TOS = 72 h, (d) TOS = 96 h, (e) TOS = 120 h, (f) TOS = 150 h: (○) phenol conversion, (●) temperature: p = 1 h, s = 0.8:  $P_{O_2}$ ,  $T_{inlet} = 162^\circ\text{C}$ ,  $F_L = 58$  h,  $W_{cat} = 7$  g,  $F_G = 9$  NL/h,  $C_{Ph} = 5$  g/L.

## ABOUT THE AUTHOR

**Nigus Gabbiye Habtu** was born in Alamata region (**Ethiopia**) on 22<sup>th</sup> August , 1976. After accomplishing his high school education, he joined Bahir Dar University and obtained his B.Sc degree in Chemical Engineering in 2001. In 2004 he obtained his M.Sc. degree in Chemical Engineering at University of Addis Ababa with the dissertation topic "*Modelling and Simulation of Interface Mass Transfer with Chemical Reaction*". In 2007 he obtained his M.Sc. degree in Chemical and Process Engineering at Rovira i Virgili University with the dissertation topic of "*Catalytic Wet Air Oxidation of Phenol over Activated Carbon in Multi-Phase Reactor*". In October 2007 he started his Ph.D. research at the Department of Chemical Engineering of Rovira i Virgili University.

## Publication

- **N. Habtu, J. Font , A. Fortuny, C. Bengoa, A. Fabregat, P. Haure, A. Ayude, F. Stüber**; Heat Transfer in Trickle Bed Column with Constant and Modulated Feed Temperature: Experiments and Modeling, Chemical engineering science; Accepted (In Press), Refrence: CES9533.
- **Nigus Gabbiye, Josep Font, Agusty, Fortuny, Christophe Bengoa, Azael Fabregat, Frank Stüber**. Performance of Trickle Bed Reactor and Active Carbon in the Liquid phase oxidation of phenol;International Journal of Chemical Reactor; 8; A76;2010 .
- **N. Gabbiye, F. Stber, J. Font, C. Bengoa, A. Fortuny, A. Fabregat, P. Haure, A. Ayude**; Feed Temperature Modulation in Trickle Bed Reactor: Experiments And Modelling. In Proceedings of the 8<sup>th</sup> World Congress of Chemical Engineering, 2009, Montral, Quebec, Canada

## Contribution in Congresses

- **N. Habtu, J. Font, A. Fortuny, C. Bengoa, A. Fabregat, P. Haure, A. Ayude, F. Stüber**; Heat Transfer in Trickle Bed Column with Constant and Modulated Feed Temperature: Experiments and Modeling; 10<sup>th</sup> international conferences on Gas-Liquid and Gas-Liquid-Solid reactor Engineering; Accepted for Oral presentation, June, 26-29 - 2011, Braga, Portugal

- **N. Habtu, J. Font, A. Fortuny, C. Bengoa, A. Fabregat, P. Haure, A. Ayude, F. Stüber;** Heat Transfer in Trickle Bed Column with Constant and Modulated Feed Temperature: Experiments and Modeling, Asociacin Argentina de Ingenieros Quimicos (AAIQ ), Oral presentation, VI CAIQ 2010
- **N. Habtu, J. Font, A. Fortuny, C. Bengoa, A. Fabregat, F. Stüber;** Periodic Operation of Trickle Bed Reactor for Improving the Stability of Activated Carbon in CWAO Processes. Oral presentation. 19<sup>th</sup> International Congress of Chemical and Process Engineering and 7<sup>th</sup> European Congress of Chemical Engineering, Prague (Czech Republic), 28 Aug 1 Sept 2010.
- **G. Mezohegyi, F. Goncalves, J. J. M. Orfao, C. Bengoa, F. Stüber, F. Font, A. Fortuny , A. Fabregat, N. G. Habtu;** Activated carbon as catalyst in the anaerobic removal of azo colourants: Influence of the surface chemistry. Poster. 19<sup>th</sup> International Congress of Chemical and Process Engineering and 7<sup>th</sup> European Congress of Chemical Engineering, Prague (Czech Republic), 28 Aug 1 Sept 2010; accepted.
- **N. Gabbiye, F. Stüber, J. Font, C. Bengoa, A. Fortuny, A. Fabregat, P. Haure, A. Ayude;** Feed Temperature Modulation in Trickle Bed Reactor: Experiments And Modelling. Oral presentation; 8<sup>th</sup> World Congress of Chemical Engineering, August 23 - 27, 2009, Montral, Quebec, Canada
- **N. Gabbiye, J. Font, A. Fortuny, C. Bengoa, A. Fabregat, F. Stüber:** Trickle Bed Reactor for The Oxidation of Phenol over Active Carbon Catalyst. 2<sup>nd</sup> international congress of Green Process Engineering; and 2<sup>nd</sup> European Congress Process Intensification Conference; Oral presentation 14-17 June, 2009; Venice, Italy

## Research Stage

From 17/06/2010 to 17/09/2010: Visit to the research group of Prof.dr.ir. Jaap Schouten (Chemical Reactor Engineering group) at the Department of Chemical Engineering and Chemistry, Eindhoven Univeristy of Technology (TU/e), Eindhoven, The Netherlands